UNIVERSITY OF CRETE

DEPARTMENT OF PHYSICS

PhD THESIS

Holography and the phase structure of gravity theories.

Ιωάννης Ιατράκης

Advisor: *Prof.* Ηλίας Κυρίτσης - University of Crete

UNIVERSITY OF CRETE
DEPARTMENT OF PHYSICS

PhD THESIS

Doctor of Philosophy
of
- High energy Physics -

Defended by
Ιωαννης Ιατρακης

Holography and the phase structure of gravity theories

COMMITTEE

Prof.	Ηλίας Κυρίτσης	-	University of Crete
Prof.	Νικόλαος Τσάμης	-	University of Crete
Prof.	Αναστάσιος Πέτκου	-	University of Crete
Prof.	Θεόδωρος Τομαράς	-	University of Crete
Prof.	Νικόλαος Παπανικολάου	-	University of Crete
Prof.	Javier Mas	-	Universidade de Santiago de Compostela
Prof.	Κωνσταντίνος Αναγνωστόπουλος	-	National Technical University of Athens

Date of the defense:
30/08/2013

Περίληψη

Η αντιστοιχία βαρυτικών θεωριών με θεωρίες βαθμίδας χρησιμοποιείται για την κατασκευή ενεργών ολογραφικών μοντέλων που περιγράφουν την Κβαντική Χρωμοδυναμική (Κ.Χ.Δ.) στο όριο ισχυρής σύζευξης. Υποθετοντάς ότι $N_f << N_c$, κατασκευάζουμε ένα ολογραφικό μοντέλο που περιγράφει την φυσική του μεσονικού τομέα των ισχυρών αλληλεπιδράσεων, όπως το σπάσιμο της chiral συμμετρίας, την αποκατάστασή της πάνω απο την θερμοκρασία της αλλαγής φάσης απο την φάση περιορισμού χρώματος στην απελευθέρωσή του και το φάσμα των μαζών των μεσονίων. Το μοντέλο επίσης χρησιμοποιείται για την μελέτη του εγκάρσιου μέρους της συναρτησης συσχετισής του διανυσματικού-ψευδοδιανυσματικού ρεύματος γεύσης υπό την παρουσία ασθενούς εξωτερικού ηλεκτρικού πεδίου, η οποία είναι σημαντική στον υπολογισμό κβαντικών διορθώσεων της μαγνητικής ροπής του μυονίου. Στη συνέχεια το μοντέλο γενικεύεται, ώστε να περιγράψει την Κ.Χ.Δ. στο όριο του Veneziano, που τα N_f και N_c τείνουν στο άπειρο αλλά ο λόγος, $x = \frac{N_f}{N_c}$, είναι σταθερός. Τα κύρια αποτελέσματα είναι το διακριτό φάσμα μαζών για $x < x_c$, όπου x_c είναι το σημείο της σύμμορφης αλλαγής φάσης. Καθώς $x \to x_c$, όλες οι παράμετροι της θεωρίας με μη-τερτιμμένη διάσταση μάζας τείνουν στο μηδέν ακολουθώντας την ασυμπτωτική συμπεριφορά Miransky. Ο ρυθμός διαχύσης Chern-Simons, Γ_{CS}, υπολογίζεται στο πλαίσιο της Improved Holographic QCD (IHQCD). Ο Γ_{CS} είναι μία σημαντική ποσότητα για το chiral magnetic effect στο πλάσμα κουάρκ-γλοιονίων και είναι ανάλογο με το όριο μηδενικής ορμής και συχνότητας του φανταστικού μέρους της καθυστερημένης συνάρτησης Green του περιττού υπό τον CP μετασχηματισμό τελεστή, $Tr\left[F \wedge F\right]$, όπου F είναι ο YM τανυστής τάσης του πεδίου.

Abstract

The gauge/gravity duality is used in order to construct effective holographic models that describe strongly coupled QCD. Assuming $N_f << N_c$, a holographic model is built that describes the physics of the meson sector of strong interactions, such as chiral symmetry breaking, chiral symmetry restoration above confinement/deconfinement phase transition and the meson mass spectrum. This model is also used to study the transverse part of the vector-axial vector flavor current correlator in the presence of weak external electric field, which is important for the calculation of the two-loop electroweak radiative corrections to the muon anomalous magnetic moment. It is then generalized to describe the spectrum of QCD in the Veneziano limit of large N_f and N_c but at fixed $x = \frac{N_f}{N_c}$. The main results include discrete and gapped spectrum for $x < x_c$, where x_c is the conformal transition point. As $x \to x_c$ all the parameters of the theory with non trivial mass dimension approach zero following Miransky scaling. The Chern-Simons diffusion rate, Γ_{CS} is studied in the context of Improved Holographic QCD model. Γ_{CS} is an important quantity for the chiral magnetic effect in the quark-gluon plasma and is proportional to the zero-momentum, zero-frequency limit of the imaginary part of the retarded two-point function of the CP-odd operator $\mathrm{tr}\,[F \wedge F]$, where F is the YM field strength.

Acknowledgements

I would like to deeply thank my advisor Elias Kiritsis for his guidance and support during my diploma and PhD years. I am also grateful to my collaborators A. Paredes, B. S. Kim, M. Järvinen, U. Gürsoy, F. Nitti, A. O'Bannon, D. Areán from whom I learned a lot. I am also indebted to the members of the Crete Center for Theoretical Physics and in particular professors N. Papanicolaou, T. Tomaras, T. Petkou, N. Tsamis and the members of C.N. Yang Institute for Theoretical Physics P. van Nieuwenhuizen, G. Sterman, L. Rastelli and M. Rocek for teaching me interesting courses in theoretical physics. I would also like to thank the students who participated in the graduate program of the Physics Department of the University of Crete in the recent years for contributing in the formation of a very stimulating environment. We had many discussions from which I have been greatly benefited. Moreover, I would like to thank Y. Constantinou for proof-reading of this thesis. Last but not least, I would like to thank Polina and my family for their endless support.

This work was funded by the Physics Department of the University of Crete and Manassaki fellowship from September 2008 to September 2009. I would also like to thank A.S. Onassis Foundation for financial support from October 2009 to August 2010. From September 2010 to August 2013, this work has been supported by the project "IRAKLITOS II - University of Crete" of the Operational Programme for Education and Lifelong Learning 2007 - 2013 (E.P.E.D.V.M.) of the NSRF (2007 - 2013), which is co-funded by the European Union (European Social Fund) and National Resources.

Contents

1 Introduction

The strong interaction is one of the four fundamental forces of nature and is responsible for the stability of protons and neutrons in nuclei. This interaction is described very successfully in the context of Quantum Field Theory (QFT) as an $SU(3)$ gauge theory known as Quantum Chromodynamics (QCD). It's spectrum contains six quarks in the fundamental representation of $SU(3)$ interacting by exchanging gauge bosons, the gluons, transforming in the adjoint of $SU(3)$. A main feature of strong interaction is that it is asymptotically free. This was first revealed by deep inelastic scattering experiments which showed that hadrons behave as nearly free particles in the limit of large momentum transfer during the scattering, [1]. In the early seventies, non-abelian gauge theories were proven to have coupling constant which decreases with increasing energy scale, [2; 3]. Hence, QCD was proposed by Fritzsch and Gell-Mann, [4], as a non-abelian gauge theory describing strong interactions which accurately matches the experimental data from high energy scatterings.

The theory is strongly coupled in the low energy regime and it is very difficult to make predictions or postdictions. To date, the main approaches to answer questions about low energy phenomena of the strong interaction are Lund Monte-Carlo model, lattice QCD and low energy effective field theories. Hadron-hadron collisions produce multiparticle strongly coupled backgrounds. It is impossible to calculate even gross properties of the products of the collision using standard QCD since the products of the scattering are strongly interacting. Lund Monte-Carlo describes a partonic system

which eventually hadronizes to the observed particles by string fragmentation, [5]. Lund string model assumes that QCD is linearly confined, therefore quarks are connected with a relativistic string of width at the order of hadronic size. As the quarks which are attached to the string endpoints move apart the string energy increases and it may break. The string fragmentation continuous until ordinary hadrons are formed.

In the context of lattice QCD, the theory is formulated on discretized Euclidean spacetime and its path integral is directly computed using numerical techniques, [6; 7]. Some of the successes of this non-perturbative approach include evidence in favor of confinement, computation of hadron masses which are compared to experimental data. Lattice methods also give a good description of finite temperature phases of the theory in equilibrium. Since, lattice QCD is de facto Euclidean it cannot answer questions related to time dependent processes as scattering or finite temperature dynamical phenomena. On the other hand, low energy effective models answer questions about specific low energy phenomena. For instance, chiral perturbation theory (ChPT) is an effective theory which successfully describes low energy interactions of light hadrons, [8; 9]. This Lagrangian of the model is organized as an expansion in momenta and requiring that it respects the global symmetries of QCD. The Lagrangian of order up to $\mathcal{O}(p^4)$ has twelve free parameters. QCD has an approximate global symmetry called flavor (or chiral) symmetry $U_L(N_f) \times U_R(N_f)$, where N_f is the number of quarks that are taken to be approximately massless and L/R refer to left and right handed quarks. Chiral symmetry is spontaneously broken by the QCD vacuum to the vector subgroup $U_V(N_f)$ and it is responsible for various low energy phenomena of QCD.

This thesis is devoted to the study of low energy phenomena of QCD using the concept of gauge/gravity duality (or holography) coming from the area of string theory. Gauge/gravity duality states that a d-dimensional $SU(N)$ gauge theory in the limit of large N has a dual description in terms of a $(d+1)$-dimensional gravitational theory. The prototype example of this, is AdS/CFT, which was discovered through the study of black holes and D-branes in string theory, [10]. AdS/CFT is the duality between $\mathcal{N} = 4$ super Yang Mills theory and type IIB supergravity in $AdS_5 \times S^5$. As it is explained in section 2.2, QCD is an $SU(N_c)$ gauge theory whose large N_c expansion resembles the perturbative expansion of string theory. This suggests that QCD dynamics can be described by a string theory dual. Until now, several models have been built starting from D-brane constructions (top-down models) which try to model pure Yang-Mills, either in critical string theory set-up [11] or in non-critical [12]. Another approach includes the bottom-up models which are formulated as two-derivative actions in asymptotically AdS spacetimes. The first simplest effort for treating pure

gluon QCD is in [13]. Those phenomenological models use boundary conditions which match QCD in order to describe IR dynamics of the theory. There are also efforts to include flavor degrees of freedom in holographic models, for a review see [14]. The usual approach is to consider a small number of flavors $N_f << N_c$. In top-down models, N_f flavor branes are introduced in the background created by N_c color branes, [15]. Initial efforts to treat meson physics with bottom-up models include the hard and soft wall models, [16]. We are using intuition from the original AdS/CFT in order to construct effective holographic models which are closer to QCD.

This thesis is organized as follows:

- in chapter 2, we present an introduction to AdS/CFT. We firstly analyze the large N_c expansion of $SU(N_c)$ gauge theories, we then review basic string theory and D-branes. We discuss how AdS/CFT correspondence is motivated from the physics of D_3-branes. Then, AdS geometry is analyzed and the prescription for computation of field theory correlation functions is described. Wilson loop is then computed holographically in order to find the static potential of two "quarks" in the field theory. Then, we present the holographic analysis of finite temperature theories and their thermal transitions. Finally, we introduce an effective holographic model for non-supersymmetric 4D Yang Mills theory called Improved Holographic QCD (IHQCD) and a holographic model for the flavor sector of QCD for the limit of $N_f << N_c$, which we call Tachyon AdS/QCD, [17; 18].

- In chapters 3, 4 and 5, our work in the Tachyon AdS/QCD model is presented. For this work the glue part of the gauge theory is modeled holographically by a simple gravitational background (AdS_6 soliton) which is described in chapter 4 (see for references therein). Chapter 3 includes a phenomenological analysis of the model. We focus on the computation of the meson spectrum, and we find the dependence of the meson masses of different meson towers (vectors, axial vectors, pseudoscalars, scalars) on the quark mass and then we fit to experimental data. We use light mesons with isospin one. We also make a fit to heavier "hypothetical states" which are are made of a pair of strange quark-antiquark. In chapter 4, there is a thorough analysis of the model. The flavor vacuum of the model is analyzed and spontaneous breaking of chiral symmetry is shown at zero temperature and its restoration above the deconfinement transition. The holographic renormalization of the action is performed and a detailed analysis of the meson spectrum and decay constants follows. In chapter 5, the transverse part of the vector-axial vector flavor current correlator in the presence of weak

external electric field is studied in the context of the above holographic model. This correlator plays a role in the calculation of two-loop electroweak radiative corrections to the muon anomalous magnetic moment. In the context of simpler AdS/QCD models Son and Yamamoto proposed a relation of this correlator to the difference of the two-point functions of the vector flavor minus axial-vector flavor currents. In our model, this relation is verified in the IR.

- In chapter 6, we study a combination of the IHQCD model with tachyon AdS/QCD, called V-QCD. V-QCD is dual to a 4D $SU(N_c)$ Yang Mills theory with N_f flavors in the Veneziano limit where N_c and N_f are large but with finite ratio, $x = \frac{N_f}{N_c}$, [19]. There are Making reasonable assumptions the model produces a phase diagram which has similar structure as QCD in the Veneziano limit and does not depend on the details of the potentials. Thus it is found that there is a point x_c where a conformal phase transition happens. Below x_c the theory exhibits chiral symmetry breaking and confinement in the IR. Above x_c there is an IR fixed point which is at strong coupling for x close to x_c but it moves at weak coupling as x increases. Above the point $x = 11/2$ the theory is not asymptotically free any more. The region $x_c < x < 11/2$ is called "conformal window" and the theory is chirally symmetric. Upon matching the β-function of the Yang-Mills coupling and the anomalous dimension of $\overline{q}q$ to the QCD result in the UV, x_c is found to be close to 4. In our work, we make a fluctuation analysis of the model, calculate the meson masses, the decay constants and the S-parameter in terms of x. The spectrum of the theory falls into two distinct classes, the singlet-flavor states and the non-singlets. The singlet sector includes scalar mesons, tensor and scalar glueballs. The non-singlet class has vector, axial-vector, scalar and pseudoscalar mesons. It is found that below x_c all spectra are discrete and gaped, except for the pseudoscalar Goldstone bosons. In addition, all spectra fall to zero following Miransky scaling as $x \to x_c$. There is mixing and level crossing of the states of the singlet sector at leading order in $1/N_c$ since we are in the Veneziano limit. No light dilaton state was found in the spectrum signaling the breaking of conformal as argued in [20]. The S-parameter is computed to increase in terms of x and reach a finite constant at $x = x_c$ contrary to previous results [21].

- Finally, in chapter 7, we calculate the Chern-Simons diffusion rate, Γ_{CS}, in the context of IHQCD model. Γ_{CS} is found by the zero-momentum and frequency limit of the retarded two-point function of the CP-odd operator tr $[F \wedge F]$, with F the YM field strength. The Chern-Simons diffusion rate is a crucial ingredient for

the chiral magnetic effect in the quark-gluon plasma (QGP). Γ_{CS} is non-zero for instanton configurations, which are though suppressed in the vacuum. However, Γ_{CS} can become non zero at finite temperature due to thermal fluctuations which excite sphaleron gauge field configurations in the medium. In this way bubbles of net chirality are created in the QGP. Non-central heavy ion collisions create QGP with finite angular momentum and magnetic field. Then, an electric current parallel to the magnetic field is created in the medium due to its net chirality. This is the chiral magnetic effect which is possible to be detected in heavy ion collisions even though until now there is not conclusive. Γ_{CS} cannot be computed with perturbative techniques since the QGP is strongly coupled. Lattice methods also face difficulties in calculating Γ_{CS}, since it is defined as a real-time correlation function. In our work, we calculate Γ_{CS} in IHQCD by considering axion (which is the dual field of $\mathrm{tr}\,[F \wedge F]$) fluctuations in IHQCD black hole backgrounds.

The main results of this work are summarized in the following.

1. *Tachyon AdS/QCD:*

   - Chiral symmetry is broken dynamically at zero temperature and it is restored at the confinement-deconfinement transition.
   - The meson masses depend on the quark mass linearly in the limit of small quark mass.
   - The Gell-Mann-Oakes-Renner relation between the pion and the quark mass is shown to be valid in the model. In case of zero quark mass there are N_f^2 Goldstone bosons in the spectrum. The masses of highly excited states follow linear Regge trajectories.
   - The masses and some decay constants are fitted to the experimental data quite successfully, with error $\epsilon_{rms} = 14.5\%$.
   - The Wess-Zumino action of the system reproduces the correct anomaly.
   - The formula, which was proposed by Son and Yamamoto in [22], relating the vector-axial vector flavor current correlator in weak electric field to the difference of the vector and axial vector two-point functions was found to be valid only for low Euclidean momenta in our model.

2. *V-QCD:*

   - In the conformal window the spectra are continuous. Below the conformal window, $x < x_c$ ($x = N_f/N_c$ and x_c is the conformal transition point), the spectra are discrete, except for the pions.

- All the massive parameters of the theory are obeying Miransky scaling, $sim\Lambda_{\rm UV}\exp(-\frac{\kappa}{\sqrt{x_c-x}})$, in the walking region.
- All singlet and non-singlet mass ratios asymptote to finite constants as $x \to x_c$. Therefore there is no "dilaton" state. Miransky scaling signals the approximate conformal symmetry of the "walking region".
- There is mixing and level crossings of singlet mesons and glueballs at finite x.
- The S-parameter in units of $N_f N_c$ is an increasing function of x and asymptotes to a finite constant as $x \to x_c$.

3. *Chern-Simons Diffusion rate, Γ_{CS}, in IHQCD:*

- Γ_{CS} is shown to be proportional to the dilaton dependent function, $Z(\lambda)$, which multiplies the axion kinetic term in the IHQCD action.
- The value of Γ_{CS} as a function of temperature is bounded from below by it's value at infinite T.
- Γ_{CS} is calculated for various choices of $Z(\lambda)$, which match the lattice results for topological susceptibility and for axial glueball mass ratios. Γ_{CS} is always increasing as the temperature approaches the confinement/deconfinement transition temperature. Γ_{CS} at $T = T_c$ is found to be bounded by the values $1.64 \leq \Gamma_{CS}(T_c)/T_c^4 \leq 2.8$.
- The renormalized spectral function signals the presence of an excitation with energy of order of the lightest axial glueball mass at $T = 0$.

Bibliography

[1] L. Montanet *et al.*[Particle Data Group], *"Review of Particle Properties,"* Phys. Rev. D **50**, 1173 (1994) 1

[2] D. J. Gross and F. Wilczek, *"Ultraviolet Behavior of Nonabelian Gauge Theories,"* Phys. Rev. Lett. **30** (1973) 1343. 1

[3] H. D. Politzer, *"Reliable Perturbative Results for Strong Interactions?,"* Phys. Rev. Lett. **30** (1973) 1346. 1

[4] H. Fritzsch, M. Gell-Mann, Proceedings of the International Conference on Duality and Symmetry, Tel-Aviv, 1971;
H. Fritzsch, M. Gell-Mann, Proc. XVI Intern. Conf. on High energy physics, Chicago, **2** (1972), 135 ;
H. Fritzsch, M. Gell-Mann and H. Leutwyler, *"Advantages of the Color Octet Gluon Picture,"* Phys. Lett. B **47** (1973) 365. 1

[5] H. -U. Bengtsson and T. Sjostrand, *"The Lund Monte Carlo for Hadronic Processes: Pythia Version 4.8,"* Comput. Phys. Commun. **46** (1987) 43. 2

[6] J. M. Drouffe and C. Itzykson, *"Lattice Gauge Fields,"* Phys. Rept. **38** (1978) 133. 2

[7] K. G. Wilson, *"Confinement of Quarks,"* Phys. Rev. D **10** (1974) 2445. 2

[8] J. Gasser and H. Leutwyler, *"Chiral Perturbation Theory to One Loop,"* Annals Phys. **158** (1984) 142. 2

[9] H. Leutwyler, *"On the foundations of chiral perturbation theory,"* Annals Phys. **235** (1994) 165 [ArXiv:hep-ph/9311274]. 2

[10] J. M. Maldacena, *"The large N limit of superconformal field theories and supergravity,"* Adv. Theor. Math. Phys. **2**, 231 (1998) [Int. J. Theor. Phys. **38**, 1113 (1999)] [ArXiv:hep-th/9711200];

S. S. Gubser, I. R. Klebanov and A. M. Polyakov, *"Gauge theory correlators from non-critical string theory,"* Phys. Lett. B **428**, 105 (1998) [ArXiv:hep-th/9802109]; E. Witten, *"Anti-de Sitter space and holography,"* Adv. Theor. Math. Phys. **2**, 253 (1998) [ArXiv:hep-th/9802150]. 2

[11] E. Witten, *"Anti-de Sitter space, thermal phase transition, and confinement in gauge theories,"* Adv. Theor. Math. Phys. **2** (1998) 505 [ArXiv:hep-th/9803131]; J. M. Maldacena and C. Nunez, *"Towards the large N limit of pure N = 1 super Yang Mills,"* Phys. Rev. Lett. **86** (2001) 588 [ArXiv:hep-th/0008001]; A. H. Chamseddine and M. S. Volkov, *"Non-Abelian BPS monopoles in N = 4 gauged supergravity,"* Phys. Rev. Lett. **79** (1997) 3343 [ArXiv:hep-th/9707176]; I. R. Klebanov and M. J. Strassler, *"Supergravity and a confining gauge theory: Duality cascades and χSB-resolution of naked singularities,"* JHEP **0008** (2000) 052 [ArXiv:hep-th/0007191]. 2

[12] S. Kuperstein and J. Sonnenschein, *"Non-critical supergravity (d > 1) and holography,"* JHEP **0407** (2004) 049 [ArXiv:hep-th/0403254]; S. Kuperstein and J. Sonnenschein, *"Non-critical, near extremal AdS_6 background as a holographic laboratory of four dimensional YM theory,"* JHEP **0411** (2004) 026 [ArXiv:hep-th/0411009]; I. R. Klebanov and J. M. Maldacena, *"Superconformal gauge theories and non-critical superstrings,"* Int. J. Mod. Phys. A **19** (2004) 5003 [ArXiv:hep-th/0409133]; F. Bigazzi, R. Casero, A. L. Cotrone, E. Kiritsis and A. Paredes, *"Non-critical holography and four-dimensional CFT's with fundamentals,"* JHEP **0510**, 012 (2005) [ArXiv:hep-th/0505140]; R. Casero, A. Paredes and J. Sonnenschein, *"Fundamental matter, meson spectroscopy and non-critical string / gauge duality,"* JHEP **0601**, 127 (2006) [ArXiv:hep-th/0510110]. 2

[13] J. Polchinski and M. J. Strassler, *"Hard scattering and gauge / string duality,"* Phys. Rev. Lett. **88**, 031601 (2002) [ArXiv:hep-th/0109174]. 2

[14] J. Erdmenger, N. Evans, I. Kirsch and E. Threlfall, Eur. Phys. J. A **35** (2008) 81 [arXiv:0711.4467 [hep-th]]. 3

[15] J. Babington, J. Erdmenger, N. J. Evans, Z. Guralnik and I. Kirsch, *"Chiral symmetry breaking and pions in non-supersymmetric gauge / gravity duals,"* Phys. Rev. D **69**, 066007 (2004). [ArXiv:hep-th/0306018]; N. J. Evans and J. P. Shock, *"Chiral dynamics from AdS space,"* Phys. Rev. D **70**,

046002 (2004) [ArXiv:hep-th/0403279];
M. Kruczenski, D. Mateos, R. C. Myers and D. J. Winters, *"Towards a holographic dual of large-N(c) QCD,"* JHEP **0405**, 041 (2004) [ArXiv:hep-th/0311270];
T. Sakai and S. Sugimoto, *"Low energy hadron physics in holographic QCD,"* Prog. Theor. Phys. **113**, 843 (2005) [ArXiv:hep-th/0412141]. 3

[16] J. Erlich, E. Katz, D. T. Son and M. A. Stephanov, *"QCD and a Holographic Model of Hadrons,"* Phys. Rev. Lett. **95**, 261602 (2005) [ArXiv:hep-ph/0501128];
L. Da Rold and A. Pomarol, *"Chiral symmetry breaking from five dimensional spaces,"* Nucl. Phys. B **721**, 79 (2005) [ArXiv:hep-ph/0501218];
A. Karch, E. Katz, D. T. Son and M. A. Stephanov, *"Linear Confinement and AdS/QCD,"* Phys. Rev. D **74**, 015005 (2006) [ArXiv:hep-ph/0602229]. 3

[17] U. Gursoy and E. Kiritsis, *"Exploring improved holographic theories for QCD: Part I,"* JHEP **0802** (2008) 032 [ArXiv:0707.1324][[hep-th]];
U. Gursoy, E. Kiritsis and F. Nitti, *"Exploring improved holographic theories for QCD: Part II,"* JHEP **0802** (2008) 019 [ArXiv:0707.1349][[hep-th]]. 3

[18] R. Casero, E. Kiritsis and A. Paredes, *"Chiral symmetry breaking as open string tachyon condensation,"* Nucl. Phys. B **787**, 98 (2007) [ArXiv:hep-th/0702155]. 3

[19] M. Järvinen and E. Kiritsis, *"Holographic Models for QCD in the Veneziano Limit,"* JHEP **1203**, 002 (2012) [ArXiv:1112.1261][[hep-ph]]. 4

[20] K. Yamawaki, M. Bando and K. -i. Matumoto, *"Scale Invariant Technicolor Model and a Technidilaton,"* Phys. Rev. Lett. **56** (1986) 1335. 4

[21] F. Sannino, *"Mass Deformed Exact S-parameter in Conformal Theories,"* Phys. Rev. D **82**, 081701 (2010) [ArXiv:1006.0207][[hep-lat]]. 4

[22] D. T. Son and N. Yamamoto, *"Holography and Anomaly Matching for Resonances,"* [ArXiv:1010.0718][[hep-ph]]. 5

2 AdS/CFT

2.1 Introduction

Modern string theory is understood as a theory of quantum gravity, [1; 2; 3; 4; 5; 6; 7; 8; 9; 10]. However, it was historically discovered as an attempt to describe low energy spectrum of bound states formed by the strong interaction, [11]. This effort was inspired by the observation that the spectrum of orbitally excited hadrons obeys a linear relation $M^2 \sim TJ + c$, where M^2 is the mass of the hadron, J is the total angular momentum, T and c are constants. Hence, hadrons lie in linear trajectories on the plot of M^2 in terms of J, which are called linear Regge trajectories. The regime of validity of the linear relation of M^2 and J is for large J and the slope of the linear trajectories of mesons and baryons is universal. A spinning relativistic string of tension T can reproduce such a relation. Therefore, it was attempted to construct a theory of strong interactions using strings as the fundamental degrees of freedom of the model. The appearance of tachyonic and massless modes in the spectrum of the theory in four dimensions and the agreement of QCD with experiment led to the abandonment of string theory.

Quantum Chromodynamics was later formulated and successfully describes strong interactions, [12]. In the limit of high energies the theory is treated perturbatively since it is asymptotically free, i.e. it's coupling decreases at high energy, [13; 14] . On the

other hand, in the low energy limit the theory is non-perturbative and very difficult to calculate with. For large enough coupling quarks are confined in $SU(3)$ singlet states. In the context of gauge theory, mesons can be interpreted as a pair of quark and anti-quark connected by a gauge flux tube. The typical width of the tube is proportional to the QCD energy scale. Hence, the cost of energy increases when we try to separate the two quarks. The dynamics of such a state are resembled by a string with two massive quarks at the end. Closed strings can be matched to glueballs, which are low energy bound states of gluons.

G. 't Hooft proposed to study QCD in the limit of large number of colors. Instead of taking $N_c = 3$ he considered $N_c \to \infty$ and then did an expansion in $1/N_c$, [15]. Such an expansion suggests that the theory is a free string theory at large N_c. The reason is that the large N_c expansion can be matched to the topological expansion of string theory if we replace the string coupling by the $1/N_c$ parameter of the gauge theory. This argument applies to more general adjoint theories and not only to QCD. Using the above arguments it is reasonable to expect that some kind of string theory can be used to reformulate certain gauge theories in some limits.

The most recent proposal is AdS/CFT which arose from the study of black holes and D-brane dynamics in the context of modern string theory, [17]. D-branes are hypersurfaces where open string end, however they are dynamical objects since there is momentum flowing on them by the open string which are attached on them, [18], [19]. In the low energy limit, where the string coupling (g_s) is small, the effective theory of those open strings is a gauge field theory, described by Dirac-Born-Infeld action. Branes can also be introduced as charged solitonic objects under the massless forms which appear in the Ramond-Ramond sector of the spectrum of type II string theories, [20]. Those are called p-branes, where p are the spatial dimensions of the brane. p-branes in ten dimensions are found as solutions of the classical equations of motion of type IIA/B supergravities which are the low energy limit of the corresponding string theories. Stable solutions are in general supersymmetric, meaning that they are invariant under some of the supersymmetry transformations of the action. p-branes are found to be the same as the string theory D-branes. This "open/closed duality" is the predecessor of AdS/CFT.

In particular, we may consider a system of N D_3-branes on top of each other. Then, the supergravity solution has a characteristic scale, L, which determines the curvature of the solution. As it will be shown, it turns out that $\frac{L^4}{\ell_s^4} \sim g_s N$, where ℓ_s is the string length. Then, D_3-branes can be described either as a gauge theory when $g_s N_c << 1$ or as a classical gravitational background when $g_s N_c >> 1 \Rightarrow L >> \ell_s$. In

the second case, the gauge theory description of D_3-branes fails due to strong coupling but the solution of two derivative supergravity action provides a good description of the system. The detailed analysis of this system eventually led to AdS/CFT, and will be analyzed in detail in this chapter. Pedagogical presentations of AdS/CFT can be found in the books [3; 4; 5; 6] and reviews [21; 22; 23].

2.2 Large N_c QCD

The connection of non-abelian gauge theories with string theory becomes more precise in the large N_c limit of the field theory. Some reviews on the subject are in [24] and [25]. We consider an $SU(N_c)$ gauge theory with a fixed number (N_f) of flavor fields in the fundamental representation. Hence, the theory includes $N_c^2 - 1$ independent gauge fields $A^i_{\mu\, j}$ and fermion fields ψ^i_a, where $i = 1, \ldots, N_c$ and $a = 1, \ldots, N_f$, with Lagrangian

$$\mathcal{L} = -\frac{1}{4g_{YM}^2}\mathbb{T}rF_{\mu\nu}F^{\mu\nu} + \sum_{a=1}^{N_f}\overline{\psi}_a\left(i\not{D} - m_a\right)\psi_a\,. \tag{2.2.1}$$

The theory possesses a dimensionless coupling constant, g_{YM}, which is transmuted to the dimensionfull energy scale, Λ_{QCD}. Thus, it is interesting to study the limit $N_c \to \infty$ with fixed N_f. In order to understand how g_{YM} scales with N_c so as Λ_{QCD} to remain finite as $N_c \to \infty$ we should look at the one loop β-function of the theory

$$\mu\frac{dg_{YM}}{d\mu} = -N_c\left(\frac{11}{3} - \frac{2}{3}\frac{N_f}{N_c}\right)\frac{g_{YM}^3}{(4\pi)^2}\,. \tag{2.2.2}$$

By redefining 't Hooft coupling, $\lambda = g_{YM}^2 N_c$, the leading term of it's β-function is independent of N_c, $\mu\frac{d\lambda}{d\mu} = -\left(\frac{22}{3} - \frac{4}{3}\frac{N_f}{N_c}\right)\frac{\lambda^4}{(4\pi)^2}$. The second term is suppressed as $N_c \to \infty$. Thus, the appropriate limit is to take N_c large, while 't Hooft coupling is fixed. Then flavor degrees of freedom have subleading effects with respect to the color ones. Another interesting limit which we will consider in this thesis is the Veneziano limit where N_f is also taken to infinity but the ratio $\frac{N_f}{N_c}$ is kept fixed. Then, the flavor degrees of freedom play an equally important role as the color and both terms of the β-function, 2.2.2, are of the same order.

We will study the structure of large N_c perturbation theory, in a general theory with matrix fields, X_M, in the adjoint representation of $SU(N_c)$, where M includes all

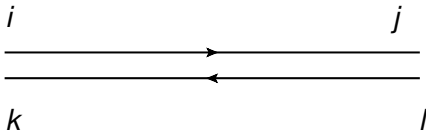

Figure 2.1: The gluon propagator in double line notation.

the possible Lorentz, flavor, etc indices. The gauge invariant Lagrangian is of the form

$$\mathcal{L} = \mathbb{T}r\left[dX_M dX_N + g_{YM} f_1^{MNL} X_M X_N X_L + g_{YM}^2 f_2^{MNLK} X_M X_N X_L X_K + \ldots\right] . \tag{2.2.3}$$

By rescaling the fields $\tilde{X}_M = g_{YM} X_N$ it becomes

$$\mathcal{L} = \frac{N_c}{\lambda}\mathbb{T}r\left[d\tilde{X}_M d\tilde{X}_N + f_1^{MNL}\tilde{X}_M\tilde{X}_N\tilde{X}_L + f_2^{MNLK}\tilde{X}_M\tilde{X}_N\tilde{X}_L\tilde{X}_K + \ldots\right] , \tag{2.2.4}$$

where λ is t' Hooft coupling. As $N_c \to \infty$, the overall coupling goes to zero and this is a semi-classical limit.

Any field in the adjoint can be written as $X^i_{M\,j}$, where i and j are indices of the fundamental and anti-fundamental representations, respectively. In this notation the propagator of X_M is

$$\left\langle X^i_{M\,k}(x) X^l_{N\,j}(y)\right\rangle = \frac{1}{2}\left(\delta^i_j\delta^l_k - \frac{1}{N_c}\delta^i_k\delta^l_j\right)\Delta_{MN}(x-y) , \tag{2.2.5}$$

where $\Delta_{MN}(x-y)$ is the propagator of a single gauge field. The mixing term comes from the fact that the gluon is traceless but it will not play any role since it is subleading in N_c. Hence, Feynman diagrams of the Lagrangian (2.2.4) can be analyzed using the double line notation, where each adjoint field propagates on two parallel lines of opposite orientations. In terms of index structure, each line represents the propagator of a quark/antiquark field.

To show how the large N_c perturbation series is organized, we begin by studying vacuum diagrams, where each line makes a closed oriented loop. In each diagram every propagator is proportional to $\frac{\lambda}{N_c}$, every vertex to $\frac{N_c}{\lambda}$ and each loop a N_c because of the trace in gauge indices. Then, a diagram of E propagators, V vertices and F loops scales as

$$\left(\frac{\lambda}{N_c}\right)^E \left(\frac{N_c}{\lambda}\right)^V N_c^F = N^\chi \lambda^{E-V} , \tag{2.2.6}$$

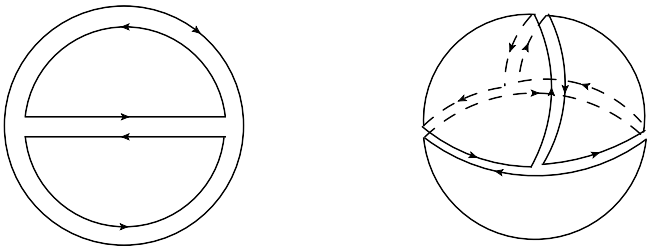

Figure 2.2: A planar diagram of order λN_c^2 and it's associated Riemann surface which has the topology of a sphere.

where $\chi = V - E + F$. A closed double line diagram can be matched to a simplicial decomposition of an oriented Riemann surface. Each propagator corresponds to an edge of the surface, a closed loop to a face and a vertex to a simplicial vertex. The number χ is then the Euler number of the closed surface which is topological invariant of surfaces and is also given by $\chi = 2-2h-b$, where h is the number of handles (genus) and b is the number of boundaries of the surface. For a closed surface $b = 0$. Graphs of adjoint fields consist only of double lines so they do not have boundaries. Therefore, the large N_c expansion of any vacuum diagram of (2.2.4) is

$$\mathcal{D} = \sum_{h=0}^{\infty} N_c^{\chi} \sum_{n=0}^{\infty} c_{g,n} \lambda^n \,. \tag{2.2.7}$$

It is observed that for large N_c the series is led by diagrams of order N_c^2 which correspond to a closed surface with $h = 0$. Such a surface is topologically equivalent to a sphere, see Fig. (2.2). Those are planar diagrams and can be drawn on a plane without any crossing of lines. The next terms are non-planar graphs corresponding to surfaces with handles. For example, the second term in the series has $h = 1$ represents a surface with the topology of a torus.

The expansion (2.2.7) is the same as the perturbative expansion of closed string theory if $\frac{1}{N_c}$ is identified with the string coupling. Such a correspondence would imply that the large N_c limit of a gauge theory is matched to weakly-coupled closed string theory.

In the case of a theory with N_f fields in the fundamental representation, the Feynman diagrams would have single lines as well. Remember that each single line corresponds to a fundamental or anti-fundamental index. The existence of single lines in the diagrams leads to less N_c factors because in a closed loop of a double line there is a trace over the gauge indices which is proportional to N_c but a closed line of a quark

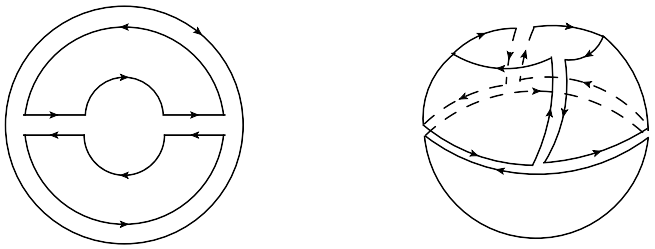

Figure 2.3: A planar graph with a quark loop. The diagram is of order $\lambda N_f N_c$ and it's associated Riemann surface has a boundary.

has no such factor. The flavor index of the fundamental field is though summed and give an additional contribution analogous to N_f. Hence, quark loops are suppressed by powers of $\frac{N_f}{N_c}$. The corresponding surfaces of graphs with single lines are surfaces with boundaries, i.e. $b \neq 0$, see Fig. (2.3). Then Eq. (2.2.7) is associated to the perturbative expansion of a theory with both open and closed strings. This kind of expansion contains boundaries which are created by the open strings.

Eq. (2.2.7) was shown only for vacuum diagrams but it actually holds for any correlation function of single trace gauge invariant operators, $\mathcal{O}_i$. To calculate the connected correlation function $\langle \prod_{I=1}^{n} \mathcal{O}_I \rangle$ we deform the action as $S \to S + N_c \sum_I J_I \mathcal{O}_\jmath$ and differentiate the generating functional of connected vacuum diagrams

$$\left\langle \prod_{I=1}^{n} \mathcal{O}_I \right\rangle = \frac{1}{(iN_c)^n} \left. \frac{\partial^n W[J]}{\partial J_1 \dots \partial J_n} \right|_{J_I=0} . \tag{2.2.8}$$

The scaling of the above correlator in terms of N_c is the same as for the vacuum diagrams but now there are also insertions of operators which correspond to vertices that come with $1/N_c$ factors. Thus, for operators made of adjoint fields the leading diagram of the above correlation function scales as $\sim N_c^{2-n}$. If we consider the operators $\mathcal{B}_I$, containing fundamental fields then the leading contribution is $\sim N_c^{1-n}$. If we normalize them such as their two point function is N_c independent ($\mathcal{B}'_I = \sqrt{N_c} B_I$), then their n-point function scales as $\sim N_c^{1-\frac{n}{2}}$. Concluding, we point out that at $N_c \to \infty$ limit interactions vertices scale as inverse powers of N_c, so there is an infinite tower of stable single-particle states in the spectrum of the theory.

2.3 String theory

As it was mentioned above, AdS/CFT was formulated in the context of string theory and in particular in the study of D-brane dynamics. In this section, we will present a quick introduction to string theory. Firstly, we analyze the bosonic string, then move to the superstring and finally introduce D-branes as extended solitonic gravitational objects but also as dynamical objects in perturbative string theory.

2.3.1 The bosonic string

A bosonic string in D dimensional spacetime with metric $G_{MN}(X)$ is described by the Polyakov action

$$S = -\frac{1}{2}T\int_{-\infty}^{+\infty} d\tau \int_0^{\pi} d\sigma\sqrt{-h}h^{\mu\nu}(\partial_\mu X^M \partial_\nu X^N)G_{MN}(X)\,, \tag{2.3.1}$$

where $X^M, M = 0, \dots D-1$ are the string coordinates, $h^{\mu\nu}, \mu, \nu = 0, 1$ is the worldsheet metric and T is the string tension which can be expressed in terms of the string length, ℓ_s,

$$T = \frac{1}{2\pi\alpha'} = \frac{1}{\pi\ell_s^2}\,. \tag{2.3.2}$$

The parameters $\sigma \in [0, \pi]$ and τ parametrize the string worldsheet. The above action has two gauge symmetries

- Diffeomorhism symmetry, $\delta X^M = \xi^\mu \partial_\mu X^M$ and $\delta h_{\mu\nu} = \partial_\mu \xi^\rho h_{\rho\nu} + \partial_\nu \xi^\rho h_{\rho\mu} + \xi^{rho}\partial_\rho h_{\mu\nu} = \nabla_\mu \xi_\nu + \nabla_\nu \xi_\mu$
- Weyl Symmetry, $\delta X^M = 0$, $\delta h_{\mu\nu} = \lambda(x) h_{\mu\nu}$.

We will study the bosonic string in flat background metric $G_{MN}(X) = \eta_{MN}$ and fix the above gauge semmetries by choosing the conformal gauge, $h_{\mu\nu} = \eta_{\mu\nu}$.

The variation of the action is

$$\delta S = T\int d^2x \delta X \cdot \Box X + T\int_0^{\pi} d\sigma \dot{X}\cdot\delta X\Big|_{\tau_i}^{\tau_f} - T\int_{\tau_1}^{\tau_f} d\tau X'\cdot\delta X\Big|_0^{\pi}. \tag{2.3.3}$$

The second term is zero since $\delta X^M(\tau_i = -\infty) = \delta X^M(\tau_f = \infty) = 0$. The third term will vanish due to the boundary conditions (b.c.) which will be imposed in the following. The equations of motion of string coordinates then are

$$\Box X^M = (\partial_\sigma^2 - \partial_\tau^2) X^M(\sigma, \tau) = 0\,. \tag{2.3.4}$$

The most general solution of the above equation is

$$X^M(\sigma, \tau) = \frac{1}{2} X_L^M(\tau + \sigma) + \frac{1}{2} X_R^M(\tau - \sigma)\,, \tag{2.3.5}$$

where

$$X_L^M(\tau + \sigma) = x^M + 2\alpha' p_0^M(\tau + \sigma) + i\sqrt{2\alpha'} \sum_{n \neq 0} \frac{1}{n} \alpha_n^M e^{-i2n(\tau+\sigma)}\,, \tag{2.3.6}$$

$$X_R^M(\tau - \sigma) = \tilde{x}^M + 2\alpha' \tilde{p}_0^M(\tau - \sigma) + i\sqrt{2\alpha'} \sum_{n \neq 0} \frac{1}{n} \tilde{\alpha}_n^M e^{-i2n(\tau-\sigma)}\,. \tag{2.3.7}$$

For the study of *closed* strings we have to impose periodic b.c. in σ coordinate

$$X^M(\sigma, \tau) = X^M(\sigma + \pi, \tau) \quad , \quad \partial_\sigma X^M(\sigma, \tau) = \partial_\sigma X^M(\sigma + \pi, \tau)\,, \tag{2.3.8}$$

we also consider $x^M = \tilde{x}^M$, $p_0^M = \tilde{p}_0^M \equiv p^M$, and the solution becomes

$$X_L^M(\tau + \sigma) = x^M + 2\alpha' p^M(\tau + \sigma) + i\sqrt{2\alpha'} \sum_{n \neq 0} \frac{1}{n} \alpha_n^M e^{-i2n(\tau+\sigma)}\,, \tag{2.3.9}$$

$$X_R^M(\tau - \sigma) = x^M + 2\alpha' p^M(\tau - \sigma) + i\sqrt{2\alpha'} \sum_{n \neq 0} \frac{1}{n} \tilde{\alpha}_n^M e^{-i2n(\tau-\sigma)}\,, \tag{2.3.10}$$

where p^M is the momentum of the center of mass of the string as it will be seen in Eq.(2.3.19). The possible boundary conditions (b.c.) for the *open* string which cancel the second term of Eq.(2.3.3)are

$$\begin{gathered} \text{Neumann boundary condition:} \quad \partial_\sigma X^M \Big|_{\sigma=0}^{\sigma=\pi} = 0\,, \\ \text{Dirichlet boundary condition:} \quad \delta X^M \Big|_{\sigma=0}^{\sigma=\pi} = 0\,. \end{gathered} \tag{2.3.11}$$

In case of Neumann b.c., we have $x^M = \tilde{x}^M$, $p_0^M = \tilde{p}_0^M \equiv p^M$, $a_n^M = \tilde{a}_n^M$ and the factor of two in the exponential is absent

$$X^M(\sigma, \tau) = x^M + 2\alpha' p^M \tau + i\sqrt{2\alpha'} \sum_{n \neq 0} \frac{a_n^M}{n} e^{-in\tau} cos(n\sigma)\,. \tag{2.3.12}$$

The case of Dirichlet b.c. will be studied later.

Even if, the worldsheet metric is fixed, it's equations of motion should be satisfied. The equations of motion of the metric are known to give the energy momentum tensor

$$T_{\mu\nu} = -\frac{4\pi\alpha'}{\sqrt{-h}}\frac{\delta S}{\delta h^{\mu\nu}} = \partial_\mu X \cdot \partial_\nu X - \frac{1}{2}\eta_{\mu\nu}\eta^{\rho\sigma}\partial_\rho X \cdot \partial_\sigma X = 0\,. \tag{2.3.13}$$

These provide constraints to the string coordinates that eliminate the ghosts which would have been created by the X^0 field. The constraints may be written explicitly as

$$T_{01} = \dot{X} \cdot X' = 0 \quad , \quad T_{00} = T_{11} = \frac{1}{2}(\dot{X}^2 + X'^2) = 0\,. \tag{2.3.14}$$

The above constraints can also be written in terms of worldsheet lightcone coordinates, $x^{\pm} = t \pm \sigma$, as

$$T_{++} = (\partial_+ X)^2 = 0 \quad , \quad T_{--} = (\partial_- X)^2 = 0\,, \tag{2.3.15}$$

and they may be expanded in Fourier modes of *closed* string

$$\begin{aligned} T_{--} &= \frac{\alpha'}{2}\sum_{n,m=-\infty}^{\infty} \alpha_{m-n}\cdot\alpha_n e^{-imx^-} = \alpha'\sum_{n=-\infty}^{\infty} L_m e^{-imx^-}\,, \\ T_{++} &= \frac{\alpha'}{2}\sum_{n,m=-\infty}^{\infty} \tilde{\alpha}_{m-n}\cdot\tilde{\alpha}_n e^{-imx^+} = \alpha'\sum_{n=-\infty}^{\infty} \tilde{L}_m e^{-imx^+}\,, \end{aligned} \tag{2.3.16}$$

where we have defined $\alpha_0^M = \tilde{\alpha}_0^M = \sqrt{\frac{\alpha'}{2}}p^M$. We have also set

$$L_m = \frac{1}{2}\sum_{n,m=-\infty}^{\infty} \alpha_{m-n}\cdot\alpha_n \quad , \quad \tilde{L}_m = \frac{1}{2}\sum_{n,m=-\infty}^{\infty} \tilde{\alpha}_{m-n}\cdot\tilde{\alpha}_n\,, \tag{2.3.17}$$

which are the Virasoro generators. The constraints (2.3.15) on the energy momentum tensor lead to

$$L_n = \tilde{L}_n = 0 \quad , \quad n = 0, 1, \ldots \tag{2.3.18}$$

Those are interpreted as constraint equations. The $n = 0$ part of the above equation constrains the mass spectrum as it will be shown in the following. Polyakov action also enjoys Poincare symmetry of the background which is interpreted as a global symmetry in the worldsheet. The charges of this symmetry are the momentum and the angular momentum

$$P^M = T\int_0^\pi \dot{X}^M d\sigma = p^M \quad , \quad J^{MN} = T\int_0^\pi (\dot{X}^M X^N - \dot{X}^N X^M)\,, \tag{2.3.19}$$

The Hamiltonian is then found to be

$$H = \int_0^\pi T_{00} d\sigma = T \int_0^\pi (\dot{X}^2 + X'^2) d\sigma \,, \tag{2.3.20}$$

which is set to zero due to Eq.(2.3.14). For the closed string it takes the form

$$H_{cl} = \sum_{n=-\infty}^{\infty} (\tilde{\alpha}_{-n} \cdot \tilde{\alpha}_n + \alpha_{-n} \cdot \alpha_n) = \alpha' p^2 + 2N + 2\tilde{N} \,, \tag{2.3.21}$$

where $N = \sum_{n=1}^{\infty} \alpha_{-n} \cdot \alpha_n$ and $\tilde{N} = \sum_{n=1}^{\infty} \tilde{\alpha}_{-n} \cdot \tilde{\alpha}_n$. We may follow the same procedure for the open string and similarly find that

$$H_{op} = \frac{1}{2} \sum_{n=-\infty}^{\infty} \alpha_{-n} \alpha_n = \alpha' p^2 + N \,. \tag{2.3.22}$$

Upon quantization of the theory, the $H = 0$ constraint is used to find the mass spectrum. It is noticed that $H_{cl} = 2(L_0 + \tilde{L}_0)$ and $H_{op} = L_0$, where L_0 for the open string has the same form as for the closed.

2.3.1.1 Lightcone quantization

The gauge fixed action of the bosonic string has a remaining symmetry

$$\delta X^M = \xi^\mu \partial_\mu X^M \quad , \quad \xi^+ = \xi^+(x^+) \quad , \quad \xi^- = \xi^-(x^-) \,. \tag{2.3.23}$$

The above transformation leaves the lightcone invariant, it therefore is a conformal symmetry. We may use the above transformation to go to a coordinate frame $(\tilde{\tau}, \tilde{\sigma})$ where the coordiantate $\tilde{X}^+(\tilde{\sigma}, \tilde{\tau})$ has the following form

$$\tilde{X}^+(\tilde{\sigma}, \tilde{\tau}) = \tilde{x}_0^+ + \alpha' p^+ \tilde{\tau} \,. \tag{2.3.24}$$

Taking into account that the string coordinates transform like scalars under diffeomorphism and Weyl transformations on the worldsheet, i.e. $X^+(\sigma, \tau) = \tilde{X}^+(\tilde{\sigma}, \tilde{\tau})$, we find $\tilde{\tau} = \tilde{p}^+ \alpha'(X^+ - \tilde{x}_0^+)$, where we have also used the lightcone coordinates of the string, defined as $X^\pm = X^0 \pm X^{D-1}$. Using the constraints (2.3.15), we may express X^- in terms of the transverse string coordinates

$$2\partial_+ X^- \partial_+ X^+ = \sum_{I=1}^{D-2} \partial_+ X^I \partial_+ X^I \quad , \quad 2\partial_- X^- \partial_- X^+ = \sum_{I=1}^{D-2} \partial_- X^I \partial_- X^I \,. \tag{2.3.25}$$

These imply for the oscillators that

$$a_n^- = \frac{1}{p^+\sqrt{2\alpha'}} \sum_{m=-\infty}^{\infty} a_{n-m}^I a_m^I = \frac{1}{p^+\sqrt{2\alpha'}} \sum_{m=-\infty}^{\infty} \tilde{a}_{n-m}^I \tilde{a}_m^I \,. \tag{2.3.26}$$

Hence, $X^\pm$ fields are fixed in the lightcone gauge and only the X^I, $I = 1, \ldots, D-2$ are propagating fields. The action in the lightcone gauge reads

$$S = -\frac{1}{2} T \int_{-\infty}^{+\infty} dt \int_0^\pi d\sigma \; \eta^{\mu\nu} (\partial_\mu X^I \partial_\nu X^I) \quad , \quad I = 1, \ldots, D-2 \tag{2.3.27}$$

where summation over I is implied. To quantize the theory, we impose the canonical commutation relations

$$[x^I, p^J] = i\delta^{IJ} \quad , \quad [x^-, p^+] = -i \quad , \quad [\alpha_n^I, \alpha_m^J] = [\tilde{\alpha}_n^I, \tilde{\alpha}_m^J] = m\delta^{IJ}\delta_{m+n,0}$$

Since $\alpha_0^- = \sqrt{\frac{\alpha'}{2}} p^-$, Eq.(2.3.26) for $n = 0$ gives

$$2p^+p^- = p^I p^I + \sum_{n=1}^{\infty} \alpha_{-n}^I \alpha_n^I = p^I p^I + \sum_{n=1}^{\infty} \tilde{\alpha}_{-n}^I \tilde{\alpha}_n^I \tag{2.3.28}$$

Hence the mass shell condition $M^2 = -p^2$ can be written in terms of the creation and annihilation operators

$$M^2 = 2p^+p^- - p^I p^I = \frac{4}{\alpha'}(N - a_{cl}) = \frac{4}{\alpha'}(\tilde{N} - \tilde{a}_{cl}) \tag{2.3.29}$$

where $N = \sum_{n=1}^{\infty} \alpha_{-n}^I \alpha_n^I$ and $\tilde{N} = \sum_{n=1}^{\infty} \tilde{\alpha}_{-n}^I \tilde{\alpha}_n^I$, the summation over I runs from 1 to $D-2$. Since, p^- is not an independent degree of freedom we must impose the above constraints on the states, which coincide with the mass shell condition. The two constants a_{cl} and $\tilde{a}_{cl}$ parametrize the ordering ambiguity of the sums of creation and annihilation operators that appears for $n = 0$. These constants will be determined by physical arguments on the spectrum. By a similar procedure, the open string mass shell condition is found

$$M^2 = 2p^+p^- - p^I p^I = \frac{1}{\alpha'} \sum_{n=1}^{\infty} \alpha_{-n}^I \alpha_n^I = \frac{1}{\alpha'}(N - a_{op}) \,, \tag{2.3.30}$$

where a_{op} also appears due to the ordering ambiguity of the creation and annihilation operators. N is given by the same formula as in the closed string case.

The vacuum is defined by

$$\hat{p}^+ |0, p^+, p^I\rangle = p^+ |0, p^+, p^I\rangle \quad , \quad \hat{p}^I |0, p^+, p^I\rangle = p^I |0, p^+, p^I\rangle \quad , \tag{2.3.31}$$

$$\alpha_n^I|0,p^+,p^I\rangle = \tilde{\alpha}_n^I|0,p^+,p^I\rangle = 0\,. \tag{2.3.32}$$

The states which are produced by the creation operators are eigenstates of the $\hat{p}^-$ operator with eigenvalue

$$p^- = \frac{1}{2\alpha' p^+}\left(8(N-a_{cl}) + 2\alpha' p^I p^I\right) = \frac{1}{2\alpha' p^+}\left(8(\tilde{N}-\tilde{a}_{cl}) + 2\alpha' p^I p^I\right)\,, \tag{2.3.33}$$

for the closed string and

$$p^- = \frac{1}{2\alpha' p^+}\left(2(N-a_{op}) + 2\alpha' p^I p^I\right)\,, \tag{2.3.34}$$

for the open string. Hence, now the constraints are not written as operator equations but as eigenvalue equations. Then, if we assume $a_{cl} = \tilde{a}_{cl}$ for the closed string, Eq.[2.3.29] leads to

$$N = \tilde{N} \quad , \quad \alpha' M^2 = 4N - 4\alpha_{cl}\,. \tag{2.3.35}$$

The vacuum state of the closed string is $|0,p^+,p^I\rangle$ and its mass is $\alpha' M^2 = -4a_{cl}$. This state is a negative mass state, i.e. it's a tachyon. The next excitation includes

$$\alpha_{-1}^{((I}\alpha_{-1}^{J))}|0,p^+,p^I\rangle \quad , \quad \alpha_{-1}^{[I}\alpha_{-1}^{J]}|0,p^+,p^I\rangle \quad , \quad \sum_{I=1}^{D-2}\alpha_{-1}^I\alpha_{-1}^I|0,p^+,p^I\rangle\,, \tag{2.3.36}$$

with mass $\alpha' M^2 = 4(1-a_{cl})$. These states form a symmetric traceless representation, an antisymmetric and a scalar representation of $SO(D-2)$, which is the little group of $SO(1,D-1)$ for massless states. Hence, the above states are ineterpreted as a spin 2 massless field (graviton) with $\frac{1}{2}(D-2)(D-1)-1$ degrees of freedom, a massless antisymmetric tensor field (gauge field) with $\frac{1}{2}(D-2)(D-3)$ states, and a scalar field, called dilaton. Since, the above excitations are massless states, the mass formula gives

$$a_{cl} = \tilde{a}_{cl} = 1 \tag{2.3.37}$$

The open string mass formula is given by (2.3.30). The vacuum is $|0,p^+,p^I\rangle$ and its mass is $\alpha' M^2 = -a_{op}$, which corresponds to a tachyonic state. The first excitation is $\alpha_{-1}^I|0,p^+,p^I\rangle$ with $D-2$ degrees of freedom. Therefore, this is a vector representation of the $SO(D-2)$ little group. Hence, it must be a massless vector state. The mass formula (2.3.30) accordingly gives

$$\alpha' M^2 = 1 - a_{op} = 0 \quad , \quad \alpha_{op} = 1\,. \tag{2.3.38}$$

Choosing the lightcone gauge to quantize the theory leads to explicit breaking of the Lorentz invariance of the background, which is a global symmetry from the worldsheet point of view. This may lead to anomalies in the quantum level of the theory. The requirement of nonanomalous Lorentz symmetry leads to a $D = 26$ dimensional spacetime for the bosonic string.

2.3.2 The superstring

Type IIA/B theories are the two consistent ten dimensional closed string theories with maximal supersymmetry. These two theories have $\mathcal{N} = 2$ supersymmetry in ten dimensions, hence there are 32 supercharges. D-branes are contained in the type II superstring theories.

We study the superstring using the Neveu-Schwarz and Ramond formulation. We thus introduce a fermion field on the worldsheet

$$\Psi^{\alpha M} = \begin{pmatrix} \psi_-^M \\ \psi_+^M \end{pmatrix} \quad , \quad M = 0, ..., D-1 \quad , \quad \alpha = 1, 2 \tag{2.3.39}$$

which is 2-component real spinor on the worldsheet (α: spinor index), and spacetime vectors M: spacetime vector index. Its components, ψ_-^M and ψ_+^M, are left and right handed spinors, respectively.

The superstring action is constructed by coupling the scalar fields (X^M) and the fermions to 2 dimensional supergravity. The resulting action is

$$\begin{aligned} S = T \int d^2x\, e \Big[& -\frac{1}{2} h^{\mu\nu} \partial_\mu X^M \partial_\nu X^N - \frac{1}{2} \overline{\Psi}^M \gamma^\mu \partial_\mu \Psi^N + \frac{1}{2} F^M F^N \\ & + (\overline{\chi}_\mu \gamma^\nu \gamma^\mu \Psi^M)(\partial_\nu X^N) + \frac{1}{4} (\overline{\Psi}^M \Psi^N)(\overline{\chi_\mu} \gamma^\nu \gamma^\mu \chi_\nu) \Big] \eta_{MN} \end{aligned} \tag{2.3.40}$$

where χ_μ^α is a gravitino field (μ : worldsheet index) and F^M are auxiliary fields. The above action enjoys the following local symmetries

1. Einstein symmetry
2. Local Lorentz symmetry
3. Weyl symmetry
4. Superconformal symmetry
5. Supergravity (local supersymmetry)

To find the spectrum of the superstring we must fix its gauge symmetries. The gauge symmetries are fixed by choosing a flat worldsheet metric. In the bosonic case the equations of motion of e^a_μ, i.e. $T_{\mu\nu} = 0$, provide the constraints that guarantee the absense of longitudinal and timelike degrees of freedom in the string spectrum. The satisfaction of the equations of motion of the gravitino field ensures the same for the field Ψ^M of the superstring. Hence the constraints for the superstring are

$$T_{++} = \partial_+ X \partial_+ X + \frac{i}{2}\psi_+ \partial_+ \psi_+ \quad , \quad T_{--} = \partial_- X \partial_- X + \frac{i}{2}\psi_+ \partial_- \psi_- \,, \tag{2.3.41}$$

where both indices of the energy momentum tensor are obviously vector indices. The gravitino equation of motion gives the supercurrent

$$J^{\mu,\alpha} \equiv \frac{1}{4T}\frac{\delta S}{\delta \bar{\chi}_{\mu,\alpha}} = 0 \,, \tag{2.3.42}$$

where α is a two dimensional spinor index. Eq.(2.3.42) in components reads

$$J_{++} = \psi_+ \partial_+ X = 0 \quad , \quad J^{-,-} = \psi_- \partial_- X = 0 \,, \tag{2.3.43}$$

where one index in J is vector and the other spinor.The constraints $T_{\mu\nu} = 0$ and $J^{\mu,\alpha} = 0$ are also generators of residual symmetries of the flat worldsheet space which depend either on $t + \sigma$ or $t - \sigma$. These symmetries are fixed by transforming the coordinates to go to the lightcone gauge

$$X^+ = x^+ + l^2 p^+ t \quad , \quad \Psi^+ = \Psi^0 + \Psi^{D-1} = 0 \,. \tag{2.3.44}$$

The action in the lightcone gauge becomes

$$S = T \int d^2x \left[-\frac{1}{2}\eta^{\mu\nu}\partial_\mu X^I \partial_\nu X^I - \frac{1}{2}\overline{\psi}^I \gamma^\mu \partial_\mu \psi^I \,. \right] \tag{2.3.45}$$

where $I = 1, \ldots, D-2$. The field equations for the fermions are

$$(\partial_\tau - \partial_\sigma)\psi^I_+ = (\partial_\tau + \partial_\sigma)\psi^I_- = 0 \,. \tag{2.3.46}$$

Hence, right handed fermions are left-moving and left handed fermions are right-moving. The boundary conditions for *closed* string fermions may be either periodic, which correspond to the Ramond sector of the closed string, or antiperiodic which lead to the Neveu-Schwarz sector. The mode expansions of the femions for the *closed* string

are

$$\text{Ramond case}\,, \qquad \psi_+^I(\sigma,\tau) = \sum_{n\in\mathbb{Z}} d_n^I e^{-2in(\tau+\sigma)} \quad , \quad \psi_-^I(\sigma,\tau) = \sum_{n\in\mathbb{Z}} \tilde{d}_n^I e^{-2in(\tau-\sigma)}\,,$$
$$\text{Neveu Schwarz case}\,, \qquad \psi_+^I(\sigma,\tau) = \sum_{r\in\mathbb{Z}+\frac{1}{2}} b_r^I e^{-2ir(\tau+\sigma)} \quad , \quad \psi_-^I(\sigma,\tau)au = \sum_{r\in\mathbb{Z}+\frac{1}{2}} \tilde{b}_r^I e^{-2ir(\tau-\sigma)}\,.$$

The canonical commutation relationships for the oscillator modes are

$$\{d_m^I, d_n^J\} = \{\tilde{d}_m^I, \tilde{d}_n^J\} = \delta_{m+n}\delta^{IJ}\,,$$
$$\{b_r^I, b_s^J\} = \{\tilde{b}_r^I, \tilde{b}_s^J\} = \delta_{r+s}\delta^{IJ}\,.$$

The boundary conditions which *open* strings obey are

$$\psi_+^I(\sigma=0,\tau) = \psi_-^I(\sigma=0,\tau)\,,$$
$$\text{Ramond case}\,, \qquad \psi_+^I(\sigma=\pi,\tau) = \psi_-^I(\sigma=\pi,\tau)\,,$$
$$\text{Neveu Schwarz case}\,, \qquad \psi_+^I(\sigma=\pi,\tau) = -\psi_-^I(\sigma=\pi,\tau)\,.$$

These boundary conditions are the same for all I in order to preserve Lorentz invariance of spacetime. In case of open string the mode expansions of the femions become

$$\text{Ramond case}\,, \qquad \psi_+^I(\sigma,\tau) = \frac{1}{\sqrt{2}}\sum_{n\in\mathbb{Z}} d_n^I e^{-in(\tau+\sigma)} \quad , \quad \psi_-^I(\sigma,\tau) = \frac{1}{\sqrt{2}}\sum_{n\in\mathbb{Z}} d_n^I e^{-in(\tau-\sigma)}\,,$$
$$\text{Neveu Schwarz case}\,, \qquad \psi_+^I(\sigma,\tau) = \frac{1}{\sqrt{2}}\sum_{r\in\mathbb{Z}+\frac{1}{2}} b_r^I e^{-ir(\tau+\sigma)} \quad , \quad \psi_R^I(\sigma,\tau) = \frac{1}{\sqrt{2}}\sum_{r\in\mathbb{Z}+\frac{1}{2}} b_r^I e^{-2ir(\tau-\sigma)}\,.$$

The modes satisfy the following commutation relationships

$$\{d_m^I, d_n^J\} = \delta_{m+n}\delta^{IJ}\,,$$
$$\{b_r^I, b_s^J\} = \delta_{r+s}\delta^{IJ}\,.$$

The constraint equations can now be written in terms of the open string oscillator modes. In Ramond sector, the Fourier modes of the energy momentum tensor of open strings are

$$L_m = \frac{1}{2}\sum_{n=-\infty}^{\infty}\left(\alpha_{m-n}\cdot\alpha_n + (n+\frac{m}{2})d_{m-n}\cdot d_n\right) \tag{2.3.47}$$

and the Fourier modes of the supercurrent read

$$F_m = \sum_{n=-\infty}^{\infty} d_{m-n} \cdot a_n \tag{2.3.48}$$

In the Neveu-Schwarz sector, the energy momentum tensor modes are

$$L_m = \frac{1}{2} \sum_{n=-\infty}^{\infty} \left(\alpha_{m-n} \cdot \alpha_n + (n + \frac{m}{2}) b_{m-n} \cdot b_n \right) \tag{2.3.49}$$

and the supercurrent modes are written as

$$G_r = \sum_{n=-\infty}^{\infty} b_{r-n} a_n \,. \tag{2.3.50}$$

The fermion number operator is given by

$$\begin{aligned} \text{Ramond}\,,\; N &= \sum_{I=1,8} \sum_{n \in \mathbb{Z}} n d^I_{-n} d^I_n \,, \\ \text{Neveu-Schwarz}\,,\; N &= \sum_{I=1,8} \sum_{r \in \mathbb{Z}+\frac{1}{2}} r b^I_{-r} b^I_r \end{aligned} \tag{2.3.51}$$

for the Ramond and the Neveu-Schwarz case respectively. The mass of a state is then found by

$$\alpha' M^2 = -\alpha' p^2 = N - a \,. \tag{2.3.52}$$

In open string theory, for the Neveu Schwarz sector we have $a(NS) = \frac{1}{2}$ and for the Ramond, $a(R) = 0$, as we will see later. Using Eq. (2.3.51) for the fermion number operator in each sector we may express the mass in terms of creation and annihilation operators.

Neveu Schwarz sector :

$$\alpha' M^2 = \sum_{I=1}^{8} \left(\sum_{n \in \mathbf{Z}} \alpha^I_{-n} \alpha^I_n + \sum_{r \in \mathbf{Z}+\frac{1}{2}} r b^I_{-r} b^I_r \right) - a(NS) \,.$$

The ground state has mass $\alpha' M^2 = -a(NS)$. The first excited state is

$$b^I_{-r} |0, p\rangle \tag{2.3.53}$$

is a vector state with 8 degrees of freedom, which means that it is a massless bosonic state. Thus, we find $a(NS) = \frac{1}{2}$, and the ground state is a tachyon.

Ramond sector :
The mass formula now reads

$$\alpha' M^2 = \sum_{I=1}^{8} \sum_{n=1}^{\infty} \left(\alpha_{-n}^I \alpha_n^I + n d_{-n}^I d_n^I \right) - a(R) \,.$$

In this sector the ground state is a spinor. Since the operators d_0^I satisfy the Clifford algebra,

$$\{d_0^I, d_0^J\} = \delta^{IJ} \,, \tag{2.3.54}$$

they may be considered as Dirac matrices up to normalization, $d_0^M \equiv \frac{1}{\sqrt{2}} \Gamma^M$. We may define the annihilation and creation operators

$$\begin{aligned} d^a &= \sqrt{\frac{1}{2}} (d_0^I + i d_0^{I+1}) \quad , \quad I = 1, 3, 5, 7 \\ d_a^\dagger &= \sqrt{\frac{1}{2}} (d_0^I - i d_0^{I+1}) \quad , \quad I = 1, 3, 5, 7 \,, \end{aligned} \tag{2.3.55}$$

where $a = 1, 2, 3, 4$. These satisfy

$$\{d^a, d_b^\dagger\} = \delta_b^a \quad , \quad \{d^a, d^b\} = \{d_a^\dagger, d_b^\dagger\} = 0 \,. \tag{2.3.56}$$

The vacuum for these operators is defined as

$$d^a |\Omega\rangle = 0 \,. \tag{2.3.57}$$

Then, the creation operators acting on the vacuum give 16 states

$$|\Omega\rangle \ , \ d_a^\dagger |\Omega\rangle \ , \ d_a^\dagger d_b^\dagger |\Omega\rangle \ , \ d_a^\dagger d_b^\dagger d_c^\dagger |\Omega\rangle \ , \ d_a^\dagger d_b^\dagger d_c^\dagger d_d^\dagger |\Omega\rangle \,, \tag{2.3.58}$$

which form a spinor representation of $SO(8)$, since d_as satisfy Clifford algebra. Action with d_0^I on the above states results again in linear combination of the same states. Hence, a 16×16 matrix representation of the d_0^I operators was constructed. The states with even number of creation operators do not mix with states with odd number of $d^\dagger$ operators. The spinor then decomposes into two spinors, one with even number of $d^\dagger s$ denoted by $\mathbf{8_s}$ and the other with odd number of $d^\dagger s$ called $\mathbf{8_c}$. Thus, the ground state is in the chiral spinor representation of $SO(8)$ group. There are two degenerate chiral ground states that are denoted by

$$|a\rangle \ \text{ and } \ |\bar{a}\rangle \,, \tag{2.3.59}$$

both with mass $\alpha' M^2 = -a(R, open)$. These are 8 dimensional spinors of $SO(8)$ that can be embedded in the 10 dimensional spinors which are in the Majorana-Weyl (real and chiral) representation of $SO(1,9)$. They also have opposite chiralities $\Gamma_{11}|a\rangle = |a\rangle$ and $\Gamma_{11}|\bar{a}\rangle = -|\bar{a}\rangle$, where Γ_{11} is the ten dimensional chirality matrix, the same is valid by acting with the eight dimensional chirality matrix. These spinors have 16 real components which correspond to 8 on shell states that make a massless Majorana-Weyl spinor. Thus, we must have $a(R, open) = 0$.

The spectrum that we get from the above procedure is not supersymmetric. Moreover, the requirement of modular invariance, coming from string interactions, implies that we have to truncate the spectrum that we have found, by GSO projection. In the NS sector, the GSO operator is

$$\Pi_{NS} = \frac{1}{2}(1 - (-1)^F) \quad , \quad F = \sum_{r=\frac{1}{2}}^{\infty} b^i_{-r} b^i_r \,, \tag{2.3.60}$$

where F counts the number of b^i_{-r}. The tachyon of the NS sector and all states with even number of b^i_{-r} are projected out.

In the Ramond sector there are two choices for defining GSO operator

$$\Pi_{Ram} = \frac{1}{2}(1 + \gamma_c(-1)^F) \quad , \quad \bar{\Pi}_{Ram} = \frac{1}{2}(1 - \gamma_c(-1)^F) \quad , \quad F = \sum_{n=1}^{\infty} d^i_{-n} d^i_n \,, \tag{2.3.61}$$

where $\gamma_c = \gamma^1 \dots \gamma^2$ (with $\gamma^i = d^i_0$) and F counts the number of d^i_{-n}. The two choices are equivalent in case of open superstring. For any of the two choices, GSO reduction will project out one of the two possible Ramond ground states.

Thus, the **open superstring** massless spectrum contains a ten dimensional massless vector from the NS sector one ten dimensional massless chiral spinor. As it will be mentioned later, this is the field content of the maximally supersymmetric Yang Mills theory in 10 dimensions.

The spectrum of the closed superstring comes from four sectors: $NS \otimes NS$, $R \otimes R$, $NS \otimes R$,$R \otimes NS$. After tensoring states from left and right moving sectors and applying the GSO projection to the spectrum we get the closed superstring spectrum. Here we project out the states from left moving sector with $\Pi_{NS,\,L}$ and $\Pi_{Ram,\,L}$ projectors, where the index L shows that they act on the left movers. For the right moving sector we use $\Pi_{NS,\,R}$. If we choose to project the right moving Ramond states by $\Pi_{Ram,\,R}$ we conclude to the spectrum of type IIA, whereas if we use $\bar{\Pi}_{Ram,\,R}$ we are led to type IIB. The massless spectrum of the two closed superstring theories follows:

Type IIA ($\Pi_{NS,\,L}$,$\Pi_{NS,\,R}$,$\Pi_{Ram,\,L}$ and $\Pi_{Ram,\,R}$)

- $NS \otimes NS$: graviton, $g_{\mu\nu}$, dilaton, ϕ, antisymmetric 2-form, $B_{\mu\nu}$.
- $R \otimes R$: real vector, C_μ, real 3-form $C_{\mu\nu\rho}$.
- $NS \otimes R$: massless right-handed gravitino, χ^μ_α and a massless left-handed spin 1/2 state, λ_α.
- $R \otimes NS$: massless left-handed gravitino, $\chi^\mu_{\dot\alpha}$ and a massless left-handed spin 1/2 state, $\lambda_{\dot\alpha}$.

Since, the fermionic part of the spectrum includes two gravitinos and spin 1/2 fields of opposite chiralities, type IIA is nonchiral.

Type IIB ($\Pi_{NS,\,L}$,$\Pi_{NS,\,R}$,$\Pi_{Ram,\,L}$ and $\bar{\Pi}_{Ram,\,R}$)

- $NS \otimes NS$: graviton, $g_{\mu\nu}$, dilaton, ϕ, antisymmetric 2-form, $B_{\mu\nu}$.
- $R \otimes R$: a massles scalar C_0, real 2-form, $C_{\mu\nu}$ and a selfdual 4-form $C_{\mu\nu\rho\sigma}$
- $NS \otimes R$: massless gravitino, χ^μ_α and a massless spin 1/2 state, λ_α.
- $R \otimes NS$: massless gravitino of the same chirality as the one from $NS \otimes R$ sector, χ^μ_α and a massless spin 1/2 state of opposite chirality, λ_α.

In type IIB, all fermions have the same chirality, therefore the theory is chiral.

2.3.3 p-Branes

The forms in the $R \otimes R$ sector of the IIA/B transform under a generalized gauge symmetry

$$C_p \to C_p + d\Lambda_{p-1}\,, \tag{2.3.62}$$

and for each form we can define a gauge invariant field strength

$$F_{p+1} = dC_p\,. \tag{2.3.63}$$

By taking the hodge dual of the field strengths of the forms that appear in the type II spectrum

$$\begin{aligned} \tilde{F}_{10-p} &= \star F_p\,, \\ \tilde{F}_{\mu_1\cdots\mu_{10-p}} &= \frac{1}{p!}\epsilon_{\mu_1\cdots\mu_{10-p}}{}^{\nu_1\cdots\nu_p} F_{\nu_1\cdots\nu_p} \end{aligned} \tag{2.3.64}$$

we find their duals. We may consider the C_p forms as electric potentials and the potentials, $\tilde{C}_{9-p}$, which are defined by $\tilde{F}$ as

$$\tilde{F}_{10-p} = d\tilde{C}_{9-p} \tag{2.3.65}$$

are the magnetic potentials. Thus, in the spectrum of type IIA the following forms exist: C_1, C_3 and their duals $\tilde{C}_7$ and $\tilde{C}_5$ respectively. In type IIB there exist the C_0 and C_2 forms, their duals $\tilde{C}_8$ and $\tilde{C}_6$ and the selfdual C_4. Hence, type IIA contains all the odd forms and type IIB the even ones.

A state which is charged under a RR form, C_{p+1}, is a p-brane, where p is the number of its spatial dimensions. p-branes are $p+1$ dimensional objects in total. A particle of mass m and charge q couples to the spacetime and to the $U(1)$ gauge field in the following way

$$S = T \int ds + iQ \int dx^\mu A_\mu \tag{2.3.66}$$

This is naturally generalized to the coupling of a C_{p+1} form to the background where it is located and a p-brane

$$S = T_p \int \sqrt{-g}\, d^{p+1}x + iQ_p \int C_{p+1} \tag{2.3.67}$$

where $\int C_{p+1} = \int dx^{\mu_1} \wedge \cdots \wedge dx^{\mu_{p+1}} C_{\mu_1 \cdots \mu_{p+1}}$ and g is the determinant of the world-volume metric of the p-brane. T_p is the tension of the p-brane i.e. its mass per unit volume in the p spacelike directions and Q_p is the electric charge density. The electric charge is defined by the flux on a sphere surrounding the source. The transverse space of p-branes is $\mathbb{R}^{9-p}$. To compute the electric charge, we must consider an S^{8-p} sphere which surrounds the p-brane. The electric charge of the solution is calculated from the flux through a $8-p$ sphere at infinity

$$NT_p = \frac{1}{2\kappa_{10}} \int_{S^{8-p}} \star F_{p+2}\,. \tag{2.3.68}$$

Branes are not states that appear in the perturbative spectrum of type II superstrings. The RR vertex operator contains only the field strength and not the potentials, hence couplings of the form (2.3.67) are impossisble to appear in string perturbation theory.

The massless spectra of IIA/B superstrings are the same as those of IIA/B supergravities. Therefore, the two derivative effective action that describes the low energy

dynamics of the IIA/B superstrings is that of the IIA/B supergravities. The action describing the bosonic massless modes of the superstring at low energies are

$$S = \frac{1}{\kappa_{10}^2}\int d^{10}x\left[\sqrt{-g}\,e^{-2\phi}\left[R + 4(\nabla\phi)^2 - \frac{1}{12}H_3\right] - \frac{\sqrt{-g}}{2(p+2)!}{F'_{p+2}}^2\right], \tag{2.3.69}$$

where $H_3 = dB$ and $F'_{p+1} = dC_p - B\wedge dC_{p-2}$. We are interested in p-branes which are not charged under the B field, therefore we may set it to zero. The equations of motion for the metric and the RR form are

$$\begin{aligned} &R_{\mu\nu} + 2\nabla_\mu\nabla_\nu\phi = \frac{e^{2\phi}}{2(p+1)!}\left(F_{\mu\nu\cdots\mu_{p+2}}F^{\mu_1\cdots\mu_{p+2}} - \frac{g_{\mu\nu}}{2(p+2)}F^2\right) \\ &d\star F_{p+2} = 0\,. \end{aligned} \tag{2.3.70}$$

Longitudinal coordinates on the brane will denoted by x and the transverse by y. We require the p-brane to be spherically symmetric in $(10-p)$ dimensions. The problem is then reduced to finding a spherically symmetric charged black hole solution in $(10-p)$ dimensions. The ansatz reads

$$ds^2 = \frac{-f(r)^2dt^2 + dx_idx^i}{\sqrt{H(r)}} + \sqrt{H(r)}\left(\frac{dr^2}{f(r)} + r^2d\Omega_{8-p}^2\right), \tag{2.3.71}$$

where $d\Omega_{8-p}$ is the infinitesimal distance on a $(8-p)$ dimensional unit-sphere and the functions $H(r)$ and $f(r)$ are harmonic functions in $9-p$ dimensions, satisfying

$$\Box H(r) = 0\,,\ \Box f(r) = 0\,. \tag{2.3.72}$$

The solutions are

$$\begin{aligned} H(r) = 1 + \tfrac{L^{7-p}}{r^{7-p}}\,,\ f(r) = 1 + \tfrac{r_0^{7-p}}{r^{7-p}} \\ e^{\phi(r)} = g_sH(r)^{\frac{3-p}{4}} \\ A_{0\ldots p} = \sqrt{1 + \tfrac{r_0^{7-p}}{L^{7-p}}}\,\tfrac{H_p(r)-1}{H_p(r)}\,. \end{aligned} \tag{2.3.73}$$

The p-brane electric charge is given by Eq.(2.3.68),

$$NT_p = \frac{(7-p)\,\Omega_{8-p}}{2\kappa_{10}^2}\sqrt{L^{7-p}(r_0^{7-p} + L^{7-p})}\,. \tag{2.3.74}$$

The corresponding ADM mass of the p-brane is

$$M = \frac{\Omega_pV_p}{2\kappa_{10}}\left[(8-p)r_0^{7-p} + (7-p)L^{7-p}\right], \tag{2.3.75}$$

with V_p being the p-brane worldvolume.

At the points $r = 0$ and $r = r_0$ the metric becomes infinite. Calculating the the Ricci scalar for the above solution we find

$$R_r = \frac{(3-p)(p-7)^2 L^{7-p}}{4\, r^{23-3p} H_p(r)^{\frac{5}{2}}} \left(4(rr_0)^{7-p} + L^{7-p}((p+1)r^{7-p} - (p-3)r_0^{7-p})\right) , \quad (2.3.76)$$

and observe that in case of D_3-branes there is no curvature singularity. For $-1 \leq p < 3$, R_r is regular but if we transform the metric from the string to Einstein frame, $g^E_{\mu\nu} = e^{-\frac{\Phi}{2}} g_{\mu\nu}$ and $R^E_r \sim r^{-\frac{(p-3)^2}{8}}$ which diverges at $r = 0$ for any $p \neq 3$, thus there is a curvature singularity. In order for this not to be a naked singularity, the condition $r_0 > 0$ must be valid. This yields the Bogomol' ny bound

$$\frac{M}{V_p} \geq N T_p \, , \quad (2.3.77)$$

where we have used Eqs. (2.3.74, 2.3.75). In the extremal case, of D_3-branes the above bound is saturated and $r_0 = 0$. The region close to $r = 0$ is known as the "throat" of spacetime. The metric is of the form

$$ds^2 = \frac{-dt^2 + dx_i dx^i}{\sqrt{H(r)}} + \sqrt{H(r)} \left(dr^2 + r^2 d\Omega^2_{8-p}\right) . \quad (2.3.78)$$

The above solution can also be shown to be supersymmetric. When it is inserted in the supersymmetry transformations of the fermions we are led to $\delta\psi = 0$ for half of the supersymmetry parameters. Thus, half of the sypersymmetries are preserved and D_3-branes are considered to be half BPS objects.

2.3.4 D branes: Perturbation theory

D_p-branes are extended objects of p spatial dimensions which can be introduced as planes where open strings end due to Dirichlet boundary conditions. In [19], Polchinski argued that the D-branes are dynamical objects whose fluctuations are the same with the fluctuations of the open strings which are attached on the brane. The massless spectrum of the open strings coincides with the collective excitations of the brane. Consider the case of the bosonic string and a D_p-brane in 26 dimensions. The open string action in conformal gauge is mentioned again

$$S = -\frac{T}{2} \int d^2x \, \eta^{\mu\nu} \, \partial_\mu X \cdot \partial_\nu X \, . \quad (2.3.79)$$

There are two different kinds of boundary conditions for the equations of motion that come from this action, Eq.(2.3.11). Dirichlet boundary conditions imply that the string endpoints lie at a constant position, $X^M = x^{(0)}$. In case that there is a D$_p$-brane, the boundary conditions become

$$\begin{aligned} \text{Neumann b.c. } &: \partial_\sigma X^\mu \Big|_0^\pi = 0 \quad , \quad \text{for } \mu = 0, \ldots, p \,, \\ \text{Dirichlet b.c. } &: \delta X^I \Big|_0^\pi = 0 \quad , \quad \text{for } I = p+1, \ldots, 25 \,, \end{aligned} \tag{2.3.80}$$

where it should noticed that now the greek index μ parametrizes the worldvolume of the D_p-brane and not the string worldsheet. Since, the endpoints of the string are restricted to a $p+1$ dimensional plane, Lorentz symmetry breaks to $SO(1,25) \to SO(1,p) \times SO(25-p)$. The Neumann boundary conditions impose $\alpha_n^\mu = \tilde{\alpha}_n^\mu \equiv \alpha_n^\mu$ and the Dirichlet $x^I = x^{(0)\,I}$, $p^I = 0$ and $\alpha_n^I = -\tilde{\alpha}_n^I \equiv \alpha_n^I$. Then, Eq.(2.3.6) and (2.3.7) become

$$X^\mu(\tau,\sigma) = x^\mu + 2\alpha' p^\mu \tau + i\sqrt{2\alpha'} \sum_{n\neq 0} \frac{1}{n} \alpha_n^\mu e^{-in\tau} cos(n\sigma) \,, \tag{2.3.81}$$

$$X^I(\tau,\sigma) = x^{(0)\,i} + i\sqrt{2\alpha'} \sum_{n\neq 0} \frac{1}{n} \alpha_n^I e^{-in\tau} sin(n\sigma) \,. \tag{2.3.82}$$

We observe that there are no zero modes for momenta in the transverse directions. Therefore, the brane degrees of freedom propagate only on the longitudinal coordinates of the D$_p$-brane. The spectrum of the bosonic string in the presence of the D$_p$-brane is found similarly as in the case of the closed string. We use the lightcone gauge ($X^\pm = \frac{1}{\sqrt{2}}(X^0 \pm X^p)$) and find the mass formula

$$M^2 = \frac{1}{\alpha'} \left(\sum_{\mu=1}^{p-1} \sum_{n>0} \alpha_{-n}^\mu \alpha_n^\mu + \sum_{I=p+1}^{25} \sum_{n>0} \alpha_{-n}^I \alpha_n^I - 1 \right) . \tag{2.3.83}$$

The ground state is annihilated by all annihilation operators

$$\alpha_n^\mu |0,p\rangle = \alpha_n^I |0,p\rangle = 0 \quad , \quad n>0, \;\; \mu = 0, \ldots, p \;\; , \;\; I = p+1, \ldots, 25 \,. \tag{2.3.84}$$

Using Eq.(2.3.83) we find the mass of the ground state

$$M^2 = -\frac{1}{\alpha'}, \,. \tag{2.3.85}$$

Therefore, the ground state is tachyonic.

The states of the first excitation level are massless. The longitudinal states to the brane are

$$\alpha_n^\mu|0,p\rangle \quad , \quad \mu = 1,\ldots,p \tag{2.3.86}$$

and transform as a vector under the $SO(1,p)$ Lorentz group of the brane worldvolume, hence a brane vector field A_μ is associated with this state. It is known that we may assign Chan Paton factors to the open string, i.e. put global charges at the ends of the open string. This is needed in case that we have more than one D-brane where the endpoints of the open string may lie. Then, the above vector field is promoted to a non-abelian gauge field. The massless state is $\alpha_n^\mu|i,j;p\rangle \to A_\mu^A T_{ij}^A$, where T_{ij}^A are $U(N)$ generators. N is the number of coincident branes at a point of the transverse space where the open string ends.

The transverse states are

$$\alpha_n^I|0,p\rangle \quad , \quad I = p+1,\ldots,D-1\,, \tag{2.3.87}$$

which are $D-p-1$ scalars under the $SO(1,p)$ Lorentz group of the brane worldvolume, but they transfrorm as vectors under the $SO(D-p-1)$ rotation group of transverse rotations, which is a global symmetry from the worldvolume viewpoint. These scalars will be understood as fluctuations of the position of the brane in the transverse space.

The same procedure may be followed for the superstring. The boundary conditions for the fermions in the Neveu Schwarz and Ramond sectors are

$$\begin{aligned} \text{Neumann b.c. : } & b_r^\mu = -\tilde{b}_r^\mu \quad , \quad d_n^\mu = \tilde{d}_n^\mu \\ \text{Dirichlet b.c. : } & b_r^i = \tilde{b}_r^i \quad , \quad d_n^i = -\tilde{d}_n^i\,, \end{aligned} \tag{2.3.88}$$

where we strees again that $\mu = 0,\ldots,p$ is not a worldsheet index but it parametrizes the worldvolume of the D_p-brane. Upon GSO projection, the open superstring spectrum involves the massless states

$$b_{-\frac{1}{2}}^\mu|0,p\rangle \quad , \quad b_{-\frac{1}{2}}^I|0,p\rangle\,, \tag{2.3.89}$$

which are one worldvolume vector and $D-p-1$ scalars. In Ramond sector, GSO projection gives a spinorial ground state $|a\rangle$ which is a 10 dimensional real chiral spinor. Hence, the massless spectrum of open superstrings in the presence of N coincident D_p-branes is the same as the dimensional reduction of the 10 dimensional, $SU(N)$, super Yang Mills action, which will be analyzed in the following section.

2.3.4.1 Dimensional reduction of $10d$ super Yang Mills

In the presence of multiple D-branes there are several different branes where the endpoinds of an open string have the choice to lie. Hence, the endpoints of each string are labelled by indices which show what brane they lie on. Chan-Paton indices are interpreted as those labels that indicate on which brane the open strings end. As it was mentioned above, the low energy worldvolume theory on N coincident D-branes turns out to be the dimensional reduction of the 10 dimensional $U(N)$ super Yang Mills (SYM) to $p+1$ dimensions. Ten dimensional super Yang Mills involves a gauge vector field $A_M(x)$ and a Majorana-Weyl spinor field, $\Psi(x)$. The action of the theory reads

$$S_{10d} = -\frac{1}{g_{YM}^2}\int d^{10}x \ \mathrm{Tr}\left(\frac{1}{4}F_{MN}F^{MN} + \bar{\Psi}\Gamma^M D_M\Psi\right) , \tag{2.3.90}$$

where the field strength of A_M is $F_{MN} = \partial_{[M}A_{N]} + [A_M, A_N]$ and the covariant derivative reads $D_M\Psi = \partial_M\Psi + [A_M, \Psi]$. The above theory is supersymmetric and it contains a ten dimensional massless vector field with eight degrees of freedom and a Majorana-Weyl spinor which also has eight on shell degrees of freedom. Here, we concentrate on the bosonic part of the action. When we dimensionally reduce the theory to $p+1$ dimensions the vector breaks in a $(p+1)$-dimensional vector and $9-p$ scalars

$$A_M(x,y) \longrightarrow A_\mu(x) \quad , \quad \phi_I(x) \, , \tag{2.3.91}$$

where x^μ are the longitudinal directions and y_I the transverse ones. The fields do not to depend on the transverse coordinates. They are also in the adjoint representation of the gauge group, $U(N)$. Then, the bosonic part of the action reduces to

$$S_{(p+1)d} = \frac{1}{4g_{YM}^2}\int d^{p+1}x \mathrm{Tr}\left(F_{\mu\nu}F^{\mu\nu} + 2D_\mu\phi_I D^\mu\phi^I + [\phi_I, \phi_J]\ [\phi^I, \phi^J]\right) , \tag{2.3.92}$$

where sum over I and J is implied. It is noticed that Lorentz symmetry breaks to the Lorentz symmetry of the D_p-brane worldvolume and a global symmetry

$$SO(9,1) \to SO(p,1) \times SO(9-p) \, . \tag{2.3.93}$$

The above lagrangian is the effective theory of the open string gauge boson and the transverse scalars which are the lightest bosonic states in the string spectrum in the presence of a D_p-brane.

The vaccua of the above field theory are static field configurations which minimize the potential

$$V(\phi) = [\phi_I, \phi_J]\ [\phi^I, \phi^J]\,. \tag{2.3.94}$$

The fermion fields and the gauge field strength are set to zero. For supersymmetric vaccua, we seek solutions of $V(\phi) = 0$ up to gauge equivalence. Then,

$$\left[\phi^I, \phi^J\right] = 0\,. \tag{2.3.95}$$

This implies that the scalar fields are simultaneously diagonalizable

$$\phi^I = \begin{pmatrix} \phi_1^I & & 0 \\ & \ddots & \\ 0 & & \phi_N^I \end{pmatrix}\ ,$$

where ϕ_i^I, $(i = 1 \dots N)$ gives the position of the i^{th} brane in the I^{th} direction of transverse space. Dimensional analysis actually shows that the positions of the branes are $X_i^I = \alpha' \phi_i^I$. The moduli space of vacua of the above field theory is $\left(\mathbb{R}^{9-p}\right)^N / S_N$, where $\left(\mathbb{R}^{9-p}\right)^N$ corresponds to the positions of the N D_p-branes in the transverse space and the permutation S_N acts on the eigenvalues of the scalar fields as the Weyl group of $U(N)$. This is interpreted as the permutations of N indistinguishable D_p-branes.

We now examine a concrete example of two D-branes which are seperated in the transverse space. Then, the vacuum expectation values (vevs) of the p scalar fields are 2×2 hermitian matrices

$$\phi^I = \begin{pmatrix} \phi_1^I & 0 \\ 0 & \phi_2^I \end{pmatrix}\ .$$

Since, the scalar has nonzero vacuum expectation value, the gauge symmetry breaks in its Cartan subgroup, $U(2) \to U(1) \times U(1)$. We may check that a gauge transformation of the form

$$g = \begin{pmatrix} e^{i\theta_1} & 0 \\ 0 & e^{i\theta_2} \end{pmatrix}$$

leaves the scalar vevs invariant. The gauge field fluctuations around the above vacuum are given by

$$A_\mu = \begin{pmatrix} A_\mu^{11} & A_\mu^{12} \\ A_\mu^{21} & A_\mu^{22} \end{pmatrix}$$

Then, the kinetic term of scalars in the action (Eq.[2.3.92]) results in the following term

$$Tr\left(D_\mu\phi_I D^\mu\phi^I\right) \to Tr[A_\mu,\phi^I]^2 = \sum_I \left(\phi_1^I - \phi_2^I\right)^2 |A_\mu^{12}|^2 \tag{2.3.96}$$

Hence, similarly to Higgs mechanism the diagonal part of the gauge field remained massless (A_μ^{11}, A_μ^{22}) corresponding to the generators of the remaining $U(1)\times U(1)$ gauge symmetry. The non-diagonal fields obtain a mass

$$m_{A^{12}}^2 = \sum_i \left|\phi_1^i - \phi_2^i\right|^2 = \frac{1}{\alpha'^{\,2}} \sum_i \left|X_1^i - X_2^i\right|^2 \tag{2.3.97}$$

Geometrically, the above mass corresponds to the minimum energy of the strings stretched between the two D-branes.

2.3.4.2 Bulk fields

In section (2.3.3), we described the minimal coupling of a p-brane to the background and the corresponding C_{p+1} RR form by the action [2.3.67]. However, this can be generalized to the Dirac-Born-Infield (DBI) and the Wess-Zumino action. DBI generalizes the interaction of the brane with the gravitational and other background fields of spacetime

$$S_{DBI} = \hat{T}_p \int d^{p+1}e^{-\phi}\sqrt{-det\left(g_{\mu\nu}^{(pb)} + 2\pi\alpha' F_{\mu\nu} + B_{\mu\nu}^{(pb)}\right)}\,. \tag{2.3.98}$$

The action above shows how the fields on the brane (A_μ, ϕ_I) (where $\mu = 0,\ldots,p$ and $I = p+1,\ldots,D-1$) couple to the NS-NS fields ($g_{\mu\nu}^{(pb)}, B_{\mu\nu}^{(pb)}, \phi$), where $g_{\mu\nu}$ and $B_{\mu\nu}$ are the pull-backs of the spacetime fields on the brane. The scalars ϕ_I appear in the pull-back of the metric

$$g_{MN}^{(pb)} dx^M dx^N = g_{\mu\nu}dx^\mu dx^\nu + g_{IJ}dX^I dX^J = g_{\mu\nu}dx^\mu dx^\nu + g_{IJ}\frac{dX^I}{dx^\mu}\frac{dX^J}{dx^\nu}dx^\mu dx^\nu\,, \tag{2.3.99}$$

where $M,N = 0,\ldots,D-1$. Eventually we take

$$g_{\mu\nu}^{(pb)} = g_{\mu\nu} + g_{IJ}\frac{dX^I}{dx^\mu}\frac{dX^J}{dx^\nu}\,, \tag{2.3.100}$$

where we have identified the transverse coordinates with the scalar fields $X^I(x_\mu)$, which also depend on the worldvolume coordinates, x_μ. The pull-back of B field is also defined

as

$$B^{(pb)}_{\mu\nu} = B_{MN}\frac{dx^M}{dx^\mu}\frac{dx^N}{dx^\nu} \tag{2.3.101}$$

In flat spacetime we have $g_{\mu\nu} = \eta_{\mu\nu}$, $g_{IJ} = \delta_{IJ}$ and $B_{\mu\nu} = 0$. If we expand the action [2.3.98] in powers of α' and keep up to two derivative terms we take the Yang-Mills action

$$S_{DBI} = \frac{(2\pi\alpha')^2\hat{T}_p}{4}\int d^{p+1}x\, e^{-\phi}\left(F_{\mu\nu}F^{\mu\nu} + 2\partial_\mu X^I\partial^\mu X^I\right) + \mathcal{O}(\alpha') \tag{2.3.102}$$

where $g_s = \langle e^{-\phi}\rangle$, i.e. the expectation value of the dilaton. We then read the Yang-Mills coupling constant

$$g^2_{YM} = \frac{g_s}{\hat{T}_p(2\pi\alpha')^2} = \frac{1}{T_p(2\pi\alpha')^2}\,. \tag{2.3.103}$$

where $\hat{T}_p = g_s T_p$. T_p is the p-brane tension which was defined in section 2.3.3. Hence, the Yang Mills action describes the light strings attached to a D_p-brane in the limit of small string length.

Even if there are non abelian generalizations of the DBI action, it is not known if they are compatible with string amplitudes to a;; orders. The interaction of the p-brane with the RR field (second part of action 2.3.67) is extended to the Wess-Zumino (WZ) action

$$S_{WZ} = \hat{T}_p\int d^{p+1}x\, \mathcal{C}\wedge e^{2\pi\alpha' F_{(2)}+B_{(2)}} \tag{2.3.104}$$

where $\mathcal{C} = \sum_k C_k$, is a formal sum of all RR forms and eventually we have to keep only the $(p+1)$-form of the above wedge product. For instance, in the case of a D_3-brane the WZ action reads

$$S_{WZ} = \hat{T}_p\int d^4x\, C_{(4)} + C_{(2)}\wedge(2\pi\alpha' F_{(2)}+B_{(2)}) + \frac{1}{2}C_{(0)}\wedge(2\pi\alpha' F_{(2)}+B_{(2)})\wedge(2\pi\alpha' F_{(2)}+B_{(2)}) \tag{2.3.105}$$

Hence, the WZ couplings express the interactions of the brane fields with the RR-forms.

2.3.4.3 D-branes as BPS configurations

Dirichlet boundary conditions for the fermions imply the identification

$$\psi^\mu_+ = \psi^\mu_- \quad , \quad \psi^i_+ = -\psi^i_- \tag{2.3.106}$$

where ψ_+ and ψ_- are the left and right closed string movers in Ramond sector. The identification of the modes of the Fourier expansion is given in Eq.(2.3.88). We consider the identification of the following form

$$|\alpha\rangle_L = P|\bar{b}\rangle_R \tag{2.3.107}$$

where $|\alpha\rangle_L$ and $|\bar{\alpha}\rangle_R$ are the left and right handed Ramond ground states of the left and right moving sectors. The indices L and R show the sector of the state. The operator P acts on spacetime spinors by changing their chirality and parity. In order for the above transformation to be compatible with the identification of d_0^I and d_0^μ (given in Eq.[2.3.88]), which can be mapped to gamma matrices, we require

$$\{P, \Gamma_I\} = 0 \quad , \quad [P, \Gamma_\mu] = 0 \tag{2.3.108}$$

Then, it is readily then checked that

$$P = \Gamma_{11}\Gamma_I \tag{2.3.109}$$

If we consider a single D_p-brane, Dirichlet boundary conditions are imposed on $9-p$ directions. Then, left and right handed ten dimensional spinors must be identified according to Eq.(2.3.107), but then we use $P = \prod_{I=p+1}^{9}(\Gamma_{11}\Gamma_I)$. Type II superstring theories have two ten dimensional spinor parameters ϵ_L (left mover) and ϵ_R (right mover). These have the same chirality in type IIB and opposite in type IIA. In the presence of D_p-branes they must satisfy

$$\epsilon_L = \prod_{i=p+1}^{9}(\Gamma_{11}\Gamma_i)\,\epsilon_R = \Gamma_{p+1}\ldots\Gamma_9\epsilon_R = \Gamma_0\ldots\Gamma_p\epsilon_R \tag{2.3.110}$$

as any other spacetime spinor of the theory. The above equalities are valid up to a sign which does not change our physical conclusions. Then, it follows that the presence of a D_p-brane leads to conservation of half of the supersymmetries, since ϵ_L and ϵ_R are no more independent. Leading to the conclusion the D_p-branes are BPS objects. Since, Γ_i changes the chirality and ϵ_L and ϵ_R have the same chirality for type IIB and opposite for type IIA, D_p-branes exist in IIA for even p and in IIB for odd p.

The interaction which is depicted in Fig.(2.4) is an one-loop vacuum energy for a supersymmetric open string, thus it is zero. But, it can also be seen in the closed string channel as a tree level exchange of bosonic NS-NS and R-R fields, see [19].

Since, the result of the diagram is zero, the force between the D-branes is zero. By explicit calculation, we find that the tension of the brane is related to its R-R charge

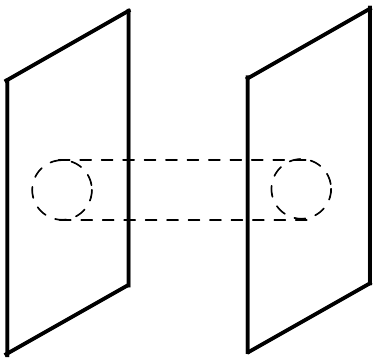

Figure 2.4: A system of two D-branes interacting through the exchange of an closed string. The diagram can also be interpreted as a tree level interaction of open strings.

by the BPS condition

$$T_p = \frac{1}{(2\pi)^p g_s \ell_s^{p+1}} \,. \tag{2.3.111}$$

2.4 Motivating the AdS/CFT correspondence

AdS/CFT was discovered along the study black holes in string theory. On the one hand, they are described as charged solitonic objects generating curved gravitational backgrounds and on the other hand their low energy fluctuations are described effectively by gauge field theories. Taking certain limits of the above descriptions, it turns out that they describe the same physical system from two different perspectives. One is a gravitational and the other a gauge theory description. This led to the gauge/gravity duality.

2.4.1 The decoupling limit

Consider N coincident D_3-branes in a ten-dimensional spacetime. As it was analyzed in section 2.3.4 the light open-string degrees of freedom of the system are described by $\mathcal{N} = 4$ super Yang Mills theory, in the limit of small string length, i.e. $\alpha' \to 0$. Hence, the theory contains one vector gauge field, six scalars and four Weyl fermions. As it is

mentioned in Eq.(2.3.93), the gauge theory also has an $SO(6) \simeq SU(4)$ global symmetry, under which the vector is singlet, scalars are in the antisymmetric representaion (**6**) and fermions in the fundamental (**4**). The theory is conformal at quantum level as well.

There are also closed string excitations in the background spacetime. At energies lower than the string scale those are described by type IIB supergravity. It's spectrum contains a graviton, a dilaton, a two-form, Ramond-Ramond form, two gravitini and two fermions.

The total action describing the system is

$$S_{\text{total}} = S_{\text{closed}} + S_{\text{open}} + S_{\text{op-cl}}\,, \tag{2.4.1}$$

where the first two terms include the interactions of closed and open strings among themselves and the third term the combined open-closed string interaction. The interactions of open and closed strings are described by higher derivative terms, which can be neglected at low energies.

To study the low energy limit of the system, we expand the gravitational (closed-string) action in powers of κ_{10} and write the metric as a background metric plus the graviton fluctuation, $g_{\mu\nu} = \eta_{\mu\nu} + \kappa_{10} h_{\mu\nu}$. Then, the total string action is

$$\begin{aligned} S_{\text{total}} &\sim \frac{1}{2\kappa_{10}} \int d^{10}x\, \sqrt{g} R + \ldots + \frac{1}{4g_{YM}^2} \int d^4x \sqrt{-g} \mathbb{T}r\left(F^2\right) + \ldots \\ &\sim \int d^{10}x\, \left[(\partial h)^2 + kh(\partial h)^2 + \ldots\right] + \frac{1}{4g_{YM}^2} \int d^4x\, \left(F_{\mu\nu}F^{\mu\nu}\right) \\ &+ \frac{\kappa_{10}}{4g_{YM}^2} \int d^4x\, \mathbb{T}r h^{\mu\nu} \left(F_{\mu\rho}F^{\rho}_{\nu} - \frac{\delta_{\mu\nu}}{4}F^2\right) + \ldots \end{aligned} \tag{2.4.2}$$

The low energy limit can be taken by considering the characteristic scale of the theory small, $\ell_s \to 0$, keeping all the other dimensionless parameters finite. Extracting the low energy string effective action, which is typically a supergravity action we may express Newton's gravitational constant in terms of g_s and ℓ_s,

$$\kappa_{10} = \sqrt{\frac{(2\pi)^7}{2}} g_s l_s^4\,, \tag{2.4.3}$$

see for instance [3]. Thus, when string length is approaching zero open strings are described by $\mathcal{N} = 4$ SYM theory (see section 2.3.4)) and all the closed string interactions, either with open or among themselves are small. Concluding, as $\ell_s \to 0$

$$S_{\text{total}} = S_{\text{free gr}} + S_{\text{SYM}}\,, \tag{2.4.4}$$

where the first part describes free gravitons.

2.4.2 The p-Brane viewpoint

As it was analyzed in section 2.3.3 N coincident D_3-branes are described as extremal solutions of classical type IIB supergravity. The background fields are reminded

$$\begin{aligned} ds^2 &= \frac{-dt^2 + dx_i dx^i}{\sqrt{H(r)}} + \sqrt{H(r)}\left(dr^2 + r^2 d\Omega_5^2\right) , \\ A_{0123} &= \frac{L^4/r^4}{1+\frac{L^4}{r^4}} \ , \ \ H(r) = 1 + \frac{L^4}{r^4} . \end{aligned} \tag{2.4.5}$$

Using Eqs. (2.3.74) and (2.3.111) we determine L in terms of the parameters of the theory

$$L^4 = 4\pi g_s \ell_s^4 N . \tag{2.4.6}$$

To take the corresponding low energy limit we have to take into account the gravitational redshift. An observer at infinity measures energy which is related to the energy measured at r by $E_\infty = H(r)^{-1/4} E_r$. Meaning that modes of arbitrary energy are measured at infinity to be low energetic if they are located at small distance, $r << L$. He also observes the standard low energy modes in the bulk. These two types of modes are decoupled, in the sense that if the observer at infinity emits low energy modes towards the throat of the solution ($r < L$ region) the cross section is ω^3, where ω is the frequency of the mode. Hence, at low energy the two kinds of modes interact very weakly. Consequently, in the low energy limit, gravitational fluctuations of D_3-brane background are described by the action

$$S_{\text{total}} = S_{\text{free gr}} + S_{\text{IIB hor}} , \tag{2.4.7}$$

where the first term is the action of the bulk large wavelength modes which are described by free graviton action, and the second term is the type IIB supergravity action which describes the gravitons at the $r << L$ region. Taking the limit $r << L$ in the metric of Eq. (2.4.5) we find

$$ds^2 = \frac{r^2}{L^2}\left(-dt^2 + dx_i dx^i\right) + \frac{r^2}{L^2} dr^2 + L^2 d\Omega_5^2 , \tag{2.4.8}$$

which is the metric of five dimensional anti-de Sitter times a $5d$ sphere ($AdS_5 \times S^5$) spacetime. Both AdS_5 and S^5 have radius L.

Concluding, the low energy limit of D_3-branes was described using two different viewpoints. In both cases, the action describing the system has a free supergravity part. On the one hand, the remaining part is $\mathcal{N} = 4$ super Yang Mills theory and on the other hand type IIB supergravity action in $AdS_5 \times S^5$ background. Hence, the conjecture that the these two theories are equivalent seems to be reasonable.

2.4.3 Matching the two theories

$\mathcal{N} = 4$ SYM enjoys two global symmetries, the conformal $SO(2,4)$ symmetry and $SO(6)$, which were mentioned above. $SO(2,4)$ is also the isometry group of AdS_5 and $SO(6)$ is the isometry group of S_5, as it will be seen in section (2.5.1). The gauge theory is a;so supersymmetric with 16 supercharges. Taking into account the conformal group supersymmetry is enhanced to the superconformal symmetry with 32 supercharges. It can be shown that even if the D_3-brane solution is left invariant under the type IIB supergravity transformations only for 16 parameters, $AdS_5 \times S^5$ is invariant under 32 supergravity parameters. As a result the symmetries of the two theories match.

$U(N)$ SYM theory is equivalent to a free $U(1)$ and an $SU(N)$ gauge theory. Geometrically, the $U(1)$ part corresponds to the motion of center of mass of D_3-branes in the bulk spacetime. In the low energy this motion appears as zero modes travelling in the whole bulk spacetime. In the low energy limit, those modes were omitted. Therefore, type IIB supergravity action in $AdS_5 \times S^5$ does not describe this $U(1)$ free theory but only the $SU(N)$ part.

SYM theory has two dimensionless parameters, the order of the gauge group N and t' Hooft coupling $\lambda = g_{YM}^2 N$. On the supergravity side, the dimensionless parameters are L/ℓ_s and g_s. Eqs. (2.3.103), (2.3.111), (2.4.3) and (2.4.6) relate the parameters of the two theories

$$\frac{L^4}{\ell_s^4} = 4\pi g_s N = 2\lambda \ , \ \ g_s^2 = \frac{2}{(2\pi)^7}\frac{\kappa_{10}^2}{\ell_s^8} = (2\pi)^5 \frac{\lambda}{N} \, . \tag{2.4.9}$$

We notice that the low energy limit of the D_3-branes is valid when g_s is small, thus string loop amplitudes are subleading. The above relations imply that this is happening for $N >> 1$. Higher string states corrections to supergravity action are also suppressed in the limit of large $NL/\ell_s >> 1$, which yields that $\lambda >> 1$. Thus, a weakly coupled two-derivative supergravity in $AdS_5 \times S^5$ is dual to strongly coupled , $\mathcal{N} = 4$ SYM theory. We point out that supersymmetry was not used in the above argumentation. Therfore, it does not seem to be an important ingredient of the conjecture even though it is crucial in checking the correspondence by comparing correlation functions of the

gauge theory operators to bulk field correlators.

2.5 The geometry of AdS_{d+1}

Anti-de Sitter space AdS_{d+1} of dimension $d+1$ can be defined as a hyperboloid

$$X_0 + X_{d+1} - \sum_{i=1}^{d} X_i^2 = L^2 \tag{2.5.1}$$

embedded in a flat $d+2$ space $\mathbb{R}^{d,2}$ with metric

$$ds^2 = -dX_0^2 - dX_{d+1}^2 + \sum_{i=1}^{d} dX_i^2. \tag{2.5.2}$$

The isometry group of the space is $SO(d,2)$. Using the following parameterization

$$X_0 = L\ cosh\rho\ cos\tau, \qquad X_{d+1} = L\ cosh\rho\ sin\tau, \tag{2.5.3}$$

$$X_i = L\ sinh\rho\ \Omega_i \qquad (i = 1, \cdots, d;\ \sum_i \Omega_i^2 = 1) \tag{2.5.4}$$

we find the metric of the AdS_{d+1} space

$$ds^2 = L^2(-cosh^2\rho\ d\tau^2 + d\rho^2 + sinh^2\rho\ d\Omega^2), \tag{2.5.5}$$

where Ω_i are the standard coordinates of the d-Sphere S^d. If we consider $0 \leq \rho < \infty$ and $0 \leq \tau < 2\pi$ the metric covers the whole hyperboloid. Hence, the coordinates (τ, ρ, Ω_i) are called global. Near $\rho = 0$ the metric is approximated as

$$ds^2 \simeq L^2(-d\tau^2 + d\rho^2 + \rho^2\ \ d\Omega^2). \tag{2.5.6}$$

So, the topology of the hyperboloid is $S^1 \times \mathbb{R}^d$, where S^1 yields that there are closed timelike curves in the τ direction. By taking the covering space of the S^1 coordinate $(-\infty < \tau < \infty)$ we avoid closed timelike curves. The boundary of the space has two disconnected boundary components, one to the right and another to the left part of the hyperboloid. In the case of AdS_2 space the boundary is a zero dimensional sphere S^0 which is just two points.

It is now convenient to bring the endpoints of the ρ coordinate to finite values. Therefore, we set

$$\tan\theta = \sinh\rho\,, \tag{2.5.7}$$

where $0 \leq \theta < \pi/2$. Then the metric reads

$$ds^2 = \frac{L^2}{cos^2\theta}(-d\tau^2 + d\theta^2 + sin^2\theta \; d\Omega^2) \tag{2.5.8}$$

The space that is described by the above metric is causally equivalent to the metric of Einstein static universe ($ds^2 = -d\tau^2 + d\theta^2 + sin^2\theta \; d\Omega^2$). In our case though, the coordinate θ is restricted to the values $[0, \frac{\pi}{2})$ and not to the full range $[0, \pi)$. The boundary of the space is at $\theta = \frac{\pi}{2}$. There is also another coordinate system which is defined as

$$\begin{aligned} X^0 &= \frac{1}{2u}\left(1 + u^2(L^2 + \vec{x}^{\;2} - t^2)\right), \\ X_{d+1} &= L \; u \; t \;, \;\; X^i = L \; u \; x^i \quad (i = 1, \cdots, d) \\ X^d &= \frac{1}{2u}\left(1 - u^2(L^2 - \vec{x}^{\;2} + t^2)\right), \end{aligned} \tag{2.5.9}$$

where $0 < u$ and $\vec{x} \in \mathbb{R}^d$. These coordinates are called Poincaré coordinates and cover one half of the hyperboloid. The metric in Poincaré coordinates takes the form

$$ds^2 = L^2\left(\frac{du^2}{u^2} + u^2(-dt^2 + d\vec{x}^{\;2})\right). \tag{2.5.10}$$

We can finally set $z = \frac{1}{u}$, the metric then becomes

$$ds^2 = \frac{L^2}{z^2}\left(dz^2 - dt^2 + d\vec{x}^{\;2}\right), \tag{2.5.11}$$

with the boundary being at $z = 0$. It is noticed that at $z = 0$ the above metric blows up. Hence, this is not really the boundary of the space but it is a conformal boundary, whose metric is conformally equivalent to $\mathrm{R}^{d-1,1}$ flat minkowski metric $ds^2_B = \frac{L^2}{z^2}(-dt^2 + d\vec{x}^{\;2})$.

By making a Wick rotation in time ($\tau \to \tau_E = -i\tau$) the metric (2.5.11) is analytically continued in Euclidean signature, i.e.

$$ds^2 = \frac{L^2}{z^2}\left(dz^2 + dt_E^2 + d\vec{x}^{\;2}\right), \tag{2.5.12}$$

which is the metric of Lobachevsky space. The Euclidean space AdS_2 in Poincare coordinates is the upper half complex plane described by the Poincare metric. So, if we set $Z = t_E + iz$ and $L = 1$ the Poincare metric reads

$$ds^2 = \frac{dZd\overline{Z}}{(Im \; Z)^2}. \tag{2.5.13}$$

By making the transformation

$$w = \frac{1+iZ}{1-iZ} \tag{2.5.14}$$

The upper half plane is mapped into a disk, and infinity of the complex plane is mapped to a point of the boundary of the disk. Therefore, we generalize to the case of Euclidean AdS_{d+1} that is mapped to a $d+1$ disk. The boundary then at $y=0$ is mapped to the boundary of the disk S^d with one point removed. This point corresponds to the the boundary at $y=\infty$. Indeed, the surface $y=\infty$ in Lorentzian case is a null surface, hence it is mapped to a point after the Euclidean rotation.

2.5.1 Mapping of the global symmetries

The symmetries of the Anti-de Sitter space is the isometry group of the hyperboloid and the d dimensional Poincaré symmetry which includes the $SO(d-1,1)$ Lorentz group and the d-dimensional translations. In general, if the Lorentz group of a space of signature (p,q) is $SO(p,q)$, then the conformal group is $SO(p+1,q+1)$. The boundary of AdS_{d+1} has $(d-1,1)$ signature. The conformal group of the space is $SO(d,2)$ which is the same as the isometry group of the AdS_{d+1}. $SO(d,2)$ has the maximal subgroup $SO(d)\times SO(2)$. $SO(2)$ corresponds to translations of coordinate τ and $SO(d)$ to rotations on S^{d-1}. In conclusion, the conformal transformations in the boundary correspond to the plain isometries of the bulk space. For example, if we make a dilatation transformation in the boundary

$$\begin{aligned} \vec{x} &\to \lambda\vec{x} \\ t &\to \lambda t \\ z &\to \lambda z\,, \end{aligned}$$

the metric of the boundary becomes

$$ds'^{\,2}_{bound} = \lambda^2 ds^2_{bound} = \lambda^2(-dt^2 + d\vec{x}^{\,2})\,. \tag{2.5.15}$$

However, the metric of the bulk remains invariant

$$ds'^{\,2}_{bulk} = \frac{L^2}{(\lambda z)^2}(d(\lambda z)^2 - d(\lambda t)^2 + d(\lambda\vec{x})^{\,2}) = ds^2_{bulk}\,, \tag{2.5.16}$$

and we observe that a dilatation is a conformal transformation in the boundary and corresponds to an isometry in the bulk.

2.6 Correlation functions in AdS/CFT

A precise formulation of AdS/CFT correspondence should be set. Since $\mathcal{N} = 4$ SYM is a conformal field theory, hence we cannot define an S-matrix in its context. The natural observables of the theory are correlation functions of gauge invariant operators. For instance, the Lagrangian density operator is a marginal operator which has as a source the Yang-Mills coupling, g_{YM}. Eq. (2.3.103) relates this to the string coupling which is given by the dilaton expectation value at the boundary of AdS_5 spacetime, $g_s = \langle e^{-\phi_{\text{bound.}}} \rangle$. Hence, the above discussion yields that deforming the field theory by a local gauge invariant operator ($S \to S + \int d^4x\, \phi_{\text{bound.}}(x)\mathcal{O}(x)$), the value of the dilaton at the boundary changes. The mapping of the field theory operators to the bulk fields arises from the couplings of background fields to the D-brane fluctuations in the DBI action.

Therefore, AdS/CFT relates any local gauge invariant operator to an on shell bulk field of string theory in $AdS_5 \times S^5$. The precise correspondence reads

$$\langle e^{\int d^4x \phi_I(x)\mathcal{O}^I(x)} \rangle_{SYM} = \mathcal{Z}_{\text{str.}} \left[\phi_I(x, z = 0) = z^{4-\Delta} \phi_I(x) \right] , \tag{2.6.1}$$

where AdS_5 metric is taken in Poincaré coordinates, Eq. (2.5.11), and the boundary is at $z = 0$. Thus, the source of the operator $\mathcal{O}(x)$ is the boundary value of the bulk field, $\phi_I(x)$, where x are the Minkowski coordinates and z is the AdS_5 coordinate. This motivates us to consider that the field theory lives at the boundary of AdS_5. In the large N and large λ limit the string theory partition function is approximated by $\mathcal{Z}_{\text{str.}} \sim e^{-S_{\text{sugra.}}}$.

To find which is the dual bulk field of a certain operator we must know the details of the string theory which is reduced either to the gauge or to the supergravity theory. An easier way to find the dual pairs is by symmetries. In particular, the bulk field and the operator should have the same $SO(2, 4)$ quantum numbers. Some conserved currents have obvious couplings which are of the form

$$\int d^4x \sqrt{-g} \left[A_\mu(x) J^\mu(x) + h_{\mu\nu}(x) T^{\mu\nu}(x) \right] . \tag{2.6.2}$$

J^μ is a global conserved current ($\partial_\mu J^\mu = 0$) in the gauge theory, thus A_μ is gauge field in the bulk which has as a gauge transformation $\delta A_\mu = \partial_\mu \epsilon$ which leaves invariant the above coupling. $T_{\mu\nu}$ is the energy-momentum tensor operator which is conserved in a translationally invariant gauge theory. Then, $h_{\mu\nu}$ is a graviton transforming as

$\delta h_{\mu\nu} = \partial_{(\mu}\xi_{\nu)}$ under diffeomorphisms. In conclusion, we notice that global symmetries of the boundary theory are mapped to local symmetries in the bulk.

Hence, any theory with a conserved stress-energy tensor has a dual graviton field, meaning that the bulk theory is a gravity theory. Eq. (2.6.1) also yields that a d-dimensional field theory is dual to a gravity theory in $AdS_{d+1} \times K$, where K is a compact manifold. In case that the field theory is not conformal, the bulk spacetime cannot be AdS since the symmetries of the two descriptions would not match, see section (2.5.1).

2.6.1 Mass dimension relation

We consider a scalar field in AdS_{d+1} spacetime, which is dual to some local operator of the boundary field theory. It's action is

$$S = \frac{1}{2}\int d^5x\sqrt{-g}\left[(\partial\phi)^2 + m^2\phi^2\right] , \tag{2.6.3}$$

and the equation of motion is

$$(\Box - m^2)\phi = 0\,. \tag{2.6.4}$$

In Poincaré coordinates, it becomes

$$\phi'' - \frac{d-1}{z}\phi' + \partial_\mu\partial^\mu\phi - \frac{m^2L^2}{z^2}\phi = 0\,. \tag{2.6.5}$$

We apply Fourier transformation at the field in Minkowski slices of AdS_5

$$\phi(x,z) = \int \frac{d^dq}{(2\pi)^d}\phi(q,z)e^{iq\cdot x}\,. \tag{2.6.6}$$

The solution of the equation of motion reads

$$\phi(q,z) = c_1 z^{d/2} I_\nu(qz) + c_2 z^{d/2} K_\nu(qz)\,, \tag{2.6.7}$$

where $\nu = \frac{1}{2}\sqrt{d^2 + 4m^2L^2}$. The field close to the boundary, $z \to 0$ reads

$$\phi(q,z) = c_1 z^\Delta + c_2 z^{d-\Delta}\ ,\ \ \Delta = \frac{d}{2} + \frac{1}{2}\sqrt{d^2 + 4m^2L^2}\,. \tag{2.6.8}$$

Thus, the leading solution at the boundary is

$$\phi(x,\epsilon) = z^{d-\Delta}\phi_0(x) \tag{2.6.9}$$

This solution is non-normalizable in the UV, since $\int_{\partial \mathrm{AdS}} d^d x \sqrt{-h}|\phi|^2 = \infty$, where $h_{\mu\nu}$ is the induced boundary metric. Then $\phi_0(x)$ is the source of the dual operator while the normalizable solution, i.e. the first term in Eq.(2.6.8) is the vacuum expectation value of the dual operator. Since the field ϕ is dimensionless, ϕ_0 has dimension $\Delta - d$ and Eq.(2.6.1) yields that its dual operator has dimension $[\mathcal{O}] = \Delta$. The mass dimension relation can be rewritten as

$$\Delta(\Delta - d) = 4m^2 L^2 \,. \tag{2.6.10}$$

We immediately notice that marginal operators correspond to massless fields, irrelevant operators to massive and relevant ones to fields with negative mass square. Fields in AdS with $m^2 < 0$ do not break unitarity if their mass is above Breitenlohner-Freedman (BF) bound, which is $4m^2L^2 \geq -d^2$, [26].

2.6.2 Two-point function

To calculate correlation functions of local operators, $\mathcal{O}_I(x)$, in $\mathcal{N} = 4$ SYM we may differentiate Eq.(2.6.1) with respect to the source, $\phi_0^I(x)$. $\mathcal{Z}_{str.}$ is the generating functional of string theory S-matrix elements in $AdS_5 \times S^5$ spacetime, and it depends on the boundary values of the massless string theory fields. As it is mentioned above in the limit of large λ and $N \to \infty$ it is approximated by

$$\mathcal{Z}_{\mathrm{str}} \sim \sum_i e^{-S_{\mathrm{sugra},i}(\phi_0(x))} \,, \tag{2.6.11}$$

where on the right hand side, we calculate the on-shell supergravity action with the Dirichlet boundary conditions for the bulk fields, depending on their dual operator. It is possible that supergravity equations of motion have several solutions with the same boundary conditions. Hence, one should add the contributions from all the solutions, even though in practice there is one solution that is the global minimum of the action and this contributes mainly in the sum.

We now present the calculation of the two point function of a local scalar field operator, $\mathcal{O}(x)$, using the above prescription. Consider the scalar field of section (2.6.1) in AdS_{d+1}. It's on-shell action reads

$$S_{\text{on-shell}} = \frac{1}{2}\int_{AdS} d^5x\, \partial_\mu \left(\sqrt{-g}\,\phi \partial_\mu \phi\right) = -\frac{1}{2}\int_{\partial AdS} d^4x\, \sqrt{-h}\,\phi \partial_z \phi\Big|_{z=\epsilon} \,, \tag{2.6.12}$$

where we take AdS_{d+1} in Poincaré coordinates. The general solution for the scalar field is given in Eq. (2.6.7), from which we keep only the $z^{d/2}K_\nu(qz)$ part since it is

normalizable in the interior of AdS_5. The first term of (2.6.7) diverges for large z. The normalization constant is set by requiring that $\phi(q, z = \epsilon) = \phi_0(q)\epsilon^{d-\Delta}$, which is the source of the corresponding operator. Then,

$$\phi(q, z) = \frac{z^2}{\epsilon^2}\frac{K_\nu(qz)}{K_\nu(q\epsilon)}\phi_0(q)\epsilon^{d-\Delta} \tag{2.6.13}$$

and the two point function is

$$\langle \mathcal{O}(p)\mathcal{O}(q)\rangle = \frac{\partial^2 e^{S_{\text{sugra}}}}{\partial\phi_0(p)\phi_0(q)} = \text{const.}\,\delta^4(p+q)\,p^{2\Delta-d} + \dots\,, \tag{2.6.14}$$

where there are also infinite terms which are absorbed by holographic renormalization procedure. The two-point function in coordinate space reads

$$\langle \mathcal{O}(x)\mathcal{O}(y)\rangle = \frac{1}{|x-y|^{2\Delta}}\,. \tag{2.6.15}$$

To compute n-point functions we must differentiate $e^{S_{\text{sugra}}}$ n times with respect to the source

$$\langle \mathcal{O}_I(x_1)\dots\mathcal{O}_J(x_n)\rangle = \frac{\delta^n e^{-S_{\text{sugra}}}}{\delta\phi_0^I(x_1)\dots\delta\phi_0^J(x_n)}\,. \tag{2.6.16}$$

2.7 Wilson Loops

The Wilson loop is an important non-local gauge invariant operator of Yang-Mills theory. It is defined as

$$W(\mathcal{C}, R) = \mathbb{T}r_R\left[Pe^{i\int_{\mathcal{C}} A_\mu dx^\mu}\right]\,, \tag{2.7.1}$$

where P is the path ordering of the integral over the gauge field. This resolves the ambiguity of the ordering of the non-abelian gauge field in the integral. The trace can be taken in any representation R of the gauge group. We now take it to be the fundamental. $\mathcal{C}$ is a closed path of integration. We consider $\mathcal{C}$ as a rectangular in $t-x$ plane with length T along t axis and ℓ along x, with $T >> \ell$. A Wilson loop then describes the creation of a static pair of quak-antiquark at distance ℓ interacting for time T. The vacuum expectation value of the Wilson loop then gives potential energy of the pair

$$\langle W(\mathcal{C})\rangle = e^{-TV(\ell)}\,. \tag{2.7.2}$$

In case of, $V(\ell) \sim \ell$, for large ℓ the gauge theory is confined, whereas if $V(\ell) \sim \frac{1}{\ell}$ the interaction is of Coulomb type.

Holography may be used to calculate the Wilson loop of a gauge theory, [27; 28]. Already, intuition from gauge theory implies that the Wilson loop is related to a string connecting the quark-antiquark pair. From the AdS/CFT point of view, the pair of quarks lives at the boundary of spacetime and the string stretches in the ten dimensional bulk space. A simple motivation of the above picture in $\mathcal{N} = 4$ SYM, is to consider a system of $N + 1$ D_3-branes where one of them (probe brane) is put at a finite distance from the others along the AdS direction. The gauge symmetry then is Higgsed to $U(N) \times U(1)$ and the strings stretching from the stack of N branes to the probe transform in the fundamental under the $U(N)$. In order for the ground state of those strings to be a very heavy quark the probe brane should be put at $r = \infty$ thus the string ends at the boundary of AdS. Thus, in the bulk side, we should compute the partition function of a string scanning a worldsheet which ends at the boundary and stretches at the bulk. In the limit of large λ and $N \to \infty$ supergravity approximation may be used.

We will calculate now a rectangular Wilson loop for $T >> \ell$, with the pair of quarks to be put at $X^1 = \pm\ell/2$. The string stretches in the bulk and is located at point in S^5. The Nambu-Goto action for the string reads

$$S = \frac{1}{2\pi\ell_s^2}\int_0^T d\tau \int_{-\ell/2}^{\ell/2} d\sigma \sqrt{(\partial_\mu X^M \partial_\nu X^N) G_{MN}(X)} = \frac{TL^2}{2\pi\ell_s^2}\int_{-\ell/2}^{\ell/2} d\sigma \frac{\sqrt{(\partial_\sigma z)^2 + 1}}{z^2}\,, \tag{2.7.3}$$

where we have used the static frame, $\tau = X^0, \sigma = X^1, X^{2,3}(\sigma,\tau) = \text{const.}$ and $z(\sigma,\tau) = z(\sigma)$. Since, the action does not have explicit dependence on σ there is a conserved charge

$$(\partial_\sigma z)p_z - \mathcal{L} = \frac{L^2}{z^2}\frac{1}{\sqrt{1 + (\partial_\sigma z)^2}} = \text{const.}\,, \tag{2.7.4}$$

where $\mathcal{L} = \frac{\sqrt{(\partial_\sigma z)^2+1}}{z^2}$ and $p_z = \frac{\delta\mathcal{L}}{\delta z}$. We then find

$$z^2\sqrt{1 + (\partial_\sigma z)^2} = c^2 \Rightarrow \sigma(z) = c\int_{z/(Lc)}^1 \frac{y^2}{\sqrt{1 - y^4 dy}}\,. \tag{2.7.5}$$

In the limit $z \to 0$, $\sigma \to \ell/2$, this determines $c = \frac{\Gamma\left(\frac{1}{4}\right)}{(2\pi)^{3/2}}\ell$. Then, Eqs. (2.7.3) and

(2.7.5) give

$$S = \frac{TL^2}{\pi \ell_s^2 c} \int_\epsilon^1 \frac{dy}{y^2 \sqrt{1-y^4}}\,, \tag{2.7.6}$$

where the lower limit of integration corresponds to the AdS boundary. The above integral diverges as $\epsilon \to 0$. To cancel this singularity we have to subtract by the action of two non interacting quarks

$$S_{\text{free}} = \frac{T}{\pi \ell_s} \int_\epsilon^\infty dz \frac{L^2}{z^2}\,. \tag{2.7.7}$$

Then, we find

$$S_{\text{ren}} = S - S_{\text{free}} = \frac{TL^2}{\pi \ell_s^2 c} \left[-1 + \int_\epsilon^1 \frac{dy}{y^2} \left(\frac{1}{\sqrt{1-y^4}} - 1 \right) \right]\,. \tag{2.7.8}$$

In the limit of small ϵ we find

$$S_{ren} = -\frac{4\pi\sqrt{2\lambda}\,T}{\Gamma\left[\frac{1}{4}\right]^4} \frac{1}{\ell}\,. \tag{2.7.9}$$

The potential between two static quarks is Coulomb ($V(\ell) \sim 1/\ell$) because the theory is conformal. We also notice the the dependence on λ is $\sqrt{\lambda}$ for large λ, whereas at weak coupling it is λ.

2.8 Finite temperature AdS/CFT

To describe a CFT at finite temperature we must consider appropriate gravitational backgrounds, which are supposedly black holes, [29]. Possible thermal backgrounds dual to thermal $\mathcal{N} = 4$ SYM in $S^1 \times S^3$ spacetime are the thermal AdS background (which is the Euclidean AdS spacetime) and the Euclidean AdS-Schwarzschild black hole, which arises from the black D_3-brane solution after its reduction on the S^5. Making a Wick rotation in time coordinate t, time is made compact with period $\beta = \frac{1}{T}$, where T is the temperature. The metric reads

$$ds^2 = \left(1 + \frac{r^2}{L^2} - \frac{wM}{r^2}\right) dt^2 + \left(1 + \frac{r^2}{L^2} - \frac{wM}{r^2}\right)^{-1} dr^2 + r^2 d\Omega_3^2\,, \tag{2.8.1}$$

where $w = \frac{16 g_5}{3\pi^2,}$ and M is the ADM mass of the black hole. The boundary of the above metric is at $r = \infty$ and its topology is $S^1 \times S^3$, with radius of S^3 to be r. Taking $r \to \infty$

we recover $S^1 \times \mathbb{R}^3$ boundary. For $M = 0$ the above solution is the Euclidean AdS metric. In this case the t-coordinate circle is not contractible thus the temperature can be arbitrary. On the other hand the time circle is contractible for the black hole ($M \neq 0$) and the temperature is found by requiring that there is no conical singularity in the background

$$\beta = \frac{2\pi L^2 r_h}{2r_h^2 + L^2}\,, \tag{2.8.2}$$

with r_h being the position of the horizon. We observe that β has a maximum so that the temperature has a minimum. The effective radius of time circle S^1 is $\sqrt{g_{tt}}\beta$. Close to the boundary, we have $\beta_\infty = \frac{r}{L}\beta$. Then, we may define the dimensionless temperature, which is identified with the field theory dimensionless temperature, as

$$\mathcal{T} = \frac{R_{S^3}}{\beta_\infty} = \frac{L}{\beta} = \frac{2r_h^2 + L^2}{2\pi L r_h}\,, \tag{2.8.3}$$

where in the numerator of the second equality we have used that the radius of S^3 is $R_{S^3} = r$. There are two black holes for each temperature which have different horizon positions

$$r_h = \frac{\pi L^2}{\beta}\left[1 \pm \sqrt{1 - \frac{\beta^2}{\pi^2 L^2}}\right]\,. \tag{2.8.4}$$

Hence, there are black holes with horizon size $r_h < L$ which are qualitatively similar to Schwarzschild black holes in asymptotically flat spacetime, meaning that they are thermodynamically unstable due to Hawking radiation. In the second case, where $r_h > L$ the black hole is stable with positive specific heat.

As it is pointed out above, holography states that the generating functional of correlation functions in boundary field theory is equal to the functional of string theory in the bulk spacetime. As it is stated in Eq. (2.6.11), there can be different bulk manifolds $\mathcal{M}_i$ with the same boundary $\partial\mathcal{M}$. The string theory functional will receive contributions from string theories in all those saddle points. All of them have the same boundary conditions at $\partial\mathcal{M}$. We write this as

$$\mathcal{Z}_{FT}(\partial\mathcal{M}) = \mathcal{Z}_{\text{str}} \simeq \sum_i e^{-S_{\text{sugra}}(\mathcal{M}_i)} \simeq \sum_i e^{-N^2 F(\mathcal{M}_i)}\,, \tag{2.8.5}$$

where F is the free energy of the bulk theory. In our particular case, we have to compare the on-shell actions of the thermal AdS background and black hole in order

to find which has the minimum free energy. The action from which the metric (2.8.1) arises is

$$S_{sugra} = -\frac{1}{16\pi G_5}\int d^5x\,\sqrt{g}\left[R+\frac{12}{L^2}\right] - S_{HG}\,, \tag{2.8.6}$$

where the last term is the Hawking-Gibbons term which is important in order to have a well-defined variational problem, [16]. In our discussion it will not play any role since it will cancel in the difference of actions that we will consider. This happens because it is a boundary term and the backgrounds that we will compare have the same boundary asymptotics. However, this is not a general property. Hawking-Gibbons term should be taken into account in similar calculations in asymptotically AdS spacetime. The difference of the on-shell actions reads

$$\begin{aligned}\Delta S = S_{\rm bh} - S_{\rm th} &= \frac{1}{2\pi G_5 L^2}\int d\Omega_3\left[\int_0^{\beta} dt\int_{r_h}^{1/\epsilon} dr\, r^3 - \int_0^{\beta'} dt\int_0^{1/\epsilon} dr\, r^3\right]\\ &= \frac{\pi^2}{8G_5L^2}\left[\beta\left(\frac{1}{\epsilon^4}-r_h^4\right)-\frac{\beta'}{\epsilon^4}\right],\end{aligned} \tag{2.8.7}$$

where β and β' are such that the two metrics to be the same at the regulated boundary of spacetime which is at $r=\epsilon$. Then, $\beta'\sqrt{1+\frac{1}{\epsilon^2L^2}} = \beta\sqrt{1+\frac{1}{\epsilon^2L^2}-wM\epsilon^2}$ and the difference of the actions becomes

$$\Delta S|_{\epsilon\to 0} = \frac{\pi^3}{8G^5}\frac{r_h^3(L^2-r_h^2)}{2r_h^2+L^2} \tag{2.8.8}$$

Therfore, for $r_h < L$, thermal AdS background is favored and for $r_h > L$ the black hole is preferred. So, there is a phase transition in the corresponding boundary field theory at $\mathcal{T} = \frac{3}{2\pi}$. As it is argued in [29] the thermal AdS background is dual to a confined phase of the dual field theory, and the black hole to a deconfined phase.

2.9 Holographic 4D Yang Mills

Until now, we have studied the AdS/CFT correspondence between the conformal $\mathcal{N}=4$ SYM theory and type IIB supergravity in $AdS_5\times S^5$. Now, we will describe a holographic model which intends to describe 4-dimensional Yang-Mills (YM) gauge theory with no supersymmetry or conformal symmetry. The D-brane construction whose low energy limit is YM theory is not known yet and it is a very difficult problem to solve. Critical 10-dimensional string theory models describe successfully some qualitative IR

features of YM but they typically face the problem of Kaluza-Klein (KK) modes which have masses of order of the dynamical gauge theory scale, [30]. Hence, there is notable deviation of the holographic models from YM above this scale. Alternatively, non critical 5-dimensional string theory duals of YM gauge theory do not have KK modes but the two-derivative supergravity action is not expected to be a good approximation for large-N_c YM, [31]. In general, there are higher curvature terms in the action which are of the string scale. Therefore, the expansion in powers of α' cannot be trusted.

An alternative scenario is the construction of semi-phenomenological holographic models which describe the main IR features of YM theory. In the original models, the gravitational background is an AdS_5 slice with a constant dilaton in it, [33]. Boundary conditions are set in the IR and UV cutoffs of space. In this approach, main phenomena such as confinement and chiral symmetry breaking (in the meson sector) are described by setting certain boundary conditions.

The model which will be analyzed here is an effective holographic model for pure large-N_c, 4-dimensional YM theory and is named Improved Holographic QCD (IHQCD), [34], [35]. It is built by using intuition from string theory and matching the asymptotics of the solutions to expectations from QCD. The action is (4+1)-dimensional Einstein-dilaton gravity with a well-chosen dilaton potential. The main bulk fields are dual to the operators of the YM with the lowest dimension in the UV. The graviton is dual to the energy-momentum tensor $T_{\mu\nu} \simeq \mathbb{T}r\left[F_{\mu\rho}F^{\rho}_{\nu} - \frac{\delta_{\mu\nu}}{4}F^2\right]$, the dilaton, dual to $\mathbb{T}r\left[F^2\right]$ and the axion is dual to $\mathbb{T}r\left[F\wedge F\right]$. Moreover, the model should contain a RR four form which sources the D_3-branes which is non propagating in 5 dimensions. It can be integrated out though and generate new terms in the dilaton potential. It is also assumed that higher curvature and derivative terms generate a finite constant term in the dilaton potential when they integrated out, for more details see [34]. In terms of the holographic 't Hooft coupling $\lambda \equiv e^{\Phi}$, the bulk action is

$$S = M_p^3 N_c^2 \int d^5x\sqrt{-g}\left[R - \frac{4}{3}\frac{(\partial\lambda)^2}{\lambda^2} + V(\lambda) - \frac{Z(\lambda)}{2N_c^2}(\partial\alpha)^2\right], \tag{2.9.1}$$

where M_p is the Planck mass, related to the (4+1)-dimensional Newton's constant G_5 as $M_p^3 = 1/(16\pi G_5 N_c^2)$, $V(\lambda)$ is the dilaton potential. $Z(\lambda)$ encodes the interaction of the axion with the dilaton. This term in suppressed with respect to the rest of the action by a factor of $\frac{1}{N_c^2}$, because axion is a RR field in string theory and its action has not the $e^{-2\Phi}$ factor, [35]. In case of $V(\lambda) = 12/L^2$ with a constant length scale L, the action becomes as Eq.(2.8.6). One solution of the equations of motion is constant λ and an AdS metric with radius of curvature L, Eq.(2.5.11).

For a general $V(\lambda)$, the background solutions have the general form

$$ds^2 = e^{2A_0(z)}(dz^2 + \eta_{\mu\nu}dx^\mu dx^\nu)\ ,\ \ \lambda = \lambda(z)\,, \tag{2.9.2}$$

where $e^{A_0(z)}$ is the metric scale factor. As $z \to 0$, the metric approaches AdS_5, so $e^{A_0(z)} \to L/r + \mathcal{O}(1/\log(r))$ and that λ vanishes logarithmically, $\lambda \to -1/\log r$, so as to match the running of the large-N_c YM coupling.

Pure YM theory is strongly coupled in the IR and weakly coupled in the UV. So, large-N_c YM in the IR regime, is expected to have a two-derivative gravitational dual theory which will describe the $z \to \infty$ region (which corresponds to the IR of the field theory) appropriately. As it is mentioned above, intuition from AdS/CFT yields that the AdS coordinate corresponds to the energy scale of the boundary field theory. The boundary region of AdS corresponds to the UV of the theory where the coupling is small. Then, the low energy supergravity description is not valid. However, the equations of motion of the bulk fields are solved in the whole region from $z = \infty$ to $z = \epsilon \to 0$, where the boundary conditions of the fields are set. Then, as it is mentioned in section (2.6) the physical observables of the field theory are computed in the gravity side by the bulk solution for th fields and by setting the suitable boundary conditions at $z = \epsilon$. The role of the axion field will not be analyzed in this section because it is suppressed by $1/N_c^2$ compared to the background field. It is described though in detail in chapter 7.

The IHQCD describes the IR phenomena of YM theory. One needs however the UV asymptotics of the two dual theories to be matched. For instance, to find the YM free energy for $T \gtrsim T_c$ with the correct normalization, the IHQCD free energy should follow Stefan-Boltzmann law of a gluon gas at high T. This determines L in units of the Planck mass, $(M_pL)^{-3} = 45\pi^2$, [36].

The perturbative UV β-function of YM constrains the asymptotics of $V(\lambda)$ in the $z \to 0$ region, where $\lambda \to 0$. It is found that $V(\lambda)$ has a regular series expansion

$$V(\lambda) = \frac{12}{L^2}\left(1 + v_0\lambda + v_1\lambda^2 + \mathcal{O}\left(\lambda^3\right)\right). \tag{2.9.3}$$

Matching field theory energy scale to AdS coordinate, $E \equiv E_0\, e^{2A_0(z)}$, where E_0 can be fixed by matching to the lowest glueball mass, determines the coefficients v_0 and v_1 in terms of the coefficients of the perturbative large-N_c YM β-function:

$$\beta(\lambda_t) = -\beta_0\lambda_t^2 - \beta_1\lambda_t^3 + \mathcal{O}(\lambda_t^4)\ ,\ \ \beta_0 = \frac{22}{3(4\pi)^2}, \qquad \beta_1 = \frac{51}{121}\beta_0^2\,, \tag{2.9.4a}$$

where λ_t is taken to be 't Hooft coupling and

$$v_0 = \frac{8}{9}\beta_0, \qquad v_1 = \frac{4}{9}\beta_1 + \frac{23}{81}\beta_0^2\,. \tag{2.9.4b}$$

In the vacuum solutions, generically λ diverges at the bottom of spacetime. IR features of the theory constrain the IR aymptotics of the potential, which is

$$V(\lambda) \propto \lambda^{2Q}(\log\lambda)^{P}\,. \tag{2.9.5}$$

The potential presents a good IR singularity for $Q < 2\sqrt{2}/3$. A good singularity is a repulsive singularity, which cannot be probed arbitrarily deep by finite energy modes, [37]. It also generates a confining background for $Q > 2/3$ or $Q = 2/3$ and $P > 0$. The most common choice is $Q = 2/3$. $P = 1/2$ in order for the asymptotic glueball spectra for large excitation number, n, to be linear. Therefore,

$$V(\lambda) \propto \lambda^{\frac{4}{3}}\sqrt{\log\lambda}\,. \tag{2.9.6}$$

The asymptotic solution of the fields in the IR reads

$$e^{2A_0(z)} \propto e^{-(z\Lambda_{IR})^2}\ ,\ \ \lambda(z) \propto z\Lambda_{IR}\ e^{\frac{3}{2}(z\Lambda_{IR})^2}\,, \tag{2.9.7}$$

where Λ_{IR} is a scale determined by the value of λ at the boundary $z = \epsilon$. The IR asymptotics of $e^{2A_0(z)}$ are such that there is confinement in the dual field theory. The metric actually has a repulsive singularity at $r = \infty$, which guarantees that we do not need extra boundary conditions at $z \to \infty$ when we solve for the fluctuations of the fields in order to determine the spectrum of the theory.

2.9.1 The quark-antiquark potential in the IHQCD

We now follow the analysis of section 2.7, in order to compute the static potential of a quark-antiquark pair in the IHQCD, [34], which is a criterion for confinement. The Wilson loop is computed by the Nambu-Goto action of a string stretching in the bulk spacetime and its endpoints in a rectungular loop with sides ℓ (distance of the quark-antiquark pair) and T (time interval of evolution of the system). We consider a general form for the 5-dimensional metric

$$ds^2 = g_{zz}(z)dz^2 - g_{00}(z)dt^2 + g_{xx}(z)d\vec{x}^2\,. \tag{2.9.8}$$

In [28], it was showed, for differentiable worldsheets, that the on-shell action produces a potential

$$V(\ell) = \frac{1}{2\pi\ell_s}f(z_F)\ell - 2T_f\int_\epsilon^{z_F} ds\frac{g(z)}{f(z)}\sqrt{f^2(z) - f^2(z_F)} \tag{2.9.9}$$

where ϵ is the location of the boundary of spacetime and z_F is the turning point of the worldsheet. $f(s)$ and $g(s)$ are defined as

$$f^2(z) = g_{00}(z)g_{xx}(z)\,,\; g^2(z) = g_{00}(z)g_{zz}(z) \tag{2.9.10}$$

From momentum conservation, it is found that z_F depends on ℓ

$$\ell = 2\int_\epsilon^{z_F} dz \frac{g(z)}{f(z)} \frac{1}{\sqrt{f^2(z)/f^2(z_F) - 1}}, \tag{2.9.11}$$

In the limit of large ℓ, the second term in Eq. (2.9.9) is suppressed.

Witting the metric in Einstein frame, we have

$$(g_S)_{\mu\nu}(z) = e^{2A_S(z)}\eta_{\mu\nu}\,,\; A_S(z) = A(z) + \frac{2}{3}\Phi(z)\,,\; f(z) = g(z) = e^{2A_S(z)}\,, \tag{2.9.12}$$

and Eq. 2.9.11 becomes

$$\ell = 2\int_\epsilon^{z_F} dz \frac{1}{\sqrt{e^{4A_S(z) - 4A_S(z_F)} - 1}}. \tag{2.9.13}$$

Close to $z = \epsilon \to 0$ the integral is finite, because the integrand behaves as $e^{-2A_S(z)} \sim z^2$. Then $z_F \sim \ell^3$ for small ℓ. In the vicinity of z_F the denominator reads

$$\frac{1}{\sqrt{e^{4A_S(z) - 4A_S(z_F)} - 1}} \simeq \frac{1}{\sqrt{4A_S'(z_F)(z_F - z) + 8A_S''(z_F)(z_F - z)^2 + \ldots}}\,. \tag{2.9.14}$$

In general, the integral in Eq. (2.9.13) is finite, except for the case that $z_F \to z_*$, where z_* is the location of a minimum of $A_S(z)$, $A_S'(z_*) = 0$. Then, the integral goes to infinity. Hence,

$$z_F \to z_* \;\; as \;\; \ell \to \infty. \tag{2.9.15}$$

Eq. (2.9.9) yields that the quark-antiquark potential energy is

$$V(\ell) \sim \frac{e^{2A_S(r_*)}}{2\pi\ell_s^2}\ell \tag{2.9.16}$$

which exhibits an area law if and only if A_S is finite at its minimum. This requirement constraints the dilaton potential, in Eq. (2.9.5), to have $Q > 2/3$ and $P > 0$.

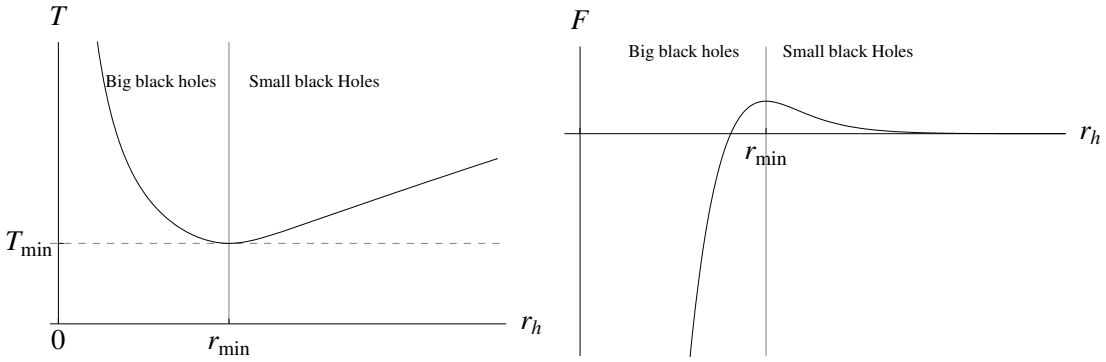

Figure 2.5: The two branches of black hole solution in the IHQCD. Left: The temperature in terms of the horizon radius. We observe that for each temperature above T_{min}, there is a small and large black hole branch. Right: The free energy of two black hole branches in terms of the horizon radius.

2.9.2 Holographic 4D Yang Mills at finite temperature

Action (2.9.1) has also black hole solutions which is dual to a finite quantum field theory as states in section 2.8, [36]. We consider a metric of the form

$$ds^2 = e^{2A(z)}\left(\frac{dz^2}{f(z)} - f(z)dt^2 + dx^i dx_i\right) . \tag{2.9.17}$$

The function $f(z)$ has roots, $f(z_h) = 0$, which indicate the position of the black hole horizon ($z = z_h$). The corresponding Hawking temperature can be calculated by applying a Wick rotation in time coordinate and making compact with period β. The temperature then reads $T = 4\pi f'(z_h)$. As in the simple case of action ((2.8.6)), black hole solutions only exist for temperatures above a value $T_{\rm min}$, and in fact two branches of solutions exist, the large and small black holes for $z_h > L$ and $z_h < L$ respectively, see Fig. (2.5). Near horizon asymptotics of the scale factor are $e^{A(z\to z_h)} = $ const. for both branches. Its actual value determines the entropy density, $s = e^{3A(z_h)}/(4G_5)$, and as $z \to 0$, $A(z) \to -\log(r/L)$, indicates that the field theory thermal energy density and pressure are both of order N_c^2.

There is also another possible background solution at finite T which is the Euclidean form of (2.9.2), and is called the thermal gas background. As mentioned above, the thermodynamically preferred vacuum of the theory is the one with the less free energy, which is dual to the bulk on-shell Euclidean action, see Fig. (2.5). The system sits in the thermal gas vacuum for low temperature and at $T = T_c$ it undergoes a first order phase transition to the large black hole background. The thermal gas solution is dual

to a confined phase of the gauge theory and the black hole corresponds to a deconfined phase.

Eventually, the potential which was used for the numerical solution of the equations of motion is of the form

$$V(\lambda) = \frac{12}{\ell^2}\left[1 + V_0\lambda + V_1\lambda^{4/3}\sqrt{\log\left(1 + V_2\lambda^{4/3} + V_3\lambda^2\right)}\right] . \tag{2.9.18}$$

the parameters V_0 and V_2 are determined by the matching of the β-function coefficients to the near boundary expansion of $V(\lambda)$. Then, V_1 and V_3 are determined by matching to lattice results for two thermodynamic quantities of large-N_c YM, the latent heat at $T = T_c$ and the pressure at $T = 2T_c$. Then, the model describes succesfully various IR features of the theory at $T = 0$, like glueball spectrum and several thermodynamic quantities at finite T.

2.10 Tachyon AdS/QCD

In this section, we will try to set a general framework for the holographic study of the flavor sector of QCD. The most striking low-energy phenomenon, related to flavors, in QCD is chiral symmetry breaking, $U(N_f)_L \times U(N_f)_R \to U(N_f)_V$, where N_f is the number of flavors. Initially, top-down models were formulated by taking N_f branes in non-supersymmetric backgrounds generated by N_c color branes, [38]. In this context, $U(1)_A$ is an isometry of spacetime and it breaks due to the flavor branes. Then, one reproduces correctly the Gell Mann-Oakes-Renner (GOR) relation for the quark condensate for small quark mass, $f_\pi^2 m_\pi^2 = -2m_q\langle\bar{q}q\rangle$. The shortcoming of this model is that the flavor symmetry can not be generalized to the non-abelian case. Another approach is the Sakai-Sugimoto model where N_f probe D_8-$\overline{D}_8$ branes are put in a D_4-brane background, with $N_f << N_c$ so they do not backreact to the geometry, [39]. Chiral symmetry, $U(N_f)_L \times U(N_f)_R$, is generated by the brane-antibrane pairs and breaks due to the recombination of the pairs in the IR of background spacetime. Successes of the model include N_f^2 massless Goldstone bosons in the spectrum, calculation of chiral anomaly by WZW term and good phenomenological fit of low mass meson states to experimental data. The main disadvantage of the model is the absence of parameter which corresponds to quark mass or condensate and the fact that there are no massive pseudoscalar states in the spectrum.

The flavor sector of QCD can be also described by using phenomenological holographic models, mostly called AdS/QCD models, [40]. In those approaches, the back-

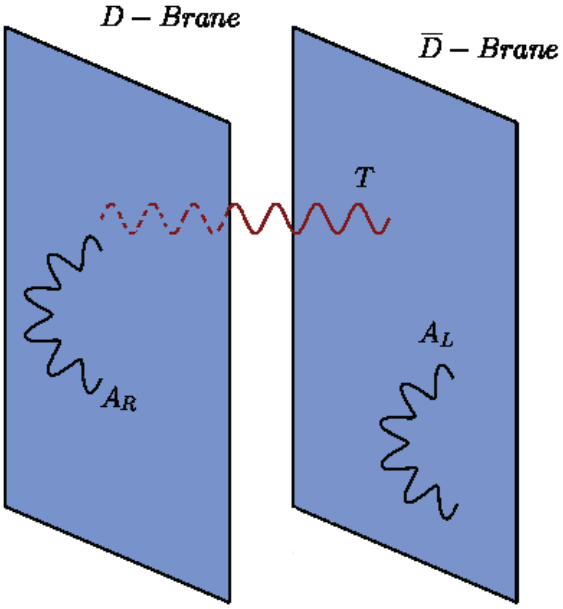

Figure 2.6: A system of D − $\bar{\text{D}}$ branes. The lightest states from the strings attached to them is a complex scalar, a left and right gauge field.

ground spacetime is usually AdS_5, which has either an IR cutoff or some modified IR geometry which reproduces confinement and other IR features of QCD. Then, the bulk action which describes the dual quark bilinear operators is introduced by hand. It usually contains a left and right vector fields corresponding to the left and right flavor currents of QCD and a bulk scalar field which is dual to $\bar{q}q$ and it receives an non-trivial vacuum expectation value by IR boundary conditions which are set by hand. Such models successfully incorporate characteristics as GOR relation, the existence of Goldstone bosons, vector meson dominance. The fit of the models to experimental data is also at the order of 10%.

We will now present a phenomenological holographic model which is a fusion of Sakai-Sugimoto and AdS/QCD models, [41]. Initially, a confining asymptotically AdS background of the form

$$ds_5^2 = g_{xx}(z)\eta_{\mu\nu} + g_{zz}(z)dz^2 \ , \ \ g_{xx}(z\to 0) = g_{zz}(z\to 0) = \frac{L^2}{z^2} + \dots \qquad (2.10.1)$$

is used where a stack of N_f coincident D_p brane- $\overline{\text{D}}_p$ antibrane pairs is introduced.

The lightest state of the string stretching among the branes and antibranes is the open string tachyon field and transforms under $U(N_f)_L \times U(N_f)_R$. This is a complex scalar which is dual to the operator $\overline{q}q$. Strings having both their endpoints on D/$\bar{\text{D}}$ brane transform in the adjoint of $U(N_f)_{L/R}$ and their lightest state is a vector field $A_{L/R}$ dual to the left/right flavor current of QCD, see figure (2.6). The low energy regime of the system is studied using a generalization of DBI and WZW action, including the tachyon field.

The DBI action for the simpler case of one D$_p$ brane- $\overline{\text{D}}_p$ antibrane pair reads

$$S = -\int d^{p+1}x\, V(\tau^2)\left(\sqrt{-\det \mathbf{A}_L} + \sqrt{-\det \mathbf{A}_R}\right) , \tag{2.10.2}$$

where

$$\begin{aligned} A_{(i)MN} &= \hat{g}_{MN} + 2\pi\alpha' F^{(i)}_{MN} + \pi\alpha'(D_M T)^*(D_N T) + \pi\alpha'(D_N T)^*(D_M T) \\ F^{(i)}_{MN} &= \partial_M A^{(i)}_N - \partial_N A^{(i)}_M \ , \ \ D_M T = (\partial_M + iA^L_M - iA^R_M)T \, , \end{aligned} \tag{2.10.3}$$

where $i = L, R$ and $\hat{g}$ is the pullback of the background metric on the worldvolume of the brane-antibrane pair, where B_{MN} and transverse scalars are not included since they do not have a dual interpretation in QCD. Hence, the flavor fields are the complex tachyon $T = \tau e^{i\theta}$, form which τ is dual to $\overline{q}q$ and θ to $\overline{q}\gamma_5 q$. $A_{L/R}(x)$ are dual to $\overline{q}_{l/R}\gamma_\mu q_{L/R}$ currents of QCD. The tachyon potential in front of the action is derived in flat background using string field theory

$$V(\tau) = \mathcal{K} e^{-\mu^2\tau^2} \, . \tag{2.10.4}$$

This potential cannot be generalized straightforwardly in curved backgrounds. However, in this context the above form of the potential is assumed. As it will be shown in chapter 4, eventually this choice of potential leads to many expected characteristics of QCD in the IR regime like linear Regge trajectories for highly excited mesons. Most of the other physical observables do not depend on the details of the potential.

The vacuum solution that arises from the action (2.10.2) has $A_L = A_R = \theta = 0$ and $\tau = \tau(z)$. The worldvolume action (2.10.2) for τ is

$$S = -2\mathcal{K}\int d^4x dz e^{-\frac{1}{2}\mu^2\tau^2} g_{tt}^{\frac{1}{2}} g_{xx}^{\frac{3}{2}} \sqrt{g_{zz} + 2\pi\alpha'\lambda(\partial_z\tau)^2} \tag{2.10.5}$$

and the corresponding equation of motion:

$$\tau'' + 4\pi\alpha' \frac{g'_{xx}}{g_{xx}g_{zz}}\tau'^3 + \frac{\tau'}{2}\left(4\frac{g'_{xx}}{g_{xx}} - \frac{g'_{zz}}{g_{zz}}\right) + \left(\frac{g_{zz}}{2\pi\alpha'} + \tau'^2\right)\mu^2\tau = 0 \, . \tag{2.10.6}$$

Eq. (2.6.10), relates the mass of the tachyon bulk field to the dimension of the $\overline{q}q$

$$\frac{L^2\mu^2}{2\pi\alpha'} = 3\,. \tag{2.10.7}$$

The solution of (2.10.6) close to the the boundary of spacetime $z = 0$ is

$$\tau = (m_q z + \dots) + (\sigma z^3 + \dots) \tag{2.10.8}$$

The first term is a non-normalizable solution which corresponds to the source of the dual operator, the coupling in the boundary field theory $\int d^4x\, m_q\, \overline{q}(x)q(x)$. The parameter σ is proportional to $\langle\overline{q}q\rangle$. σ is related to m_q by requesting regularity at IR. In case of this model the regularity condition is $\tau_{IR} = \infty$. This condition is natural to consider in order to reproduce correctly the dual field theory anomaly.

Using the Wilson loop criterion, presented in (2.7), for the background (2.10.1) we find that it describes a confined gauge theory if at some z_0, $g_{zz}(z_0) \to \infty$ while $g_{xx}(z_0)$ is finite. Assuming to have a metric with $g_{zz} = b(z_0 - z)^{-1}$, the solution of Eq.(2.10.6) for large τ is of the form $\tau \simeq (z_0 - z)^n$, where $n = \frac{\mu^2}{4\pi\alpha'}\left.\frac{g_{xx}}{g'_{xx}}\right|_{z=z_0}$. Usually the derivative of g_{xx} is negative, therefore the tachyon diverges. The tachyon, τ, may diverge only at the end of AdS coordinate.

It was argued above, that confining gravitational backgrounds lead to chiral symmetry breaking, $U(N_f)_L \times U(N_f)_R \to U(N_f)_V$, through the diverging tachyon in the IR. In [42], Coleman and Witten proved that in the large N_c massless QCD chiral symmetry is spontaneously broken if the following assumptions hold:

1. existence of the large N_c limit of QCD.
2. Confinement at large N_c.
3. There is one order parameter of the spontaneous breaking, that is $\overline{q}q$ operator transforming in the bifundamental of $U(N_f)_L \times U(N_f)_R$.
4. Its vev can be found by minimizing some potential.
5. The potential does not have degenerate minima.

For any holographic QCD model, the assumptions 1) and 2) are true. Since, there is not an exact string theory dual of QCD until now, one should also assume the existence of a hologrphic dual of QCD. Assumption 3) and 4) are automatic in our model since the tachyon field, which is dual to $\overline{q}q$, provides us with the necessary order parameter of the symmetry breaking. The vev, $\langle\overline{q}q\rangle$ is found by minimizing the bulk action. In other

words, we solve the equations of motion of the tachyon with UV boundary condition $m_q = 0$ and IR regularity condition $\tau_I R \to \infty$. This determines holographically $\langle \overline{q} q \rangle$. The final assumption, 5), cannot be proven in the general set-up which is considered here. This should be taken as a further assumption of the present setup. Hence, the Tachyon AdS/QCD provides holographic version of Coleman-Witten theorem.

Gell-Mann-Oakes-Renner relation is also proved holographically in the context of the Tachyon AdS/QCD model, see section 4.5.4. We consider an expansion of the pseudoscalar fluctuation equation for small pseudoscalar mass, which is identified with pion mass. Pion decay constant is defined as the pole of the axial-vector current two-point function at zero momentum. This is determined by solving the fluctuation equation of the bulk axial-vector wavefunction, with the appropriate boundary conditions. Then, one can prove the GOR relation, $-4m_q\langle \overline{q} q \rangle = m_\pi^2 f_\pi^2$, which holds in the limit $m_q \to 0$.

Another appealing feature of the model is that the generic IR behavior of the tachyon potential yields linear Regge trajectories for the masses of the fluctuations in terms of the excitation number, n, as $n \to \infty$, see section 4.5.1.1. The tachyon potential decreases exponentially in the IR if the tachyon asymptotes toinfinity, (2.10.4). If one formulates the fluctuation equations in Schrödinger form, the corresponding Schrödinger potentials asymptote to the IR as $V(u) \sim u^2$, where u is the Schrödinger AdS coordinate. WKB approximation then shows that the masses of the fluctuations follow linear Regee trajectories for large n.

The Wess-Zumino coupling of a pair of branes-antibranes is a generalization of the standard term, (2.3.104), and it correctly reproduces the flavor anomaly of QCD if $\tau(z \to z_0) = \infty$, as it will be analyzed in chapter 5.

Bibliography

[1] M. B. Green, J. H. Schwarz, E. Witten, *"Superstring Theory, Vols. I and II,"* Cambridge University Press, Cambridge, 1987. 10

[2] J. Polchinski, *"String Theory, Vols. I and II,"* Cambridge University Press, Cambridge, 1998. 10

[3] E. Kiritsis, *"String Theory in a Nutshell,"* Princeton University Press, Princeton, 2007. 10, 12, 40

[4] K. Becker, M. Becker, J. Schwarz, *"String Theory and M-theory,"* Cambridge University Press, Cambridge, 2007. 10, 12

[5] R. Blumenhagen, D, Lüst, S. Theisen, *"Basic Concepts of String Theory,"* Springer, 2013. 10, 12

[6] C. V. Johnson, *"D-branes,"* Cambridge University Press, Cambridge, 2003. 10, 12

[7] B. Zwiebach, *"A first Course in String Theory,"* Cambridge University Press, Cambridge, 2004. 10

[8] M. Rocek, P. van Nieuwenhuizen, *"Introduction to Modern String theory,"* Unpublished Lecture Notes. 10

[9] E. Kiritsis, *"Introduction to superstring theory,"* (Leuven notes in mathematical and theoretical physics. B9) [ArXiv:hep-th/9709062]. 10

[10] D. Tong, *"String Theory,"* [ArXiv:0908.0333][hep-th]. 10

[11] G. Veneziano, *"Construction of a crossing - symmetric, Regge behaved amplitude for linearly rising trajectories,"* Nuovo Cim. A **57** (1968) 190. 10

[12] H. Fritzsch, M. Gell-Mann, Proceedings of the International Conference on Duality and Symmetry, Tel-Aviv, 1971;

H. Fritzsch, M. Gell-Mann, Proc. XVI Intern. Conf. on High energy physics, Chicago, **2** (1972), 135 ;
H. Fritzsch, M. Gell-Mann and H. Leutwyler, *"Advantages of the Color Octet Gluon Picture,"* Phys. Lett. B **47** (1973) 365. 10

[13] D.J. Gross, F. Wilczek, *"Ultraviolet behavior of non abelian gauge theories,"* Phys. Rev. Lett. **30** (26) 1973 1343-1346. 10

[14] David H. Politzer, *"Reliable Perturbative Results for Strong Interactions?"* Phys. Rev. Lett., **30** (26) (1973) 1346 -1349. 10

[15] G. 't Hooft, *"A Planar Diagram Theory for Strong Interactions,"* Nucl. Phys. B **72** (1974) 461. 11

[16] G. W. Gibbons and S. W. Hawking, *"Action Integrals and Partition Functions in Quantum Gravity,"* Phys. Rev. D **15** (1977) 2752. 53

[17] J. M. Maldacena, *"The large N limit of superconformal field theories and supergravity,"* Adv. Theor. Math. Phys. **2**, 231 (1998) [Int. J. Theor. Phys. **38**, 1113 (1999)] [ArXiv:hep-th/9711200];
S. S. Gubser, I. R. Klebanov and A. M. Polyakov, *"Gauge theory correlators from non-critical string theory,"* Phys. Lett. B **428**, 105 (1998) [ArXiv:hep-th/9802109];
E. Witten, *"Anti-de Sitter space and holography,"* Adv. Theor. Math. Phys. **2**, 253 (1998) [ArXiv:hep-th/9802150]. 11

[18] J. Dai, R. G. Leigh, J. Polchinski, *"New Connections Between String Theories„"* Mod. Phys. Lett. **A4** (1989) 2073. 11

[19] J. Polchinski, *"Dirichlet Branes and Ramond-Ramond charges„"* Phys. Rev. Lett. **75** (1995) 4724-4727 [ArXiv:hep-th/9510017]. 11, 31, 38

[20] G. T. Horowitz and A. Strominger, *"Black strings and P-branes,"* Nucl. Phys. B **360** (1991) 197. 11

[21] O. Aharony, S. S. Gubser, J. M. Maldacena, H. Ooguri and Y. Oz, *"Large N field theories, string theory and gravity,"* Phys. Rept. **323** (2000) 183 [ArXiv:hep-th/9905111]. 12

[22] A. Zaffaroni, *"Introduction to the AdS-CFT correspondence,"* Class. Quant. Grav. **17** (2000) 3571. 12

[23] D. Mateos, *"String Theory and Quantum Chromodynamics,"* Class. Quant. Grav. **24**, S713 (2007) [ArXiv:0709.1523][hep-th]. 12

[24] S. Coleman *"Aspects of Symmetry: Selected Erice Lectures,"* Cambridge University Press, Cambridge, 1995. 12

[25] A. V. Manohar, *"Large N QCD,"* [ArXiv:hep-ph/9802419]. 12

[26] P. Breitenlohner and D. Z. Freedman, *"Positive Energy in anti-De Sitter Backgrounds and Gauged Extended Supergravity," http://www.sciencedirect.com/science/article/pii/037026938290643*8Phys. Lett. B **115** (1982) 197;
P. Breitenlohner and D. Z. Freedman, *"Stability in Gauged Extended Supergravity,"* Annals Phys. **144** (1982) 249. 48

[27] S. J. Rey and J. T. Yee, *"Macroscopic strings as heavy quarks in large N gauge theory and anti-de Sitter supergravity,"* Eur. Phys. J. C **22**, 379 (2001) [ArXiv:hep-th/9803001];
J. M. Maldacena, *"Wilson loops in large N field theories,"* Phys. Rev. Lett. **80**, 4859 (1998) [ArXiv:hep-th/9803002]. 50

[28] Y. Kinar, E. Schreiber and J. Sonnenschein, *"Q anti-Q potential from strings in curved spacetime: Classical results,"* Nucl. Phys. B **566**, 103 (2000) [ArXiv:hep-th/9811192]. 50, 56

[29] E. Witten, *"Anti-de Sitter space, thermal phase transition, and confinement in gauge theories,"* Adv. Theor. Math. Phys. **2** (1998) 505 [ArXiv:hep-th/9803131]. 51, 53

[30] J. M. Maldacena and C. Nunez, *"Towards the large N limit of pure N = 1 super Yang Mills,"* Phys. Rev. Lett. **86** (2001) 588 [ArXiv:hep-th/0008001];
A. H. Chamseddine and M. S. Volkov, *"Non-Abelian BPS monopoles in N = 4 gauged supergravity,"* Phys. Rev. Lett. **79** (1997) 3343 [ArXiv:hep-th/9707176];
I. R. Klebanov and M. J. Strassler, *"Supergravity and a confining gauge theory: Duality cascades and χSB-resolution of naked singularities,"* JHEP **0008** (2000) 052 [ArXiv:hep-th/0007191]. 53

[31] S. Kuperstein and J. Sonnenschein, *"Non-critical supergravity (d > 1) and holography,"* JHEP **0407** (2004) 049 [ArXiv:hep-th/0403254];
S. Kuperstein and J. Sonnenschein, *"Non-critical, near extremal AdS_6 background*

as a holographic laboratory of four dimensional YM theory," JHEP **0411** (2004) 026 [ArXiv:hep-th/0411009];
I. R. Klebanov and J. M. Maldacena, *"Superconformal gauge theories and non-critical superstrings,"* Int. J. Mod. Phys. A **19** (2004) 5003 [ArXiv:hep-th/0409133];
F. Bigazzi, R. Casero, A. L. Cotrone, E. Kiritsis and A. Paredes, *"Non-critical holography and four-dimensional CFT's with fundamentals,"* JHEP **0510**, 012 (2005) [ArXiv:hep-th/0505140];
R. Casero, A. Paredes and J. Sonnenschein, *"Fundamental matter, meson spectroscopy and non-critical string / gauge duality,"* JHEP **0601**, 127 (2006) [ArXiv:hep-th/0510110]. 54

[32] F. Bigazzi, R. Casero, A. L. Cotrone, E. Kiritsis and A. Paredes, *"Non-critical holography and four-dimensional CFT's with fundamentals,"* JHEP **0510** (2005) 012 [ArXiv:hep-th/0505140];
R. Casero, C. Nunez and A. Paredes, *"Towards the string dual of N=1 SQCD-like theories,"* Phys. Rev. D **73** (2006) 086005 [ArXiv:hep-th/0602027];
C. Nunez, A. Paredes and A. V. Ramallo, *"Unquenched Flavor in the Gauge/Gravity Correspondence,"* Adv. High Energy Phys. **2010** (2010) 196714 [ArXiv:1002.1088][hep-th].

[33] J. Polchinski and M. J. Strassler, *"Hard scattering and gauge / string duality,"* Phys. Rev. Lett. **88**, 031601 (2002) [ArXiv:hep-th/0109174]. 54

[34] U. Gursoy and E. Kiritsis, *"Exploring improved holographic theories for QCD: Part I,"* JHEP **0802** (2008) 032 [ArXiv:0707.1324][hep-th];
U. Gursoy, E. Kiritsis and F. Nitti, *"Exploring improved holographic theories for QCD: Part II,"* JHEP **0802** (2008) 019 [ArXiv:0707.1349] [hep-th]. 54, 56

[35] E. Kiritsis, *"Dissecting the String Theory Dual of QCD,"*, *Fortsch.Phys.* **57** (2009) 396–417, [arXiv:0901.1772]. 54

[36] U. Gursoy, E. Kiritsis, L. Mazzanti and F. Nitti, *"Deconfinement and Gluon Plasma Dynamics in Improved Holographic QCD,"* Phys. Rev. Lett. **101**, 181601 (2008) [ArXiv:0804.0899][hep-th];
U. Gursoy, E. Kiritsis, L. Mazzanti and F. Nitti, *"Holography and Thermodynamics of 5D Dilaton-gravity,"* JHEP **0905** (2009) 033 [ArXiv:0812.0792][hep-th];
U. Gursoy, E. Kiritsis, L. Mazzanti and F. Nitti, *"Improved Holographic QCD at finite Temperature: comparison with data,"* Nucl. Phys. B **820** (2009) 148 [ArXiv:0903.2859][hep-th];

U. Gursoy, E. Kiritsis, G. Michalogiorgakis and F. Nitti, *"Thermal Transport and Drag Force in Improved Holographic QCD,"* JHEP **0912** (2009) 056 [ArXiv:0906.1890][hep-ph]. 55, 57

[37] S. S. Gubser, Adv. Theor. Math. Phys. **4** (2000) 679 [hep-th/0002160]. 56

[38] J. Babington, J. Erdmenger, N. J. Evans, Z. Guralnik and I. Kirsch, *"Chiral symmetry breaking and pions in non-supersymmetric gauge / gravity duals,"* Phys. Rev. D **69**, 066007 (2004). [ArXiv:hep-th/0306018];
N. J. Evans and J. P. Shock, *"Chiral dynamics from AdS space,"* Phys. Rev. D **70**, 046002 (2004) [ArXiv:hep-th/0403279];
M. Kruczenski, D. Mateos, R. C. Myers and D. J. Winters, *"Towards a holographic dual of large-N(c) QCD,"* JHEP **0405**, 041 (2004) [ArXiv:hep-th/0311270]. 59

[39] T. Sakai and S. Sugimoto, *"Low energy hadron physics in holographic QCD,"* Prog. Theor. Phys. **113**, 843 (2005) [ArXiv:hep-th/0412141]. 59

[40] J. Erlich, E. Katz, D. T. Son and M. A. Stephanov, *"QCD and a Holographic Model of Hadrons,"* Phys. Rev. Lett. **95**, 261602 (2005) [ArXiv:hep-ph/0501128];
L. Da Rold and A. Pomarol, *"Chiral symmetry breaking from five dimensional spaces,"* Nucl. Phys. B **721**, 79 (2005) [ArXiv:hep-ph/0501218];
A. Karch, E. Katz, D. T. Son and M. A. Stephanov, *"Linear Confinement and AdS/QCD,"* Phys. Rev. D **74**, 015005 (2006) [ArXiv:hep-ph/0602229]. 59

[41] R. Casero, E. Kiritsis and A. Paredes, *"Chiral symmetry breaking as open string tachyon condensation,"* Nucl. Phys. B **787**, 98 (2007) [ArXiv:hep-th/0702155]. 59

[42] S. R. Coleman and E. Witten, *"Chiral Symmetry Breakdown In Large N Chromodynamics*, Phys. Rev. Lett. **45**, 100 (1980). 62

3

AdS/QCD model from an effective action for open string tachyons.

Authors : Ioannis Iatrakis[a], Elias Kiritsis[a,b], Ángel Paredes[c]

[a] Crete Center for Theoretical Physics, Department of Physics, University of Crete, 71003 Heraklion, Greece.

[b] APC, Université Paris 7, Bâtiment Condorcet, F-75205, Paris, France (UMR du CNRS 7164).

[c] Departament de Física Fontamental and ICCUB Institut de Ciències del Cosmos, Universitat de Barcelona, Martí i Franquès, 1, E-08028, Barcelona, Spain.

3.1 Abstract

We construct a new, simple phenomenological model along1 the lines of AdS/QCD. The essential new ingredient in the brane-antibrane effective action including the open string tachyon was proposed by Sen. Chiral symmetry breaking happens because of tachyon dynamics. We fit a large number of low-spin meson masses at the 10 %-15 % level. The only free parameters involved in the fits correspond to the overall QCD scale and the quark masses. Several aspects of previous models are qualitatively improved.

3.2 Introduction

Understanding the strong dynamics underlying many observations related to the strong interaction remains an unsolved problem. Much progress has been made to date with different methods but new insights are always welcome. A recent development that has led to reconsidering the strong interaction has been the AdS/CFT duality. This has been applied to obtain new insights on QCD phenomenology. In this paper, we focus on the meson spectrum (see [1] for a review of the gauge-gravity literature on the issue).

There are two main ways to address the problem at hand. Top-down approaches use string theory from first principles in order to build dual theories as close as possible to QCD. Notable examples are [2], [3]. On the other hand, bottom-up approaches, starting from the works [4; 5; 6], use known QCD features to develop holographic models that are only inspired by string theory. The model we present here is more of the second kind, but includes the main stringy ingredients we expect from first principles, namely the effective action controlling the chiral dynamics. Our main observation is that merging this stringy input of top-down holographic models for flavor allows us to improve the existing bottom-up models both qualitatively and quantitatively.

3.3 The model

In [7], it was shown, quite generally, that effective actions for brane-antibrane systems derived from string theory [8] encode a set of qualitative features related to chiral symmetry breaking and QCD at strong coupling. The goal of this paper is to build a concrete model within the framework of [7]. We will consider the simplest smooth gravitational background that is asymptotically AdS, while having a confining IR in the same spirit as [9]. This turns out to be the AdS_6 soliton, which was shown to be a solution to the two-derivative approximation of subcritical string theory and used as a toy model for certain aspects of 4D Yang-Mills in [10]. The metric reads:

$$ds_6^2 = \frac{R^2}{z^2}\left[dx_{1,3}^2 + f_\Lambda^{-1} dz^2 + f_\Lambda\, d\eta^2\right] \tag{3.3.1}$$

with $f_\Lambda = 1 - \frac{z^5}{z_\Lambda^5}$. The coordinate η is periodically identified and $z \in [0, z_\Lambda]$. The dilaton is constant and we do not write the RR forms since they do not play any role in

the following. We now consider a D4-$\bar{\text{D}}$4 pair, located at fixed η in this background[1]. We write the action proposed by Sen [8] as

$$S = -\int d^4x dz V(|T|) \left(\sqrt{-\det \mathbf{A}_L} + \sqrt{-\det \mathbf{A}_R} \right) \tag{3.3.2}$$

The objects inside the square roots are defined as

$$\mathbf{A}^{(i)}_{MN} = g_{MN} + \pi\alpha' \left[2F^{(i)}_{MN} + ((D_M T)^* (D_N T) + (M \leftrightarrow N)) \right] \tag{3.3.3}$$

where $M, N = 1, \ldots, 5$, the field strengths $F^{(i)}_{MN} = \partial_M A^{(i)}_N - \partial_N A^{(i)}_M$ and the covariant derivative of the tachyon is $D_M T = (\partial_M + i A^L_M - i A^R_M) T$. The active fields in (3.3.2), (3.3.3) are two 5-d gauge fields and a complex scalar $T = \tau\, e^{i\theta}$, which are dual to the low-lying quark bilinear operators that correspond to states with $J^{PC} = 1^{--}, 1^{++}, 0^{-+}, 0^{++}$; see [7] for details. In the action of [8], the transverse scalars (namely η in the present case) are also present. We have discarded them when writing (3.3.3) since they do not have any interpretation in terms of QCD fields. Accordingly, even if the background (3.3.1) is six dimensional, the holographic model for the hadrons is effectively five dimensional and, in fact, its field content coincides with those of [5], [6]. For the tachyon potential we take, as the simplest possibility, the one computed in boundary string field theory for an unstable Dp-brane in flat space [12], although one should keep in mind that this expression for V is not top-down derived for the present situation. In the present conventions, $V = \mathcal{K}\, e^{-\frac{\pi}{2}\tau^2}$, where $\mathcal{K}$ is an overall constant that will play no role in the following since it does not enter the meson spectrum computation (it is important though, in the normalization of correlators when computing for instance decay constants [5], [6], [13]). The tachyon mass is $m_T^2 = -\frac{1}{2\alpha'}$, and we will impose $R^2 = 6\alpha'$ in order to have $m_T^2 R^2 = -3$. This should not be interpreted as a modification of the background due to the branes, but just as a (bottom-up) choice of the string scale that controls the excitations of those branes, such that the bifundamental scalar T is dual to an operator of dimension 3, as in [5], [6]. Since the AdS radius is not parametrically larger than α', the two-derivative action cannot be a controlled low enegy approximation to string theory. This is the main reason why a model of this kind cannot be considered of top-down nature. Notice the value of R^2 we take differs from the one used in [10].

[1] In 5 dimensional holographic models of QCD, the flavor branes are expected to be a D4-$\bar{\text{D}}$4 system, [11].

The tachyon vacuum and chiral symmetry breaking

As shown in [7], an essential ingredient of the present framework is that the generation of the correct flavor anomaly on the flavor branes requires the tachyon modulus τ to diverge somewhere. Therefore, τ must have a nontrivial vacuum expectation value (vev), which breaks the chiral symmetry. From the action (3.3.2) we obtain the equation determining $\tau(z)$:

$$\tau'' - \frac{4\pi\, z\, f_\Lambda}{3}\tau'^3 + (-\frac{3}{z} + \frac{f'_\Lambda}{2f_\Lambda})\tau' + \left(\frac{3}{z^2 f_\Lambda} + \pi\,\tau'^2\right)\tau = 0 \tag{3.3.4}$$

where the prime stands for derivative with respect to z. Near $z = 0$, the solution can be expanded in terms of two integration constants as

$$\tau = c_1 z + \frac{\pi}{6}c_1^3 z^3 \log z + c_3 z^3 + \mathcal{O}(z^5) \tag{3.3.5}$$

where, on general AdS/CFT grounds, c_1 and c_3 are related to the quark mass and condensate (see [13] for a careful treatment). From (3.3.4), we find that τ can diverge only at $z = z_\Lambda$. There is a one-parameter family of diverging solutions in the IR:

$$\tau = \frac{C}{(z_\Lambda - z)^{\frac{3}{20}}} - \frac{13}{6\pi C}(z_\Lambda - z)^{\frac{3}{20}} + \dots \tag{3.3.6}$$

The interpretation is the following: for a given c_1 (namely quark mass[1]) fixed in the UV (near $z = 0$), the value of c_3 (namely the quark condensate) is determined dynamically by requiring that the numerical integration of (3.3.4) leads to the physical IR (near $z = z_\Lambda$) behavior (3.3.6). Hence, for any value[2] of c_1, one can obtain numerically the function for the vev $\langle\tau\rangle$.

Meson spectrum: numerical results

There is a rather standard method for computing the meson spectrum in holographic models; see [1] for a review. Each bulk field is dual to a boundary operator. By looking at normalizable fluctuations of the bulk fields, one typically encounters discrete towers of masses for the physical states with the corresponding quantum numbers. Eventually, the computation translates into a Schrödinger-like problem. We just quote here the results of these numerical computations. Further details will appear in [13].

[1] For the present work, we will just use that c_1 is proportional to m_q. Finding the proportionality coefficient requires normalizing the action and fields as in [14].

[2] In practice, we have been able to perform numerics in a controlled manner only for $0 \leq c_1 < 1$.

By computing the different towers at different values of c_1, we found the following expressions to be very good approximations to the numerical results, in the range $0 < c_1 < 1$ where we could perform the numerics reliably. For the vectors,

$$\begin{aligned} z_\Lambda\, m_V^{(1)} &= 1.45 + 0.718 c_1 \quad , \quad z_\Lambda\, m_V^{(2)} = 2.64 + 0.594 c_1 \\ z_\Lambda\, m_V^{(3)} &= 3.45 + 0.581 c_1 \quad , \quad z_\Lambda\, m_V^{(4)} = 4.13 + 0.578 c_1 \\ z_\Lambda\, m_V^{(5)} &= 4.72 + 0.577 c_1 \quad , \quad z_\Lambda\, m_V^{(6)} = 5.25 + 0.576 c_1 . \end{aligned}$$

For the axial vectors,

$$\begin{aligned} z_\Lambda\, m_A^{(1)} &= 1.93 + 1.23 c_1 \quad , \quad z_\Lambda\, m_A^{(2)} = 3.28 + 1.04 c_1 \\ z_\Lambda m_A^{(3)} &= 4.29 + 0.997 c_1 \quad , \quad z_\Lambda m_A^{(4)} = 5.13 + 0.975 c_1 \\ z_\Lambda\, m_A^{(5)} &= 5.88 + 0.962 c_1 \quad , \quad z_\Lambda\, m_A^{(6)} = 6.55 + 0.954 c_1 . \end{aligned}$$

For the pseudoscalars,

$$\begin{aligned} z_\Lambda\, m_P^{(1)} &= \sqrt{2.47 c_1^2 + 5.32 c_1} \quad , \quad z_\Lambda\, m_P^{(2)} = 2.79 + 1.16 c_1 \\ z_\Lambda\, m_P^{(3)} &= 3.87 + 1.08 c_1 \quad , \quad z_\Lambda\, m_P^{(4)} = 4.77 + 1.04 c_1 \\ z_\Lambda\, m_P^{(5)} &= 5.54 + 1.01 c_1 \quad , \quad z_\Lambda\, m_P^{(6)} = 6.24 + 0.997 c_1 . \end{aligned}$$

For the scalars,

$$\begin{aligned} z_\Lambda\, m_S^{(1)} &= 2.47 + 0.683 c_1 \quad , \quad z_\Lambda\, m_S^{(2)} = 3.73 + 0.488 c_1 \\ z_\Lambda\, m_S^{(3)} &= 4.41 + 0.507 c_1 \quad , \quad z_\Lambda\, m_S^{(4)} = 4.99 + 0.519 c_1 \\ z_\Lambda\, m_S^{(5)} &= 5.50 + 0.536 c_1 \quad , \quad z_\Lambda\, m_S^{(6)} = 5.98 + 0.543 c_1 . \end{aligned}$$

It turns out that meson masses increase linearly with c_1. Namely, they increase linearly with the bare quark mass, as expected from an expansion in m_q and in qualitative agreement with lattice results; see for instance [15],[16],[17]. The exception, of course, is the first pseudoscalar for which m_π is proportional to $\sqrt{m_q}$ (for small m_q), as expected from the Gell-Mann-Oakes-Renner relation. Actually, the behavior $m_\pi = \sqrt{b\, m_q + d\, m_q^2}$ was also found in the lattice [15].

3.4 Fitting the meson spectrum

We now proceed to make a phenomenological comparison of the results above for the meson masses to the experimental values quoted by the Particle Data Group [18]. Obviously, we can only model those mesons with $J^{PC} = 1^{--}, 1^{++}, 0^{-+}, 0^{++}$. From [18], we will just take the central value quoted for each resonance. We do not discuss decay widths here (in the strict $N_c \to \infty$ limit they are, of course, zero).

Isospin 1 mesons

We start by looking at mesons composed of the light quarks u and d. In particular, we discuss the isovectors. In Table 3.1, we show all the mesons listed in [18] under *light unflavored mesons* which have isospin 1 and the J^{PC}'s present in our model. The exceptions are $a_0(980)$, which is considered to be a four-quark state [18] and $\rho(1570)$ which is a non-confirmed state[1]. We have fitted the parameters of the model to these observables by minimizing the rms error $\varepsilon_{rms} = 100 \times \frac{1}{\sqrt{n}} \left(\sum_O \left(\frac{\delta O}{O} \right)^2 \right)^{\frac{1}{2}}$, where $n = 11 - 2 = 9$ is the number of observables minus the number of parameters. We obtain for the parameters

$$z_\Lambda^{-1} = 503\text{MeV} , \qquad \text{c}_{1,\text{l}} = 0.0135 \tag{3.4.1}$$

with $\varepsilon_{rms} = 11\%$.

J^{PC}	Meson	Measured (MeV)	Model (MeV)
1^{--}	$\rho(770)$	775	735
	$\rho(1450)$	1465	1331
	$\rho(1700)$	1720	1742
	$\rho(1900)$	1900	2083
	$\rho(2150)$	2150	2380
1^{++}	$a_1(1260)$	1230	980
	$a_1(1640)$	1647	1661
0^{-+}	π_0	135.0	135.3
	$\pi(1300)$	1300	1411
	$\pi(1800)$	1816	1955
0^{++}	$a_0(1450)$	1474	1249

Table 3.1: A comparison of the results of the model to the experimental values for light unflavored meson masses.

In Table 3.2, we display the resonance masses with isospin 1 listed in [18] under *other light unflavored mesons*. These are, namely, states considered as "poorly established that thus require confirmation." For the results given by our model, we use (3.4.1) and therefore no further parameter is fitted here. For this set of observables we get

[1] We however include in the fit other non-confirmed states as $\rho(1900)$ and $\rho(2150)$ because they rely on firmer experimental grounds than $\rho(1570)$. We thank S. Eydelman for useful explanations on the issue.

$\varepsilon_{rms} = 23\%$, where we have inserted $n = 8 - 0 = 8$. One should keep in mind that it is plausible that some of these "un-confirmed" states may not be real or may be misinterpreted as part of the meson towers. In this sense, our model seems to favor the $\rho(2150)$ as the fourth member of the ρ-meson tower [19]. We have not included $\rho(1570)$ in Table 3.2 because its excitation number is smaller than $\rho(1700)$ which was included in the previous fit. In case $\rho(1570)$ gets confirmed as a member of this tower, the fit should be redone. We observe that the model tends to consistently overestimate the masses of the excited axial vectors and pions. This is connected to the fact the model yields a Regge slope for axial mesons larger than the one for the vectors [7]. If the experimental results of Table 3.2 are confirmed, one should think of improving the model in order to ameliorate this discrepancy.

J^{PC}	Meson	Measured (MeV)	Model (MeV)
1^{--}	$\rho(2270)$	2270	2649
1^{++}	$a_1(1930)$	1930	2166
	$a_1(2096)$	2096	2591
	$a_1(2270)$	2270	2965
	$a_1(2340)$	2340	3303
0^{-+}	$\pi(2070)$	2070	2406
	$\pi(2360)$	2360	2798
0^{++}	$a_0(2020)$	2025	1883

Table 3.2: A comparison of the results of the model to the experimental values for other light unflavored meson masses.

$s\bar{s}$ states

A nice feature of the present model compared to AdS/QCD is that it incorporates the dependence of the hadron masses on the quark mass. This allows us to study $s\bar{s}$ states. More precisely, it allows us to discuss “hypothetically states" with quark content $s\bar{s}$ assuming no mixing with other states. In the real world, the mixing for pseudoscalars and scalars is important (see Chapter 14 of [18]), and therefore it is not possible to compare directly the outcome of the model to the experimental results. Nevertheless, as in [20], we can estimate the masses of these “hypothetical" $s\bar{s}$ mesons from the light-strange and light-light mesons. Then, using quotation marks for the hypothetical states, and using the quark model classification (Table 14.2 of [18]), we can write

$m(\text{“}\eta\text{”}) = \sqrt{2m_K^2 - m_\pi^2}$, $m(\text{“}\phi(1020)\text{”}) = 2m(K^*(892)) - m(\rho(770))$, $m(\text{“}\eta(1475)\text{”}) = 2m(K(1460)) - m(\pi(1300))$, etc. Keeping the value of z_Λ found in (3.4.1), we fit the value of c_1 associated with the strange quark to the “experimental" values of Table 3.3, obtaining

$$c_{1,s} = 0.350 \tag{3.4.2}$$

The rms error for this set of observables ($n = 6 - 1$) is $\varepsilon_{rms} = 11\%$.

J^{PC}	Meson	Measured (MeV)	Model (MeV)
1^{--}	“$\phi(1020)$”	1009	857
	“$\phi(1680)$”	1363	1432
1^{++}	“$f_1(1420)$”	1440	1188
0^{-+}	“η”	691	740
	“$\eta(1475)$”	1620	1608
0^{++}	“$f_0(1710)$”	1386	1365

Table 3.3: A comparison of the results of the model to the hypothetical states with $s\bar{s}$ quark content.

We end this section by commenting on the estimates given by the model on two other physical quantities. Without fixing the proportionality coefficient between c_1 and the quark mass, from (3.4.1), (3.4.2), we can infer the ratio of the strange quark to the light quark mass: $\frac{2m_s}{m_u+m_d} \approx \frac{c_{1,s}}{c_{1,l}} \approx 26$. Moreover, the background studied here experiences a first order deconfinement phase transition in full analogy with [9]. The deconfinement temperature is given by $T_{deconf} = \frac{5}{4\pi\, z_\Lambda} \approx 200$ MeV. Both of these values are close to the experimental values.

3.5 Conclusions

We have built a new phenomenological model for the meson sector of QCD. In this paper we have discussed the mass spectrum. We note the simplicity of the construction, whose essential point is the use of Sen's action [8] including the open string tachyon field. We have applied it to one of the simplest backgrounds exhibiting confinement [10]. Despite the minimal input, we have found the following interesting qualitative properties:

- The model includes towers of excitations with $J^{PC} = 1^{--}, 1^{++}, 0^{-+}, 0^{++}$, namely all low-lying operators that do not need a dual excited stringy state.

- Chiral symmetry breaking is consistently realized. Moreover, the value of the quark condensate is computed dynamically and is not a tunable input. Hence, the number of tunable parameters coincides with those present in QCD: they are just the dynamically generated scale and the quark masses.

- We find Regge trajectories for the excited states $m_n^2 \propto n$, as in the soft wall model [21]. This allows good predictions for the higher excitations, as opposed to the hard wall model [5; 6]. Notwithstanding, the Regge slope for axial vectors is bigger than the one for vectors. This fact requires further study.

- Our model incorporates the increase of the vector meson masses due to the increase of quark massess, as $m_\rho \approx k_1 + k_2\, m_\pi^2$ for small m_π.

Previous AdS/QCD models present some of these properties, but as far as we know, no existing model is able to encompass all of them; see [22] for recent related discussions. We briefly comment on the three benchmark models: the Sakai-Sugimoto model [3] misses the first and third points listed above, the hard wall model [5; 6] misses the third one and partially the second one; and the soft wall model [21] misses the second one. All of these models [3; 5; 6; 21] and variations thereof fail to get the fourth point (although it is worth mentioning that D3D7 models with Abelian flavor symmetry do capture the physics of this fourth point; see Sec. 6.2.3 of [1]).

Moreover, the quantitative matching shown in Tables 3.1 and 3.3 with the central values of the meson resonances is excellent, at the 10%-15% level. This is a typical accuracy of AdS-QCD-like models (a recent example is [23], which accounts for excited spin states of the ρ and ω families). Since the systematic error produced by quenching is of the order of 10% [24] and the differences between quenched lattice computations with $N_c = 3$ and $N_c = \infty$ are again of the order of 10% [16; 17], it would be unexpected to get a better accuracy from any model of the kind presented here.

It would be of utmost interest to generalize the set up to the non-Abelian case, allowing several quark flavors, but this is beyond the scope of the present work.

Acknowledgments

This work was partially supported by European Union Grant No.FP7-REGPOT-2008-1-CreteHEP Cosmo-228644. The research of A.P is supported by Grants No.FPA2007-66665C02-02 and No. DURSI 2009 SGR 168, and by the CPAN CSD2007-00042 project of the Consolider-Ingenio 2010 program. I.I. has been supported by Manasaki Graduate Scholarship and the Physics Department of the University of Crete until September 2009 and by A.S. Onassis Foundation Graduate Scholarship from October 2009.

Bibliography

[1] J. Erdmenger, N. Evans, I. Kirsch and E. Threlfall, Eur. Phys. J. A **35**, 81 (2008). 70, 72, 77

[2] I. R. Klebanov and M. J. Strassler, JHEP **0008**, 052 (2000). J. Babington, J. Erdmenger, N. J. Evans, Z. Guralnik and I. Kirsch, Phys. Rev. D **69**, 066007 (2004). M. Kruczenski, D. Mateos, R. C. Myers and D. J. Winters, JHEP **0405**, 041 (2004). 70

[3] T. Sakai and S. Sugimoto, Prog. Theor. Phys. **113** (2005) 843. 70, 77

[4] J. Polchinski and M. J. Strassler, Phys. Rev. Lett. **88**, 031601 (2002) [arXiv:hep-th/0109174]. 70

[5] J. Erlich, E. Katz, D. T. Son and M. A. Stephanov, Phys. Rev. Lett. **95**, 261602 (2005). 70, 71, 77

[6] L. Da Rold and A. Pomarol, Nucl. Phys. B **721**, 79 (2005). 70, 71, 77

[7] R. Casero, E. Kiritsis and A. Paredes, Nucl. Phys. B **787**, 98 (2007). 70, 71, 75

[8] A. Sen, Phys. Rev. D **68**, 066008 (2003). 70, 71, 76

[9] E. Witten, Adv. Theor. Math. Phys. **2**, 505 (1998). 70, 76

[10] S. Kuperstein and J. Sonnenschein, JHEP **0411**, 026 (2004). 70, 71, 76

[11] F. Bigazzi, R. Casero, A. L. Cotrone, E. Kiritsis and A. Paredes, JHEP **0510**, 012 (2005); U. Gursoy and E. Kiritsis, JHEP **0802** (2008) 032; U. Gursoy, E. Kiritsis and F. Nitti, JHEP **0802** (2008) 019; U. Gursoy, E. Kiritsis, L. Mazzanti and F. Nitti, JHEP **0905** (2009) 033. 70

[12] D. Kutasov, M. Marino and G. W. Moore, JHEP **0010** (2000) 045. 71

[13] I. Iatrakis, E. Kiritsis and A. Paredes, *in preparation* 71, 72

[14] L. Da Rold and A. Pomarol, JHEP **0601**, 157 (2006). 72

[15] E. Laermann and P. Schmidt, Eur. Phys. J. C **20**, 541 (2001). 73

[16] L. Del Debbio, B. Lucini, A. Patella and C. Pica, JHEP **0803**, 062 (2008). 73, 77

[17] G. S. Bali and F. Bursa, JHEP **0809**, 110 (2008). 73, 77

[18] C. Amsler *et al.* [Particle Data Group], Phys. Lett. B **667**, 1 (2008). 73, 74, 75

[19] Indeed there us much more experimental evidence for $\rho(2150)$ than for $\rho(1900)$ or $\rho(1570)$. We thank S. Eydelman for very useful explanations. 74

[20] C. R. Allton, V. Gimenez, L. Giusti and F. Rapuano, Nucl. Phys. B **489**, 427 (1997). 75

[21] A. Karch, E. Katz, D. T. Son and M. A. Stephanov, Phys. Rev. D **74**, 015005 (2006). 77

[22] T. Gherghetta, J. I. Kapusta and T. M. Kelley, Phys. Rev. D **79**, 076003 (2009); Y. Q. Sui, Y. L. Wu, Z. F. Xie and Y. B. Yang, Phys. Rev. D **81**, 014024 (2010). 77

[23] G. F. de Teramond and S. J. Brodsky, arXiv:1001.5193 [hep-ph]. 77

[24] S. Aoki *et al.* [CP-PACS Collaboration], Phys. Rev. Lett. **84**, 238 (2000). 77

4 An AdS/QCD model from tachyon condensation: II

Authors : Ioannis Iatrakis[a], Elias Kiritsis[a,b], Ángel Paredes[c]

[a] Crete Center for Theoretical Physics, Department of Physics, University of Crete, 71003 Heraklion, Greece.
[b] APC, Université Paris 7, Bâtiment Condorcet, F-75205, Paris, France (UMR du CNRS 7164).
[c] Departament de Física Fontamental and ICCUB Institut de Ciències del Cosmos, Universitat de Barcelona, Martí i Franquès, 1, E-08028, Barcelona, Spain.

4.1 Abstract

A simple holographic model is presented and analyzed that describes chiral symmetry breaking and the physics of the meson sector in QCD. This is a bottom-up model that incorporates string theory ingredients like tachyon condensation which is expected to be the main manifestation of chiral symmetry breaking in the holographic context. As a model for glue the Kuperstein-Sonnenschein background is used. The structure of the flavor vacuum is analyzed in the quenched approximation. Chiral symmetry breaking is shown at zero temperature. Above the deconfinement transition chiral symmetry is

restored. A complete holographic renormalization is performed and the chiral condensate is calculated for different quark masses both at zero and non-zero temperatures. The $0^{++}, 0^{-+}, 1^{++}, 1^{--}$ meson trajectories are analyzed and their masses and decay constants are computed. The asymptotic trajectories are linear. The model has one phenomenological parameter beyond those of QCD that affects the $1^{++}, 0^{-+}$ sectors. Fitting this parameter we obtain very good agreement with data. The model improves in several ways the popular hard-wall and soft wall bottom-up models.

4.2 Introduction

The AdS/CFT correspondence [1] has been one of the most fruitful arenas for research in fundamental physics in the last decade. Having the possibility of mapping strongly-coupled field theories to weakly coupled gravity has set the stage for a large amount of effort devoted to use this idea in order to obtain new results on the physics of the strong interactions (see [2], for an introduction). It is clear that a precise and controllable string dual of QCD is far from our present understanding. However, it is possible to build models that describe interesting strong coupling phenomena which share many similarities with real world physics. For the physics of pure glue, models descending from string theory, [3; 4; 5] have provided important clues towards the confinement of color. Phenomenological models for glue inspired and motivated from the AdS/CFT correspondence ranged from very simple like AdS/QCD [6] to more sophisticated versions, namely "Improved Holographic QCD" that capture rather accurately the dynamics of glue at both zero [7] and finite temperature [8].

In this context, the holographic description of chiral symmetry breaking (χSB) has been thoroughly studied. Early examples were studied in the Maldacena-Nunez [4] and Klebanov-Strassler backgrounds [5]. Later, more QCD-like χSB, in the sense that the operator condensing was bilinear of fundamental fields, was described in [9; 10]. In the beginning chiral symmetry breaking involved abelian chiral symmetry, [4; 5; 9; 10]. A major breakthrough was the Sakai-Sugimoto model [11] where the broken symmetry is non-abelian $U(N_f)_L \times U(N_f)_R \to U(N_f)_V$, as opposed to just a $U(1)$. However, the model of [11] and generalizations of it have its own limitations. Just as an example, one can mention the absence of a tower of excited pions.

All the aforementioned models come from well controlled approximations to string theory and, accordingly, are top-down approaches. A different possibility is to use string theory just as inspiration and define *ad hoc* holographic models using some QCD features as inputs. This is the bottom-up approach. The obvious question is whether

the output extracted from such models is larger than their input, and we believe that experience has shown that the answer is yes. The benchmark bottom-up models for chiral symmetry breaking and meson physics are the hard wall model [12; 13] based on the Polchinski-Strassler background [6] and the soft wall model [14].

In the present work, we analyze in detail several aspects of a bottom-up model presented first in [15]. It gives a explicit realization of the framework for chiral symmetry breaking first advocated in [16]: the quarks and antiquarks are introduced by a brane-antibrane pair. A key point of the dynamics is the condensation of the lowest lying bifundamental scalar which comes from the strings connecting the brane to the antibrane. Around flat space this scalar has negative mass squared and this is called the tachyon. This corresponds precisely to a QCD-like chiral symmetry breaking. We need an effective action to describe this dynamics and we will resort to the tachyon-DBI action proposed by Sen in [17]. Once we have decided that we will use this action, we still have to choose an expression for the tachyon potential and a holographic geometry in order to use as curved background. For these choices, we will constrain ourselves to the (arguably) simplest possibilities. Another interesting property of considering brane-antibrane tachyonic actions is that there is a natural Wess-Zumino term, which correctly incorporates to the model features like parity and charge conjugation symmetries and anomalies; see the discussions in [16].

So far our ingredients are those of a top-down approach. However, it is not possible to stay in a limit in which the approximation to string theory is controlled if one wants to reproduce some QCD features in this context. For instance, we will need a background with curvature comparable to the string scale. We do not regard this point as a negative feature, but just as a sign that our approach should be considered of the bottom-up type. This has its own advantages, since for instance it seems impossible to get Regge trajectories for excited mesons $m_n^2 \sim n$ from any top-down approach, because in those cases the meson mass scale is parametrically smaller than the QCD string tension scale, see for instance [18]. Therefore, the model discussed in this work should be regarded as a phenomenological model, partly inspired by top-down consideration and in particular by Sen's action [17]. These top-down inputs will generate some dynamics (compared to other bottom-up approaches) which will be crucial in the successful modeling of several QCD features, see the discussions in [16] and also in section 4.7.1.

We will constrain ourselves to the abelian case of a single quark flavor but, unlike [9; 10], this is not an essential limitation, since we can make the model non-abelian by piling up branes and antibranes, in the spirit of [11]. This elaboration, however, is left for future work.

In section 4.3, we will discuss the backgrounds (both for confined and deconfined phases) and the gravity action of which they are solutions. In section 4.4, we will study in detail the equation for the tachyon modulus τ and its bulk vacuum expectation value. In other words, we find the open string vacuum and show how it dynamically breaks the chiral symmetry. In section 4.5, we discuss in detail linearized open string excitations around the vacuum, namely the meson physics. A good review of this kind of analysis in different holographic frameworks is [19]. Apart from remarking several general qualitative properties, we end the section with a quantitative phenomenological analysis. Section 4.6 provides a brief analysis of the same kind of excitations, but in the deconfined phase. We conclude in section 4.7 with several discussions; we will convey the pros and cons of the present model and give some ideas for future directions. We have relegated various technical comments to eight appendices. In particular, in order to facilitate the reading of the text, we review the meaning of the different constants and parameters that will appear throughout the paper and for which physical reasons some of them are fixed in appendix A .

4.3 The gravitational background

As acknowledged in the introduction, the model we will discuss does not come from any controlled approximation to string theory. Notwithstanding, we will follow general insights coming from string theory and effective actions developed in that framework, especially in the non-critical setting, [20]-[24]. In this sense, the meson physics (in the quenched approximation) is described by the dynamics of a D4-anti D4 system in a fixed closed string background, [16].

We take the following gravitational two-derivative action [20] for the background fields:

$$S = \int d^6x \sqrt{g_{(6)}} \left[e^{-2\phi} \left(\mathcal{R} + 4(\partial\phi)^2 + \frac{c}{\alpha'} \right) - \frac{1}{2}\frac{1}{6!} F^2_{(6)} \right] , \tag{4.3.1}$$

with a constant c. We consider the solution discussed in [21] whose metric is given by:

$$ds_6^2 \equiv -g_{tt}dt^2 + g_{zz}dz^2 + g_{xx}dx_3^2 + g_{\eta\eta}d\eta^2 = \frac{R^2}{z^2}\left[dx_{1,3}^2 + f_\Lambda^{-1}dz^2 + f_\Lambda\, d\eta^2 \right] \tag{4.3.2}$$

with:

$$f_\Lambda = 1 - \frac{z^5}{z_\Lambda^5} \tag{4.3.3}$$

This is the AdS soliton, a double Wick rotation of an AdS_6 Schwartszchild black hole. The only active RR-form we consider is:

$$F_{(6)} = \frac{Q_c}{\sqrt{\alpha'}}\sqrt{-g_{(6)}}\, d^6x \tag{4.3.4}$$

for some constant Q_c which is proportional to the number of colors and that will not be important in the following. The dilaton is constant:

$$e^{\phi} = \frac{1}{Q_c}\sqrt{\frac{2c}{3}} \tag{4.3.5}$$

The coordinate η is compactified and regularity of the metric at $z = z_\Lambda$ requires the following periodicity condition:

$$\eta \sim \eta + \delta\eta \ , \qquad \delta\eta = \frac{4\pi}{5} z_\Lambda = \frac{2\pi}{M_{KK}} \ . \tag{4.3.6}$$

The AdS radius is given by:

$$R^2 = \frac{30}{c}\alpha' \tag{4.3.7}$$

The application of this geometry for a phenomenological non-critical strings/gauge duality was first discussed in [20; 21]. The solution is dual to 1+4 dimensional gauge theory compactified in a circle with (susy-breaking) antiperiodic boundary conditions for the fermions. Thus, the low energy theory is 1+3 dimensional confining gauge theory coupled to a set of massive Kaluza-Klein fields.

One can consider the theory at non-zero temperature by compactifying to Euclidean time t_E. When both circles t_E and η are compactified, there is a second solution competing with (4.3.2):

$$ds_6^2 = \frac{R^2}{z^2}\left[-f_T dt^2 + dx_3^2 + f_T^{-1}dz^2 + d\eta^2\right] \tag{4.3.8}$$

while (4.3.4), (4.3.5), (4.3.7) still hold. We have introduced:

$$f_T = 1 - \frac{z^5}{z_T^5} \tag{4.3.9}$$

and z_T is related to the period of the euclidean time and therefore to the temperature as:

$$t_E \sim t_E + \delta t_E \ , \qquad \delta t_E = \frac{4\pi}{5} z_T = \frac{1}{T} \ . \tag{4.3.10}$$

Since when we Euclideanize (4.3.2), (4.3.8) both solutions are related by the interchange $t_E \leftrightarrow \eta$, $z_T \leftrightarrow z_\Lambda$, the symmetry makes obvious that there is a deconfining first order phase transition at

$$T_c = \frac{M_{KK}}{2\pi} = \frac{5}{4\pi\, z_\Lambda} \tag{4.3.11}$$

For $T < T_c$, the confining solution (4.3.2) is preferred and, conversely, (4.3.8) dominates for $T > T_c$. Of course, this discussion is just a straightforward generalization of [25].

4.4 The tachyon vacuum expectation value

Our main interest will be to study a "tachyon-DBI" action for a single brane-antibrane pair of the form advocated in [17]. In section 4.7.2 we will comment about the literature related to effective actions including open string tachyon fields and the possible impact of different choices of actions in a holographic model of this kind.

We take the brane-antibrane pair to be at a fixed value of η and we will not consider oscillations of the transverse scalar, which has no QCD counterpart[1]. The brane and antibrane are at zero distance and are therefore overlapping. We have therefore a 5D model for the quarks embedded in a 6D model for the glue. The Sen action reads:

$$S = -\int d^4x dz V(|T|)\left(\sqrt{-\det \mathbf{A}_L} + \sqrt{-\det \mathbf{A}_R}\right) \tag{4.4.1}$$

The quantities inside the square roots are defined as:

$$\mathbf{A}_{(i)MN} = g_{MN} + \frac{2\pi\alpha'}{g_V^2} F^{(i)}_{MN} + \pi\alpha'\lambda\left((D_M T)^*(D_N T) + (D_N T)^*(D_M T)\right) \tag{4.4.2}$$

where $(i) = L, R$ and the complex tachyon will be denoted $T = \tau e^{i\theta}$. Indices M, N run over the 5 world-volume dimensions while we will use μ, ν for the Minkowski directions (indices to be contracted using $\eta_{\mu\nu}$). With respect to [17], we have included two constants g_V, λ in (4.4.2), which are related to the normalization of the fields to be discussed later.

The covariant derivative of the tachyon field is defined as:

$$D_M T = (\partial_M + iA^L_M - iA^R_M)T \tag{4.4.3}$$

For the tachyon potential we take:

$$V = \mathcal{K}\, e^{-\frac{1}{2}\mu^2\tau^2} \tag{4.4.4}$$

where $\mathcal{K}$ is a constant[2] which in principle should be related to the tension of the D4-branes. The gaussian is a simple choice that has been discussed in different situations for instance in [26; 27; 28], but we warn the reader that it is not at all top-down derived for the present situation and thus should be considered as an ingredient of the bottom-up approach. We will comment further in section 4.7.2. For book-keeping, let us enumerate

[1] A different construction involving D4-anti D4 in this background was considered in [24]. The present scenario is more successful in describing different features of QCD.

[2] We have included the constant dilaton in $\mathcal{K}$, in order to avoid unnecessary cluttering of formulae.

here the constants that have been introduced up to now: $R, \alpha', \lambda, g_V, \mathcal{K}, \mu, z_\Lambda$. In the following, we will impose, on physical grounds, some relations among these constants and in appendix A we will summarize these arguments.

We must first find the vacuum of the theory. We should set θ, A_L, A_R to zero because of Lorentz invariance, but τ must have non-trivial dynamics, at least in the confined phase, as will be argued below. We thus discuss here the function $\tau(z)$ that defines the vacuum. The corresponding reduced action reads:

$$S = -2\mathcal{K}\int d^4x dz e^{-\frac{1}{2}\mu^2\tau^2} g_{tt}^{\frac{1}{2}} g_{xx}^{\frac{3}{2}} \sqrt{g_{zz} + 2\pi\alpha'\lambda(\partial_z\tau)^2} \tag{4.4.5}$$

and the corresponding equation of motion:

$$\tau'' + \frac{\pi\alpha'\lambda}{g_{zz}}\tau'^3\left(\frac{g'_{tt}}{g_{tt}} + 3\frac{g'_{xx}}{g_{xx}}\right) + \frac{\tau'}{2}\left(\frac{g'_{tt}}{g_{tt}} + 3\frac{g'_{xx}}{g_{xx}} - \frac{g'_{zz}}{g_{zz}}\right) + \left(\frac{g_{zz}}{2\pi\alpha'\lambda} + \tau'^2\right)\mu^2\tau = 0 \tag{4.4.6}$$

We want to study this equation in both the confined and deconfined backgrounds of section 4.3. For this, we need to explicitly substitute the components of the metric of each background, as given in section 4.3. We will make these studies separately in the following subsections. Before that, since the UV of both solutions is identical (up to $\mathcal{O}(z^5)$), the analysis of the UV asymptotics of (4.4.6) is the same. We find that the near-boundary limit $z \to 0$ limit is given in terms of the two integration constants as:

$$\tau = c_1 z + \frac{\mu^2}{6}c_1^3 z^3 \log z + c_3 z^3 + \mathcal{O}(z^5) \tag{4.4.7}$$

In order to find this expansion, we have imposed that:

$$\frac{R^2\mu^2}{2\pi\alpha'\lambda} = 3\ . \tag{4.4.8}$$

This enforces that the scalar bifundamental operator dual to the scalar field (which has mas $m_\tau^2 = -\mu^2/(2\pi\alpha'\lambda)$) has UV dimension 3 matching the dimension of $\bar{q}q$ in QCD. This is in agreement with the usual AdS/CFT rule $\Delta(\Delta - 4) = m_\tau^2 R^2$. It is worth stressing that (4.4.8) should be understood as a bottom-up condition on the parameters determining the open string data μ, α', λ and not on R, since in the quenched approximation one should not think of the flavor branes affecting the closed string background.

The asymptotic expansions for τ in the confined and deconfined backgrounds start differing at order $\mathcal{O}(z^6)$. On the other hand, the IR behaviour for both cases is very different, as will be discussed below.

4.4.1 The confined phase

Inserting the metric for the confining background (4.3.2) into (4.4.6), we obtain the following equation of motion for the order parameter:

$$\tau'' - \frac{4\mu^2 z f_\Lambda}{3}\tau'^3 + (-\frac{3}{z} + \frac{f'_\Lambda}{2f_\Lambda})\tau' + \left(\frac{3}{z^2 f_\Lambda} + \mu^2\tau'^2\right)\tau = 0 \tag{4.4.9}$$

Before going on, notice that equation (4.4.9) depends on two constants z_Λ and μ. However, such dependence can be easily reabsorbed by redefining the field and radial coordinate as $z \to \tilde{z} = z/z_\Lambda$, $\tau \to \tilde{\tau} = \mu\tau$. The plots in this section will be performed by taking $z_\Lambda = 1$, $\mu^2 = \pi$, but it is automatic to find the solution for different values of the constants by rescaling as mentioned above.

According to the discussion of [16], since the background is confining, we must require the tachyon to blow up somewhere. Heuristically, one can think of the diverging tachyon as a brane-antibrane recombination; if the tachyon were finite until the bottom of the space one would have an open brane (and antibrane). In [16], it was argued that this would lead to bulk flavor anomalies that do not match those of QCD[1]. The fact that confinement requires brane recombination (and therefore, chiral symmetry breaking) is a Coleman-Witten-like theorem [30] for the present set-up, and it is analogous to a similar discussion of [31] for the Sakai-Sugimoto model [11]. The difference is that the realization of chiral symmetry breaking in [31] is geometrical while here it is driven by the field τ.

Equation (4.4.9) only allows the tachyon to diverge at exactly the end of space (the tip of the cigar) $z = z_\Lambda$, see appendix B for details.

In the IR, generically the two linearly independent solutions behave as a constant and $\sqrt{z - z_\Lambda}$ and they are regular at the tip. There is however a one parameter "boundary" family of solutions that (1) depends on a single parameter (2) diverges at the tip. This is the solution we should allow in the IR. If we call the single parameter C then the acceptable IR solution is:

$$\tau = \sum_{n=0}^{\infty}(z_\Lambda - z)^{\frac{3(2n-1)}{20}} C_n \; g_n(z) \tag{4.4.10}$$

where

$$g_n(z) = 1 + \sum_{m=1}^{\infty} D_{n,m}\left(1 - \frac{z}{z_\Lambda}\right)^m \tag{4.4.11}$$

[1] Anomalies in the hard wall model have been discussed in [29]. In that case, appropriate IR boundary conditions have to be imposed on the gauge fields in order to get rid of the IR contribution to the gauge variation of the Chern-Simons term. In our case, that contribution is killed due to the divergent tachyon.

For the first few constants we have

$$C_0 = C \quad , \quad C_1 = -\frac{13}{6\mu^2 C} \quad , \quad C_2 = \frac{247}{72\mu^4 C^3} \quad , \quad C_3 = -\frac{26975}{1296\mu^6 C^5} \tag{4.4.12}$$

$$C_4 = \frac{6381505}{31104\mu^8 C^7} \quad , \quad C_5 = -\frac{276207997}{103680\mu^{10} C^9} \quad , \quad C_6 = \frac{1402840243831}{33592320\mu^{12} C^{11}}$$

and the first few functions

$$g_0(z) = 1 - \frac{9}{20}\left(1 - \frac{z}{z_\Lambda}\right) + \mathcal{O}\left(\left(1 - \frac{z}{z_\Lambda}\right)^2\right) \tag{4.4.13}$$

$$g_1(z) = 1 - \frac{1479}{3380}\left((1 - \frac{z}{z_\Lambda}\right) + \mathcal{O}\left(\left(1 - \frac{z}{z_\Lambda}\right)^2\right) \tag{4.4.14}$$

$$g_2(z) = 1 - \frac{8481}{4940}\left((1 - \frac{z}{z_\Lambda}\right) + \mathcal{O}\left(\left(1 - \frac{z}{z_\Lambda}\right)^2\right) \tag{4.4.15}$$

$$g_3(z) = 1 - \frac{396189}{82004}\left((1 - \frac{z}{z_\Lambda}\right) + \mathcal{O}\left(\left(1 - \frac{z}{z_\Lambda}\right)^2\right) \tag{4.4.16}$$

As C increases, the radius of convergence of this series increases.

The condition that the solution should end up in the one parameter family described above is our "'regularity condition". It relates the two UV initial conditions, the source (mass) c_1 and the vev (chiral condensate) c_3. This is a dynamical determination of the condensate as a function of the mass by the condition $\tau(z = z_\Lambda) = \infty$. This relation will be found numerically.

In practice, one has to solve numerically the equation of motion (4.4.9) arranging the asymptotics to be (4.4.7) in the UV and (4.4.10) in the IR. One can implement a standard shooting routine whose inputs are c_1 and some UV and IR cutoffs, where the numerical solution is required to match the mentioned asymptotics. The value of c_3 leading to (4.4.10) is the limiting point between a behavior of diverging derivative of τ and a behaviour where τ remains finite everywhere, see figure 4.1.

In fact, for fixed c_1 there are two values of c_3 for which τ diverges at z_Λ, since τ can diverge to $+\infty$, for a particular $c_3 > 0$; or to $-\infty$, for a particular $c_3 < 0$, (we are assuming by convention that $c_1 > 0$). However, the $c_3 < 0$ solution is unstable and should be discarded. This can be understood by comparing the free energy of both solutions or, alternatively, by realizing that there is a tachyonic mode in the pseudoscalar sector. In the massless quark case $c_1 = 0$, both solutions are related by $\tau \to -\tau$ and are physically equivalent. They are just related by a rotation in the direction of the Goldstone pion, which is exactly massless. This behaviour is completely

analogous to the one described in [10]. For illustrative purposes, we plot in figure 4.1 the result of numerically integrating (4.4.9) and the behaviour of $\tau(z)$ for different values of c_3.

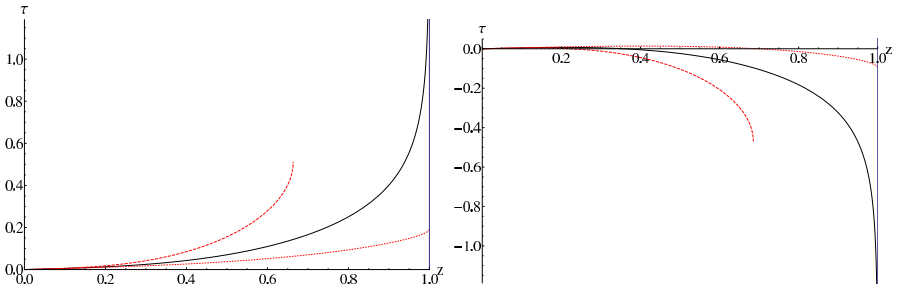

Figure 4.1: All the graphs are plotted using $z_\Lambda = 1$, $\mu^2 = \pi$ and $c_1 = 0.05$. The vertical line at $z = z_\Lambda = 1$ represents the IR end of space (tip of the cigar). On the left, the solid black line represents a solution with $c_3 \approx 0.3579$ for which τ diverges at z_Λ. The red dashed line has a too large c_3 - in particular, it corresponds to $c_3 = 1$ - such that there is a singularity at $z = z_s$ where $\partial_z \tau$ diverges while τ stays finite (a behaviour of the type $\tau = k_1 - k_2\sqrt{z_s - z}$, that is unacceptable since the solution stops at $z = z_s$ where the energy density of the flavor branes diverges). The red dotted line corresponds to $c_3 = 0.1$; this kind of solution ought to be discarded because the tachyon stays finite everywhere. The plot in the right is done with the same conventions but with negative values of $c_3 = -0.1, -0.3893, -1$. For $c_3 \approx -0.3893$ there is a solution of the differential equation such that τ diverges to $-\infty$. As explained in the text, this solution is unstable. Thus, the physical solution for this particular value of c_1 is uniquely determined to be the solid line of the graph on the left.

In figure 4.2, we plot the values of c_3 and C obtained dynamically, as a function of c_1.

4.4.2 The deconfined phase

Inserting the metric (4.3.8) in (4.4.6), we obtain the following equation for τ in the deconfined phase:

$$\tau'' + \frac{\mu^2 z^2 f_T}{3}\tau'^3\left(-\frac{4}{z} + \frac{f_T'}{2f_T}\right) + (-\frac{3}{z} + \frac{f_T'}{f_T})\tau' + \left(\frac{3}{z^2 f_T} + \mu^2\tau'^2\right)\tau = 0 \qquad (4.4.17)$$

The IR behaviour of this equation is quite different from the one of (4.4.9). First of all τ is not allowed to diverge at any point. The difference with respect to the confining case is that since there is a horizon, one can allow the branes not to recombine as long as they end on the horizon. Then, they will not generate any anomaly.

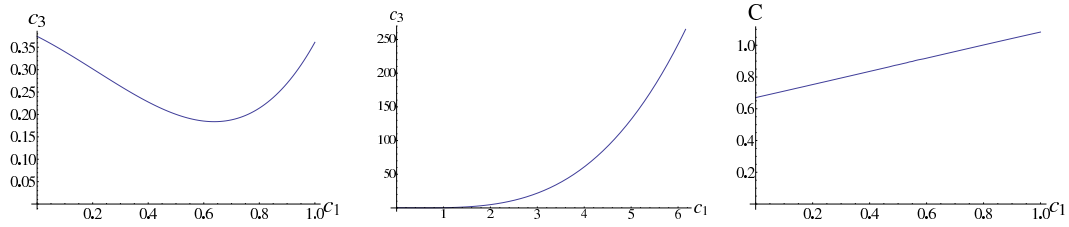

Figure 4.2: The values of c_3 and C determined numerically as a function of c_1. In the first plot we portray c_3 in terms of c_1, for $c_1 \leq 1$. In the second plot we show c_3 for a larger range of c_1. The third plot depicts the constant C entering the IR expansion as a function of c_1. Again, we have used $z_\Lambda = 1$, $\mu^2 = \pi$ for the plots.

Still, one has to discard solutions for which τ' diverges at some $z < z_T$ (with τ remaining finite). Those solutions yield infinite energy density and are physically inconsistent, just as in the confining case. It turns out that this condition uniquely selects a value for c_3, for which τ reaches the horizon at $z = z_T$ taking there a finite value, say $\tau|_{z=z_T} = c_T$, as shown in the first plot of figure 4.3.

Thus, we have a one parameter family of physical solutions (which again fix c_3 in terms of c_1 as expected on physical grounds). In a similar fashion to the confined case, by redefining the field and radial coordinate as $z \to \tilde{z} = z/z_T$, $\tau \to \tilde{\tau} = \mu\tau$, the dependence of the equation on these two parameters can be reabsorbed. Near the IR, these solutions read, in terms of the parameter $\tau(z_T) \equiv c_T$:

$$\tau = c_T - \frac{3c_T}{5z_T}(z_T - z) - \frac{9c_T}{200z_T}(8 + \mu^2 c_T^2)(z_T - z)^2 + \dots \tag{4.4.18}$$

Once c_1 is fixed, c_3 and c_T are dynamically determined by this IR condition, and their values can be found numerically; using a standard shooting technique. Notice that for $c_1 = 0$, the solution is simply $\tau = 0$ and chiral symmetry is unbroken. We display some plots with numerical results in figure 4.3.

4.4.3 Holographic renormalization, the quark mass and the quark condensate

On general AdS/CFT grounds, we expect the integration constants c_1, c_3 of the UV expansion (4.4.7) to be related to the source and vacuum expectation value of the boundary operator associated to the bulk field τ, which is the scalar quark bilinear $\bar{q}q$. Namely c_1 should be, essentially, the quark mass and c_3 the quark condensate. In this section, we will make this connection precise.

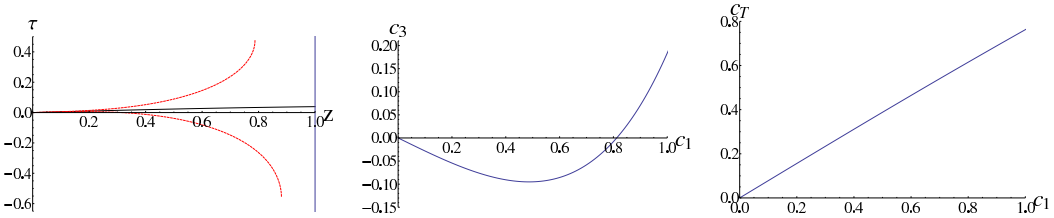

Figure 4.3: Plots corresponding to the deconfined phase. All the graphs are plotted using $z_T = 1$, $\mu^2 = \pi$. For the first plot we have taken $c_1 = 0.05$. The solid line displays the physical solution $c_3 = -0.0143$ whereas the dashed lines ($c_3 = -0.5$ and $c_3 = 0.5$) are unphysical and end with a behaviour of the type $\tau = k_1 - k_2\sqrt{z_s - z}$. The second and third plots give the values of c_3 and c_T determined numerically by demanding the correct IR behaviour of the solution, as a function of c_1.

As has been pointed out many times -see for instance [32], [33]-, in QCD the quark mass runs all the way to zero in the far UV, a fact that cannot be matched in a holographic model with AdS asymptotics (such that the m_q we will define is the UV value, which does not run further). If we want to make a phenomenological analysis, the most natural option is to identify the m_q of the model with the QCD quark mass measured at a scale around 1 or 2 GeV. It is conceivable that this feature can be ameliorated by using the tachyon action in a holographic setup which incorporates asymptotic freedom, as in "Improved holographic QCD" [7].

The quark condensate is defined as:

$$\langle \bar{q}\, q \rangle = -\frac{\delta S_{ren}}{\delta m_q} \tag{4.4.19}$$

where in order to find S_{ren} we have to follow the procedure of holographic renormalization, see for instance [36]. The first step is to regularize the action by placing a UV cut-off at $z = \epsilon$, namely $S_{reg} = \int_\epsilon^{z_\Lambda} \mathcal{L}$, where we have defined, from (4.4.5):

$$\mathcal{L} = -2\mathcal{K}\, e^{-\frac{1}{2}\mu^2\tau^2}\, g_{tt}^{\frac{1}{2}} g_{xx}^{\frac{3}{2}} \sqrt{g_{zz} + 2\pi\alpha'\lambda(\partial_z\tau)^2} \tag{4.4.20}$$

Since we are just concerned with the variation of S_{reg} with respect to m_q, we compute the functional derivative with respect to τ:

$$\delta S_{reg} = \int_\epsilon^{z_\Lambda} \left(\delta\tau \frac{\partial \mathcal{L}}{\partial \tau} + \delta\tau' \frac{\partial \mathcal{L}}{\partial \tau'} \right) dz = \int_\epsilon^{z_\Lambda} \frac{d}{dz} \left(\delta\tau \frac{\partial \mathcal{L}}{\partial \tau'} \right) \tag{4.4.21}$$

and therefore

$$\frac{\delta S_{reg}}{\delta \tau} = -\frac{\partial \mathcal{L}}{\partial \tau'}\Big|_{z=\epsilon} \tag{4.4.22}$$

We are interested in $\frac{\delta S_{reg}}{\delta c_1} = \frac{\delta \tau}{\delta c_1}\frac{\delta S_{reg}}{\delta \tau}$. In order to compute $\frac{\delta \tau}{\delta c_1}$, one should take into account that c_3 is a non-trivial function of c_1. We find by explicit computation, using the UV expansion (4.4.7):

$$\frac{\delta S_{reg}}{\delta c_1} = \mathcal{K} R^5 \mu^2 \left(\frac{2c_1}{3\epsilon^2} + \frac{2}{3}c_1^3\mu^2 \log\epsilon + 2c_3 - \frac{1}{3}c_1^3\mu^2 + \frac{2}{3}c_1\partial_{c_1}c_3 \right) \tag{4.4.23}$$

where we have disregarded terms that vanish as $\epsilon \to 0$. We now have to write the appropriate covariant counterterms that should be added to S_{reg} in order to define the subtracted action $S_{sub} = S_{reg} + S_{ct}$:

$$S_{ct} = -\mathcal{K} R \int d^4x \sqrt{-\gamma} \left(-\frac{1}{2} + \frac{\mu^2}{3}\tau^2 + \frac{\mu^4}{18}\tau^4 \log\epsilon + \frac{\mu^4}{12}\alpha\,\tau^4 \right) \tag{4.4.24}$$

where γ corresponds to the induced metric at $z = \epsilon$, namely $\sqrt{-\gamma} = R^4\epsilon^{-4}$. We have introduced a constant α which captures the scheme dependence of the condensate and reflects an analogous scheme dependence in field theory. It will be further discussed in appendix C. The renormalized action is just $S_{ren} = \lim_{\epsilon\to 0} S_{sub}$. It is now straightforward to find:

$$\frac{\delta S_{ren}}{\delta c_1} = -(2\pi\alpha'\mathcal{K} R^3\lambda)\left(-4c_3 + c_1^3\mu^2(1+\alpha) \right) \tag{4.4.25}$$

Notice that the term with $c_1\partial_{c_1}c_3$ in (4.4.23) drops out because there is one with the opposite sign in $\frac{\delta S_{ct}}{\delta c_1}$ that cancels it. We now want to evaluate the quark condensate (4.4.19). The quark mass is proportional to c_1, and we take it to be

$$m_q = \beta\, c_1 \tag{4.4.26}$$

where β is a constant.

The arbitrariness of this multiplicative constant related to the normalization of the fields has been stressed (in analogous situations) in [33], [37]. We finally obtain

$$\langle \bar{q}q \rangle = \frac{1}{\beta}(2\pi\alpha'\mathcal{K} R^3\lambda)\left(-4c_3 + \left(\frac{m_q}{\beta}\right)^3 \mu^2(1+\alpha) \right) \tag{4.4.27}$$

4.4.4 The jump of the condensate at the phase transition

The first term of the expression for the quark condensate (4.4.27) depends on the quantity c_3 that is determined dynamically via the numerical integration. The second term depends on the quark mass and a scheme dependent constant α. We now compute an observable which is independent of this second term by finding the jump of the quark condensate when the theory is heated such that it undergoes the deconfinement phase

transition. Concretely, we take a fixed mass (fixed c_1) and compare c_3 for a confined theory and deconfined theories, such that $z_\Lambda = z_T$, namely at the phase transition point. We have that $\Delta\langle\bar{q}q\rangle \equiv \langle\bar{q}q\rangle_{conf} - \langle\bar{q}q\rangle_{deconf} = -4\frac{1}{\beta}(2\pi\alpha'\mathcal{K}R^3\lambda)\Delta c_3$. In figure 4.4 we plot Δc_3, which in practice is nothing else that the difference between the first plot in figure 4.2 and the second plot of figure 4.3. It turns out to be a monotonously decreasing function, at least in the range of c_1 which we have been able to study numerically. We plot the result in figure 4.4.

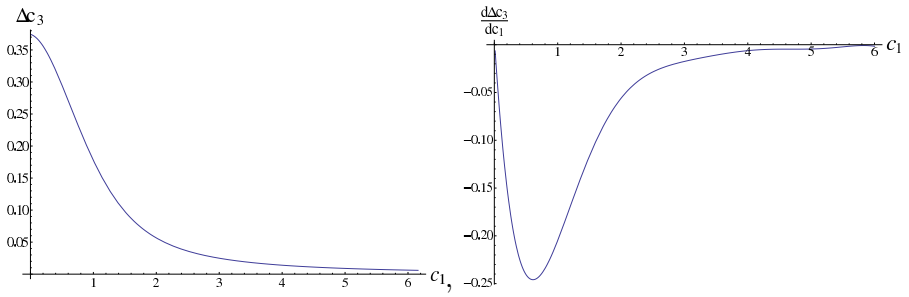

Figure 4.4: The finite jump of the quark condensate and its derivative with respect to c_1 when the confinement-deconfinement transition takes place. The values $z_\Lambda = z_T = 1$ and $\mu^2 = \pi$ have been used in the plot.

Let us now discuss how the quark condensate changes when tuning the temperature, while keeping fixed the quark mass and the QCD scale. We will plot the quantity:

$$\langle\bar{q}q\rangle_R = \frac{m_q}{T_c^4}(\langle\bar{q}q\rangle_T - \langle\bar{q}q\rangle_0)\,, \tag{4.4.28}$$

where $\langle\bar{q}q\rangle_T$ is the condensate evaluated at temperature T. We have included the power of T_c in the denominator in order to make the quotient dimensionless. Let us start by computing the explicit value of $\langle\bar{q}q\rangle_0$ from (4.4.27). We will consider small quark masses (compared to the QCD scale or M_{KK}) so we can neglect the last term of (4.4.27) and use the value $c_3 \approx 0.37 z_\Lambda^{-3}$ computed for small c_1 in the first plot[1] of figure 4.2. Inserting the value of z_Λ in terms of T_c (4.3.11) and advancing the value of the normalization constant that will be found in (4.5.34), we have $\langle\bar{q}q\rangle_0 \approx -0.3 N_c \beta\, T_c^3$. Turning on the temperature but staying below the phase transition, the functions of the metric do not depend on the temperature and therefore $\langle\bar{q}q\rangle_R = 0$ for $T < T_c$. This is just a consequence of large-N volume independence. In order to compute the result in the deconfined phase, we would like to use the values of c_3 as a function of

[1]We remind the reader that the plots were done by fixing $z_\Lambda = 1$ and $z_T = 1$ respectively. The values for generic z_Λ, z_T are obtained just by rescaling $c_1 = (c_1|_{z_\Lambda=1}) z_\Lambda^{-1}$ and $c_3 = (c_3|_{z_\Lambda=1}) z_\Lambda^{-3}$, and similarly in the deconfined phase, substituting z_Λ by z_T.

c_1 plotted in figure 4.3. From the figure, one can fit, for small $c_1 z_T$ the value of c_3 to be $c_3 z_T^3 \approx -0.286 c_1 z_T$. Using this expression, together with (4.4.26), (4.3.10), (4.5.34), we have $\langle \bar{q}q \rangle_T \approx 0.09 N_c m_q T^2$. Finally, we reach the result:

$$\langle \bar{q}q \rangle_R \approx N_c \frac{m_q}{T_c^4} (0.3\beta\, T_c^3 + 0.09 m_q T^2) \ , \qquad (T > T_c) \tag{4.4.29}$$

We illustrate the behaviour of $\langle \bar{q}q \rangle_R$ in figure 4.5. Notice that, since we are considering light quarks, the constant term is the largest until $T \gg T_c$.

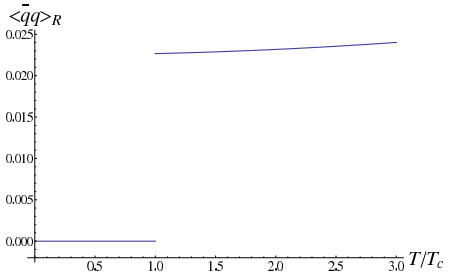

Figure 4.5: Behaviour of $\langle \bar{q}q \rangle_R$ as a function of the temperature. We have taken $N_c = 3$, $\beta = 1$, $m_q/T_c = 1/40$ for the plot.

This is in rough qualitative agreement with lattice results, see figure 4 of [38]. In our case, the jump at the phase transition is sharp due to the large N limit.

4.5 Meson excitations: the confined phase

Up to now, we have discussed the vacuum (saddle point) of the model. We will now discuss in turn the different excitation modes, by expanding the action (4.4.1) up to quadratic order in all the fields. In this section, we will only refer to the confined phase and therefore $\langle \tau \rangle(z)$ is computed as in section 4.4.1.

We define the vector and axial vector fields as:

$$V_M = \frac{A_M^L + A_M^R}{2} \ , \qquad A_M = \frac{A_M^L - A_M^R}{2} \tag{4.5.1}$$

The notation for the associated field strengths will be V_{MN}, A_{MN}. We use a gauge $A_z = V_z = 0$. We split the relevant fields as:

$$\begin{aligned} V_\mu(x^\mu, z) &= \psi^V(z)\, \mathcal{V}_\mu(x^\mu) \ , \\ A_\mu(x^\mu, z) &= A_\mu^\perp(x^\mu, z) + A_\mu^\parallel(x^\mu, z) = \psi^A(z)\, \mathcal{A}_\mu(x^\mu) - \varphi(z)\, \partial_\mu(\mathcal{P}(x^\mu)) \ , \\ \theta(x^\mu, z) &= 2\, \vartheta(z)\, \mathcal{P}(x^\mu) \ , \\ \tau(x^\mu, z) &= \langle \tau \rangle(z) \ + \ s(x^\mu, z) = \langle \tau \rangle(z) \ + \ \psi^S(z)\, \mathcal{S}(x^\mu) \ . \end{aligned} \tag{4.5.2}$$

where $\mathcal{V}_\mu$ and $\mathcal{A}_\mu$ are transverse vectors $\partial^\mu \mathcal{V}_\mu = \partial^\mu \mathcal{A}_\mu = 0$. A few comments are in order: we have used the residual gauge freedom to make V_μ transverse. We have anticipated the behaviour of the equations of motion in order to write down the terms containing $\mathcal{P}(x)$, associated to the pseudoscalars. The symbol $\langle\tau\rangle(z)$ represents the tachyon vev in the bulk, as discussed in section 4.4.

The different bulk fields are dual to the field theory quark bilinears due to the boundary couplings[1]: $\int d^4x \mathcal{V}_\mu \mathcal{J}_V^\mu$, $\int d^4x \mathcal{A}_\mu \mathcal{J}_A^\mu$, $\int d^4x \mathcal{P}\mathcal{J}_P$, $\int d^4x \mathcal{S}\mathcal{J}_S$, where the $\mathcal{J}$'s are the different bilinear quark currents: $\mathcal{J}_V^\mu = \bar{q}\gamma^\mu q$, $\mathcal{J}_A^\mu = \bar{q}\gamma^\mu\gamma^5 q$, $\mathcal{J}_P = \bar{q}\gamma^5 q$, $\mathcal{J}_S = \bar{q}q - \langle\bar{q}q\rangle$.

We also define the useful quantity:

$$\tilde{g}_{zz} = g_{zz} + 2\pi\alpha'\lambda(\partial_z\langle\tau\rangle)^2 \tag{4.5.3}$$

In the rest of this section, we will discuss the explicit prescriptions to compute the masses and decay constants for the different mesonic modes. In particular, the decay constants will require computing two-point correlators for which one has to holographically renormalize. We give here the complete set of counterterms which make the on-shell action finite.

$$S_{ct} = -\mathcal{K}R\int d^4x\sqrt{-\gamma}\Bigg(-\frac{1}{2} + \frac{\mu^2}{3}\tau^2 + \frac{\mu^4}{18}\tau^4\log\epsilon + \frac{\mu^4}{12}\alpha\tau^4 +$$
$$+\frac{(2\pi\alpha')^2}{g_V^4}\frac{1}{2}\gamma^{\mu\rho}\gamma^{\nu\delta}(V_{\mu\nu}V_{\rho\delta} + A_{\mu\nu}A_{\rho\delta})(\log\epsilon + \frac{1}{2}) + \frac{R^2\mu^2}{3}\gamma^{\mu\nu}(D_\mu T)^*(D_\nu T)(\log\epsilon + \frac{1}{2})\Bigg) \tag{4.5.4}$$

This expression completes (4.4.24) by including all the active fields we are considering. The terms of 1/2 inside the brackets of the second line are finite contact terms that have been chosen for convenience.

We now discuss in turn each of the modes.

4.5.1 Vector mesons

The quadratic action corresponding to the vector mesons that comes from expanding (4.4.1) reads:

$$S_V = -\frac{(2\pi\alpha')^2}{g_V^4}\mathcal{K}\int d^4x\, dz e^{-\frac{1}{2}\mu^2\tau^2}\left[\frac{1}{2}\tilde{g}_{zz}^{\frac{1}{2}}V_{\mu\nu}V^{\mu\nu} + g_{xx}\tilde{g}_{zz}^{-\frac{1}{2}}\partial_z V_\mu \partial_z V^\mu\right], \tag{4.5.5}$$

where we have constrained ourselves to the confining phase in which $g_{tt} = g_{xx}$. Here and in the following, it should be understood that the μ, ν indices are contracted using

[1] The various discrete symmetries and their realization are detailed in [16].

the flat Minkowski metric, since we have explicitly written the factor of $g_{xx} = R^2/z^2$. The equation of motion can be easily derived:

$$\frac{1}{e^{-\frac{1}{2}\mu^2\tau^2}\tilde{g}_{zz}^{\frac{1}{2}}}\partial_z\left(e^{-\frac{1}{2}\mu^2\tau^2}g_{xx}\tilde{g}_{zz}^{-\frac{1}{2}}\partial_z\psi^V(z)\right) - q^2\psi^V(z) = 0 \tag{4.5.6}$$

where we have gone to Fourier space and defined the 4d-momentum such that for the eigenmodes it corresponds to the mass eigenvalues $q^2 = -m_V^2$. The above equation explicitly depends on only two parameters z_Λ and μ^2. It is easy to check that z_Λ just gives an overall scale to m_V^2 (and, in fact, to all dimensionful quantities that will appear later) and μ^2 only enters through the combination $\tilde{\tau}^2 = \mu^2\tau^2$. This was the same combination in the tachyon equation (see the comment below (4.4.9)), and in fact one can fix the value of μ^2 without any loss of generality. From now on, we will set $\mu^2 = \pi$, $z_\Lambda = 1$ in all the plots, although we will keep the parameters explicit in the equations.

Finally, notice that (4.5.6) depends implicitly on c_1 (the quark mass) through the bulk vacuum expectation value of τ. In short, the vector spectrum given by the model depends just on a multiplicative constant z_Λ and the parameter c_1, namely the quark mass. All the other parameters that we have defined drop out from this computation.

4.5.1.1 Schrödinger formalism and the mass spectrum

In order to gain some insight in the problem, let us transform equation (4.5.6) to a Schrödinger problem, following appendix D. We immediately read $C(z) = M(z) = 0$ and:

$$A(z) = e^{-\frac{1}{2}\mu^2\tau^2}g_{xx}\tilde{g}_{zz}^{-\frac{1}{2}} \ , \qquad B(z) = e^{-\frac{1}{2}\mu^2\tau^2}\tilde{g}_{zz}^{\frac{1}{2}} \ , \tag{4.5.7}$$

such that the Schrödinger radial variable is defined by:

$$u = \int_0^z \sqrt{\frac{B(\tilde{z})}{A(\tilde{z})}}d\tilde{z} = \int_0^z \sqrt{\frac{\tilde{g}_{zz}(\tilde{z})}{g_{xx}(\tilde{z})}}d\tilde{z} \ . \tag{4.5.8}$$

Notice that $u \in [0, \infty)$. It is now a straightforward exercise to obtain the Schrödinger-like potential (D.7), for a given c_1. One has to compute numerically $\tau(z)$ as in section 4.4.1, then evaluate (D.7) and finally implement the variable change (4.5.8). Some examples are plotted in figure 4.6.

We observe that the potentials move up as we increase c_1. This is of course expected on general grounds, since meson masses should grow with increasing quark masses, but this feature is missing from the hard wall or soft wall models. In [15], we made

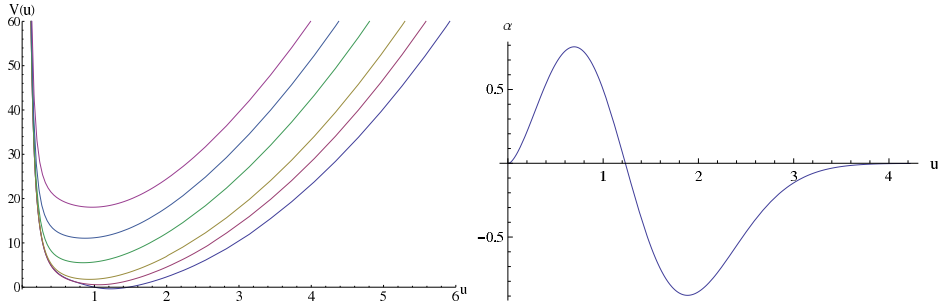

Figure 4.6: The Schrödinger potential associated to the vector excitation for different values of the quark mass. From bottom to top $c_1 = 0, 0.5, 1, 2, 3, 4$. For illustrative purposes, on the right we plot the second normalizable "wavefunction" for $c_1 = 1$.

a phenomenological fit including the strange-strange meson masses in the analysis, finding good agreement with experimental data.

One can check that the leading contribution to $V(u)$ near $u = 0$ is of the form $V(u) = \frac{3}{4}u^{-2} + \ldots$. This just comes from the UV AdS asymptotics. Let us now find the leading IR contribution to $V(u)$. For large u (namely near $z = z_\Lambda$), we have that $g_{xx} \approx R^2/z_\Lambda^2$ and $\tilde{g}_{zz} \approx 2\pi\alpha'\lambda(\partial_z\tau)^2$. Using the expressions in appendix D, a little algebra shows that for large u, we have $\frac{du}{dz} \approx \frac{\mu}{\sqrt{3}} z_\Lambda \partial_z \tau$ and therefore $u \sim \frac{\mu}{\sqrt{3}} z_\Lambda \tau$. The function Ξ behaves as $\Xi \approx \left(\frac{R}{z_\Lambda}\right)^{\frac{1}{2}} e^{-\frac{3u^2}{4z_\Lambda^2}}$ what finally leads to $V(u) = \frac{9}{4z_\Lambda^4}u^2 + \mathcal{O}(u)$. Therefore, $V(u)$ grows quadratically at large u, a fact that leads to standard Regge trajectories for large excitation number n [14]. Asymptotically, the slope of these trajectories is $\lim_{n\to\infty} \frac{dm_n^2}{dn} = \frac{6}{z_\Lambda^2}$, as can be found by evaluating (D.9).

By using standard numerical shooting techniques, we have computed the mass spectrum. In particular, we have computed the first seven states, changing the quark mass parameter in the range $0 < c_1 < 5$. We plot some results in figure 4.7. It turns out that for small c_1 the growth of meson mass on the quark mass is linear. This is just what one expects from a Taylor expansion if we consider the meson masses as function of the quark masses. This was a result already found in [15]. We have:

$$\begin{aligned} z_\Lambda\, m_V^{(1)} &\approx 1.45 + 0.718c_1 \quad , \quad z_\Lambda\, m_V^{(2)} \approx 2.64 + 0.594c_1 \quad , \quad z_\Lambda\, m_V^{(3)} \approx 3.45 + 0.581c_1 \quad , \quad (c_1 \leq 1) \\ z_\Lambda\, m_V^{(4)} &\approx 4.13 + 0.578c_1 \quad , \quad z_\Lambda\, m_V^{(5)} \approx 4.72 + 0.577c_1 \quad , \quad z_\Lambda\, m_V^{(6)} \approx 5.25 + 0.576c_1. \end{aligned} \tag{4.5.9}$$

At around $c_1 \geq 1$, the graphs start departing from the straight line, as can be seen on the second plot in figure 4.7.

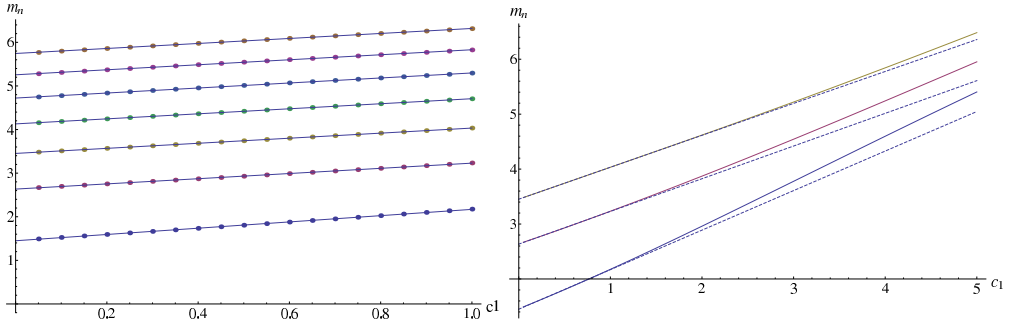

Figure 4.7: Vector meson masses as a function of c_1 (proportional to the quark mass). On the left, we plot the fitted straight lines together with several points computed numerically, for the seven lowest-lying vector modes, in the range $c_1 < 1$. On the right, we go to larger values of c_1 and, for clarity, only plot the three ligthest states. The dashed lines correspond to the linear fits valid for small c_1 whereas the solid line are the actual values found numerically.

4.5.1.2 Current-current correlator and normalization of the action

We have discussed the vector spectrum, but we are also interested in the decay constants of each state. In order to compute them, we have to fix the multiplicative constant associated to the normalization of the action associated to the vector modes. We will follow the reasoning of [12; 13] and match the correlator Π_V to the quark bubble perturbative computation at large Euclidean momentum. In fact, all the discussion of this subsection is completely parallel to [12; 13], since it only depends on the asymptotically AdS structure. We however repeat the argument in the present notation for the sake of clarity.

The current-current correlator is defined as:

$$\int d^4x\, e^{iqx}\langle J_\mu(x)J_\nu(0)\rangle = (\eta_{\mu\nu}q^2 - q^\mu q^\nu)\Pi_V(q^2)\ . \tag{4.5.10}$$

As usual, we compute it holographically from the on-shell action. Integrating by parts in (4.5.5) and adding the counterterm from (4.5.4), we find:

$$\begin{aligned} S_V = \frac{(2\pi\alpha')^2\mathcal{K}}{g_V^4}\int\frac{d^4q}{(2\pi)^4}e^{-\frac{1}{2}\mu^2\tau^2}g_{xx}\tilde{g}_{zz}^{-\frac{1}{2}}V_\mu(q,z)\partial_z V^\mu(-q,z)\Big|_{z=\epsilon} + \\ -\frac{\mathcal{K}R^5(2\pi\alpha'^2)}{g_V^4}\int\frac{d^4q}{(2\pi)^4}\left(q^2V_\mu(q,\epsilon)V^\mu(-q,\epsilon)(\log\epsilon+\frac{1}{2})\right) \end{aligned} \tag{4.5.11}$$

where $V_\mu(q,z) = \psi^V(q,z)V_0^\mu(q)$, and $\psi^V(q,z)$ is the solution to (4.5.6) subject to $V(q,\epsilon) = 1$ and with normalizable behaviour in the IR. At small z, the solution for

$\psi^V(q,z)$ can be expanded in terms of two integration constants as:

$$\psi^V = b_1(q) + \left(b_2(q) + \frac{1}{2}b_1(q)q^2\log z\right) z^2 + \dots \tag{4.5.12}$$

Substituting this expression into (4.5.11) and taking two derivatives with respect to $V_0^\mu(q)$, we find that:

$$\Pi_V(q^2) = -4\frac{\mathcal{K}R(2\pi\alpha')^2}{g_V^4}\frac{b_2}{q^2} \tag{4.5.13}$$

where we have set $b_1(q) = 1$ consistent with the two-point function prescription and the non-trivial q^2-dependence comes through $b_2(q)$, which has to be found by integrating numerically and demanding the physical IR behaviour.

Before entering into numerical integration, we are interested in computing the limiting behaviour for Π_V for large q^2. In order to do this, we consider again the equation written in Schrödinger form and notice that, for small z:

$$u \simeq z\ , \qquad \alpha(u) \simeq u^{-\frac{1}{2}}\psi^V(u) \tag{4.5.14}$$

The leading large q behaviour is not affected by the details of the Schrödinger potential, so we may just approximate it by an expression that interpolates between its UV and IR behaviours, as discussed in subsection 4.5.1.1. Namely, we can just write:

$$-\partial_u^2\alpha + \left(\frac{3}{4u^2} + c^2u^2\right)\alpha + q^2\alpha = 0\,, \tag{4.5.15}$$

where we should take $c^2 = \frac{9}{4z_\Lambda^4}$. However, we will see that the value of c^2 does not matter for the normalization we want to make. (4.5.15) is nothing else than the soft wall model of [14]. The general solution of (4.5.15) is:

$$\alpha(u) = k_1\frac{e^{\frac{-cu^2}{2}}}{\sqrt{u}}U(\frac{q^2}{4c},0,cu^2) + k_2\frac{e^{\frac{-cu^2}{2}}}{\sqrt{u}}L^{-1}_{\frac{-q^2}{4c}}(cu^2) \tag{4.5.16}$$

where U stands for the confluent hypergeometric function and L for a generalized Laguerre polynomial. IR normalisability requires $k_2 = 0$. We now substitute in (4.5.14) and fix k_1 by demanding that $\lim_{z\to 0}\psi^V(q,z) = \lim_{u\to 0}u^{\frac{1}{2}}\alpha(u) = 1$.

$$\psi^V(q,u) = \frac{q^2}{4c}\Gamma\left(\frac{q^2}{4c}\right)e^{\frac{-cu^2}{2}}U(\frac{q^2}{4c},0,cu^2) \tag{4.5.17}$$

We can now expand this expression for small $u \approx z$ and compare to (4.5.12), in order to read b_2 and, accordingly Π_V from (4.5.13). The leading pieces at large q^2 for b_2 read:

$$\lim_{q^2\to\infty}\frac{b_2}{q^2} = \frac{1}{4}\log q^2 - \frac{1}{4}(1+\log 4 - 2\gamma) - \frac{c^2}{3q^4} + \dots\ , \tag{4.5.18}$$

where γ is Euler's constant. Therefore, the leading piece which we can compare to the quark bubble via (4.5.13) is:

$$\Pi_V(q^2) = -\frac{\mathcal{K}R(2\pi\alpha')^2}{g_V^4}\log q^2 \tag{4.5.19}$$

By matching this expression to the perturbative result, we find[1]:

$$\frac{(2\pi\alpha')^2\mathcal{K}R}{g_V^4} = \frac{N_c}{12\pi^2} \tag{4.5.20}$$

One may wonder how good the results obtained from the simple Schrödinger problem we have discussed (4.5.15) are as an approximation to the full problem (4.5.6). In figure 4.8, we compare (4.5.18) to the value of $b_2(q^2)/q^2$ computed numerically.

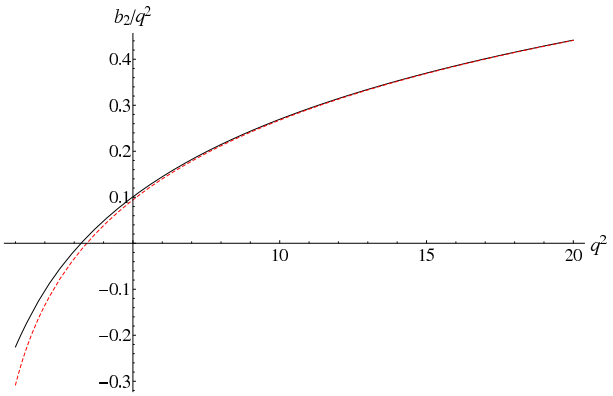

Figure 4.8: We plot the value of b_2/q^2, proportional to the vector current-current correlator. The plot is a comparison of the approximation found in the text from a simplified Schrödinger problem, Eq.(4.5.18) (red dashed line) to the actual numerical result (solid line). The numerical plot was made by taking $c_1 = 0.1$, $\mu^2 = \pi$.

4.5.1.3 Decay constants

We are now interested in determining the decay constants of our mesonic states. We start by writing the current-current correlator as a sum rule.

$$\Pi_V(q^2) = \sum_n \frac{F_n^2}{(q^2 + m_n^2 - i\epsilon)} \tag{4.5.21}$$

[1]Notice that we are dealing with abelian flavor symmetry. There is a factor of $\frac{1}{2}$ difference with respect to [12] since in that paper they deal with a non-abelian case and define $\mathrm{Tr}(t^a t^b) = \frac{1}{2}\delta^{ab}$. This also makes different the definition of the decay constants, for instance the f_π defined in [12] is the f_π we will use divided by $\sqrt{2}$.

The idea is to derive the form of the sum rule holographically. In appendix E we give a general description on how to write holographically a two-point correlator as an infinite sum. Then we use properties of the normalizable modes in order to determine the values of F_n. The argument follows [12; 13] so we directly quote the result in the present notation[1]:

$$F_n^2 = \frac{N_c}{6\pi^2}\frac{R}{m_n^2}\left(\frac{d^2\psi_V^{(n)}}{dz^2}\Big|_{z=0}\right)^2 \tag{4.5.22}$$

where $\psi_V^{(n)}$, $n = 1, 2, \ldots, \infty$ are the solutions of (4.5.6) normalized as:

$$\int B(z)(\psi_V^{(n)})^2 dz = 1 \tag{4.5.23}$$

with $B(z)$ given in (4.5.7). Again, we can compute numerically the values of the decay constants given by the model. We have plotted them in figure 4.9. One can see that the dependence on excitation number is rather mild for small quark masses and for a large number of modes.

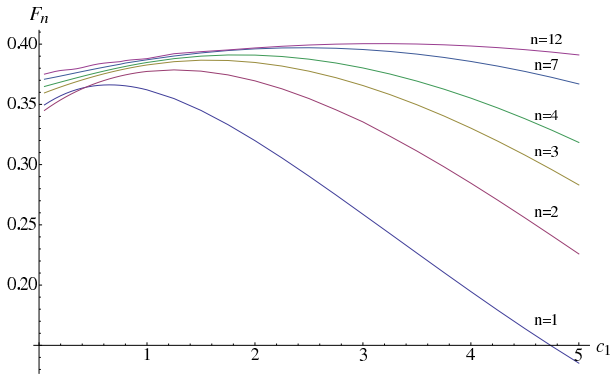

Figure 4.9: The decay constant, in units of z_Λ^{-1} for the four lowest-lying, the seventh and the twelve-th vector mode (from bottom to top), as a function of c_1. The numerical plot was made by taking $\mu^2 = \pi$ and $N_c = 3$.

4.5.1.4 Regge trajectories for vector mesons and linear confinement

Typical holographic models lead to a behaviour of the masses with the excitation number as $m_n^2 \propto n^2$, for large n [39]. However, experiment and semiclassical quantization of a hadronic string (assuming linear confinement) suggest that $m_n^2 \propto n$ in QCD. Circumventing this problem was the motivation for developing the soft-wall model [14].

[1] Notice our definition of F_n is different from [12].

As pointed out above and also in [16], a model including an open string tachyon with action (4.4.1) and gaussian tachyon potential, naturally implements this behaviour. In figure 4.10, we plot the results of some numerical computations which display this feature. We remind the reader that, as we saw in section 4.5.1.1, for vector mesons $\lim_{n\to\infty} m_{n+1}^2 - m_n^2 = 6/z_\Lambda^2$. This seems to be born out by the figure.

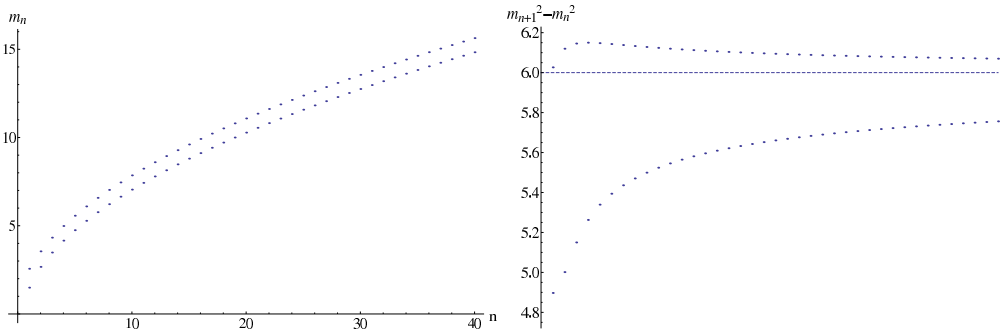

Figure 4.10: Results corresponding to the forty lightest vector states with $c_1 = 0.05$ and $c_1 = 1.5$. On the right, the horizontal line signals the asymptotic value 6 of the Regge trajectory, the lower line corresponds to $c_1 = 0.05$ and the upper line to $c_1 = 1.5$. Masses are given in units of z_Λ^{-1}.

4.5.2 Axial-vector mesons

The quadratic action corresponding to the axial vector mesons that comes from expanding (4.4.1) picks an extra term with respect to (4.5.5), coming from the covariant derivative of the tachyon:

$$S_A = -\frac{(2\pi\alpha')^2}{g_V^4}\mathcal{K}\int d^4x\, dz e^{-\frac{1}{2}\mu^2\tau^2}\left[\frac{1}{2}\tilde{g}_{zz}^{\frac{1}{2}}A_{\mu\nu}A^{\mu\nu} + g_{xx}\tilde{g}_{zz}^{-\frac{1}{2}}\partial_z A_\mu \partial_z A^\mu + \frac{4R^2 g_V^4}{3(2\pi\alpha')^2}\mu^2\tau^2 g_{xx}\tilde{g}_{zz}^{\frac{1}{2}}A_\mu A^\mu\right] \tag{4.5.24}$$

The equation of motion can be derived to be:

$$\frac{1}{e^{-\frac{1}{2}\mu^2\tau^2}\tilde{g}_{zz}^{\frac{1}{2}}}\partial_z\left(e^{-\frac{1}{2}\mu^2\tau^2}g_{xx}\tilde{g}_{zz}^{-\frac{1}{2}}\partial_z\psi^A(z)\right) - k\frac{\mu^2\tau^2}{z^2}\psi^A(z) - q^2\psi^A(z) = 0 \tag{4.5.25}$$

where we have introduced a new constant k as the combination:

$$k = \frac{4R^4 g_V^4}{3(2\pi\alpha')^2} \tag{4.5.26}$$

We observe that τ only enters through the combination $\mu\tau$ so μ is immaterial since it can be rescaled away. On the other hand, the constant k, that did not enter the

parity even sector does affect the physics. In fact, by comparing (4.5.6) to (4.5.25), one can see that the difference between the equation for the vectors and the one for the axials in controlled by k. Therefore, it is natural to guess that k somehow enhances or suppresses the effects of chiral symmetry breaking on the P-odd spectra. In the following, we will see how the physics depends on this parameter. The model of our previous work [15] was more constrained since, in terms of the present notation, k was fixed to $\frac{12}{\pi^2}$.

4.5.2.1 Schrödinger formalism and the mass spectrum

The functions for converting to a Schrödinger problem $A(z)$, $B(z)$ are as before (4.5.7). On top of that, we have here a non-trivial $M(z)$ given by $M(z) = B(z)\, k\, \mu^2\tau^2/z^2$. It is easy to check that the leading piece in the UV of the Schrödinger potential is $3/4u^2$ as for the vectors. However, the leading IR behaviour is modified due to the term proportional to k to $V_{IR}(u) = \frac{9}{4z_\Lambda^4}\left(1+\frac{4k}{3}\right)u^2$. From this observation, one can immediately realize that the model gives different Regge slopes for vectors and axials and that the leading behaviour of $\Pi_A(q^2)$ at large Euclidean momentum coincides, consistently, with the vector one (4.5.19). We will later comment further on these issues.

The qualitative appearance of the Schrödinger potentials for the axial excitation is similar to the ones for the vectors. But the value of the potentials in the axial case is always higher due to the terms coming from $M(z)$. Thus, for equal excitation number and quark mass, the axial mode is always heavier than the vector mode (with the difference controlled by k). For small values of c_1, the dependence of the meson masses on the quark masses is linear

$$\begin{aligned} z_\Lambda\, m_A^{(1)} &\approx 2.05 + 1.46c_1\ , \qquad z_\Lambda\, m_A^{(2)} \approx 3.47 + 1.24c_1\ , \qquad z_\Lambda\, m_A^{(3)} \approx 4.54 + 1.17c_1\ , \qquad (c_1 \leq 1) \\ z_\Lambda\, m_A^{(4)} &\approx 5.44 + 1.13c_1\,, \qquad z_\Lambda\, m_A^{(5)} \approx 6.23 + 1.11c_1\,, \qquad z_\Lambda\, m_A^{(6)} \approx 6.95 + 1.10c_1\ . \qquad (4.5.27) \end{aligned}$$

For this calculation, we used $k = \frac{18}{\pi^2}$ as it is found by the fit of the parameters in section (4.5.5), whereas in [15], we used $k = \frac{12}{\pi^2}$. For larger c_1, the plots of the meson mass dependence on the quark mass for the axial excitation look similar to the vector case, see the plot on the right of figure 4.7.

4.5.2.2 Current-current correlator and the pion decay constant

By explicit computation it is easy to check that the UV expansion of the solution to (4.5.25) is given in terms of the two integration constants as:

$$\psi^A = b_1 + \left(b_2 + \frac{1}{2}b_1(q^2 + \pi\, k\, c_1^2)\log z\right) z^2 + \dots \tag{4.5.28}$$

For the case of the axial vector, the corresponding sum rule generalising (4.5.21) reads:

$$\Pi_A(q^2) = \frac{f_\pi^2}{q^2} + \sum_n \frac{F_n^2}{(q^2 + m_n^2 - i\epsilon)} \tag{4.5.29}$$

where of course now the n run over the axial resonances. The F_n here are computed in essentially the same way as for the vector case, namely using (4.5.22) with a normalization condition (4.5.23).

Now, we are also be able to compute the value of f_π. We do this by directly computing the 2-point function at zero-momentum, namely:

$$f_\pi^2 = -\frac{N_c}{6\pi^2} b_2|_{q=0} \tag{4.5.30}$$

where we have used the expansion (4.5.28), which up to that order, is also valid for the axial case. The value of b_2 to be inserted in (4.5.30) is found numerically by solving (4.5.25) with $q^2 = 0$, with initial condition $\psi^A|_{z=\epsilon} = 1$ and demanding IR normalizability.

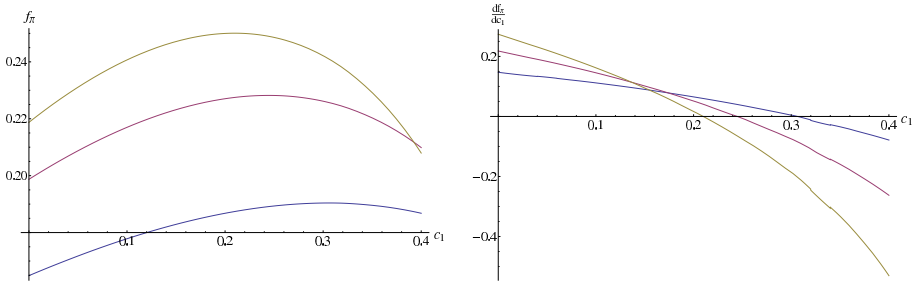

Figure 4.11: The pion decay constant and its derivative as a function of c_1 - the quark mass. The different lines correspond to different values of k. From bottom to top (on the right plot, from bottom to top in the vertical axis) $k = \frac{12}{\pi^2}, \frac{24}{\pi^2}, \frac{36}{\pi^2}$. The pion decay constant comes in units of z_Λ^{-1}.

From the figure, we observe that the decay constant grows with the quark mass for small quark masses and then starts decreasing. We can also observe that increasing the parameter k, increases the value of the pion decay constant. This is in agreement with the intuitive notion given above that k somehow controls the amount of chiral symmetry breaking.

4.5.3 Scalar mesons

We now deal with the scalar excitation. The quadratic action reads:

$$\begin{aligned} S &= -2\pi\alpha'\mathcal{K}\lambda\int d^4xdze^{-\frac{1}{2}\mu^2\tau^2}\Big[g_{xx}^2g_{zz}\tilde{g}_{zz}^{-\frac{3}{2}}(\partial_z s(x,z))^2 - 2\mu^2 g_{xx}^2\tilde{g}_{zz}^{-\frac{1}{2}}\tau(z)\tau(z)'s(x,z)\partial_z s(x,z) \\ &+ \frac{\mu^2}{2\pi\alpha'\lambda}(\mu^2\tau(z)^2-1)g_{xx}^2\tilde{g}_{zz}^{\frac{1}{2}}s(x,z)^2 + g_{xx}g_{zz}\tilde{g}_{zz}^{-\frac{1}{2}}(\partial_\mu s(x,z))^2\Big] \end{aligned} \tag{4.5.31}$$

From (4.4.1), it can be seen that there is also a linear term in the bulk action, but can be easily shown to be a total derivative.

We can read the functions that are used to rewrite this problem is Schrödinger form, as defined in appendix D:

$$\begin{aligned} A(z) &= e^{-\frac{1}{2}\mu^2\tau^2}g_{xx}^2\frac{g_{zz}}{\tilde{g}_{zz}^{3/2}}, & B(z) &= e^{-\frac{1}{2}\mu^2\tau^2}g_{xx}\frac{g_{zz}}{\tilde{g}_{zz}^{1/2}}, \\ C(z) &= -2\mu^2e^{-\frac{1}{2}\mu^2\tau^2}\frac{g_{xx}^2}{\tilde{g}_{zz}^{1/2}}\tau(z)\partial_z\tau(z), & M(z) &= \frac{\mu^2}{2\pi\alpha'\lambda}e^{-\frac{1}{2}\mu^2\tau^2}(\mu^2\tau^2-1)g_{xx}^2\tilde{g}_{zz}^{\frac{1}{2}}. \end{aligned} \tag{4.5.32}$$

Notice that $B(z)/A(z)$ takes the same value as for the vector and axial excitations, which means that the definition of the u-radial coordinate is the same as in those cases. The expression built from $B(z)$, $C(z)$ and $M(z)$ which enters the Schrödinger potential takes a remarkably simple form:

$$\frac{1}{B(z)}\left(M(z)-\frac{1}{2}\partial_z C(z)\right) = -\frac{3}{z^2} \tag{4.5.33}$$

We will find the UV and IR limiting behaviour of the associated Schrödinger potential. At small $z\approx u$, we find $\Xi\approx R^{\frac{3}{2}}/u^{\frac{3}{2}}$ and one can immediately compute from (D.7) the UV leading term to be $V(u)=\frac{3}{4u^2}$. Similarly, the term that dominates for large u is quadratic $\frac{9u^2}{4z_\Lambda^2}$. Thus, we have found that the UV and IR asymptotics are the same as for the vector case and, as a first approximation, we can use the soft wall equation (4.5.15). Thus, we can again match the asymptotic behaviour of the current-current correlator to the perturbative result. For that, we make an argument similar to [32] assume that the $q\bar{q}$ operator is dual to the tachyon rescaled by some constant β, such that the boundary coupling is, schematically, $\int\beta(\tau/z)q\bar{q}$. This is what we anticipated in the relation between c_1 and the quark mass (4.4.26). Then, matching the large q^2 result $\Pi_S(q^2)=\frac{N_c}{8\pi^2}q^2\log q^2$ and reasoning as in the the vector case, we find:

$$\frac{(2\pi\alpha')\mathcal{K}R^3\lambda}{\beta^2} = \frac{N_c}{8\pi^2} \tag{4.5.34}$$

In figure 4.12, we depict the associated Schrödinger potential for different values of c_1. Comparing figure 4.12 to figure 4.6, one can check that the potentials for the scalars

are above those of the vectors. Thus, for equal excitation number, scalar mesons are typically heavier than vectors in the present model.

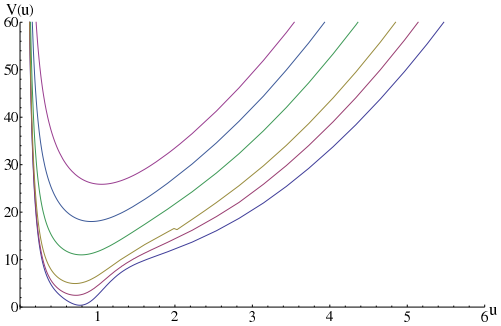

Figure 4.12: The Schrödinger potentials associated to the scalar excitation for $c_1 = 0, 0.5, 1, 2, 3, 4$.

The relation of the lowest scalar meson masses to c_1 follows

$$\begin{aligned} z_\Lambda\, m_S^{(1)} &\approx 2.47 + 0.683 c_1\ , \qquad z_\Lambda\, m_S^{(2)} \approx 3.73 + 0.488 c_1\ , \qquad z_\Lambda\, m_S^{(3)} \approx 4.41 + 0.507 c_1\ , \qquad (c_1 \leq 1) \\ z_\Lambda\, m_S^{(4)} &\approx 4.99 + 0.519 c_1\ , \qquad z_\Lambda\, m_S^{(5)} \approx 5.50 + 0.536 c_1\ , \qquad z_\Lambda\, m_S^{(6)} \approx 5.98 + 0.543 c_1\ . \qquad (4.5.35) \end{aligned}$$

We point out that the scalar meson masses do not depend on the parameter k.

4.5.4 Pseudoscalar mesons

We now focus on the pseudoscalar mesons. With respect to the previous modes, there is an extra complication because the physical modes are a combination of two bulk fields θ and $A_\mu^{\parallel}$. However, we will see that it is possible to find a combination of the fields for which one obtains a standard Sturm-Liouville problem.

The quadratic action reads:

$$\begin{aligned} S &= -(2\pi\alpha')^2 \mathcal{K} \int d^4x dz e^{-\frac{1}{2}\mu^2\tau^2} \Big[\frac{1}{g_V^4} g_{xx} \tilde{g}_{zz}^{-\frac{1}{2}} (\partial_z A_\mu^{\parallel})^2 \\ &+ \frac{\lambda}{2\pi\alpha'} \tau^2 g_{xx}^2 \tilde{g}_{zz}^{-\frac{1}{2}} (\partial_z \theta)^2 + \frac{\lambda}{2\pi\alpha'} \tau^2 g_{xx} \tilde{g}_{zz}^{\frac{1}{2}} (\partial_\mu \theta + 2A_\mu^{\parallel})^2 \Big] \qquad (4.5.36) \end{aligned}$$

Defining $\varphi(z)$ and $\vartheta(z)$ as in (4.5.2) and Fourier transforming $\mathcal{P}(x^\mu)$, we can write the equations of motion for $A_\mu^{\parallel}$ and θ as:

$$\frac{1}{e^{-\frac{1}{2}\mu^2\tau^2} \tilde{g}_{zz}^{\frac{1}{2}}} \partial_z (e^{-\frac{1}{2}\mu^2\tau^2} g_{xx} \tilde{g}_{zz}^{-\frac{1}{2}} \partial_z \varphi(z)) - k \frac{\mu^2\tau^2}{z^2} (\varphi(z) - \vartheta(z)) = 0 \qquad (4.5.37)$$

$$k \frac{\mu^2\tau^2}{z^2} \partial_z \vartheta(z) + q^2 \partial_z \varphi(z) = 0 \qquad (4.5.38)$$

These two equations can be combined into one by solving (4.5.37) for ϑ and inserting this into (4.5.38).

$$e^{-\frac{1}{2}\mu^2\tau^2}\tau^2 g_{xx}^2\tilde{g}_{zz}^{-\frac{1}{2}}\partial_z\left[\frac{1}{e^{-\frac{1}{2}\mu^2\tau^2}\tau^2 g_{xx}\tilde{g}_{zz}^{\frac{1}{2}}}\partial_z\psi^P(z)\right]-k\frac{\mu^2\tau^2}{z^2}\psi^P(z)-q^2\psi^P(z)=0 \tag{4.5.39}$$

where we have defined:

$$\psi^P(z)=-e^{-\frac{1}{2}\mu^2\tau^2}g_{xx}\tilde{g}_{zz}^{-\frac{1}{2}}\partial_z\varphi(z) \tag{4.5.40}$$

and we have used the definition of k in (4.5.26). We can transform equation (4.5.39) to a Schrödinger form following appendix D. Comparing (4.5.39) to (D.2) (and inserting $C(z)=0$) , we find:

$$A(z)=e^{\frac{1}{2}\mu^2\tau^2}\tau^{-2}g_{xx}^{-1}\tilde{g}_{zz}^{-\frac{1}{2}}\,,\qquad B(z)=e^{\frac{1}{2}\mu^2\tau^2}\tau^{-2}g_{xx}^{-2}\tilde{g}_{zz}^{\frac{1}{2}}\,,\qquad \frac{M(z)}{B(z)}=k\frac{\mu^2\tau^2}{z^2}\,. \tag{4.5.41}$$

Notice that the value of B/A coincides with those for the rest of modes and, therefore, the Schrödinger coordinate u is the same for all the possible excitations. Let us compute the IR (large u) leading behaviour of such a Schrödinger potential. It turns out to be $V_{IR}(u)\approx\frac{9}{4z_\Lambda^4}(1+\frac{4k}{3})u^2$, as for the axials. The coefficient of this quadratic term is what controls the slope of the Regge trajectories for highly excited mesons. Thus, the outcome of the present model in this respect is that vectors and scalars have the same Regge slope, whereas the slopes for axials and pseudoscalars coincide and are larger than the vector one.

An important observation is that the natural normalization condition is not (D.4) but, looking for the kinetic term of the pseudoscalar field in (4.5.36), we obtain:

$$(2\pi\alpha')^2\mathcal{K}\int_0^{z_\Lambda}dze^{-\frac{1}{2}\mu^2\tau^2}\Big[\frac{1}{g_V^4}g_{xx}\tilde{g}_{zz}^{-\frac{1}{2}}(\partial_z\varphi_n(z))^2+\frac{4\lambda}{2\pi\alpha'}\tau^2 g_{xx}\tilde{g}_{zz}^{\frac{1}{2}}(\vartheta_n(z)-\varphi_n(z))^2\Big]=\frac{1}{2}\,. \tag{4.5.42}$$

Rewriting this expression in terms of ψ^P, we find:

$$\begin{aligned}\frac{1}{2}&=\frac{(2\pi\alpha')^2\mathcal{K}}{g_V^4}\int_0^{z_\Lambda}dz\,e^{\frac{1}{2}\mu^2\tau^2}g_{xx}^{-1}\left(\tilde{g}_{zz}^{\frac{1}{2}}\psi_n^P(z)^2+\frac{2\pi\alpha'}{4\lambda g_V^4\tau^2}\tilde{g}_{zz}^{-\frac{1}{2}}(\partial_z\psi_n^P(z))^2\right)=\\&=\frac{(2\pi\alpha')^2\mathcal{K}}{g_V^4}\int_0^{\infty}du\left(g_{xx}\tau^2\alpha(u)^2+\frac{2\pi\alpha'}{4\lambda\,g_V^4}e^{\frac{1}{2}\mu^2\tau^2}g_{xx}^{-\frac{3}{2}}\tau^{-2}\left[\partial_u\left(e^{-\frac{1}{4}\mu^2\tau}g_{xx}^{\frac{3}{4}}\tau\alpha(u)\right)\right]^2\right)\end{aligned} \tag{4.5.43}$$

where in the last line we have changed to the Schrödinger variables following the conventions of appendix D. There are some subtleties related to the UV behaviour of (4.5.43) which are worth explaining. Since the leading UV behaviour of our model is

the same as in the hard wall [12], [13] or soft wall [14] models, the following arguments are analogous in all these cases. However, we are unaware of any reference where the discussion below is explicitly shown. It turns out that this UV behaviour is qualitatively different for massless ($c_1 = m_q = 0$) or massive ($c_1 \sim m_q > 0$) quarks. We will study both cases separately below.

4.5.4.1 The $m_q = 0$ case

We will now study the qualitative properties of the physical spectrum for $m_q = 0$. In this case, the $\tau \sim u^3$ near the UV and therefore $\Xi = (AB)^{\frac{1}{4}} \sim u^{-\frac{3}{2}}$, which implies that

$$V_{UV}(u) = \frac{15}{4u^2} + \dots \tag{4.5.44}$$

The first correction represented by the dots comes at order u^3. One can then find the UV expansion for $\alpha(u)$ that solves (D.6) in terms of the two integration constants which we denote k_1, k_2 as $\alpha(u) = k_1 u^{-\frac{3}{2}} + \frac{1}{4}k_1 m_n^2 u^{\frac{1}{2}} - \frac{1}{16}k_1 m_n^4 u^{\frac{5}{2}} \log u + k_2 u^{\frac{5}{2}} + \dots$ We now want to insert this in the last line of (4.5.43) and check whether the integral converges near $u = 0$. The first term is always convergent so we focus on the second term which behaves as $\int_0 du u^{-3}[\partial_u(u^{\frac{3}{2}}\alpha(u))]^2$. Therefore, for $m_n = 0$, this mode is UV-normalizable irrespective of the values of k_1 and k_2. Thus, one can always tune k_2/k_1 in order to find a solution that is well-behaved in the IR. This means that for $m_q = 0$ there is always a normalizable solution with $m_n = 0$, which corresponds to the expected massless Goldstone boson. On the other hand, if $m_n \neq 0$, one has to impose $k_1 = 0$ in order to have UV-normalizability. Then, as in a standard Sturm-Liouville problem, there will be a discrete set of massive modes, where m_n is selected by matching the normalizable UV and IR behaviours.

In summary, for $m_q = 0$ the UV structure of the Schrödinger potential and normalizability condition ensures the existence of a massless Goldstone boson together with a discrete tower of massive excitations, as expected.

4.5.4.2 The $m_q \neq 0$ case

Near the UV, we now have $\tau \sim u$ and therefore $\Xi = (AB)^{\frac{1}{4}} \sim u^{\frac{1}{2}}$, and

$$V_{UV}(u) = -\frac{1}{4u^2} + \dots \tag{4.5.45}$$

where the first correction in the dots is $\mathcal{O}(u^0)$. We can find again the UV solution in terms of two integration constants $\alpha(u) = k_1 u^{\frac{1}{2}} \log u + k_2 u^{\frac{1}{2}} + \mathcal{O}(u^{\frac{5}{2}})$. Now, requiring

that the last term of (4.5.43) is UV-finite requires setting $k_1 = 0$. Again, one has a Sturm-Liouville problem with a discrete spectrum.

Figure 4.13 depicts a few Schrödinger potentials for the pseudoscalar mode, for different values of c_1.

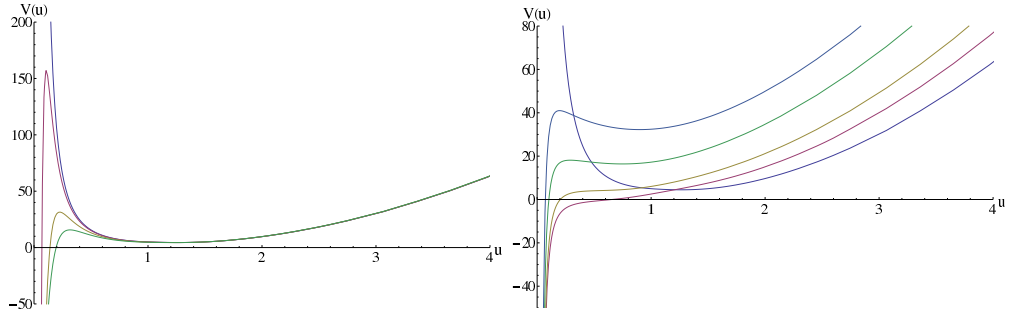

Figure 4.13: On the left, we plot the associated Schrödinger potential for small quark mass, concretely $c_1 = 0, 0.001, 0.005, 0.01$. Even if the UV behaviour is completely different for $c_1 = 0$, we see that for small c_1, the potential looks very similar to the massless case except precisely around $u = 0$. On the right, we plot the same but with larger values of c_1, in particular $c_1 = 0, 0.5, 1, 2, 3$. All plots have been done taking $k = \frac{12}{\pi^2}$. As for the axial case, increasing k amounts to pushing up the IR part of the potential.

Let us now look at the lowest-lying excitation when m_q is small. This should be a pseudo-Goldstone boson with its mass given by the Gell-Mann-Oakes-Renner relation. One indeed can find this following the argument of [12]: for zero quark mass, the $q^2 = 0$ solution of (4.5.37), (4.5.38) is given by $\vartheta(z) = -1$, $\varphi(z) = \psi^A_{q^2=0}(z) - 1$, where we have defined $\psi^A_{q^2=0}(z)$ as the solution at zero momentum of (4.5.25) with boundary condition $\psi^A_{q^2=0} = 1$. Consequently, regarding (4.5.30), $z^{-1}\partial_z \psi^A_{q^2=0}|_{z=0} = -\frac{6\pi^2}{N_c} f_\pi^2$. We now find perturbatively the small m_π^2 solution just by integrating (4.5.38) and we obtain:

$$-1 = m_\pi^2 \int \frac{z^2}{\mu^2 k \tau^2} \partial_z \psi^A_{q^2=0} dz \tag{4.5.46}$$

Using that this integral is dominated by the small z region and taking into account $\int \frac{z^3}{\tau^2} \approx \int \frac{z^3}{(c_1 z + c_3 z^3)^2} \approx \frac{1}{2c_1 c_3}$, we can substitute the relations between c_1, c_3 and $m_q, \langle \bar{q} q \rangle$ (4.4.26), (4.4.27) together with (4.4.8), (4.5.20) and (4.5.26) to find the GOR relation [40]:

$$-4 m_q \langle q \bar{q} \rangle = m_\pi^2 f_\pi^2 \tag{4.5.47}$$

We have obtained this expression by making a series of approximations. However, we can crosscheck it with the values for the mass obtained by the standard numerical computation, see figure 4.14. (4.5.47) is very accurate for small masses. When going

to larger masses (up to $c_1 \approx 1$), we can fit the mass of the lowest lying pseudoscalar to $\sqrt{a\, m_q + b\, m_q^2}$. We include here the masses of the first six pseudoscalar modes in terms of c_1

$$\begin{aligned} z_\Lambda\, m_P^{(1)} &\approx \sqrt{3.53 c_1^2 + 6.33 c_1}\ , \qquad z_\Lambda\, m_P^{(2)} \approx 2.91 + 1.40 c_1\ , \qquad z_\Lambda\, m_P^{(3)} \approx 4.07 + 1.27 c_1\ , \qquad (c_1 \leq 1) \\ z_\Lambda\, m_P^{(4)} &\approx 5.04 + 1.21 c_1\ , \qquad z_\Lambda\, m_P^{(5)} \approx 5.87 + 1.17 c_1\,, \qquad z_\Lambda\, m_P^{(6)} \approx 6.62 + 1.15 c_1\ . \qquad (4.5.48) \end{aligned}$$

where we have also set $k = \frac{18}{\pi^2}$ for this calculation.

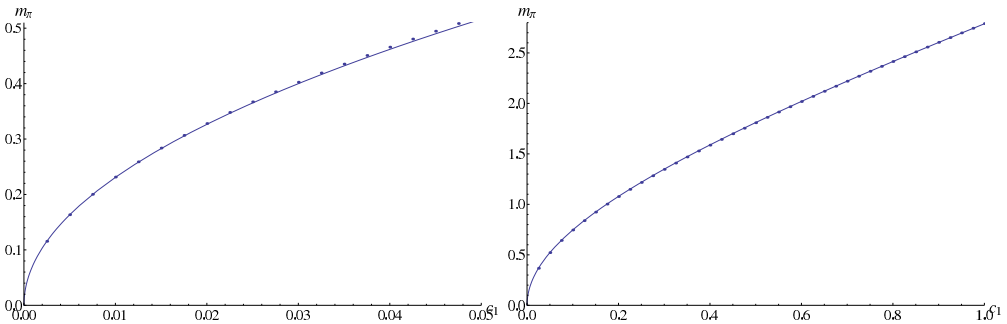

Figure 4.14: We plot the mass of the lowest lying pseudoscalar as a function of c_1 (namely, the quark mass). On the left, we crosscheck the GOR relation (where for $\langle q\bar{q}\rangle$, f_π we have introduced the result found numerically in the chiral limit) to some points computed numerically. The approximation is very good for small c_1, and deviations start seeing visible around $c_1 = 0.03$. On the right, we have fitted b in the expression $m_\pi = \sqrt{\frac{-4 m_q \langle q\bar{q}\rangle}{f_\pi^2} + b\, m_q^2}$ and checked that the fit is rather good up to $c_1 = 1$. the parameter k has been taken to be $\frac{12}{\pi^2}$ in these plots.

4.5.5 Mesonic excitations: a brief phenomenological analysis

We now make a phenomenological analysis of our model by comparing our results for the spectrum and the decay constants of *light unflavored mesons* to their experimental values. An extensive study of meson spectrum appeared in [15], without including the decay constants. We will fit the three parameters of the model, z_Λ, c_1 and k, using mesons with isospin 1 and $J^{PC} = 1^{--}, 1^{++}, 0^{-+}, 0^{++}$. Since $z_\Lambda \sim \Lambda_{QCD}^{-1}$ and $c_1 \sim m_q$, it turns out that there is a single phenomenological parameter k, apart from those inherent of QCD physics.

The experimental values of the meson masses which are used are quoted by [41].

We fit the three parameters of our model to the masses of the light mesons which appear in table [4.1] and the decay constants appearing in [4.2]. To make the fit we

minimize the rms error

$$\epsilon_{rms} = \left(\frac{1}{n} \sum_i \left(\frac{\delta O_i}{O_i} \right)^2 \right)^{\frac{1}{2}} \tag{4.5.49}$$

where n is the number of the observables minus the number of the fitted parameters, $n = 9 - 3$. The values of the parameters minimizing ϵ_{rms} read

$$z_\Lambda^{-1} = 549 \ MeV \quad , \quad c_{1l} z_\Lambda = 0.0094 \quad , \quad k = \frac{18}{\pi^2} \tag{4.5.50}$$

The rms error then is $\epsilon_{rms} = 14.5\%$ and the comparison between the experimental and model values appears in table (4.1), for the masses and in table (4.2), for the decay constants.

J^{CP}	Meson	Measured (MeV)	Model (MeV)	$100\|\delta O\|/O$
1^{--}	$\rho(770)$	775	800	3.2%
	$\rho(1450)$	1465	1449	1.1%
1^{++}	$a_1(1260)$	1230	1135	7.8%
0^{-+}	π_0	135.0	134.2	0.5%
	$\pi(1300)$	1300	1603	23.2%
0^{++}	$a_0(1450)$	1474	1360	7.7%

Table 4.1: The results of the model and the experimental values for light unflavored meson masses.

J^{CP}	Meson	Measured (MeV)	Model (MeV)	$100\|\delta O\|/O$
1^{--}	$\rho(770)$	216	190	12%
1^{++}	$a_1(1260)$	216	228.5	5.8%
0^{-+}	π_0	127	101.3	20.2%

Table 4.2: A comparison of the results to the experimental values for the decay constants of light unflavored mesons.

4.6 Meson melting in the deconfined phase

We briefly discuss in this section the fate of the mesonic modes when the gauge theory undergoes a deconfining phase transition [42], namely when we use the background of

equation (4.3.8). The first observation is that, as we saw in section 4.4.2, the tachyon cannot diverge at any point in this case and, therefore, the brane reaches the horizon, and we only have "black hole embeddings", in analogy with the terminology introduced in [43]. This means that there is no discrete spectrum above the deconfining phase transition. When we are considering small quark masses, this is perfectly realistic.

However, in the real world, charmonium and bottomonium do survive the QCD phase transition. We want to study this problem in the present model, and therefore we will compute the spectral functions at different values of m_q/T. In particular, we will focus in the vector excitation.

We start by discussing the associated Schrödinger potential for the vector excitation in the deconfined background, at zero momentum. The expressions in (4.5.7) are modified to:

$$A(z) = e^{-\frac{1}{2}\mu^2\tau^2} g_{xx}^{\frac{1}{2}} g_{tt}^{\frac{1}{2}} \tilde{g}_{zz}^{-\frac{1}{2}} \ , \qquad B(z) = e^{-\frac{1}{2}\mu^2\tau^2} g_{xx}^{\frac{1}{2}} g_{tt}^{-\frac{1}{2}} \tilde{g}_{zz}^{\frac{1}{2}} \ , \tag{4.6.1}$$

where one should remember that now $g_{\mu\nu}$ refers to the metric (4.3.8). Notice that $\sqrt{B/A}$ diverges at $z = z_T$ as a single pole, such that $\int \sqrt{B/A} dz$ diverges and the horizon $z = z_T$ corresponds to $u = \infty$ in the Schrödinger coordinate. $V(u)$ is exponentially decreasing for large u. For completeness, we write in appendix G the functions determining the potential for the rest of modes. In figure 4.15, we show several examples of potentials computed numerically, for different values of $c_1 \sim m_q z_T \sim m_q/T$. In the second and third plots, we also compare it to the potentials in the confined phase for the same value of c_1. Namely, we show how the potentials for the vector excitations are modified at the phase transition. They share the same UV behaviour, but are drastically modified in the IR due to the different behaviour of the tachyon and the metric.

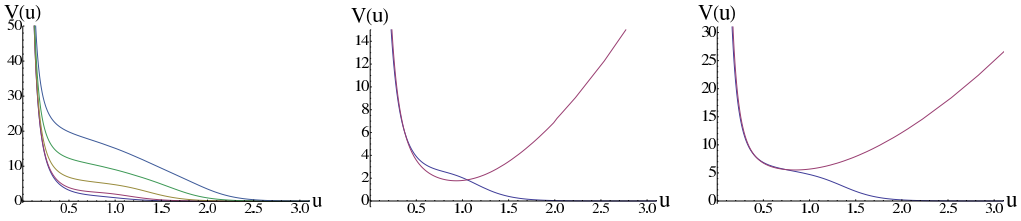

Figure 4.15: The Schrödinger potentials associated to the vector excitation in the deconfined phase, at zero momentum, for different values of $c_1 \sim m_q/T$. In the first plot $c_1 = 0.01, 1, 2, 3, 4$. The second and third plot (respectively $c_1 = 1, 2$) make a comparison with the potentials in the confined phase for the same values of c_1.

In [46], it was shown that a step-like potential gives quasi-particle behaviour. Moreover, if the position of the step coincides with that of a barrier in the confined phase,

the quasi-particle mass is related to the mass of the meson before the phase transition. The third plot seems to point along that line. However, in the present model the potentials for the deconfined phase are never step-like enough, nor present bumps, and thus do not create sharp peaks in the spectral function, as we will see below.

Once we have the potentials, it is straightforward to compute the spectral function from the retarded correlator which is computed following the prescription of [47]. In practice, what one has to do is to impose ingoing boundary conditions at the horizon ($\alpha(u) \sim e^{i\omega u}$ near $u = \infty$)[1] and find the behaviour of the wavefunction near the boundary, namely compute b_1, b_2 matching the numerical result to the UV-expansion (4.5.12). Then, the spectral function is given by:

$$\rho(\omega) = -\text{Im } G_R(\omega) = \frac{N_c}{3\pi^2}\text{Im}\left(\frac{b_2}{b_1}\right) \tag{4.6.2}$$

where we have replaced the parameters of our model by $\frac{N_c}{3\pi^2}$, using (4.5.20). We show in figure 4.16 some examples of this computation. We have plotted $\frac{12\pi}{N_c}\frac{\rho(\omega)}{\omega^2}$ in terms of ω for various values of c_1.

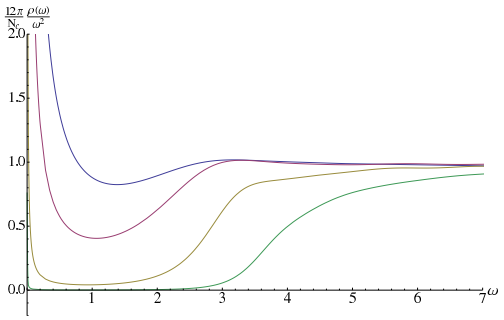

Figure 4.16: The spectral function (divided by ω^2) in units of $\frac{N_c}{12\pi}$ for $c_1 = 0.01, 1, 2, 3, 4$, from top to bottom.

In [44], a bottom-up holographic model was built in order to discuss the physics of the J/Ψ above the phase transition (see also [45] for related work). In the model of [44], there is also no discrete spectrum but, for low enough temperature, by engineering the potential, the J/Ψ shows up as a peak in the spectral function (or, alternatively, as a small negative imaginary part of the associated quasinormal frequency). Namely, it has quasi-particle behaviour.

We now discuss the results comparing to [44]. The authors of [44] showed how the Schrödinger potential should look like to find some qualitative physical properties of the

[1] Even if we use the notation with u since it is better for illustrative purposes, we have found easier to perform the numerical computations in the z-coordinate.

J/Ψ meson. In our model, the potentials are found dynamically, and look similar to [44] except for the important fact that they fail to have the dip of [44]. As a consequence, the J/Ψ decay constant is too low (see figure 4.9) and a clear peak in the spectral function is absent. One may compare our figure 4.16 to figure 3 in [44].

It does not seem possible to introduce the dip feature in our model without inserting at least a new scale in the problem. Notice that the Λ_{QCD} does not play any role in the deconfined case for the present model, apart from setting the value of T at which the transition takes place. In other words, the z_Λ does not appear at all in the deconfined background. We speculate that one should modify the background by including some dependence on Λ_{QCD} in the deconfined phase in order to improve the model in these respects. It would be interesting to investigate whether analyzing the tachyon action in the less simple but well motivated backgrounds of "improved holographic QCD" models [35] might ameliorate the issue along this path.

4.7 Discussion

4.7.1 Summary and general comments on the model

In this paper, we have analyzed in detail several issues of the holographic model presented in [15]. The main ingredient is to describe the open string (meson) physics by using tachyon condensation, captured by Sen's action [17], as first advocated in [16]. The "tachyon", namely the lowest lying bifundamental scalar of the brane-antibrane system, is dual to the quark mass scalar bilinear operator and its condensation corresponds to chiral symmetry breaking. In order to make explicit computations, it is necessary to give an explicit form of the tachyon potential and to choose a curved gravitational background. We have considered extremely simple possibilities for both, see (4.4.4) and (4.3.2).

As we have already remarked, the model is inspired by string theory but is phenomenological. It does not provide a well controlled approximation to string theory in any limit. In this sense, it should be considered a bottom-up model. Nevertheless, the main point we want to make in this work is that it can be very useful to incorporate top-down derived ingredients as (4.4.1) into bottom-up models. We will make a comparison between qualitative properties of our model and the soft wall model [14] and modifications thereof. Successes of [14] include a reasonable qualitative and quantitative matching of properties of the measured mesonic states, including the Gell-Mann-Oakes-Renner relation and the Regge trajectories. These are also found in our

model, together with the following extra appealing properties, which are automatic in our general set-up:

- The model incorporates confinement in the sense that the quark-antiquark potential computed with the usual AdS/CFT prescription [49] confines. Moreover, magnetic quarks are screened. The background solution stems from a gravitational action, that allows, for instance, to compute thermodynamical quantities. All of this are properties associated to the background geometry and were already discussed in [21].

- The string theory nature of the bulk fields dual to the quark bilinear currents is readily identified: they are low-lying modes living in a brane-antibrane pair.

- Chiral symmetry breaking is realized dynamically and consistently, because of the tachyon dynamics. See [48] for discussion and possible solutions in the soft-wall model context.

- In the present model, the mass of the ρ-meson grows with increasing quark mass, or, more physically, with increasing pion mass. This welcome physical feature is absent in the soft wall model, [14]. It occurs here because the tachyon potential multiplies the full action and in particular the kinetic terms for the gauge fields, which therefore couple to the chiral symmetry breaking vev. In our previous work [15], we exploited this fact in order to fit the strange-strange mesons together with the light-light mesons, with rather successful results. In [50], the authors added the strange quark mass to the hard wall model and computed the dependence of vector masses on the quark mass. In that case however, this dependence of the vector masses originated only from the non-abelian structure and therefore misses at least part of the physics[1].

- The soft wall requires assuming a quadratic dilaton in the closed string theory background. It has been shown that such a quadratic dilaton behaviour can never be derived from a gravitational action while keeping the geometry to be that of AdS.[2]. That the background is not found as a solution is a shortcoming if for instance one wants to study the thermodynamics of the underlying glue theory.

[1] On the other hand, the quark mass dependence of the ρ-meson can be seen in different top-down models, see [51] for a recent work in the context of the Klebanov-Strassler model.

[2] This was shown in the second reference of [8]. In [7] such behavior can be implemented for glue, but the metric changes appropriately, an important ingredient for implementing confinement in the glue sector.

The thermodynamics of the soft wall model is therefore ill-defined. In the present model, we found the background as a solution of a two-derivative approximation to non-critical string theory, see section 4.3. In order to obtain Regge behaviour, we also needed a further assumption: that the tachyon potential is asymptotically gaussian. However, this is rather natural since this potential has appeared in the literature, for instance [26; 27]. Still, we warn the reader that the formalism of [26; 27] cannot be directly and controllably connected to the present setup.

- Considering that the dynamics is controlled by a tachyon world-volume action automatically provides the model with a WZ term of the form given in [27; 52; 53]. We have not discussed this term at all in this work, but in [16] it was shown that properties like discrete symmetries (parity and charge conjugation) and anomalies are, in general, correctly described by analyzing this term.

In summary, we regard our model as being in the general framework of [14], but with several qualitative improvements due to the dynamics built in the action (4.4.1). Moreover, our starting assumptions are rather simple and well motivated from a top-down perspective, such that the *ad hoc* input is scarce. It is also encouraging to find that quantitative fits to experimental data are reasonably good, see [15] and section 4.5.5, but those are not the main aim of the present work.

We have also found several aspects in which the model does not capture features which are known from perturbative QCD.

The main issue is the leading large q^2 contribution to $\Pi_V(q^2) - \Pi_A(q^2)$ as will be discussed in section 4.7.3. We have also seen that our model does not work that well for large quark masses[1] as it would grossly underestimate the decay constants for charmonium and no clear peaks are observed in the corresponding spectral functions in the deconfined phase (see the discussion of section 4.6). It would be interesting to know whether mild corrections of the model could ameliorate these issues or whether these are unsurmountable differences of models of this class to actual QCD physics.

The behaviour of $\frac{d\langle\bar{q}q\rangle}{dm_q}$ for small m_q (figure 4.2) has been investigated in earlier classic works [54]. However, the leading IR divergence-free correction, is of order $1/N^2$ at large N, originating from a pion loop, [55]. The leading-N corrections come from the four-derivative terms and are dominated by the scalar meson contribution. The behavior is qualitatively similar to what we find. For large m_q we have not been

[1] Perhaps this is not surprising since for heavy quarkonium perturbative methods and in particular non-relativistic QCD (see [56] for reviews) are accurate and it may be naive to expect that a dual theory can be a good approximation to the physics.

able to calculate the asymptotic behavior but generically speaking we do not expect it to necessarily match that of QCD, as discussed in [54]. The reason is that the UV asymptotics of the bulk gravity solution are not necessarily the same as in QCD.

4.7.2 Comments on effective actions for the open string tachyon

The notion that a scalar bifundamental in a brane-antibrane system should be the holographic dual of QCD-like chiral symmetry breaking is rather simple and robust, see for instance [16; 57; 58; 59; 60].

What is not obvious, however, is which effective action is best in order to describe a brane-antibrane system if curved spacetime. We have used the simple proposal of [17], but one should keep in mind that other alternatives might also be useful. We provide here a short guide to the literature on the issue.

Garousi and collaborators, starting from the early work [61], have tried to use explicit string theory computations in order to constrain the tachyon generalization of the DBI and WZ actions [62], see also [63]. In [28], an action for a Dp-$\bar{\text{D}}p$ system based on a particular symmetriced trace prescription was proposed[1]. There are subtle differences between the proposal of [28] and the one by Sen [17], which may have dramatic consequences. In fact, we have checked that using the symmetrized trace action of [28] for our model, one still finds Regge trajectories for vector and axial mesons but the slope for the axials changes, see appendix H. The study of other physical properties inferred from the action of [61] is beyond the scope of the present work.

In [64], it was discussed how to take into account the brane-antibrane distance in the string action. This is important for holographic duals, specially if one wants to insist in top-down approaches. A reason is that, in the weakly coupled picture, if one has brane and antibrane on top of each other in flat space, the tachyon would create a real instability (it cannot be compensated by the AdS curvature). Therefore one should think of separated branes as in the Sakai-Sugimoto model [11]. With this in mind, generalizations of [11], based on the action proposed in [64] where constructed in [65].

In a beautiful recent paper [66], building on the work [67], Niarchos proposed a

[1] In [28], a trace is needed even for a single brane-antibrane pair since the degrees of freedom are 2×2 matrices. In order to non-abelianize the flavor group in our case, one should also deal with the problem of how to implement traces on a non-abelian generalization of Sen's action (4.4.1). Investigating the physical consequences on the dual theory of this non-abelianization and of different proposals for the effective action [62] would be very interesting, but is beyond the scope of the present work.

different way of building the effective action which should better capture the physics of a separated brane-antibrane system. This may be useful in holographic modeling and in particular to improve the Sakai-Sugimoto model. We also refer the reader to [66] for a more exhaustive overview of the literature of tachyon effective actions.

4.7.3 On the OPEs and the slope of the Regge trajectories

There has been some debate in the literature on whether the large Euclidean momentum behaviour of two-point correlators can be used to constrain the behaviour of the QCD spectrum of excited mesons. The main point is to compare infinite sums like (4.5.21) (or, more precisely, differences of such sums: vector minus axial or scalar minus pseudoscalar) to the large q^2 behaviour expected from the operator product expansion (OPE). In particular, there is the question of whether different Regge slopes in the vector and axial (or scalar and pseudoscalar) channels

$$(m_n^{V,A})^2 \sim \Lambda_{V,A}^2 n + const \qquad \text{for large } n \tag{4.7.1}$$

are consistent with the OPEs. Notice that this is a theoretical question, irrespective of the experimental observation of the spectra. Let us give a brief and incomplete overview about the debate regarding this issue. For instance, in [68], a model with $\Lambda_V \neq \Lambda_A$ was put forward. Later, in [69], it was claimed that this model was inconsistent with the OPEs, but the arguments of [69] were called into question in [70], due to subtleties in the regularization of infinite sums like (4.5.21). More recently, works like [71; 72; 73] claim that the Regge slopes should be equal whereas the opposite conclusion was reached in [74; 75; 76].

We have found above that in our model, there are different asymptotic Regge slopes $\Lambda_A > \Lambda_V$. However, the coefficients of the leading logarithms in the large q^2 correlator for vectors and axials coincide, consistently. In order to illustrate this fact, let us remember that, asymptotically in the UV, our model resembles the soft wall of [14], see equation (4.5.15). In the soft wall model, the Regge slope is controlled by the constant c of (4.5.15), but the quotient F^2/Λ^2 is independent of c [77]. This quotient is indeed what controls the coefficient of the leading logarithm [70]. We thus have $\lim_{q^2\to\infty}\left(\Pi_V(q^2) - \Pi_A(q^2)\right) = 0$ together with different Regge slopes. However, this is not enough to comply with the OPEs. The leading contribution to $\left(\Pi_V(q^2) - \Pi_A(q^2)\right)$ at large q^2 should be of order q^{-4} because QCD does not have dimensionful quantities that allow to rewrite for instance a q^{-2} term. We can resort to numerics to compute $\left(\Pi_V(q^2) - \Pi_A(q^2)\right)$ in our model and the result does not comply with the q^{-4} expectation. This fails in the axial channel as shown in appendix F.

The obvious guess is that, since our holographic model is clearly not exactly QCD, it includes operators or condensates which are absent in QCD, modifying the subleading pieces of the correlators.

The same kind of problem is present for any holographic model we are aware of, see [77] for a discussion concerning the soft wall[1]. However, this seems to us more of a technical problem that may be resolved by finding the appropriate potentials than a general obstruction to this class of models. Settling these issues requires further work.

4.7.4 Outlook

As we have discussed, our simple model is quite successful in describing many features of QCD. A lot of effort has been devoted in bottom-up models to estimate other QCD related properties as for example form factors, see for instance [78]. To reproduce such computations in the present setting and compare the results is an interesting problem that we leave open for the future. We have not studied non-trivial baryon number or chemical potentials, which would clearly be worthy extensions of the model.

There are some aspects of the present that would be worth improving, like the physics associated to heavy quarks (compared to the QCD scale). We have just explored the result of working with Sen's action in the simplest confining holographic background available in the literature [20; 21]. Therefore, it is still left to understand the consequences of implementing the tachyon action in different backgrounds, as for instance those which go under the name of improved holographic QCD [7; 35] or modifications thereof.

It could also be interesting to try to introduce the quarks beyond the quenched approximation and therefore compute the backreaction of the tachyon action for the fundamental fields on the gravity background. For a review of unquenched flavor in critical (ten-dimensional) string theory backgrounds, see [79].

Of course, it would be worth to provide a non-abelian generalization of this model, for which one should provide a technical prescription on how to take traces in the action. Another line of obvious interest would be to use the model for baryons. Since quark masses play a more dynamical role than in other bottom-up approaches, this could be interesting for the physics of the sigma-term.

Finally, and most importantly, we would like to point out that using an effective open string action like (4.4.1) in the framework of holography can well have interesting applications beyond the realm of strong interactions. For instance, many bottom-up

[1] A.P. thanks O. Cata for a discussion on this subject.

technicolor models have appeared in the literature, see [80] for a review. It is a very interesting question to understand whether chiral symmetry breaking controlled by an action like (4.4.1) may offer new dynamical possibilities for the modeling of electroweak symmetry breaking. On the other hand, in the last years, many phenomenological models have been constructed in order to address some issues of superconductors and other condensed matter systems, for a review see [81]. Again, we would like to remark that (4.4.1) could hopefully lead to interesting new dynamics in different set-ups.

4.8 Acknowledgements

We would like to thank for useful conversations and correspondence. R. Casero, O. Cata, A. Cotrone, S. Eydelman, U. Gursoy, D. Mateos, V. Niarchos, F. Nitti, M. Panero, T. Pich, A. Pomarol, M. Shifman.

E. Kiritsis would like to thank CERN, ENS, ESI and Perimeter Institute for hospitality during the present work. The research of A.P is supported by grants FPA2007-66665C02-02 and DURSI 2009 SGR 168, and by the CPAN CSD2007-00042 project of the Consolider-Ingenio 2010 program. This work was partially supported by a European Union grant FP7-REGPOT-2008-1-CreteHEPCosmo-228644. I. Iatrakis was supported by an Onassis graduate fellowship.

APPENDIX

A Book-keeping summary of the parameters of the model

We summarize here the parameters of the our model. There are two parameters coming from the background, the AdS radius R and the position of the cigar tip z_Λ.

The action of the flavor brane-antibrane pair also includes α' and two more parameters g_V and λ which are related to the normalization of the vector and tachyon fields respectively. The tachyon potential also includes two constants, $\mathcal{K}$ which is an overall factor in front of the action and μ^2. It should also noticed that μ can be absorbed in $\tau(z)$ by redefining $\tilde{\tau} \to \mu\tau$. Then this parameter disappears from all equations. We used $\mu^2 = \pi$, for the numerics through our analysis, but this does not affect any physical results of our model.

Another parameter which exists in the model is c_1 which appears in the UV asymptotic of the tachyon expectation value (4.4.7). c_1 is proportional to the quark mass, with a proportionality constant β which was introduced in (4.4.26), however β does not appear in the equations for the spectrum or the decay constants, so its value is not relevant for the model predictions.

In total we have the following parameters R, z_Λ, α', g_V, λ, $\mathcal{K}$ and c_1. R, α' and λ are related by equation (4.4.8), which relates the tachyon mass to the dimension of its dual operator. Then, we relate g_V and λ to the number of colors N_c in QCD by matching the results of the vector and scalar two point functions as calculated in bulk on the one hand and in QCD on the other hand. The results are given in (4.5.20), (4.5.34), which relate g_V to λ. Hence, finally the spectrum and the decay constants depend on z_Λ, c_1 and a combination of R, g_V and α' which was named k and is given by, (4.5.26),

$$k = \frac{4R^4 g_V^4}{3(2\pi\alpha')^2} \tag{A.1}$$

B Analysis of singularities in the tachyon differential equation

B.1 Confining Background

In this appendix, we will investigate the existence of singular solutions of the tachyon equation of motion (4.4.9). It was argued already that τ can diverge only at the tip of the cigar. Therefore what is left to investigate is solutions where $\tau'(z)$ diverges at a point $z_0 \in [0, z_\Lambda]$, but $\tau(z)$ remains finite at the same z_0. We call these solutions "spurious". Taking into account $\tau'(z) \gg \tau(z)$ in the neighborhood of z_0, the leading terms of Eq.(4.4.9) are the first and the second one. Hence, the leading order equation is (we set $\mu = 1$ in the sequel as it can be absorbed in the normalization of τ and $z_\Lambda = 1$)

$$\tau''(z) - \frac{4}{3} z f(z) \tau(z) = 0 \tag{B.1}$$

with solution in the vicinity of the divergence

$$\tau'(z) = \frac{1}{\sqrt{g(z)}} = \frac{1}{\sqrt{C - \frac{4}{3}z^2\left(1 - \frac{2}{7}z^5\right)}} \quad , \quad \tau(z) = \int_0^z \frac{dz}{\sqrt{g(z)}} + \tau_0 \tag{B.2}$$

where $g(z) = C - \frac{4}{3}z^2\left(1 - \frac{2}{7}z^5\right)$. The function $g(z)$ has either one or three real roots. In particular, there are the following three cases

1. $\mathbf{C < 0}$: There are no roots of $g(z)$ in the interval $[0, 1]$, since the only one root is at $z_0 > 1$. It should also pointed out that for $z \in [0, 1]$, $g(z)$ is negative so the solution does not exist.

2. $\mathbf{0 < C < \frac{20}{21}}$: There is a single real zero at $z_0 \in [0, 1]$. While, the other two real zeros lie outside that interval.

3. When $\mathbf{C = \frac{20}{21}}$ the divergence happens exactly at the tip of the cigar.

4. $\mathbf{C > \frac{20}{21}}$: Again there is no real zero in $[0, z_0]$.

If $g(z)$ has a real root $z_0 \in [0, 1]$, then it follows from (B.2) that $\tau'(z)$ diverges at $z = z_0$, but $\tau(z)$ is regular there. Only in case that z_0 is a double root of $g(z)$, both $\tau(z)$ and $\tau'(z)$ diverge at the same point. We are particularly interested in the above case where the acceptable solution diverges at some point z_0 in order to obtain the effect of

chiral symmetry breaking in the dual quantum field theory. This is only managed if we tune the initial conditions (C here). There are two possibilities which lead to a double root of $g(z)$, in the context of the above approximation

1. $\mathbf{C = 0}$: In that case the double root is at $z_0 = 0$. Then, Eq.(B.1) has not real solutions, so it is not considered here.

2. $\mathbf{C = \frac{20}{21}}$: The double root now is at $z = 1$.

The only rigorous result of the aforementioned analysis is that "spurious" singularities are generic if $0 < C < \frac{20}{21}$.

If the tachyon diverges as a power law $\tau \sim (z - z_0)^{-a}$ with $a > 0$, $\frac{\tau'}{\tau} \sim \frac{1}{z - z_0}$ and the approximation described above is still valid, provided $z_0 \neq 1$. But then, this is not a valid solution since the solution in the above approximation is of the form (B.2). This excludes such a divergence if $z_0 \neq 1$.

The only other option of divergence of $\tau(z)$, and/or $\tau'(z)$ at a point $z_0 \in [0, 1]$ is the case where $\tau'^2\tau$ term is dominating. The relevant equation then is

$$\tau''(z) + \tau'(z)^2\tau = 0 \tag{B.3}$$

which leads to

$$\tau'(z) = C\ e^{-\frac{1}{2}\tau(z)^2} \tag{B.4}$$

For $\tau(z) \gg 1$, an approximate solution to Eq.(B.3) is

$$\frac{1}{\tau(z)} e^{\frac{1}{2}\tau(z)^2} \simeq Cz + \dots \tag{B.5}$$

Therefore, $\tau(z)$ diverges only if $z \to \infty$ which is not allowed in the present geometry as $z \in [0, 1]$. Hence this case is excluded.

From the above mentioned, we conclude that the only place where $\tau(z)$ diverges is at $z = 1$. In order to find the solution of diverging $\tau(z)$ we must tune the initial conditions in the UV, see section 4.4. We also showed that "spurious" singularities in the interior of the interval $[0, 1]$ are generic for a range of initial conditions.

The existence of "spurious" singularities has been verified numerically, and it fits the asymptotics (B.2). An example of this behavior is shown in Fig. 17. We solve numerically eq. (4.4.9) for arbitrary initial conditions, meaning that the mass and the vev are not tuned according to the plot in Fig. 4.2. In particular, we have chosen $c_1 = 0.1$, $c_3 = 0.439$. In this case we notice that $\tau'(z_0) \gg \tau(z_0)$ at $z_0 = 0.8696 < 1$.

The right part of Fig.(17) includes the plot of the derivative of the numerical solution (red line) and the expression for $\tau'(z)$ given in Eq.(B.2) (dashed blue line), near z_0. On the left part we have plotted $\tau(z)$ and the asymptotic solution (B.2) (blue dots). The parameters of the expressions in (B.2) are $C = 2.71758 < \frac{20}{21}\pi$ and $\tau_0 = -0.28$. For those values the asymptotic solution (B.2) fits the numerical solution of the full equation near z_0.

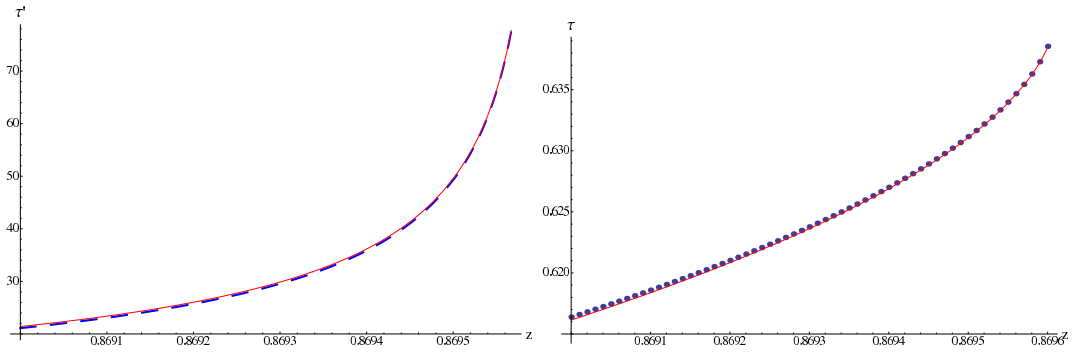

Figure 17: An example of a solution of type which diverges at $z_0 = 0.8696 < 1$ was found numerically. The numerical solution and its derivative are compared to the asymptotic solution

B.2 Deconfined Background

We now look for singular solutions of the tachyon equation of motion in the deconfined background, Eq.(4.4.17). Considering again that $\tau'(z) \gg \tau(z)$ at the vicinity of z_0, with z_0 being the point where $\tau'(z_0) \to \infty$, the leading terms of Eq.(4.4.17) near z_0 are

$$\tau''(z) + \frac{z^2}{3} f(z) \left(-\frac{4}{z} + \frac{f'(z)}{2f(z)} \right) \tau'(z)^3 = 0 \ , \tag{B.6}$$

where $f(z) = 1 - \frac{z^5}{z_T^5}$. The solution reads

$$\tau(z) = \int_0^z \frac{dz}{\sqrt{C - \frac{4}{3} z^2 \left(1 - \frac{3}{28} \frac{z^5}{z_T^5} \right)}} + \tau_0 \tag{B.7}$$

The function $g(z) = C - \frac{4}{3} z^2 \left(1 - \frac{3}{28} \frac{z^5}{z_T^5} \right)$ has a maximum in $z = 0$ and no other extrema in the interval $[0, z_T]$. If this function is zero at some point z_0, then $\tau'(z_0)$ is infinite and $\tau(z_0)$ is finite except if $g(z_0) = 0$ has a double root. Similarly to the confining background case, there are three choices

1. $\mathbf{C < 0}$: $g(z)$ is not zero in the interval $[0, z_T]$.
2. $\mathbf{0 < C < \frac{25}{21} z_T^2}$: $g(z)$ has one real root in the interval $[0, z_T]$ which is not a double root. When, $C = \frac{25}{21}$ the root of $g(z)$ is at $z_0 = 1$.
3. $\mathbf{C > \frac{25}{21} z_T^2}$: There is no root of $g(z)$ in $[0, z_T]$.

So, for a suitable range of the initial conditions (C) we may have a solution with diverging $\tau'(z)$ and finite $\tau(z)$ at some point $z_0 \in [0, 1]$. A double root is possible to be found in case of $C = 0$, and it is at $z = 0$.

The discussion about the case where the term $\tau'^2\tau$ of Eq.(4.4.17) is leading, remains the same as the one that follows Eq.(B.3) in the previous appendix. Therefore, in case of the deconfined background tachyon cannot diverge in the interval $[0, 1]$ but "spurious" singularities of the form $\tau'(z) \gg \tau(z)$ exist in general.

C Scheme dependence of the condensate and the constant α

We have introduced an arbitrary constant α in (4.4.24) associated to a counterterm that gives a finite contribution and therefore cannot be fixed by demanding the cancellation of divergences. This is a common situation in holographic renormalization and is related to scheme dependence of renormalization in the field theory side, as we now discuss.

The gauge invariant composite operator $q_L^\dagger q_R$ must be defined by a subtraction in QFT. To asses what enters in such subtractions we must study the OPE $q_L^\dagger(x) q_R(y)$ as $x \to y$. The operator can then be defined by point splitting, subtracting divergent contributions, and then taking the limit $x = y$.

Apart from the identity operator, all other operators that can appear in the OPE $q_L^\dagger(x) q_R(y)$ do not provide divergences. These include the operator itself : $q_L^\dagger(x) q_R(x)$: as well higher dimension operators. Therefore this composite operator can be defined by normal ordering. To make this precise we use a Dirac basis, so that we have the real part $\bar{q}(x)q(y)$ and the imaginary part $\bar{q}(x)\gamma^5 q(y)$. The imaginary part is finite and no subtraction is needed. For the real part we introduce a momentum cutoff Λ as we will be working in momentum space. We will therefore define

$$: \bar{q}q := \lim_{\Lambda \to \infty} \left[\bar{q}q - a_1 \Lambda^3 - a_2 m \Lambda^2 - a_3 m^2 \Lambda - a_4 m^3 \log \frac{\Lambda^2}{m^2} - a_5 m^3 \right] \tag{C.1}$$

where on the left-hand side we subtracted the most general expression of scaling dimension 3. This should be enough in a conformally invariant theory. If the theory is

asymptotically free, as in QCD, more subtractions are necessary, as there is one more relevant scale entering the problem, namely Λ_{QCD}. However in the model we consider in this paper, the physics in the UV is conformal so these subtractions are enough.

To establish the coefficients in (C.1) we must require that the (perturbative, short distance) part of the vev is finite when we remove the cutoff. We have

$$\langle : \bar{q}q : \rangle = \lim_{\Lambda\to\infty}\left[\langle\bar{q}q\rangle - a_1\Lambda^3 - a_2 m\Lambda^2 - a_3 m^2\Lambda - a_4 m^3\log\frac{\Lambda^2}{m^2} - a_5 m^3\right] \tag{C.2}$$

We calculate (in Euclidean space)

$$\begin{aligned}\langle\bar{q}q\rangle &= -N_c Tr\int\frac{d^4p}{(2\pi)^4}\frac{-i\not{q}+m}{q^2+m^2} = -4N_c m\int\frac{d^4p}{(2\pi)^4}\frac{1}{q^2+m^2} \qquad (C.3)\\ &= -2N_c\Omega_3 m\int_0^{\Lambda^2}\frac{p^2dp^2}{p^2+m^2} = -2N_c\Omega_3 m\left[\Lambda^2 - m^2\log\frac{\Lambda^2+m^2}{m^2}\right]\\ &= -2N_c\Omega_3 m\left[\Lambda^2 - m^2\log\frac{\Lambda^2}{m^2} + \mathcal{O}(\Lambda^{-2})\right]\end{aligned}$$

where Ω_3 is the volume of th unit 3-sphere.

To renormalize we must choose

$$a_1 = 0 \quad , \quad a_2 = -2N_c\Omega_3 = -a_4 \quad , \quad a_3 = 0 \tag{C.4}$$

while a_5 can be arbitrary. It is this arbitrariness that is reflected in the coefficient α in the holographic renormalization setup in (4.4.27).[1]

In some cases, this scheme dependence can be fixed on physical grounds. For instance, in supersymmetric cases, one can demand that the renormalized on-shell action is zero, see [82] for an example. We could not find any convincing prescription to fix α in the present case. A possibility would be to demand that the condensate vanishes for asymptotically large quark masses, but we have checked numerically that it is not possible. This is not surprising, since we have seen that our model works much better for small masses than for large ones.

D Appendix: converting to Schrödinger form

In many cases, it is useful to write down the Sturm-Liouville problem which determines the spectrum of any given mode as a Schrödinger-like equation. Let us start by writing

[1] In a theory like QCD, the arbitrariness involves the addition of a finite function $m^3 f\left(\frac{m}{\Lambda_{QCD}}\right)$ that reflects the presence of an extra mass scale.

a generic quadratic five-dimensional action for a field $\Psi(x^\mu, z)$:

$$S = -\frac{1}{2}\mathcal{K}_\Psi \int d^4x dz \left(A(z)(\partial_z \Psi)^2 + B(z)\eta^{\mu\nu}\partial_\mu \Psi \partial_\nu \Psi + C(z)\Psi \partial_z \Psi + M(z)\Psi^2 \right) , \tag{D.1}$$

where we have allowed an arbitrary constant multiplying the action. Let us consider $\Psi = e^{iqx}\psi(z)$ and define as m_n^2 the discrete set of values of $-q^2$ which satisfy the appropriate normalizability conditions of the Sturm-Liouville problem. The discrete set of solutions satisfy the equation of motion extracted from (D.1):

$$-\frac{1}{B(z)}\partial_z \left(A(z)\partial_z \psi_n(z) \right) + h(z)\psi_n(z) = m_n^2 \psi_n(z) \tag{D.2}$$

where we have introduced:

$$h(z) \equiv \frac{1}{B(z)} \left(M(z) - \frac{1}{2}\partial_z C(z) \right) . \tag{D.3}$$

We can define the orthonormality condition:

$$\int dz B(z)\psi_n(z)\psi_m(z) = \delta_{mn} \tag{D.4}$$

We now define a new radial variable u, and a rescaled field α in terms of a function Ξ as:

$$du = \sqrt{\frac{B(z)}{A(z)}} dz , \qquad \alpha = \Xi \psi , \qquad \Xi = (A(z)B(z))^{\frac{1}{4}} , \tag{D.5}$$

The Sturm-Liouville problem now takes the Schrödinger form:

$$-\frac{d^2\alpha_n(u)}{du^2} + V(u)\alpha_n(u) = m_n^2 \alpha_n(u) \tag{D.6}$$

where the Schrödinger potential is:

$$V(u) = \frac{1}{\Xi}\frac{d^2\Xi}{du^2} + h(u) \tag{D.7}$$

Substituting (D.4) in (D.5), we find that in the new variables, the normalization condition is the canonical one:

$$\int du \alpha_n(u)\alpha_m(u) = \delta_{mn} \tag{D.8}$$

In order to estimate the mass of the modes with large eigenvalues, it is sometimes useful to employ a WKB formula:

$$\frac{d(m_n^2)}{dn} = 2\pi \left[\int_{u_1}^{u_2} \frac{du}{\sqrt{m_n^2 - V(u)}} \right]^{-1} \tag{D.9}$$

where u_1 and u_2 are the classical turning points.

E Two-point function and sum rules

We describe here how, typically, the bulk solution needed to compute a two-point correlator from the gravity side can be written in terms of an infinite sum. Physically, two-point functions at arbitrary momenta are expressed as a sum over the discrete set of physical states. This is not a new result but, however, we believe that explicitly making the discussion as shown below can be illustrative. We remark that the argument of this appendix is not general in the sense that we have not included in the reasoning the possibility of having counterterms or other subtleties which may to be dealt with in a case by case basis.

Let us start with the equation:

$$-\frac{1}{B(z)}\partial_z\left(A(z)\partial_z\psi(z)\right)+h(z)\psi(z)=-q^2\psi(z) \tag{E.1}$$

where we have used the notation of appendix D. We want to find a solution $\psi_q(z)$ such that in the boundary $\psi_q(0)=1$, and which is IR-normalizable. Our goal is to write $\psi_q(z)$ in terms of the discrete infinite set of solutions $\psi_n(z)$ of the Sturm-Liouville problem (D.2), normalized as (D.4). Let us momentarily change to the notation with $\alpha(u)$, in which the problem is converted to:

$$-\frac{d^2\alpha(u)}{du^2}+V(u)\alpha(u)=-q^2\alpha(u) \tag{E.2}$$

and the discrete spectrum is $\alpha_n(u)$ with (D.8) as normalization and the completeness relation:

$$\sum_n \alpha_n(u)\alpha_n(u')=\delta(u-u') \tag{E.3}$$

We introduce:

$$G(u,u')=-\sum_n\frac{\alpha_n(u)\alpha_n(u')}{q^2+m_n^2} \tag{E.4}$$

such that it is a Green function, $\left[\frac{d^2}{du^2}-V(u)-q^2\right]G(u,u')=\delta(u-u')$. Let us assume now that the UV boundary is at $u=0$ and that UV-normalizability implies that $\alpha_n(0)=0$, such that $G(0,u')=0$. Regarding (D.5), $\alpha_q=\Xi\,\psi_q$, such that for generic momentum the UV condition is $\alpha_q(0)=\Xi(0)$. The solution we are looking for reads:

$$\alpha_q(u)=\Xi(u)+\int_0^\infty G(u,u')(h(u')+q^2\Xi(u'))du' \tag{E.5}$$

We can translate this back to the original variables. After some manipulations, we get our final result:

$$\psi_q(z)=1-\sum_n\frac{\psi_n(z)}{m_n^2}\int_0^\infty\frac{h(z')B(z')}{\Xi(z')}\psi_n(z')dz'-q^2A(0)\sum_n\frac{\psi_n(z)\psi_n(0)}{m_n^2(q^2+m_n^2)} \tag{E.6}$$

Two-point correlators are built from the on-shell action associated to this solution, which can be typically found by computing the derivatives fo $\psi_q(z)$ at the boundary. From the last term in (E.6) one can find the decay constants of the states in the spectrum, as in section 4.5.1.3. The second term is q-independent and in fact it can be thought of as the $q^2 = 0$ contribution. For the axial excitation, this is related to the pion decay constant whereas for the vector excitation, this term is absent since $h(z) = 0$ in that case.

F Axial current-current correlator

The axial current-current correlator is now derived following the same procedure as in section (4.5.1.2). We are interested in the two point function in the limit of large Euclidean momenta. We expect that the leading term will be the same as in the vector current correlator, but the subleading term is different.

We define the correlator as

$$\int_x e^{iqx} < J_\mu(x) J_\nu(0) >= (q^2 \eta_{\mu\nu} - q_\mu q_\nu)\Pi_A(q^2) \tag{F.1}$$

This is calculated by differentiating twice the on-shell bulk action. Integrating by parts (4.5.24) we find

$$S_{A,reg} = \frac{(2\pi\alpha')^2}{g_V^4}\mathcal{K}\int \frac{d^4q}{(2\pi)^4}\left(e^{-\frac{1}{2}\mu^2\tau^2} g_{xx}\tilde{g}_{zz}^{-\frac{1}{2}} A_\mu(q,z)\partial_z A^\mu(-q,z)\right)_{z=\epsilon} \tag{F.2}$$

where $A_\mu(q,z) = \psi^A(q,z)A_0(q)$. Then, we insert the asymptotic solution (4.5.28) into the action

$$S_A = \frac{(2\pi\alpha')^2}{g_V^4}\mathcal{K}R\int \frac{d^4q}{(2\pi)^4} A_\mu^0(q)A_0^\mu(-q)\left(2b_2(q) + (q^2 + k\mu^2 c_1^2)(\frac{1}{2} + \log\epsilon)\right) \tag{F.3}$$

where we have set $b_1 = 1$. The last term is cancelled by the corresponding counterterm from (4.5.4), so after differentiating twice with respect to $A_0(q)$ we find the final answer

$$\Pi_A(q^2) = -4\frac{\mathcal{K}R(2\pi\alpha')^2}{g_V^4}\frac{b_2(q)}{q^2} \tag{F.4}$$

We now compute $b_2(q)$ for large q^2, similarly with section (4.5.1.2). We convert (4.5.25) to Schrödinger form. Then, the new variable u reads

$$u \simeq z \ , \ \ u \simeq \frac{z_\Lambda}{\sqrt{3}}\mu\tau \tag{F.5}$$

in the UV and IR respectively. We calculate the asymptotic behavior of the Schrödinger potential in the UV and IR

$$V_{UV} \simeq \frac{3}{4u^2} + k\mu^2 c_1^2 \ , \ \ V_{IR} \simeq c^2 u^2 \tag{F.6}$$

where $c^2 = \frac{1}{z_\Lambda^4}\left(\frac{9}{4} + 3k\right)$. Adding these two contributions we finally find the equation of motion the axial modes

$$-\partial_u^2 \alpha + \left(\frac{3}{4u^2} + k\mu^2 c_1^2 + c^2 u^2\right)\alpha + q^2\alpha = 0 \tag{F.7}$$

where $\alpha(u) \simeq u^{-\frac{1}{2}}\psi^A(u)$ near $z = 0$. Its general solution reads

$$\alpha(u) = k_1 \frac{e^{\frac{-cu^2}{2}}}{\sqrt{u}} U\left(\frac{q^2 + k\mu^2 c_1^2}{4c}, 0, cu^2\right) + k_2 \frac{e^{\frac{-cu^2}{2}}}{\sqrt{u}} L^{-1}\left(\frac{q^2 + k\mu^2 c_1^2}{4c}, 0, cu^2\right), \tag{F.8}$$

we set $k_2 = 0$, since the generalized Laguerre polynomial is going to infinity in the IR. k_1 is found such that $\lim_{z\to 0}\psi^A(q,z) = 1$

$$\psi^A = \frac{q^2 + k\mu^2 c_1^2}{4c}\Gamma\left(\frac{q^2 + k\mu^2 c_1^2}{4c}\right) e^{\frac{-cu^2}{2}} U\left(\frac{q^2 + k\mu^2 c_1^2}{4c}, 0, cu^2\right) \tag{F.9}$$

By expanding the solution for large momenta we find

$$\lim_{q^2\to\infty}\frac{b_2}{q^2} = \frac{1}{4}\log\, q^2 - \frac{1}{4}(1 + \log\, 4 - 2\gamma) + \frac{k\mu^2 c_1^2(2\gamma - \log\, 4 + \log\, q^2)}{q^2} + \frac{3k^2\mu^4 c_1^4 - 8c^2}{24q^4} + \dots \tag{F.10}$$

and eventually

$$\Pi_A(q^2) = -\frac{\mathcal{K}R(2\pi\alpha')^2}{g_V^4}\left(\log\, q^2 - (1 + \log\, 4 - 2\gamma) + 4\frac{k\mu^2 c_1^2(2\gamma - \log\, 4 + \log\, q^2)}{q^2} + \frac{3k^2\mu^4 c_1^4 - 8c^2}{6q^4} + \dots\right) \tag{F.11}$$

We notice that for $c_1 = 0$ the result coincides with the vector current two point function. The $1/q^2$ term, which is absent in the QCD result, comes from the mass term of the axial field ($\sim \tau^2 A_\mu A^\mu$), see (4.5.24).

G Excitation equations in the deconfined phase

We assemble here the the Shrödinger functions, as defined in Appendix B, for the equations of motion of field excitation modes in the deconfined background (4.3.8), at vanishing spatial momentum. These modes satisfy an equation of the form (D.2) but there is no discrete spectrum.

In case of the vector excitations, we have already mentioned the functions giving rise to the Schrödinger potential approach in (4.6.1). Then, the variable u reads

$$u = \int_0^z \sqrt{\frac{\tilde{g}_{zz}(\tilde{z})}{g_{tt}(\tilde{z})}} d\tilde{z} \,, \tag{G.1}$$

which remains the same for all different excitations.

For axial-vector mesons $A(z)$ and $B(z)$ are the same as for the vectors (4.6.1), but now we also have:

$$h(z) = \frac{M(z)}{B(z)} = k\mu^2 \frac{\tau^2}{z^2} f_T(z) \,. \tag{G.2}$$

The Schrödinger functions appearing in the equations of motion of scalar excitation modes are

$$\begin{aligned} A(z) &= e^{-\frac{1}{2}\mu^2\tau^2} g_{xx}^{\frac{3}{2}} g_{tt}^{\frac{1}{2}} \frac{g_{zz}}{\tilde{g}_{zz}^{-\frac{3}{2}}} \,, & B(z) &= e^{-\frac{1}{2}\mu^2\tau^2} g_{xx}^{\frac{3}{2}} g_{tt}^{-\frac{1}{2}} \frac{g_{zz}}{\tilde{g}_{zz}^{1/2}} \,, \\ C(z) &= -2\mu^2 e^{-\frac{1}{2}\mu^2\tau^2} \frac{g_{xx}^{\frac{3}{2}} g_{tt}^{\frac{1}{2}}}{\tilde{g}_{zz}^{1/2}} \tau(z)\partial_z\tau(z) \,, & M(z) &= \frac{\mu^2}{2\pi\alpha'\lambda} e^{-\frac{1}{2}\mu^2\tau^2} (\mu^2\tau^2 - 1) g_{xx}^{\frac{3}{2}} g_{tt}^{\frac{1}{2}} \tilde{g}_{zz}^{\frac{1}{2}} \end{aligned} \tag{G.3}$$

The function $M(z)$, $B(z)$ and $C(z)$ combine to give a quite simple expression for the $h(z)$ defined in (D.3):

$$h(z) = -\frac{3}{z^2} f_T(z) \tag{G.4}$$

Finally, for the pseudoscalars we have

$$A(z) = e^{\frac{1}{2}\mu^2\tau^2} \tau^{-2} g_{xx}^{-\frac{3}{2}} g_{tt}^{\frac{1}{2}} \tilde{g}_{zz}^{-\frac{1}{2}} \,, \qquad B(z) = e^{\frac{1}{2}\mu^2\tau^2} \tau^{-2} g_{xx}^{-2} \tilde{g}_{zz}^{\frac{1}{2}} \,, \qquad h(z) = \frac{M(z)}{B(z)} = k\frac{\mu^2\tau^2}{z^2} f_T(z) \,. \tag{G.5}$$

H The action with the symmetric trace and Regge slopes

In [28], Garousi proposed an effective action for the brane-antibrane system which has subtle difference with respect to Sen's one [17], which we have used in this work. One may wonder what would be the physical consequences of using such an action in our model. We focus in this appendix on the behaviour of the spectra of highly excited vectors and axial vectors. The equations for the vectors are not modified with respect to the main text. The equations for the axials are different. It turns out that they still obey a Regge law $m_n^2 \propto n$ for large excitation number n but with different slope compared to the main text. This slope is still larger than the one for vectors. We will not deal in the present work with other possible phenomenological implication of this different tachyon action.

Garousi's action reads[1]:

$$S = -\mathrm{STr} \int d^4x dz \; e^{-\hat{T}^2} \sqrt{-\det(g_{MN} + \hat{F}_{MN} + D_M \hat{T} D_N \hat{T})} \tag{H.1}$$

where hatted symbols are 2x2 matrices:

$$\hat{T} = \begin{pmatrix} 0 & T \\ T^* & 0 \end{pmatrix}, \quad \hat{F}_{MN} = \begin{pmatrix} F^{(L)}_{MN} & 0 \\ 0 & F^{(R)}_{MN} \end{pmatrix}, \quad D_M \hat{T} = \begin{pmatrix} 0 & D_M T \\ (D_M T)^* & 0 \end{pmatrix}. \tag{H.2}$$

with $F^{(i)}_{MN} = \partial_M A^{(i)}_N - \partial_N A^{(i)}_M$ and $D_M T = \partial_M T + i(A^{(L)}_M - A^{(R)}_M)T = \partial_M T + 2iA_M T$ the usual field strength and covariant derivative, where the definition (4.5.1) has been substituted. The STr means that one has to symmetrice in $\hat{F}_{MN}$, $D_M \hat{T}$, $\hat{T}$ after expanding the square root, and then take the trace.

The expression (H.1) is quite involved but we will see that in the particular case we are interested, one can deal with it: we will consider quadratic excitations of the gauge fields, while the tachyon phase is set to a trivial constant and the tachyon modulus is a non-trivial z-dependent function (so we have to keep all orders in τ, $\partial_z \tau$). We again

[1] We adapt it to our present framework, for instance defining the covariant derivative with a different sign and disregarding the $B_{\mu\nu}$ field. With respect to the main text, we will fix the value of some of the constants that we have defined, namely $g_V^2 = 2\pi\alpha'$, $\lambda = 1/(2\pi\alpha')$, $\mathcal{K} = 1$, $\mu^2 = 2$. Regarding (4.4.8), this implies $R^2 = 3/2$. This is inessential (the constants can be easily restored) and we have done it for the sake of clarity of the equations. Our convention will be that indices M, N running over the five space-time coordinates are contracted with the metric g_{MN} whereas indices μ, ν running over the Minkowski directions are contracted with the flat metric $\eta_{\mu\nu}$.

take a gauge with $A_z^{(i)} = 0$. This is enough to compute the vector and axial spectrum in the tachyon background.

So let us compute the quadratic expansion in gauge fields. There are terms in A_μ^2 coming from the covariant derivatives and terms with $F^{(i)2}$. In principle, there could be terms with, schematically, $i\tau\partial_z\tau AF$ coming from a $DTDT\,F$ product, but these terms would make the action complex and are removed by the symmetric trace prescription. In the following, we make the computation in two steps: we first compute the A_μ^2 terms and then compute the F^2 terms.

In order to compute the A_μ^2 terms, we can consider the action:

$$\begin{aligned} S_{A^2} &= -\mathrm{STr}\int d^4x dz\; e^{-\hat{T}^2}\sqrt{-\det(g_{MN} + D_M\hat{T}D_N\hat{T})} = \\ &= -\int d^4x dz\;\sqrt{-\det g}\;\mathrm{STr}\left[e^{-\hat{T}^2}\sqrt{\det(\delta_N^M + D^M\hat{T}D_N\hat{T})}\right] \end{aligned} \tag{H.3}$$

We now compute the determinant. Being inside a STr, the $\hat{T}$ matrices can be considered as commuting objects, so $\sqrt{\det(\delta_N^M + D^M\hat{T}D_N\hat{T})} = \sqrt{1 + D^M\hat{T}D_M\hat{T}}$. We have to expand the square root. In order to simplify notation, let us define s_j, the coefficients of such expansion:

$$\sqrt{1+\xi} = \sum_{j=0}^{\infty}(-1)^{j+1}\frac{(2j-3)!!}{j!2^j}\xi^j \equiv \sum_{j=0}^{\infty} s_j\xi^j \tag{H.4}$$

Thus, also expanding the exponential:

$$\mathcal{L}_{A^2} = -\sqrt{-\det g}\sum_{k=0}^{\infty}\frac{(-1)^k}{k!}\sum_{j=0}^{\infty} s_j\mathrm{STr}\left[\hat{T}^{2k}(D^M\hat{T}D_M\hat{T})^j\right] \tag{H.5}$$

The next step is to perform the symmetriced trace, and a major simplification comes out because of the particular computation we are doing. Define:

$$\hat{J}_1 = \begin{pmatrix} 0 & 1 \\ 1 & 0 \end{pmatrix}, \quad \hat{J}_2 = \begin{pmatrix} 0 & -1 \\ 1 & 0 \end{pmatrix} \tag{H.6}$$

such that (use $T = T^* = \tau$):

$$\hat{T} = \tau\hat{J}_1 \qquad D_M\hat{T} = \partial_M\tau\hat{J}_1 - 2iA_M\tau\hat{J}_2 \tag{H.7}$$

The order zero term in A_M, *i.e.* the action for the tachyon modulus is just

$$\mathcal{L}_\tau = -2\sqrt{-\det g}\,e^{-\tau^2}\sqrt{1+\partial^M\tau\partial_M\tau}, \tag{H.8}$$

the same used in the main text. This means that the discussion of section 4.4 still holds.

We now isolate the quadratic term in A_M. One out of the j factors of $(D^M\hat{T}D_M\hat{T})^j$ has to be $g_{xx}^{-1}(-2i\tau\hat{J}_2)^2A_\mu A^\mu$ while the other $j-1$ factors are $\hat{J}_1^2 g_{zz}^{-1}(\partial_z\tau)^2$ each. Notice there cannot be crossed terms because $\partial_M\tau A^M = 0$ in the case we are conisdering. Thus:

$$\mathcal{L}_{A^2} = -g_{xx}^{-1}\sqrt{-\det g}\sum_{k=0}^{\infty}\frac{(-1)^k}{k!}\sum_{j=0}^{\infty}s_j j\ \tau^{2k}(g_{zz}^{-1}(\partial_z\tau)^2)^{j-1}(-4A_\mu A^\mu\tau^2)\mathrm{STr}\left[\hat{J}_1^{2k+2j-2}\hat{J}_2^2\right] \tag{H.9}$$

The j at the beginning of the second line of course comes because the $A_\mu A^\mu$ term can be chosen from any of the j factors in $(D^M\hat{T}D_M\hat{T})^j$. In order to perform the symmetriced trace, notice that, in general:

$$\mathrm{STr}[\hat{J}_1^{2n}\hat{J}_2^2] = \frac{1}{2n+1}\left((n+1)Tr[\hat{J}_2^2] + n\mathrm{Tr}[\hat{J}_1\hat{J}_2\hat{J}_1\hat{J}_2]\right) = -\frac{2}{2n+1} \tag{H.10}$$

where we have used that $\hat{J}_1^2$ is the 2x2 identity matrix and $\mathrm{Tr}[\hat{J}_1\hat{J}_2\hat{J}_1\hat{J}_2] = -Tr[\hat{J}_2^2] = 2$. Substituting:

$$\mathcal{L}_{A^2} = -8g_{xx}^{-1}\sqrt{-\det g}\ \sum_{k=0}^{\infty}\frac{(-1)^k}{k!}\tau^{2k+2}\sum_{j=0}^{\infty}s_j j\ (g_{zz}^{-1}(\partial_z\tau)^2)^{j-1}A_\nu A^\nu\frac{1}{2k+2j-1} \tag{H.11}$$

We should now resum the series. Let us use the identity[1]:

$$\sum_{i=0}^{\infty}\frac{1}{i!}x^i\sum_{j=0}^{\infty}\frac{j\ s_j}{2i+2j-1}y^j = \frac{y}{2}\int_0^1\frac{e^{xa^2}}{\sqrt{1+y\ a^2}}da \tag{H.12}$$

Using $x=-\tau^2$ and $y = g_{zz}^{-1}(\partial_z\tau)^2$, we finally find:

$$\mathcal{L}_{A^2} = -4g_{xx}^{-1}\sqrt{-\det g}\ \tau^2 A_\nu A^\nu\int_0^1\frac{e^{-\tau^2a^2}}{\sqrt{1+g_{zz}^{-1}(\partial_z\tau)^2a^2}}da \tag{H.13}$$

Let us now compute the F^2 terms. We want to expand the determinant of (H.1) to second order in $\hat{F}$ but to all orders in $D_z\hat{T}D_z\hat{T}$. The determinant reads:

$$-\det(g_{MN}+\hat{F}_{MN}+D_M\hat{T}D_N\hat{T}) = g_{xx}^4(g_{zz}+D_z\hat{T}D_z\hat{T})+\frac{1}{2}\hat{F}_{\mu\nu}\hat{F}^{\mu\nu}g_{xx}^2(g_{zz}+D_z\hat{T}D_z\hat{T})+g_{xx}^3\hat{F}_{\mu z}^2 \tag{H.14}$$

and thus the F^2 contribution to the square root is:

$$\frac{1}{4}g_{zz}^{\frac{1}{2}}\sqrt{(1+g_{zz}^{-1}D_z\hat{T}D_z\hat{T})}\hat{F}_{\mu\nu}\hat{F}^{\mu\nu}+\frac{1}{2}g_{xx}g_{zz}^{-\frac{1}{2}}\frac{1}{\sqrt{1+g_{zz}^{-1}D_z\hat{T}D_z\hat{T}}}\hat{F}_{\mu z}^2 \tag{H.15}$$

[1] In order to prove this, notice that $\sum_{j=0}^{\infty}js_jy^j = \frac{y}{2\sqrt{1+y}}$ and consider an auxiliary function $g(a) = \sum_{i=0}^{\infty}\frac{1}{i!}x^i\sum_{j=0}^{\infty}\frac{j\ s_j}{2i+2j-1}y^ja^{2i+2j-1}$ such that $\partial_a g(a) = a^{-2}e^{xa^2}\frac{a^2\ y}{2\sqrt{1+a^2\ y}}$. Since $g(0)=0$ and $g(1)$ is what we want to compute, we arrive at (H.12).

Let us start by computing the term with $\hat{F}_{\mu\nu}\hat{F}^{\mu\nu}$. We have to expand before taking the symmetrized trace. Notice that now $D_z\hat{T} = \partial_z\tau\hat{J}_1$ up to subleading terms. To shorten notation, we define:

$$x \equiv -\tau^2\,, \qquad y = g_{zz}^{-1}(\partial_z\tau)^2 \tag{H.16}$$

The $\hat{F}_{\mu\nu}\hat{F}^{\mu\nu}$ term in the lagrangian density (H.1) then reads:

$$\mathcal{L}_{F^2_{\mu\nu}} = -\frac{1}{4}g_{zz}^{\frac{1}{2}}\sum_{k=0}^{\infty}\frac{x^k}{k!}\sum_{j=0}^{\infty}s_j y^j \mathrm{STr}[\hat{J}_1^{2k+2j}\hat{F}_{\mu\nu}\hat{F}^{\mu\nu}] \tag{H.17}$$

It is now easy to compute the symmetriced trace:

$$\mathrm{STr}[\hat{J}_1^{2k+2j}\hat{F}_{\mu\nu}\hat{F}^{\mu\nu}] = \frac{1}{2k+2j+1}\Big((k+j+1)\mathrm{Tr}[\hat{F}_{\mu\nu}\hat{F}^{\mu\nu}] + (k+j)\mathrm{Tr}[\hat{J}_1\hat{F}_{\mu\nu}\hat{J}_1\hat{F}^{\mu\nu}]\Big) \tag{H.18}$$

Now, $\mathrm{Tr}[\hat{F}_{\mu\nu}\hat{F}^{\mu\nu}] = F^{(L)}_{\mu\nu}F^{\mu\nu(L)} + F^{(R)}_{\mu\nu}F^{\mu\nu(R)}$ which, splitting in vector and axial part and using notation of section 4.5 gives $\mathrm{Tr}[\hat{F}_{\mu\nu}\hat{F}^{\mu\nu}] = 2V_{\mu\nu}V^{\mu\nu} + 2A_{\mu\nu}A^{\mu\nu}$. Similarly, $\mathrm{Tr}[\hat{J}_1\hat{F}_{\mu\nu}\hat{J}_1\hat{F}^{\mu\nu}] = 2F^{(L)}_{\mu\nu}F^{\mu\nu(R)} = 2V_{\mu\nu}V^{\mu\nu} - 2A_{\mu\nu}A^{\mu\nu}$ and we find $\mathrm{STr}[\hat{J}_1^{2k+2j}\hat{F}_{\mu\nu}\hat{F}^{\mu\nu}] = 2V_{\mu\nu}V^{\mu\nu} + \frac{2}{2i+2j+1}A_{\mu\nu}A^{\mu\nu}$. Inserting this in (H.17):

$$\begin{aligned}\mathcal{L}_{F^2_{\mu\nu}} &= -\frac{1}{4}g_{zz}^{\frac{1}{2}}\sum_{k=0}^{\infty}\frac{x^k}{k!}\sum_{j=0}^{\infty}s_j y^j\left(2V_{\mu\nu}V^{\mu\nu} + \frac{2}{2i+2j+1}A_{\mu\nu}A^{\mu\nu}\right) = \\ &= -\frac{1}{2}g_{zz}^{\frac{1}{2}}\left[e^x\sqrt{1+y}V_{\mu\nu}V^{\mu\nu} + \left(\int_0^1 e^{a^2x}\sqrt{1+a^2y}da\right)A_{\mu\nu}A^{\mu\nu}\right]\end{aligned} \tag{H.19}$$

The fact that for non-trivial tachyon the symmetric trace produces a coupling between the left and right gauge fields was already pointed out in [28]. It results in different kinetic terms for vectors and axials. We skip the details of the similar computation leading to $\hat{F}^2_{\mu z}$:

$$\mathcal{L}_{F^2_{\mu z}} = -g_{xx}g_{zz}^{-\frac{1}{2}}\left[e^x\frac{1}{\sqrt{1+y}}(\partial_z V_\mu)^2 + \left(\int_0^1 e^{a^2x}\frac{1}{\sqrt{1+a^2y}}da\right)(\partial_z A_\mu)^2\right] \tag{H.20}$$

By comparing (H.19), (H.20) to (4.5.5), we find that the quadratic action for the vector excitation is identical regardless the choice between Sen's and Garousi's actions. Nevertheless, the axial part changes. From (H.19), (H.20) it can be read that, introducing notation of appendix D:

$$\mathcal{L}_{axial} = -\left[\frac{1}{2}B(z)A_{\mu\nu}A^{\mu\nu} + A(z)(\partial_z A_\mu)^2 + M(z)A_\mu^2\right] \tag{H.21}$$

with:

$$\begin{aligned} A(z) &= g_{xx} g_{zz}^{-\frac{1}{2}} \int_0^1 e^{-\tau^2 a^2} \left(\sqrt{1+a^2 g_{zz}^{-1}(\partial_z\tau)^2}\right)^{-1} da\,, \\ B(z) &= g_{zz}^{\frac{1}{2}} \int_0^1 e^{-\tau^2 a^2} \sqrt{1+a^2 g_{zz}^{-1}(\partial_z\tau)^2} da\,, \\ M(z) &= 4 g_{xx} g_{zz}^{\frac{1}{2}} \tau^2 \int_0^1 e^{-\tau^2 a^2} \left(\sqrt{1+a^2 g_{zz}^{-1}(\partial_z\tau)^2}\right)^{-1} da \end{aligned} \tag{H.22}$$

In order to proceed further, we need estimate the integrals near the IR, where $z \to z_\Lambda$ and the tachyon diverges, see section 4.4.1. We will use that in the limit where $-x \gg 1$ and $y \gg 1$ with $-\frac{y}{x} \gg 1$, it happens that:

$$\int_0^1 e^{x\,a^2} \sqrt{1+y\,a^2} da \approx -\frac{\sqrt{y}}{2x}\,, \qquad \int_0^1 e^{x\,a^2} (\sqrt{1+y\,a^2})^{-1} da \approx \frac{\log\left(\frac{y}{-x}\right) - \gamma + 2\log 2}{2\sqrt{y}} \tag{H.23}$$

where γ is Euler's constant. The first equality is just found by neglecting the 1 inside the square root. For the second computation, it is not possible to directly neglect the 1 since the result would be divergent, but one can express the integral as $\int_0^1 (\sqrt{1+y\,a^2})^{-1} da + \int_0^1 (e^{x\,a^2}-1)(\sqrt{1+y\,a^2})^{-1} da$, such that the first integral can be done explicitly and in the second one the 1 inside the square root can be neglected.

We are now ready to compute the leading IR behaviour of the Schrödinger potential which will determine the behaviour of the highly excited states. We will use that near the IR ($z_\Lambda - z \ll 1$), we have:

$$\begin{aligned} & g_{xx} \approx \frac{R^2}{z_\Lambda^2}\,, \qquad g_{zz} \approx \frac{R^2}{z_\Lambda^2} \frac{z_\Lambda}{5(z_\Lambda - z)}\,, \qquad \tau = \sqrt{-x} \approx C\,(z_\Lambda - z)^{-\frac{3}{20}} \\ & g_{zz}^{-1}(\partial_z\tau)^2 = y \approx \frac{9 z_\Lambda C^2}{80 R^2} (z_\Lambda - z)^{-\frac{13}{10}} \end{aligned} \tag{H.24}$$

From (H.22)-(H.24) one can readily check that $\lim_{z\to z_\Lambda} M(z)/B(z) = 0$ and therefore the term $h(u)$ does not contribute in the IR to the Schrödinger potential (D.7). On the other hand, we can obtain the relation of the z-coordinate to the u-coordinate of the Schrödinger problem (D.5):

$$\sqrt{\frac{B(z)}{A(z)}} \approx \frac{3 z_\Lambda}{20} \frac{(z_\Lambda - z)^{-1}}{\sqrt{-\log(b(z_\Lambda - z))}}\,, \qquad u \approx \frac{3}{10} z_\Lambda \sqrt{-\log(b(z_\Lambda - z))}\,. \tag{H.25}$$

where b is a positive constant that will not be important in the following. We also compute:

$$\Xi = (AB)^{\frac{1}{4}} \sim e^{-\frac{5u^2}{6 z_\Lambda^2}} \tag{H.26}$$

where we have not written multiplicative constants and powers of u which do not affect the leading IR behaviour of the Schrödinger potential. Finally, from (D.7) we find

$$V(u) \approx \frac{25}{9z_\Lambda^4} u^2 \tag{H.27}$$

Since we have a quadratic potential in the IR, the behaviour for asymptotically highly excited axials is still Regge-like. Unlike in the main text - section 4.5.2.1 -, the slope found using Garousi's action does not depend on the constant k. Comparing to the vector modes - section 4.5.1.1 -, we see that the Regge slope for the axials is slightly larger, in particular $\Lambda_A^2/\Lambda_V^2 = 10/9$, where $\Lambda_{V,A}$ are defined as in (4.7.1).

Bibliography

[1] J. M. Maldacena, *"The large N limit of superconformal field theories and supergravity,"* Adv. Theor. Math. Phys. **2**, 231 (1998) [Int. J. Theor. Phys. **38**, 1113 (1999)] [ArXiv:hep-th/9711200];
S. S. Gubser, I. R. Klebanov and A. M. Polyakov, *"Gauge theory correlators from non-critical string theory,"* Phys. Lett. B **428**, 105 (1998) [ArXiv:hep-th/9802109];
E. Witten, *"Anti-de Sitter space and holography,"* Adv. Theor. Math. Phys. **2**, 253 (1998) [ArXiv:hep-th/9802150]. 81

[2] D. Mateos, *"String Theory and Quantum Chromodynamics,"* Class. Quant. Grav. **24**, S713 (2007) [ArXiv:0709.1523][hep-th]. 81

[3] E. Witten, *"Anti-de Sitter space, thermal phase transition, and confinement in gauge theories,"* Adv. Theor. Math. Phys. **2** (1998) 505 [ArXiv:hep-th/9803131]. 81

[4] J. M. Maldacena and C. Nunez, *"Towards the large N limit of pure N = 1 super Yang Mills,"* Phys. Rev. Lett. **86** (2001) 588 [ArXiv:hep-th/0008001];
A. H. Chamseddine and M. S. Volkov, *"Non-Abelian BPS monopoles in N = 4 gauged supergravity,"* Phys. Rev. Lett. **79** (1997) 3343 [ArXiv:hep-th/9707176]. 81

[5] I. R. Klebanov and M. J. Strassler, *"Supergravity and a confining gauge theory: Duality cascades and χSB-resolution of naked singularities,"* JHEP **0008** (2000) 052 [ArXiv:hep-th/0007191]. 81

[6] J. Polchinski and M. J. Strassler, *"Hard scattering and gauge / string duality,"* Phys. Rev. Lett. **88**, 031601 (2002) [ArXiv:hep-th/0109174]. 81, 82

[7] U. Gursoy and E. Kiritsis, *"Exploring improved holographic theories for QCD: Part I,"* JHEP **0802** (2008) 032 [ArXiv:0707.1324][hep-th];
U. Gursoy, E. Kiritsis and F. Nitti, *"Exploring improved holographic theories for QCD: Part II,"* JHEP **0802** (2008) 019 [ArXiv:0707.1349] [hep-th]. 81, 91, 115, 119

[8] U. Gursoy, E. Kiritsis, L. Mazzanti and F. Nitti, *"Deconfinement and Gluon Plasma Dynamics in Improved Holographic QCD,"* Phys. Rev. Lett. **101**, 181601 (2008) [ArXiv:0804.0899][hep-th];
U. Gursoy, E. Kiritsis, L. Mazzanti and F. Nitti, *"Holography and Thermodynamics of 5D Dilaton-gravity,"* JHEP **0905** (2009) 033 [ArXiv:0812.0792][hep-th];
U. Gursoy, E. Kiritsis, L. Mazzanti and F. Nitti, *"Improved Holographic QCD at finite Temperature: comparison with data,"* Nucl. Phys. B **820** (2009) 148 [ArXiv:0903.2859][hep-th];
U. Gursoy, E. Kiritsis, G. Michalogiorgakis and F. Nitti, *"Thermal Transport and Drag Force in Improved Holographic QCD,"* JHEP **0912** (2009) 056 [ArXiv:0906.1890][hep-ph]. 81, 115

[9] J. Babington, J. Erdmenger, N. J. Evans, Z. Guralnik and I. Kirsch, *"Chiral symmetry breaking and pions in non-supersymmetric gauge / gravity duals,"* Phys. Rev. D **69**, 066007 (2004). [ArXiv:hep-th/0306018]. N. J. Evans and J. P. Shock, *"Chiral dynamics from AdS space,"* Phys. Rev. D **70**, 046002 (2004) [ArXiv:hep-th/0403279]. 81, 82

[10] M. Kruczenski, D. Mateos, R. C. Myers and D. J. Winters, *"Towards a holographic dual of large-N(c) QCD,"* JHEP **0405**, 041 (2004) [ArXiv:hep-th/0311270]. 81, 82, 89

[11] T. Sakai and S. Sugimoto, *"Low energy hadron physics in holographic QCD,"* Prog. Theor. Phys. **113**, 843 (2005) [ArXiv:hep-th/0412141]. 81, 82, 87, 117

[12] J. Erlich, E. Katz, D. T. Son and M. A. Stephanov, *"QCD and a Holographic Model of Hadrons,"* Phys. Rev. Lett. **95**, 261602 (2005) [ArXiv:hep-ph/0501128]. 82, 98, 100, 101, 108, 109

[13] L. Da Rold and A. Pomarol, *"Chiral symmetry breaking from five dimensional spaces,"* Nucl. Phys. B **721**, 79 (2005) [ArXiv:hep-ph/0501218]. 82, 98, 101, 108

[14] A. Karch, E. Katz, D. T. Son and M. A. Stephanov, *"Linear Confinement and AdS/QCD,"* Phys. Rev. D **74**, 015005 (2006) [ArXiv:hep-ph/0602229]. 82, 97, 99, 101, 108, 114, 115, 116, 118

[15] I. Iatrakis, E. Kiritsis and A. Paredes, *"An AdS/QCD model from Sen's tachyon action,"* Phys. Rev. D **81**, 115004 (2010) [ArXiv:1003.2377][hep-ph]. 82, 96, 97, 103, 110, 114, 115, 116

[16] R. Casero, E. Kiritsis and A. Paredes, *"Chiral symmetry breaking as open string tachyon condensation,"* Nucl. Phys. B **787**, 98 (2007) [ArXiv:hep-th/0702155]. 82, 83, 87, 95, 102, 114, 116, 117

[17] A. Sen, *"Dirac-Born-Infeld action on the tachyon kink and vortex,"* Phys. Rev. D **68**, 066008 (2003) [ArXiv:hep-th/0303057]. 82, 85, 114, 117, 132

[18] M. Kruczenski, D. Mateos, R. C. Myers and D. J. Winters, *"Meson spectroscopy in AdS/CFT with flavour,"* JHEP **0307**, 049 (2003) [ArXiv:hep-th/0304032]. 82

[19] J. Erdmenger, N. Evans, I. Kirsch and E. Threlfall, *"Mesons in Gauge/Gravity Duals - A Review,"* Eur. Phys. J. A **35**, 81 (2008) [ArXiv:0711.4467][hep-th]. 83

[20] S. Kuperstein and J. Sonnenschein, *"Non-critical supergravity (d > 1) and holography,"* JHEP **0407** (2004) 049 [ArXiv:hep-th/0403254];
83, 84, 119

[21] S. Kuperstein and J. Sonnenschein, *"Non-critical, near extremal AdS_6 background as a holographic laboratory of four dimensional YM theory,"* JHEP **0411** (2004) 026 [ArXiv:hep-th/0411009]. 83, 84, 115, 119

[22] I. R. Klebanov and J. M. Maldacena, *"Superconformal gauge theories and non-critical superstrings,"* Int. J. Mod. Phys. A **19** (2004) 5003 [ArXiv:hep-th/0409133].

[23] F. Bigazzi, R. Casero, A. L. Cotrone, E. Kiritsis and A. Paredes, *"Non-critical holography and four-dimensional CFT's with fundamentals,"* JHEP **0510**, 012 (2005) [ArXiv:hep-th/0505140].

[24] R. Casero, A. Paredes and J. Sonnenschein, *"Fundamental matter, meson spectroscopy and non-critical string / gauge duality,"* JHEP **0601**, 127 (2006) [ArXiv:hep-th/0510110]. V. Mazu and J. Sonnenschein, *"Non critical holographic models of the thermal phases of QCD,"* JHEP **0806**, 091 (2008) [ArXiv:0711.4273]hep-th]. O. Mintakevich and J. Sonnenschein, *"On the spectra of scalar mesons from HQCD models,"* JHEP **0808**, 082 (2008) [ArXiv:0806.0152][hep-th]. 83, 85

[25] E. Witten, *"Anti-de Sitter space, thermal phase transition, and confinement in gauge theories,"* Adv. Theor. Math. Phys. **2**, 505 (1998) [ArXiv:hep-th/9803131]. 84

[26] D. Kutasov, M. Marino and G. W. Moore, *"Some exact results on tachyon condensation in string field theory,"* JHEP **0010** (2000) 045. [ArXiv:hep-th/0009148] 85, 116

[27] T. Takayanagi, S. Terashima and T. Uesugi, *"Brane-antibrane action from boundary string field theory,"* JHEP **0103**, 019 (2001) [ArXiv:hep-th/0012210]. 85, 116

[28] M. R. Garousi, *"On the effective action of D-brane-anti-D-brane system,"* JHEP **0712**, 089 (2007) [ArXiv:0710.5469/[hep-th]]. 85, 117, 132, 135

[29] A. Pomarol and A. Wulzer, *"Baryon Physics in Holographic QCD,"* Nucl. Phys. B **809**, 347 (2009) [arXiv:0807.0316 [hep-ph]]. O. Domenech, G. Panico and A. Wulzer, *"Massive Pions, Anomalies and Baryons in Holographic QCD,"* arXiv:1009.0711 [hep-ph]. 87

[30] S. R. Coleman and E. Witten, *"Chiral Symmetry Breakdown In Large N Chromodynamics,"* Phys. Rev. Lett. **45**, 100 (1980). 87

[31] O. Aharony, J. Sonnenschein and S. Yankielowicz, *"A holographic model of deconfinement and chiral symmetry restoration,"* Annals Phys. **322**, 1420 (2007) [ArXiv:hep-th/0604161]. 87

[32] L. Da Rold and A. Pomarol, *"The scalar and pseudoscalar sector in a five-dimensional approach to chiral symmetry breaking,"* JHEP **0601**, 157 (2006) [ArXiv:hep-ph/0510268]. 91, 105

[33] A. Cherman, T. D. Cohen and E. S. Werbos, *"The chiral condensate in holographic models of QCD,"* Phys. Rev. C **79**, 045203 (2009) [ArXiv:0804.1096/[hep-ph]]. 91, 92

[34] U. Gursoy and E. Kiritsis, *"Exploring improved holographic theories for QCD: Part I,"* JHEP **0802**, 032 (2008) [ArXiv:0707.1324/[hep-th]]. U. Gursoy, E. Kiritsis and F. Nitti, *"Exploring improved holographic theories for QCD: Part II,"* JHEP **0802**, 019 (2008) [ArXiv:0707.1349/[hep-th]].

[35] U. Gursoy, E. Kiritsis, L. Mazzanti, G. Michalogiorgakis and F. Nitti, *"Improved Holographic QCD,"* [ArXiv:1006.5461][hep-th]. 114, 119

[36] K. Skenderis, *"Lecture notes on holographic renormalization,"* Class. Quant. Grav. **19**, 5849 (2002) [ArXiv:hep-th/0209067]. 91

[37] F. Jugeau, *"Towards a consistent AdS/QCD dictionary,"* [ArXiv:0902.3864][hep-ph]. 92

[38] S. Borsanyi, Z. Fodor, C. Hoelbling, S. D. Katz, S. Krieg, C. Ratti and K. K. Szabo [Wuppertal-Budapest Collaboration], *"Is there still any Tc mystery in lattice QCD? Results with physical masses in the continuum limit III,"* [ArXiv:1005.3508][hep-lat]. 94

[39] E. Schreiber, *"Excited mesons and quantization of string endpoints,"* [ArXiv:hep-th/0403226]. 101

[40] M. Gell-Mann, R. J. Oakes and B. Renner, *"Behavior of current divergences under SU(3) x SU(3),"* Phys. Rev. **175** (1968) 2195. 109

[41] C. Amsler *et al.* [Particle Data Group], *"Review of particle physics,"* Phys. Lett. B **667**, 1 (2008). 110

[42] C. Hoyos-Badajoz, K. Landsteiner and S. Montero, *"Holographic Meson Melting,"* JHEP **0704**, 031 (2007) [ArXiv:hep-th/0612169]. 111

[43] D. Mateos, R. C. Myers and R. M. Thomson, *"Holographic phase transitions with fundamental matter,"* Phys. Rev. Lett. **97**, 091601 (2006) [ArXiv:hep-th/0605046]. D. Mateos, R. C. Myers and R. M. Thomson, *"Thermodynamics of the brane,"* JHEP **0705**, 067 (2007) [ArXiv:hep-th/0701132]. 112

[44] H. R. Grigoryan, P. M. Hohler and M. A. Stephanov, *"Towards the Gravity Dual of Quarkonium in the Strongly Coupled QCD Plasma,"* Phys. Rev. D **82**, 026005 (2010) [ArXiv:1003.1138][hep-ph]. 113, 114

[45] M. Fujita, T. Kikuchi, K. Fukushima, T. Misumi and M. Murata, *"Melting Spectral Functions of the Scalar and Vector Mesons in a Holographic QCD Model,"* Phys. Rev. D **81**, 065024 (2010) [ArXiv:0911.2298][hep-ph]. 113

[46] A. Paredes, K. Peeters and M. Zamaklar, *"Mesons versus quasi-normal modes: undercooling and overheating,"* JHEP **0805**, 027 (2008) [ArXiv:0803.0759][hep-th]. 112

[47] D. T. Son and A. O. Starinets, *"Minkowski-space correlators in AdS/CFT correspondence: Recipe and applications,"* JHEP **0209**, 042 (2002) [ArXiv:hep-th/0205051]. 113

[48] T. Gherghetta, J. I. Kapusta and T. M. Kelley, *"Chiral symmetry breaking in the soft-wall AdS/QCD model,"* Phys. Rev. D **79**, 076003 (2009) [ArXiv:0902.1998][hep-ph]; Y. Q. Sui, Y. L. Wu, Z. F. Xie and Y. B. Yang, *"Prediction for the Mass Spectra of Resonance Mesons in the Soft-Wall AdS/QCD with a Modified 5D Metric,"* Phys. Rev. D **81**, 014024 (2010) [ArXiv:0909.3887][hep-ph]. 115

[49] J. Sonnenschein, *"What does the string / gauge correspondence teach us about Wilson loops?,"* [ArXiv:hep-th/0003032]. 115

[50] J. P. Shock and F. Wu, *"Three flavour QCD from the holographic principle,"* JHEP **0608**, 023 (2006) [ArXiv:hep-ph/0603142]. 115

[51] A. L. Cotrone, A. Dymarsky and S. Kuperstein, *"On vector meson masses in a holographic SQCD"* [ArXiv:1010.1017][hep-ph]. 115

[52] C. Kennedy and A. Wilkins, *"Ramond-Ramond couplings on brane-antibrane systems,"* Phys. Lett. B **464**, 206 (1999) [ArXiv:hep-th/9905195]. 116

[53] P. Kraus and F. Larsen, *"Boundary string field theory of the DD-bar system,"* Phys. Rev. D **63**, 106004 (2001) [ArXiv:hep-th/0012198]. 116

[54] M. A. Shifman, A. I. Vainshtein and V. I. Zakharov, *"QCD And Resonance Physics. Sum Rules,"* Nucl. Phys. B **147** (1979) 385;
V. A. Novikov, M. A. Shifman, A. I. Vainshtein and V. I. Zakharov, *"Are All Hadrons Alike?,"*, Appendix D. Nucl. Phys. B **191** (1981) 301. 116
J. Gasser and H. Leutwyler, *"Chiral Perturbation Theory To One Loop,"* Annals Phys. **158**, 142 (1984).

[55] G. Ecker, J. Gasser, A. Pich and E. de Rafael, *"The Role Of Resonances In Chiral Perturbation Theory,"* Nucl. Phys. B **321** (1989) 311;
A. Pich, *"Colourless mesons in a polychromatic world,"* [ArXiv:hep-ph/0205030]. 116

[56] N. Brambilla, A. Pineda, J. Soto and A. Vairo, *"Effective field theories for heavy quarkonium,"* Rev. Mod. Phys. **77**, 1423 (2005) [ArXiv:hep-ph/0410047]. J. Soto, Eur. Phys. J. A **31**, 705 (2007) [ArXiv:nucl-th/0611055]. 116

[57] S. Sugimoto and K. Takahashi, *"QED and string theory,"* JHEP **0404**, 051 (2004) [ArXiv:hep-th/0403247]. 117

[58] A. L. Cotrone, *"On the YM and QCD spectra from five dimensional strings,"* Int. J. Mod. Phys. A **24**, 4117 (2009) [ArXiv:0707.1483][hep-th]. 117

[59] O. Aharony and D. Kutasov, *"Holographic Duals of Long Open Strings,"* Phys. Rev. D **78**, 026005 (2008) [ArXiv:0803.3547][hep-th]. 117

[60] E. Kiritsis, *"Dissecting the string theory dual of QCD,"* Fortsch. Phys. **57** (2009) 396 [ArXiv:0901.1772][hep-th]. 117

[61] M. R. Garousi, *"Tachyon couplings on non-BPS D-branes and Dirac-Born-Infeld action,"* Nucl. Phys. B **584**, 284 (2000) [ArXiv:hep-th/0003122]. 117

[62] K. Bitaghsir-Fadafan and M. R. Garousi, *"Non-abelian expansion of S-matrix elements and non-abelian tachyon DBI action,"* Nucl. Phys. B **760**, 197 (2007) [ArXiv:hep-th/0607249]. M. R. Garousi and E. Hatefi, *"On Wess-Zumino terms of Brane-Antibrane systems,"* Nucl. Phys. B **800**, 502 (2008) [ArXiv:0710.5875][hep-th]. M. R. Garousi and E. Hatefi, *"More on WZ action of non-BPS branes,"* JHEP **0903**, 008 (2009) [ArXiv:arXiv:0812.4216][hep-th]. 117

[63] N. Gutierrez and Y. Lozano, *"Confinement and Non-perturbative Tachyons in Brane-Antibrane Systems,"* Phys. Rev. D **79**, 046010 (2009) [ArXiv:0809.1005][hep-th]. 117

[64] M. R. Garousi, *"D-brane anti-D-brane effective action and brane interaction in open string channel,"* JHEP **0501**, 029 (2005) [ArXiv:hep-th/0411222]. 117

[65] O. Bergman, S. Seki and J. Sonnenschein, *"Quark mass and condensate in HQCD,"* JHEP **0712**, 037 (2007) [ArXiv:0708.2839][hep-th]. A. Dhar and P. Nag, *"Sakai-Sugimoto model, Tachyon Condensation and Chiral symmetry Breaking,"* JHEP **0801**, 055 (2008) [ArXiv:0708.3233][hep-th]. A. Dhar and P. Nag, *"Tachyon condensation and quark mass in modified Sakai-Sugimoto model,"* Phys. Rev. D **78**, 066021 (2008) [ArXiv:0804.4807][hep-th]. 117

[66] V. Niarchos, *"Hairpin-Branes and Tachyon-Paperclips in Holographic Backgrounds,"* [ArXiv:1005.1650][hep-th]. 117

[67] D. Erkal, D. Kutasov and O. Lunin, *"Brane-Antibrane Dynamics From the Tachyon DBI Action,"* [ArXiv:0901.4368][hep-th]. 117

[68] M. Golterman and S. Peris, *"Large-N(c) QCD meets Regge theory: The example of spin-one two-point functions,"* JHEP **0101**, 028 (2001) [ArXiv:hep-ph/0101098]. 118

[69] S. R. Beane, *"Constraining quark hadron duality at large N(c),"* Phys. Rev. D **64**, 116010 (2001) [ArXiv:hep-ph/0106022]. 118

[70] M. Golterman and S. Peris, *"On the use of the operator product expansion to constrain the hadron spectrum,"* Phys. Rev. D **67**, 096001 (2003) [ArXiv:hep-ph/0207060]. 118

[71] M. Shifman, *"Highly excited hadrons in QCD and beyond,"* [ArXiv:hep-ph/0507246]. 118

[72] M. Shifman and A. Vainshtein, *"Highly Excited Mesons, Linear Regge Trajectories and the Pattern of the Chiral Symmetry Realization,"* Phys. Rev. D **77** (2008) 034002 [ArXiv:0710.0863][hep-ph]. 118

[73] A. A. Andrianov and D. Espriu, *"Parity doubling from Weinberg sum rules,"* Phys. Lett. B **671**, 275 (2009) [ArXiv:0803.4104][hep-ph]. 118

[74] O. Cata, M. Golterman and S. Peris, *"The operator product expansion does not imply parity doubling of hadrons,"* Phys. Rev. D **74**, 016001 (2006) [ArXiv:hep-ph/0602194]. 118

[75] J. Mondejar and A. Pineda, *"Constraints on Regge models from perturbation theory,"* JHEP **0710**, 061 (2007) [ArXiv:0704.1417/[hep-ph]]. 118

[76] J. Mondejar and A. Pineda, *"$1/N_c$ and 1/n preasymptotic corrections to Current-Current correlators,"* JHEP **0806**, 039 (2008) [ArXiv:0803.3625/[hep-ph]]. 118

[77] O. Cata, *"Towards understanding Regge trajectories in holographic QCD,"* Phys. Rev. D **75**, 106004 (2007) [ArXiv:hep-ph/0605251]. 118

[78] H. R. Grigoryan and A. V. Radyushkin, *"Form Factors and Wave Functions of Vector Mesons in Holographic QCD,"* Phys. Lett. B **650**, 421 (2007) [ArXiv:hep-ph/0703069]. S. J. Brodsky and G. F. de Teramond, *"Light-Front Dynamics and AdS/QCD Correspondence: The Pion Form Factor in the Space- and Time-Like Regions,"* Phys. Rev. D **77**, 056007 (2008) [ArXiv:0707.3859][hep-ph]. H. J. Kwee and R. F. Lebed, *"Pion Form Factor in Improved Holographic QCD Backgrounds,"* Phys. Rev. D **77**, 115007 (2008) [ArXiv:0712.1811][hep-ph]. Z. Abidin and C. E. Carlson, *"Gravitational Form Factors of Vector Mesons in an AdS/QCD Model,"* Phys. Rev. D **77**, 095007 (2008) [ArXiv:0801.3839][hep-ph]. H. R. Grigoryan and A. V. Radyushkin, *"Anomalous Form Factor of the Neutral Pion in Extended AdS/QCD Model with Chern-Simons Term,"* Phys.

Rev. D **77**, 115024 (2008) [ArXiv:0803.1143][hep-ph]. Z. Abidin and C. E. Carlson, *"Gravitational Form Factors in the Axial Sector from an AdS/QCD Model,"* Phys. Rev. D **77**, 115021 (2008) [ArXiv:0804.0214][hep-ph]. S. J. Brodsky and G. F. de Teramond, *"Light-Front Dynamics and AdS/QCD Correspondence: Gravitational Form Factors of Composite Hadrons,"* Phys. Rev. D **78**, 025032 (2008) [ArXiv:0804.0452][hep-ph]. S. S. Agaev and M. A. G. Nobary, *"Pion distribution amplitude from holographic QCD and the electromagnetic form factor $F_pi(Q2)$,"* Phys. Rev. D **77**, 074014 (2008) [ArXiv:0805.0993][hep-ph]. A. Cherman, T. D. Cohen and M. Nielsen, *"Tests of Universality of Baryon Form Factors in Holographic QCD,"* Nucl. Phys. Proc. Suppl. **199**, 103 (2010) [ArXiv:0909.5359][hep-ph]. 119

[79] C. Nunez, A. Paredes and A. V. Ramallo, *"Unquenched flavor in the gauge/gravity correspondence,"* Adv. High Energy Phys. **2010**, 196714 (2010) [ArXiv:1002.1088][hep-th]. 119

[80] M. Piai, *"Lectures on walking technicolor, holography and gauge/gravity dualities,"* [ArXiv:1004.0176][hep-ph]. 119

[81] S. A. Hartnoll, *"Lectures on holographic methods for condensed matter physics,"* Class. Quant. Grav. **26**, 224002 (2009) [ArXiv:0903.3246][hep-th]. 119

[82] A. Karch, A. O'Bannon and K. Skenderis, *"Holographic renormalization of probe D-branes in AdS/CFT,"* JHEP **0604**, 015 (2006) [ArXiv:hep-th/0512125]. 126

5 Vector-axial vector correlators in weak electric field and the holographic dynamics of the chiral condensate

Authors : Ioannis Iatrakis[a], Elias Kiritsis[a,b]

[a] Crete Center for Theoretical Physics, Department of Physics, University of Crete, 71003 Heraklion, Greece.

[b] APC, Université Paris 7, Bâtiment Condorcet, F-75205, Paris, France (UMR du CNRS 7164).

5.1 Abstract

The transverse part of the vector-axial vector flavor current correlator in the presence of weak external electric field is studied using holography. The correlator is calculated using a bottom-up model proposed recently, that includes both contributions of higher string states and the non-linear dynamics of the chiral condensate. It is shown that for low momenta the result agrees with the relation proposed by Son and Yamamoto motivated by a simpler holographic model. This suggests that the Son-Yamamoto relation is generically valid in the IR of models with the proper chiral symmetry breaking

pattern.

5.2 Introduction

Global symmetries of class3ical field theories which fail to survive quantization of the theory lead to quantum anomalies. These appear as the non-invariance of the quantum effective action under the symmetry transformation and as the violation of Ward identities of certain correlators. One such example is the chiral (triangle) anomaly with one axial and two vector currents. The longitudinal part of that correlator is not renormalized as was shown by Adler and Bardeen, [1]. However, the transverse part is not necessarily constrained.

This correlator is of importance in the context of the calculation of the two-loop electroweak radiative corrections to the muon anomalous magnetic moment, an important precision observable. In this context the transverse part of the vector - axial vector QCD flavor current correlator in the presence of weak electric field was studied in [2] and [3]. The physical significance of the above correlator led to its further study both in perturbative QCD and in the strong coupling limit, in [4] and [5]. A non-renormalization theorem beyond the one-loop term was proved, perturbatively.

At the non-perturbative level, the correlator was studied using the operator product expansion, see [2], [3] and [4]. There it was shown that the first most important non-perturbative correction at high momenta is non-perturbative, due to chiral symmetry breaking. In the absence of a model for the non-perturbative dynamics, only a high-momentum estimate can be done using the operator product expansion.

The first non-perturbative correction scales like $1/q^6$ at large q and is generated by the expectation value of the dimension three (in the UV) antisymmetric tensor current, $J^{\mu\nu}_{ij} \sim \bar{\psi}^i_R \sigma^{\mu\nu} \psi^j_L$. To be more precise, the general form of the vector-axial vector correlator is, [4]

$$\langle T\{J^a_\mu(q) J^{b\,(5)}_\nu(p)\}\rangle_{\hat{F}} = -\mathrm{Tr}(\mathcal{Q}\, t^a t^b)\frac{1}{4\pi^2}(2\pi)^4\delta^4(q+p)\Big\{w_T(q^2)(-q^2\mathcal{O}_{\mu\nu} + q_\mu q^\sigma \mathcal{O}_{\sigma\nu} - q_\nu q^\sigma \mathcal{O}_{\sigma\mu}) + w_L(q^2) q_\nu q^\sigma \mathcal{O}_{\sigma\mu}\Big\} \tag{5.2.1}$$

where $\mathcal{Q}$ is the electric charge matrix and t^a are the flavor matrices. The leading contribution comes from the dimension 2 operator $\mathcal{O}_{\mu\nu} = \frac{1}{2}\epsilon_{\mu\nu\rho\sigma}F^{\rho\sigma}$ and the coefficients read $w_L^{1\ loop} = 2w_T^{1\ loop} = 2\frac{N_c}{q^2}$, where $F^{\rho\sigma}$ is the electromagnetic field strength tensor and N_c the number of colors. In the chiral limit the next contribution comes from

non-perturbative effects (non-trivial vevs) and in the large N_c limit it reads

$$\mathcal{O}_{\mu\nu} = \epsilon_{\mu\nu\rho\sigma}\langle\bar{\psi}_R\psi_L\rangle\langle\bar{\psi}_R\sigma^{\rho\sigma}\psi_L\rangle \tag{5.2.2}$$

Its coefficient is computed at short distances and is $w_T^{non\ pert.} \sim \frac{\alpha_s}{q^6}$, where α_s is the QCD fine structure constant. It should be emphasized that the longitudinal part does not receive any correction beyond the one-loop result. Therefore, for the subleading corrections, and in particular for the correlator at lower values of q near the QCD scale one must have a non-perturbative setup in order to compute them.

In [6] a simple ansatz was used for the quadratic action of the bulk gauge fields dual to the axial and vector currents. This ansatz appeared in earlier bottom up models for Mesons like the "cosh" model [7], or the top down Sakai-Sugimoto model, [9]. In the first model the chiral symmetry breaking is done by appropriate IR boundary conditions, while in the second by the dynamics of the brane embedding in the higher dimensional space.

Son and Yamamoto (SY) have shown that for this class of actions, a relation holds between the transverse correlator w_T in (5.2.1) above and the difference between the axial-axial and vector-vector correlators, namely

$$w_T(q) = \frac{N_c}{q^2} - \frac{N_c}{f_\pi^2}\left[\Pi_A(q) - \Pi_V(q)\right] \tag{5.2.3}$$

where the transverse current two-point functions in momentum space are defined as

$$\int d^4x d^4y e^{iqx+ipy}\langle T\{J^a_{(V/A)\,\mu}(x)J^b_{(V/A)\,\nu}(y)\}\rangle = \delta^{ab}(q^2\eta_{\mu\nu}-q_\mu q_\nu)\Pi_{V/A}(q^2)(2\pi)^4\delta^{(4)}(p+q) \tag{5.2.4}$$

It is noted that in perturbative massless QCD, only the first (one-loop) term in (5.2.3) is non-zero, and the rest vanish (as they are non-perturbative)

The following points were made in [6]:

- Relation (5.2.3) implies sum rules for vector and axial vector resonances that resemble the 't Hooft matching conditions for anomalies.
- Such sum rules seem phenomenologically successful at low values of momenta.
- At large values of momenta, it is expected, based on the OPE in massless QCD, that beyond perturbation theory, both the left and right-hand side in (5.2.3) behave as $1/q^6$.
- For the "cosh" model and the Sakai-Sugimoto model that realize the action ass3umed in [6] the non-perturbative contributions on both sides of (5.2.3) are exponentially suppressed in q^2 rather than power-suppressed.

- A similar analysis in the hard-wall model, [16], has provided a different relation namely in the UV

$$w_T(q) = \frac{N_c}{q^2} - \frac{48\pi^2}{q^2}\left[\Pi_A(q) - \Pi_V(q)\right] \tag{5.2.5}$$

  while in the IR, it was found that (5.2.3) is true at $q^2 = 0$.

Although the particular models in [7] and [9] satisfying the SY relation (5.2.3) have both sides in disagreement with QCD, Son and Yamamoto suggested that the relation be valid in real QCD, [6].

This claim was subsequently analyzed in [8] who tried to test it in perturbation theory, valid at very high energy. However, as mentioned, the SY relation seems trivially satisfied in massless perturbative QCD, and therefore any non-trivial test must approach the massless limit by starting first from the massive theory. Indeed, in [8] such a limit was devised, and by removing in a specific order the regulator and taking the quark mass to zero, they have claimed that the relation fails. Despite this claim, it may still be possible for the relation to be valid if a different sequence of limits is devised, or the limit is defined in a different way.

At this stage we are faced with two questions:

- How robust is the validity of the SY relation at low energies? In particular how much is it affected by the dynamics of the chiral condensate?

- Is the SY relation valid at arbitrarily high momenta? In particular is there an appropriate massless limit in QCD compatible with (5.2.3)?

In the present work, we will try to answer (at least partly) the first of the previous two questions. We will revisit the axial correlator in question, and its calculation from holography. We will use a setup that contains contributions from higher-spin states and models the dynamics of the chiral condensate in a more realistic fashion. We will find that the low energy structure of the transverse correlator is robust and the SY relation holds at low enough energy. We will also comment on the high-energy structure of the model.

To motivate the setup it is important to revisit the low-dimension operators (dimension=3) in the flavor sector and their realization in string theory. At the spin-zero level we have the (complex) mass operator

$$\bar{\psi}^i_R \psi^j_L \leftrightarrow T_{ij} \tag{5.2.6}$$

dual to a complex scalar transforming as $(N_f, \bar{N}_f)$ under the flavor symmetry $U(N_f)_R \times U(N_f)_L$. At the spin-one level we have the two classically conserved currents

$$\bar{\psi}^i_L \sigma^\mu \psi^j_L \leftrightarrow A^\mu_{L,ij} \quad , \quad \bar{\psi}^i_R \bar{\sigma}^\mu \psi^j_R \leftrightarrow A^\mu_{R,ij} \tag{5.2.7}$$

They transform in the adjoint of the $U(N_f)_R$ respectively the $U(N_f)_L$ symmetry. The flavor symmetry is expected to arise in string theory from N_f flavor branes (R) and N_f favor antibranes (L). The precise realization and dimensionality of the branes depends on the theory. In the most popular top-down theory of Sakai and Sugimoto, [9] the flavor branes are 8-dimensional (while the full bulk is 10-dimensional and the gauge theory 5 dimensional) while in a 5-dimensional setup expected to hold for the minimal YM realization, the favor branes are expected to be space-filling D_4 branes, [10]. Due to the quantum numbers, the vectors are the lowest modes of the fluctuations of the open strings with both ends on the D branes (A^μ_R), or the anti-D branes , A^μ_L.

The bifundamental scalar T, on the other hand, is the lowest mode of the $D - \bar{D}$ strings, compatible with its quantum numbers. Its holographic dynamics is dual to the dynamics of the chiral condensate. This is precisely the scalar that in a brane-antibrane system in flat space is the tachyon whose dynamics has been studied profusely in string theory, [11]. It has been proposed that the non-linear DBI-like actions proposed by Sen and others are the proper setup in order to study the holographic dynamics of chiral symmetry breaking, [12]. This dynamics was analyzed in a toy example, [13; 14], improving several aspects of the hard [16], and soft wall models, [17]. We will keep referring to T as the “tachyon", as it indeed corresponds to a relevant operator in the UV.

Going further, the antisymmetric current

$$\bar{\psi}^i_R \sigma^{\mu\nu} \psi^j_L \leftrightarrow B^{ij}_{\mu\nu} \tag{5.2.8}$$

is dual to a two-index antisymmetric tensor[1] that transforms as $(N_f, \bar{N}_f)$ under the flavor group. It therefore originates in the $D - \bar{D}$ sector, and is a stringy descendant of the tachyon. Indeed, in flat-space open-string spectra, the antisymmetric tensor appears at the level just above the tachyon, arising from two antisymmetrized oscillators acting on the ground state, with reversed GSO projection[2].

In string theory, the effective action for low-lying states (typically massless) is often used. It is non-linear, contains an infinite series of higher-derivatives, and is generated

[1] Recent discussions on the inclusion of this antisymmetric tensor explicitly in the holographic flavor action can be found in [18].

[2] Such stringy states were recently discussed in connection with the Sakai-Sugimoto model and Mesons in [19].

by integrating out (usually at tree level) the massive modes of the relevant strings. In the particular case of open strings, it is known that the action containing all modes of the string contains only cubic interactions. Upon integrating out however the massive modes, the action becomes non-linear and non-local. In a low wavelength expansion and around nearly flat space, it has been calculated to be of the DBI type.

For the two vectors and the bifundamental scalar described above, the effective action has been proposed before by Sen. One of the characteristics of the Sen action for the tachyon, is its non-linearity, and the fact that contains (a class of) higher derivatives. In analogy with the standard DBI action, it contains contributions from all intermediate open string states, to leading order in derivatives. In the open string sector, leading order implies that the effective action for the tachyon scalar is a function of its first derivatives but not higher ones. Therefore, we expect that the DBI-like Sen action contains the corrections due to the stringy modes.

The non-linearity of the action and the fact that chiral symmetry breaking is dynamical makes an evaluation of the axial correlator in such holographic models interesting.

In this paper we will calculate this correlator using the simplified holographic model proposed and analyzed in [13], [14]. The relation (5.5.6) derived in [6] in the simpler model is not valid in general here. The reason is instructive. One can class3ify the terms that one in principle expects at the quadratic level that could contribute to the mixed correlator w_T or $\Pi_{A/V}$. For $\Pi_{A/V}$ the terms come from the CP-even sector and involve three terms: $F_{z\mu}^2$, $F_{\mu\nu}^2$ and A_μ^2. The last term is only present for the axial vector field and is the result of chiral symmetry breaking. All of these terms maybe multiplied by various combinations of the closed string fields (including the bulk metric) as well as the chiral condensate (the tachyon T). The last term, giving a mass to the axial vector is absent. This very general action is in the class3 assumed by Son and Yamamoto.

The terms that can appear in the CP-odd sector are strongly constrained by the anomaly and can only include the 5-dimensional Chern-Simons (CS) action for the gauge fields, times an overall coefficient W(T) that depends on the tachyon[1]. As long as $W(T) = W(0) = \frac{N_c}{24\pi^2}$ is a constant independent of the tachyon (and therefore matching the QCD flavor anomaly), the Son-Yamamoto relation is guaranteed to hold, as shown in [6].

In general, holographic models that contain the dynamics of the chiral condensate (alias the tachyon), also contain a quadratic term A_μ^2 that originates from the kinetic term of the tachyon field via its covariant derivative.[2] Therefore a priori we would

[1]Such a CP-odd coupling has been calculated exactly in $D - \bar{D}$ pairs around flat space, [27; 40]. There are also subleading terms that implement the proper axial anomaly.

[2]It should be stressed that in this discussion the dynamics of the tachyon is assumed to be local. For

expect that the SY relation is violated somewhere in the energy domain. Moreover, we would expect that the CS coefficient $W(TT^\dagger)$ is not constant. Indeed, general arguments due to Sen, imply that for the IR value of the tachyon, T_{IR}, $W(T_{IR}) = 0$[1]. Therefore the function $W(TT^\dagger)$ is not expected to be constant but rather to interpolate between $W(0)$ and zero.

From the general comments above we conclude that in holographic models that contain explicitly the local dynamics of a condensate,

- we expect that generically the SY relation is violated,
- only in very special cases it may be valid in at least a part of the full energy domain.

What we find in this paper is that in the class of models advocated in [12] and the specific examples analyzed in [13; 14], *the SY relation is valid at low energies.* This is a welcome result as it suggests that its IR validity seems insensitive to the details of the holographic model as long as the physics of chiral symmetry breaking is correct. We are lacking however something like a broken Ward identity that would explain the IR validity of the SY relation at low energy.

Some comments on the UV asymptotics are also pertinent. We should first stress that our model is not capable of shedding light to the question whether the SY relation is valid at high energy in QCD. The reason is that there is no guarantee that holographic models should capture the quantitative UV physics at weak coupling.

We have calculated the large momentum behavior of $\Pi_V - \Pi_A$ and find that it asymptotes to $1/q^6$ as expected in QCD. This corrects our analytic estimate in [14]. We have also examined the large q^2 behavior of w_T. We have found numerically and analytically that the first non-perturbative correction falls off as $1/q^8$. Therefore the UV structure of the present model seems somewhat different from that expected from QCD. A scaling analysis however indicates that the leading non-trivial w_T behavior will be $1/q^6$ if the subleading asymptotics of the CS tachyon function W is $W(TT^\dagger) = W(0) + \mathcal{O}(TT^\dagger)^{\frac{2}{3}})$ for small T. However, this is a fit and cannot answer the question on the UV validity of the SY relation.

this to happen, the branes and antibranes must be very close or on top of each other in the equilibrium configuration. This is expected to be the case in pure 5-dimensional models of QCD, [10], but is not the case for the Sakai-Sugimoto model, [9], where the tachyon sector is non-local as the relevant string is stretched in the extra sixth compact dimension, [15].

[1]The same is true also for the coefficients of the kinetic terms of the vectors on the D-branes. Their vanishing is interpreted as the fact that at that point the brane-antibrane pair annihilates and the world-volume gauge fields disappear from the dynamics, [11]. In the models of [13; 14], $T_{IR} \to \infty$.

We have also calculated w_T as a function of the bare quark mass. Using our earlier fits to the meson spectrum [14], we calculate the correlator for two non-zero masses. The first is the up-down quark mass, where we observe that the correlator is almost identical to that with $m_q = 0$. We also calculate it with a mass matching the strange quark mass, and find that it is larger as shown in figure 5.2.

We have good reasons to expect that the same open string sector with a proper glue sector, close to QCD, as for example in [10; 41], will provide a correlator that is quantitatively reliable at low momenta and qualitatively correct at high momenta.

5.3 Action and dynamics of holographic chiral symmetry breaking

We consider a system of N_f pairs of D_4-branes - $\bar{D}_4$-antibranes in a fixed bulk gravitational background that describes the "glue". The background was analyzed in [20] and [21] and is a solution of the non-critical string theory action in six dimensions. The metric is an AdS_6 soliton

$$ds^2 \equiv -g_{tt}dt^2 + g_{zz}dz^2 + g_{xx}dx_3^2 + g_{\eta\eta}d\eta^2 = \frac{R^2}{z^2}\left[dx_{1,3}^2 + f_\Lambda^{-1}dz^2 + f_\Lambda\, d\eta^2\right] \quad (5.3.1)$$

where $f_\Lambda = 1 - \frac{z^5}{z_\Lambda^5}$ and the η direction is cigar shaped with its tip to be at z_Λ, so $z \in [0, z_\Lambda]$. There is also a constant dilaton and a RR-form which is

$$F_{(6)} = Q\sqrt{-g_{(6)}}d^6x \quad (5.3.2)$$

Q is a constant which will be fixed by matching to the anomaly of the dual boundary field theory as it was proposed in [22] and further analysed in [23]. Although the bulk geometry is not very close to standard YM, compared to finer constructions like [10], it has the advantage of simplicity, and this is the main reason that we consider it here. It is the bulk geometry obtained from a five-dimensional supersymmetric CFT compactified on a "small" circle, with supersymmetry breaking boundary conditions for the fermion operators. Despite the simplicity of the geometry, it turns out to fulfill the main qualitative necessary ingredients .

We now consider the generalization of Sen's action [24] for describing N_f coincident pairs of D_4-branes - $\bar{D}_4$-antibranes, see [12] and references therein. For the present study, the full non-abelian "tachyon-DBI" is not necessary. The non abelian results that we need, come from a simple generalization of the abelian ones, which were found

in [12] and [14]. The D_4 - $\bar{D}_4$ pairs are taken at a fixed point in η direction[1]. The action is

$$S = -\int d^4x dz \,\mathrm{Str}\left[V(|T|)\left(\sqrt{-\det \mathbf{A}_L} + \sqrt{-\det \mathbf{A}_R}\right)\right] \tag{5.3.3}$$

where

$$\mathbf{A}_{(i)MN} = g_{MN} + \frac{2\pi\alpha'}{g_V}\mathcal{F}^{(i)}_{MN} + \pi\alpha'\lambda\left((D_M T)^*(D_N T) + (D_N T)^*(D_M T)\right) \quad , M, N = 1, \ldots, 5 \tag{5.3.4}$$

$(i) = L, R$ denotes the left and right parts of the $U(N_f)_{L/R}$ gauge field strengths $\mathcal{F} = d\mathcal{A} - i\mathcal{A}\wedge\mathcal{A}$. More details about the definitions and conventions can be found in [12].

The tachyon T is a complex bifundamental scalar. We also define

$$DT \equiv dT + iT\mathcal{A}_L - i\mathcal{A}_R T \tag{5.3.5}$$

We introduced the couplings g_V and λ which determine the normalization of the bulk fields. These two couplings can be fixed by matching the results of the vector and scalar two point functions as calculated in the bulk on the one hand and in QCD on the other hand, as was proposed in [16]. They have been matched in [14].

The tachyon potential is

$$V(\tau) = \mathcal{K}\, e^{-\frac{1}{2}\mu^2\tau^2} \tag{5.3.6}$$

where $\mathcal{K}$ is a constant. The vacuum of the above theory was analyzed in [14]. The only nonzero field is the tachyon which diverges at the tip of the cigar. As it is pointed out in [26] and [12], in case that the N_f quarks have the same mass the vacuum of the non abelian action consists of N_f copies of the abelian solution

$$\langle T\rangle = \tau(z)\mathbb{I} \tag{5.3.7}$$

The background solution for $\tau(z)$ was studied in [14]. The near-boundary expansion ($z \to 0$) of the tachyon reads

$$\tau(z) = c_1 z + \frac{\mu^2}{6}c_1^3 z^3 \log z + c_3 z^3 + \ldots \tag{5.3.8}$$

where c_1 is proportional to the quark mass and c_3 is proportional to the vacuum expectation value of the $\bar{q}q$ operator.

The study of the above model in [13], [14] led to the description of many low energy QCD properties.

[1] This is because in the 5-dimensional world, this is the case that is expected to describe the flavor sector.

- The model incorporates confinement in the sense that the quark-antiquark potential computed with the usual AdS/CFT prescription [32] confines. Moreover, magnetic quarks are screened. The background solution stems from a gravitational action, that allows, for instance, to compute thermodynamical quantities. All of this are properties associated to the background geometry and were already discussed in [21].

- The string theory nature of the bulk fields dual to the quark bilinear currents is readily identified: they are low-lying modes living in a brane-antibrane pair.

- Chiral symmetry breaking is realized dynamically and consistently, because of the tachyon dynamics. See [35] for discussion and possible solutions in the soft-wall model context.

- In this model, the mass of the ρ-meson grows with increasing quark mass, or, more physically, with increasing pion mass. This welcome physical feature is absent in the soft wall model, [17]. It occurs here because the tachyon potential multiplies the full action and in particular the kinetic terms for the gauge fields, which therefore couple to the chiral symmetry breaking vev. In our previous work [13], we exploited this fact in order to fit the strange-strange Mesons together with the light-light Mesons, with rather successful results. In [36], the authors added the strange quark mass to the hard wall model and computed the dependence of vector masses on the quark mass. In that case however, this dependence of the vector masses originated only from the non-abelian structure and therefore misses at least part of the physics[1].

- The soft wall requires assuming a quadratic dilaton in the closed string theory background. It has been shown that such a quadratic dilaton behaviour can never be derived from a gravitational action while keeping the geometry to be that of AdS.[2]. That the background is not found as a solution is a shortcoming if for instance one wants to study the thermodynamics of the underlying glue theory. The thermodynamics of the soft wall model is therefore ill-defined. In the present model, the background is a solution of a two-derivative approximation to non-critical string theory. In order to obtain Regge behaviour, we also needed a further assumption: that the tachyon potential is asymptotically gaussian. However, this

[1] On the other hand, the quark mass dependence of the ρ-meson can be seen in different top-down models, see [37] for a recent work in the context of the Klebanov-Strassler model.

[2] This was shown in [38]. In [10] such behavior can be implemented for glue, but the metric changes appropriately, an important ingredient for implementing confinement in the glue sector.

is rather natural since this potential has appeared in the literature, for instance [27; 39].

- Considering that the dynamics is controlled by a tachyon world-volume action automatically provides the model with a WZ term of the form given in [27; 28; 29; 40]. In [12] it was shown that properties like discrete symmetries (parity and charge conjugation) and anomalies are, in general, correctly described by analyzing this term and we will detail them also here.

In practice, the matching of the the predicted mass spectrum and some decay constants to experimental data is considered successful since the model has two parameters which correspond to those of QCD (quark mass and QCD scale) and one phenomenological parameter which is fitted to data[1]. Eventually, the rms error of numerical fits to spectra and decay constants is $10\% - 15\%$. In conclusion this simple bottom-up model, which is string theory inspired, incorporates many interesting QCD features.

5.4 The Wess Zumino action

The Wess-Zumino term describing the coupling of the flavor branes-antibranes to the RR background field was studied in [27], [28], [29] and is

$$S_{WZ} = T_4 \int_{\mathcal{M}_{p+1}} C \wedge \mathrm{Str}\, e^{i2\pi\alpha' \mathbf{F}} \tag{5.4.1}$$

where $C = \sum_n (-i)^{\frac{p-n+1}{2}} C_n$ is a sum of the RR fields, and $\mathbf{F} = d\mathbf{A} - i\mathbf{A} \wedge \mathbf{A}$. The integration picks up the $(p+1)$- form of the infinite sum of forms. In terms of the tachyon field and the left and right $U(N_f)$ gauge fields we have

$$i\mathbf{A} = \begin{pmatrix} i\mathcal{A}_L & T^\dagger \\ T & i\mathcal{A}_R \end{pmatrix}, \qquad i\mathbf{F} = \begin{pmatrix} i\mathcal{F}_L - T^\dagger T & DT^\dagger \\ DT & i\mathcal{F}_R - TT^\dagger \end{pmatrix} \tag{5.4.2}$$

We also set $2\pi\alpha' = 1$. The Wess-Zumino action on the worldvolume of the $D_4 - \bar{D}_4$ flavor branes in the background of N_c D_4 color branes is

$$S_{WZ} = iT_4 \int_{\mathcal{M}_5} C_{-1} \wedge \mathrm{Str}\, e^{i\mathcal{F}}\Big|_{6-\mathrm{form}} = iT_4 \int_{\mathcal{M}_5} F_{(0)} \wedge \Omega_5 \tag{5.4.3}$$

[1] It turns our that spectra and decay constants depends rather weakly on this phenomenological parameter, [14].

where $F_0 = dC_{-1}$ is proportional to the number of colors. We work in a non-critical supergravity 6-dimensional background which has a non trivial RR form with field strength given in (5.3.2). It's dual form is $F_{(0)} = \star F_{(6)} = Q$, so

$$S_{WZ} = iT_4 Q \int \Omega_5 \tag{5.4.4}$$

where $iT_4 Q = i\frac{N_c}{4\pi^2}$ was fixed by matching to the QCD chiral anomaly in [12]. Ω_5 is the 5-form that comes from the expansion of $e^{i\mathcal{F}}$ and was found in [12]

$$\begin{aligned}
\Omega_5 = \frac{1}{6}\mathrm{Tr}\, e^{-\tau^2}\Big\{ & -i\mathcal{A}_L\wedge\mathcal{F}_L\wedge\mathcal{F}_L + \frac{1}{2}\mathcal{A}_L\wedge\mathcal{A}_L\wedge\mathcal{A}_L\wedge\mathcal{F}_L + \frac{i}{10}\mathcal{A}_L\wedge\mathcal{A}_L\wedge\mathcal{A}_L\wedge\mathcal{A}_L\wedge\mathcal{A}_L \\
& + i\mathcal{A}_R\wedge\mathcal{F}_R\wedge\mathcal{F}_R - \frac{1}{2}\mathcal{A}_R\wedge\mathcal{A}_R\wedge\mathcal{A}_R\wedge\mathcal{F}_R - \frac{i}{10}\mathcal{A}_R\wedge\mathcal{A}_R\wedge\mathcal{A}_R\wedge\mathcal{A}_R\wedge\mathcal{A}_R \\
& + \tau^2\Big[i\mathcal{A}_L\wedge\mathcal{F}_R\wedge\mathcal{F}_R - i\mathcal{A}_R\wedge\mathcal{F}_L\wedge\mathcal{F}_L + \frac{i}{2}(\mathcal{A}_L-\mathcal{A}_R)\wedge(\mathcal{F}_L\wedge\mathcal{F}_R+\mathcal{F}_R\wedge\mathcal{F}_L) \\
& + \frac{1}{2}\mathcal{A}_L\wedge\mathcal{A}_L\wedge\mathcal{A}_L\wedge\mathcal{F}_L - \frac{1}{2}\mathcal{A}_R\wedge\mathcal{A}_R\wedge\mathcal{A}_R\wedge\mathcal{F}_R + \frac{i}{10}\mathcal{A}_L\wedge\mathcal{A}_L\wedge\mathcal{A}_L\wedge\mathcal{A}_L\wedge\mathcal{A}_L \\
& - \frac{i}{10}\mathcal{A}_R\wedge\mathcal{A}_R\wedge\mathcal{A}_R\wedge\mathcal{A}_R\wedge\mathcal{A}_R\Big] \\
& + i\tau^3 d\tau\wedge\Big[(\mathcal{A}_L\wedge\mathcal{A}_R - \mathcal{A}_R\wedge\mathcal{A}_L)\wedge(\mathcal{F}_L+\mathcal{F}_R) + i\mathcal{A}_L\wedge\mathcal{A}_L\wedge\mathcal{A}_L\wedge\mathcal{A}_R \\
& - \frac{i}{2}\mathcal{A}_L\wedge\mathcal{A}_R\wedge\mathcal{A}_L\wedge\mathcal{A}_R + i\mathcal{A}_R\wedge\mathcal{A}_R\wedge\mathcal{A}_R\wedge\mathcal{A}_R\Big] \\
& + \frac{i}{4}\tau^4(\mathcal{A}_L-\mathcal{A}_R)\wedge(\mathcal{A}_L-\mathcal{A}_R)\wedge(\mathcal{A}_L-\mathcal{A}_R)\wedge(\mathcal{A}_L-\mathcal{A}_R)\wedge(\mathcal{A}_L-\mathcal{A}_R)\Big\}
\end{aligned} \tag{5.4.5}$$

We now split the $U(N_f)$ gauge fields into their $U(1)$ and $SU(N_f)$ parts

$$\mathcal{A}_L = \frac{\hat{A}_L}{\sqrt{2N_f}} + A_L \quad , \quad \mathcal{A}_R = \frac{\hat{A}_R}{\sqrt{2N_f}} + A_R \tag{5.4.6}$$

where we denote as A_L, A_R the $SU(N_f)$ part and $\hat{A}_L, \hat{A}_R$ the $U(1)$ part of the gauge field. We also consider the vector combination of the $U(1)$ fields, $\hat{A}_L = \hat{A}_R = \hat{A}$. Since, we are interested in the calculation of the correlation function of the vector and the axial current in the presence of a weak electromagnetic field we expand Ω_5 to linear order in $\hat{F}$ and quadratic in the $SU(N_f)$ gauge fields. So, the relevant terms of Ω_5 are

$$\begin{aligned}
\Omega_5' = \frac{1}{6}\mathrm{Tr}\, e^{-\tau^2}\Big\{ & -i\mathcal{A}_L\wedge\mathcal{F}_L\wedge\mathcal{F}_L + i\mathcal{A}_R\wedge\mathcal{F}_R\wedge\mathcal{F}_R + \tau^2\Big[i\mathcal{A}_L\wedge\mathcal{F}_R\wedge\mathcal{F}_R - i\mathcal{A}_R\wedge\mathcal{F}_L\wedge\mathcal{F}_L \\
& + \frac{i}{2}(\mathcal{A}_L-\mathcal{A}_R)\wedge(\mathcal{F}_L\wedge\mathcal{F}_R+\mathcal{F}_R\wedge\mathcal{F}_L)\Big] + i\tau^3 d\tau\wedge(\mathcal{A}_L\wedge\mathcal{A}_R - \mathcal{A}_R\wedge\mathcal{A}_L)\wedge(\mathcal{F}_L+\mathcal{F}_R)\Big\}
\end{aligned} \tag{5.4.7}$$

We also define the vector and axial vector fields

$$V^a = \frac{A_L^a + A_R^a}{2} \quad , \quad A^a = \frac{A_L^a - A_R^a}{2} \tag{5.4.8}$$

where $a = 1, \ldots, N_f^2 - 1$. After the decomposition the action reads

$$\begin{aligned} S_{WZ}^{lin.} &= \frac{N_c}{8\pi^2} \int_{\mathcal{M}_5} e^{-\frac{1}{2}\mu^2\tau^2} \hat{F} \wedge \mathrm{Tr}\,(A_L - A_R) \wedge d(A_R + A_L) \\ &= \frac{N_c}{2\pi^2} \int_{\mathcal{M}_5} e^{-\frac{1}{2}\mu^2\tau^2} \hat{F} \wedge \mathrm{Tr}\,(A \wedge dV) \end{aligned} \tag{5.4.9}$$

In order to express the action in the above form, we have added some boundary terms to the initial action

$$S_{WZ}^{lin.} = i\frac{N_c}{4\pi^2} \int \Omega_5' + S_{b.\,1} + S_{b.\,2} + S_{b\,3} \tag{5.4.10}$$

where

$$\begin{aligned} S_{b.\,1} &= \frac{N_c}{24\pi^2} \int_{\partial\mathcal{M}_5} e^{-\frac{1}{2}\mu^2\tau^2} \hat{A} \wedge \mathrm{Tr}\,(A_R \wedge dA_R - A_L \wedge dA_L - 3A_L \wedge dA_R + 3A_R \wedge dA_L) \\ S_{b.\,2} &= \frac{N_c}{24\pi^2} \int_{\partial\mathcal{M}_5} \frac{\mu^2}{2}\tau^2 e^{-\frac{1}{2}\mu^2\tau^2} \hat{A} \wedge \mathrm{Tr}\,(A_R \wedge dA_R - A_L \wedge dA_L - 3A_L \wedge dA_R + 3A_R \wedge dA_L) \\ S_{b.\,3} &= -\frac{N_c}{24\pi^2} \int_{\partial\mathcal{M}_5} \mu^2\tau^2 d\left(e^{-\frac{1}{2}\mu^2\tau^2}\right) \wedge \hat{A} \wedge \mathrm{Tr}\,(A_L \wedge A_R) \end{aligned} \tag{5.4.11}$$

5.4.1 The chiral anomaly in the presence of the condensate

We will now calculate the anomaly under a $U(N_f)_V$ symmetry transformation in the presence of a non zero tachyon (=chiral vev). In the derivation of the expression (5.4.5), the tachyon was considered to be proportional to unity matrix (5.3.7), which breaks the flavor symmetry to its diagonal subgroup, $U(N_f)_L \times U(N_f)_R \to U(N_f)_V$. Hence we can only test transformations that preserve this form ,namely vector transformations. The variation of the action (anomaly) under the symmetry transformation can be written as

$$(D_\mu \langle J^\mu(x) \rangle)_a = \left(D_\mu \frac{\delta \mathcal{W}}{\delta A_\mu(x)} \right)_a \Bigg|_{A=0} = -\mathcal{A}_a(x) \tag{5.4.12}$$

where J^μ is the symmetry current and $\mathcal{W}$ is the generating functional of the theory. Then, the variation under the symmetry gives

$$\delta_\Lambda \mathcal{W}[A] = -\delta_\Lambda S_{bulk}[A] = \int d^4x \Lambda^a \mathcal{A}_a \tag{5.4.13}$$

where Λ is the transformation parameter. Direct calculation gives,

$$\begin{aligned}\delta S_{WZ} = -\frac{iN_c}{24\pi^2}\int_{\partial \mathcal{M}_5 \epsilon} \mathrm{Tr}\,\Lambda\Big\{ & e^{-\frac{\mu^2}{2}\tau(\epsilon)^2}(1+\frac{\mu^2}{2}\tau(\epsilon)^2)\big[-\mathcal{F}_L\wedge\mathcal{F}_L - \frac{i}{2}(\mathcal{A}_L\wedge\mathcal{A}_L\wedge\mathcal{F}_L + \\ & + \mathcal{A}_L\wedge\mathcal{F}_L\wedge\mathcal{A}_L + \mathcal{F}_L\wedge\mathcal{A}_L\wedge\mathcal{A}_L) + \frac{1}{2}\mathcal{A}_L\wedge\mathcal{A}_L\wedge\mathcal{A}_L\wedge\mathcal{A}_L + \mathcal{F}_R\wedge\mathcal{F}_R + \\ & \frac{i}{2}(\mathcal{A}_R\wedge\mathcal{A}_R\wedge\mathcal{F}_R + \mathcal{A}_R\wedge\mathcal{F}_R\wedge\mathcal{A}_R + \mathcal{F}_R\wedge\mathcal{A}_R\wedge\mathcal{A}_R) - \frac{1}{2}\mathcal{A}_R\wedge\mathcal{A}_R\wedge\mathcal{A}_R\wedge\mathcal{A}_R\big] - \\ & - \frac{\mu^2}{4}\tau(\epsilon)^2\, de^{-\frac{\mu^2}{2}\tau(\epsilon)^2}\wedge\big[(\mathcal{A}_L-\mathcal{A}_R)\wedge(\mathcal{F}_L+\mathcal{F}_R) + (\mathcal{F}_L+\mathcal{F}_R)\wedge(\mathcal{A}_L-\mathcal{A}_R) + \\ & i(\mathcal{A}_L\wedge\mathcal{A}_L\wedge\mathcal{A}_L - \mathcal{A}_L\wedge\mathcal{A}_L\wedge\mathcal{A}_R - \mathcal{A}_R\wedge\mathcal{A}_L\wedge\mathcal{A}_L + \mathcal{A}_L\wedge\mathcal{A}_R\wedge\mathcal{A}_R + \\ & + \mathcal{A}_R\wedge\mathcal{A}_R\wedge\mathcal{A}_L - \mathcal{A}_R\wedge\mathcal{A}_R\wedge\mathcal{A}_R)\big]\Big\}\end{aligned} \tag{5.4.14}$$

where ϵ is the UV cut off near the AdS boundary. We have also used the following variations of the fields

$$\begin{aligned}\delta_\Lambda \mathcal{A}_{L/R} &= -i\,D\Lambda = -i\,d\Lambda - \mathcal{A}_{L/R}\Lambda + \Lambda\mathcal{A}_{L/R} \\ \delta_\Lambda \mathcal{F}_{L/R} &= [\Lambda, \mathcal{F}_{L/R}]\end{aligned} \tag{5.4.15}$$

In case that the tachyon is a function of the radial AdS coordinate only, so the quark condensate and mass are not spacetime dependent, the term which is proportional to $de^{-\frac{\mu^2}{2}\tau(\epsilon)^2}$ in (5.4.14) is zero. Hence, we recover the known QCD flavor anomaly up to an overall consatnt term which depends on the UV cutoff, and can be reabsorbed in the coupling, T_4 of the Wess Zumino action, Eq.(5.4.1). We notice that the anomaly depends on the condensate in case that there is a finite UV cutoff and the condensate has non trivial spacetime dependence. But also in this case, when we remove the cut-off (take $\epsilon \to 0$), Eq.(5.4.14) reproduces the known QCD anomaly, see [12],

$$\begin{aligned}\delta S_{WZ} = -\frac{iN_c}{24\pi^2}\int_{\partial \mathcal{M}_5} \mathrm{Tr}\,\Lambda\Big\{ & -\mathcal{F}_L\wedge\mathcal{F}_L - \frac{i}{2}(\mathcal{A}_L\wedge\mathcal{A}_L\wedge\mathcal{F}_L + \mathcal{A}_L\wedge\mathcal{F}_L\wedge\mathcal{A}_L + \mathcal{F}_L\wedge\mathcal{A}_L\wedge\mathcal{A}_L) + \\ & \frac{1}{2}\mathcal{A}_L\wedge\mathcal{A}_L\wedge\mathcal{A}_L\wedge\mathcal{A}_L + \mathcal{F}_R\wedge\mathcal{F}_R + \frac{i}{2}(\mathcal{A}_R\wedge\mathcal{A}_R\wedge\mathcal{F}_R + \\ & \mathcal{A}_R\wedge\mathcal{F}_R\wedge\mathcal{A}_R + \mathcal{F}_R\wedge\mathcal{A}_R\wedge\mathcal{A}_R) - \frac{1}{2}\mathcal{A}_R\wedge\mathcal{A}_R\wedge\mathcal{A}_R\wedge\mathcal{A}_R\Big\}\end{aligned} \tag{5.4.16}$$

In the case of the linearized action in the presence of the external EM field, (5.4.9), that we use here, Eq.(5.4.9), it is observed that there is no triangle anomaly under $U(1)_V$ and $SU(N_f)_V$, due to the addition of the boundary terms which are given in (5.4.11). This is in agreement with treatment of anomalies in quantum field theory, where one may consider the one loop (due to fermion loops) effective action of the theory, which is a functional of external vector and axial vector fields, and add local counterterms in order to cancel the vector anomalies and be left with the axial vector anomaly. This form of the anomaly is called the Bardeen anomaly.

5.5 The Vector-Axial vector correlator

To calculate the vector-axial vector correlator in the presence of an external weak electromagnetic electric field we use the gauge, where $V_z^a = A_z^a = 0$ and the split of the relevant fields in momentum space is

$$\begin{aligned} V_\mu^a(q,z) &= P_\mu^{\perp\nu}(q) V_\nu^{a\,(0)}(q)\psi^V(q,z) \\ A_\mu^a(q,z) &= P_\mu^{\perp\nu}(q) A_\nu^{a\,(0)}(q)\psi^A(q,z) - P_\mu^{\parallel\,\nu}(q) A_{\nu\,(0)}^a(q)\phi(z) \end{aligned} \tag{5.5.1}$$

where the projection operators read $P_\mu^{\perp\nu}(q) = (\delta_\mu^\nu - \frac{q_\mu q^\nu}{q^2})$, $P_\mu^{\parallel\,\nu}(q) = \frac{q_\mu q^\nu}{q^2}$. The correlator is defined as

$$\langle T\{J_a^\mu(x) J_b^{\nu\,(5)}(y)\}\rangle_{\hat{F}} = \frac{\delta^2 S_{WZ}^{lin.}[A]}{\delta V_\mu^{a\,(0)}(x)\delta A_\nu^{b\,(0)}(y)} \tag{5.5.2}$$

In general, the correlator can be split to a transverse and a longitudinal part. So, to linear order in $\hat{F}$ it reads

$$\begin{aligned} \langle T\{J_\mu^a(q) J_\nu^{b\,(5)}(p)\}\rangle_{\hat{F}} = -\mathrm{Tr}(\mathcal{Q}\, t^a t^b)\frac{1}{4\pi^2}(2\pi)^4\delta^4(q+p)\Big\{ & w_T(q^2)(-q^2\tilde{F}_{\mu\nu} + q_\mu q^\sigma \tilde{F}_{\sigma\nu} - q_\nu q^\sigma \tilde{F}_{\sigma\mu}) \\ & + w_L(q^2) q_\nu q^\sigma \tilde{F}_{\sigma\mu}\Big\} \end{aligned} \tag{5.5.3}$$

where $\tilde{F}_{\mu\nu} = \frac{1}{2}\epsilon_{\mu\nu\rho\sigma}\hat{F}^{\rho\sigma}$. Substituting (5.5.1) in the action (5.4.9)

$$\begin{aligned} S_{WZ}^{lin.} = -\frac{\mathrm{Tr}(\mathcal{Q}\, t^a t^b)}{2}\frac{N_c}{4\pi^2}\int\frac{d^4q}{(2\pi)^4}\int dz\, e^{-\frac{1}{2}\mu^2\tau(z)^2}\epsilon^{\mu\nu z\rho\sigma}\hat{F}_{\mu\nu} \\ P_\sigma^{\perp\,\kappa}(q) P_\rho^{\perp\,\lambda}(-q) V_\kappa^{a\,(0)}(q) A_\lambda^{b\,(0)}(-q)\psi^V(q,z)'\psi^A(-q,z) \end{aligned} \tag{5.5.4}$$

where prime denotes the derivative with respect to z. By differentiating with respect to the sources twice we find

$$w_T(q^2) = -\frac{2N_c}{q^2}\int_0^{z_\Lambda} dz\, e^{-\frac{1}{2}\mu^2\tau(z)^2}\psi^V(q,z)'\psi^A(-q,z) \tag{5.5.5}$$

where $\psi^V(q,z)$, $\psi^A(-q,z)$ are the solutions of bulk equations of motion of the vector and axial vector gauge fields, Eqs.(4.6) and (4.9) of [14]. We calculate the correlator by using the numerical solutions of the vector and axial vector equations of motion. In region of low momenta, the result for $w_T(q^2)$ approximately matches the relation

$$w_T(q) = \frac{N_c}{q^2} - \frac{N_c}{f_\pi^2}\left[\Pi_A(q) - \Pi_V(q)\right] \tag{5.5.6}$$

which was proposed in [6], as it is explained below.

On the left side of Fig.(5.1), the quantities $1 - \frac{q^2}{N_c}w_T$, $\frac{q^2}{f_\pi^2}\left[\Pi_A(q) - \Pi_V(q)\right]$ and their ratio are plotted in terms of q for low momentum. We observe that the ratio of the two quantities is very close to one, so they coincide for small values of momentum, namely $q \lesssim 2\Lambda_{QCD}$. Hence Eq.(5.5.6) is satisfied in the low momentum limit. The dependence of w_T on momentum in this limit matches the chiral perturbation theory analysis, [5],

$$1 - \frac{q^2}{N_c}w_T^{(QCD)}(q^2) \sim 1 - \frac{q^2}{N_c}128\pi^2 C_{22}^W + \mathcal{O}(q^4) \quad , \quad q^2 \to 0 \tag{5.5.7}$$

where C_{22}^W is a coupling constant of the parity odd sector of the low energy chiral Lagrangian, [30]. However, there is no independent calculation of the value of C_{22}^W in order to verify Eq.(5.5.6) from the QCD viewpoint, [8]. On the right side of figure 5.1, we observe that as $q \gtrsim 2\Lambda_{QCD}$, the two quantities start differing substantially.

In Fig.(5.2), we plot the transverse part of the correlator, $1 - \frac{q^2}{N_c}w_T(q)$ for different values of the bare quark mass. The slopes of the curves in Fig.(5.2) for low momenta lead to the value of C_{22}^W for different quark masses

$$\begin{aligned} C_{22}^W &= 6.71\ 10^{-3} GeV^{-2} \quad \text{for} \quad \frac{m_q}{\Lambda_{QCD}} = 0 \\ C_{22}^W &= 6.21\ 10^{-3} GeV^{-2} \quad \text{for} \quad \frac{m_q}{\Lambda_{QCD}} = 0.0092 \\ C_{22}^W &= 4.45\ 10^{-3} GeV^{-2} \quad \text{for} \quad \frac{m_q}{\Lambda_{QCD}} = 0.31 \end{aligned} \tag{5.5.8}$$

where C_{22}^W was defined in (5.5.7) and captures the low momentum asymptotics of the correlator. We have used $\Lambda_{QCD} = 549\ MeV$, as found by the fit to meson spectra

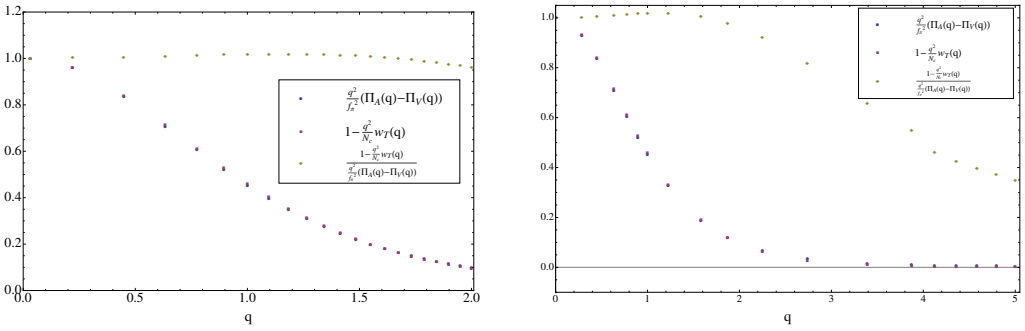

Figure 5.1: The numerical result of $1-\frac{q^2}{N_c}w_T$, the difference of the vector and axial vector two-point functions $\left(\frac{q^2}{f_\pi^2}\left[\Pi_A(q)-\Pi_V(q)\right]\right)$ that appear in Eq.(5.5.6), and their ratio are plotted a a function of q, which is measured in units of z_Λ^{-1} which is essentially Λ_{QCD}, defined in [13]. On the left, there is a zoom of the plot for small q and on the right the whole plot is depicted until large values of q.

in [14]. The mass $\frac{m_q}{\Lambda_{QCD}}=0.0092$ corresponds to $\frac{m_u+m_d}{2}$ as fit in [14]. The mass $\frac{m_q}{\Lambda_{QCD}}=0.31$ corresponds to the mass of the strange quark again from the same fit.

The transverse part of the vector-axial vector correlator times q^2/N_c, for large momentum, is plotted in Fig.(5.3). We have not been able to derive analytically the large q asymptotics of this correlator. We have therefore calculated it numerically and fitted a power law at sufficiently large q. As seen in Fig.(5.3), the subleading UV behavior of $\frac{q^2}{N_c}w_T(q)$ is $1/q^6$, instead of the $1/q^4$ expected from QCD. This is not unexpected, and suggests that in the UV of the model we are using there are lighter stringy states (before the antisymmetric tensor) that contribute to the correlator and dominate its UV asymptotics.

We observe that the subleading behavior of the correlator is subleading to the expected QCD result. In [2], [3] the nonperturbative effect to the correlator was found by using operator product expansion as it is mentioned in the introduction. It was shown that for large momentum, the subleading part of w_T^{QCD} is expected to be $\sim 1/q^6$, hence $\frac{q^2}{N_c}w_T^{QCD}\sim 1/q^4$. By finding the best fit to our numerical data we find that the subleading term of $\frac{q^2}{N_c}w_T$ is $\sim 1/q^{5.9974}$. This disagreement with QCD for large q is suggesting that for the simplistic glue theory we are using , the fermionic operator in question does not appear in the appropriate OPE of the currents.

As it is shown in the next section the difference of the vector two point function from the axial one for large momentum is found to be similar to the QCD result which is $1/q^6$, hence $\frac{q^2}{N_c}(\Pi_A(q^2)-\Pi_V(q^2)\sim 1/q^4$. Therfore, Eq.(5.5.6) is violated for large momentum since our result for the vector-axial vector correlator gives $1-\frac{q^2}{N_c}w_T\sim 1/q^{5.9974}$. A

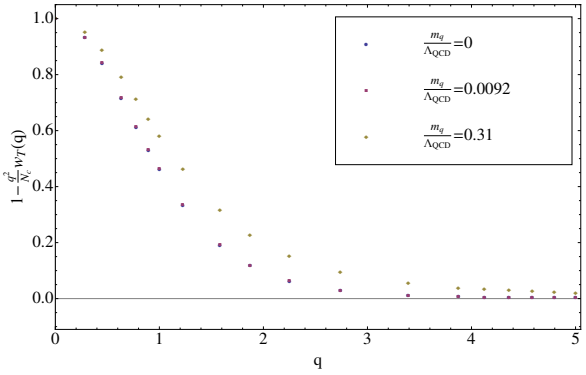

Figure 5.2: The transverse part of the vector-axial vector correlator is plotted in terms of q for different bare quark masses. We used the values for the quark mass which were found by matching to the meson spectrum in [13] and [14].

discussion of Eq.(5.5.6) in the context of QCD exists in [8]. The above outcome is similar to the result of the hard wall AdS/QCD model which is analyzed in Appendix B of [6].

5.6 Vector and Axial current-current correlators

We present here the vector and axial current-current correlators for large Euclidean momentum, following [16]. Those have already been calculated analytically in the abelian case of our model in [14] and found to contain a subleading power of $1/q^4$, (for more details see Eqs.(4.18) and (F.11) of [14]) that is absent from QCD which predicts a $1/q^6$ subleading behavior. However it turns that the analytical approximations made were unreliable. Here we will calculate the difference numerically and show agreement with QCD.

The two-point functions are defined as

$$\int d^4x d^4y e^{iqx+ipy}\langle T\{J^a_{(V/A)\,\mu}(x)J^b_{(V/A)\,\nu}(y)\}\rangle = \delta^{ab}(q^2\eta_{\mu\nu}-q_\mu q_\nu)\Pi_{V/A}(q^2)(2\pi)^4\delta^{(4)}(p+q) \tag{5.6.1}$$

We now calculate $\Pi_A(q^2)-\Pi_V(q^2)$ numerically using the full equations of motion without any approximation. The result for low momentum is shown in Fig.5.1. The above difference is plotted in terms of q, Fig.(5.4), for large Euclidean momentum and we find that the function that fits the data is $\frac{0.653}{q^{6.00933}}$. The difference of the axial

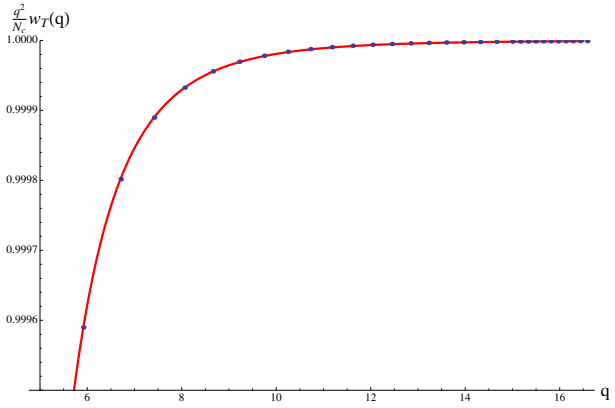

Figure 5.3: The numerical plot and the fit of the transverse part of the vector-axial vector correlator times q^2/N_c in terms q, for large Euclidean momentum. The function that fits the numerical data is $1 - \frac{18.75}{q^{5.9974}}$. As usual q is given in units of Λ_{QCD} as defined in [13].

vector and vector two point functions was calculated in QCD, using operator product expansion method, [31]. In the chiral limit the QCD result reads

$$\Pi_A(q^2) - \Pi_V(q^2) \sim \frac{2\pi\alpha_s}{q^6}\langle(\bar{\psi}_L\gamma_\mu t^a\psi_L)(\bar{\psi}_R\gamma_\mu t^a\psi_R))\rangle \tag{5.6.2}$$

whose leading power agrees with the numerical result of our calculation at large momenta.

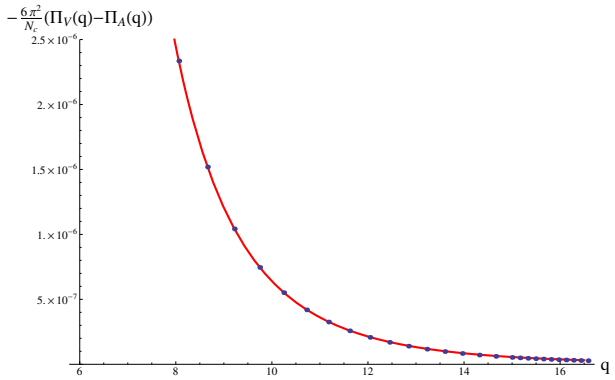

Figure 5.4: The numerical plot and the fit of the difference of the vector and axial vector 2 point functions. The fit reads $\frac{0.653}{q^{6.00933}}$. As usual q is given in units of Λ_{QCD} as defined in [13].

5.7 Conclusions

In the present work, we have shown that the relation (5.5.6) which was proposed by Son and Yamamoto relating the vector-axial vector flavor current correlator in weak electric field to the difference of the vector and axial vector two point functions is valid only for low Euclidean momenta in the context of an AdS/QCD model with non-trivial dynamics for the chiral condensate.

For large momenta, this relation is no longer valid in our model. Moreover, the dependence of the w_T correlator on q^2 for large q^2 is subleading to that expected from QCD.

We also notice that the difference of the vector and axial vector flavor current two-point functions in our model falls off as q^{-6} for large q^2 as it is expected from the operator product expansion in QCD.

This computation could be sharpened by using a more realistic theory for the glue sector, like the Improved holographic QCD model, [10]. This investigation in underway.

5.8 Acknowledgements

We would like to thank A. Paredes for discussions.

This work was partially supported by European Union grants FP7-REGPOT-2008-1-CreteHEPCosmo-228644 and PERG07-GA-2010-268246. I. Iatrakis work was supported by the project "HERakLEITOS II - University of Crete" of the Operational Programme for Education and Lifelong Learning 2007 - 2013 (E.P.E.D.V.M.) of the NSRF (2007 - 2013), which is co-funded by the European Union (European Social Fund) and National Resources.

Note added

After this paper was in its last stages, [42] appeared that studied the same correlator in the soft wall model.

Bibliography

[1] S. L. Adler and W. A. Bardeen, *"Absence of higher order corrections in the anomalous axial vector divergence equation,"* Phys. Rev. **182**, 1517 (1969). 147

[2] M. Knecht, S. Peris, M. Perrottet and E. De Rafael, *"Electroweak hadronic contributions to the muon (g-2),"* JHEP **0211** (2002) 003 [ArXiv:hep-ph/0205102]. 147, 162

[3] A. Czarnecki, W. J. Marciano and A. Vainshtein, *"Refinements in electroweak contributions to the muon anomalous magnetic moment,"* Phys. Rev. D **67**, 073006 (2003) [Erratum-ibid. D **73**, 119901 (2006)] [ArXiv:hep-ph/0212229]. 147, 162

[4] A. Vainshtein, *"Perturbative and nonperturbative renormalization of anomalous quark triangles,"* Phys. Lett. B **569**, 187 (2003) [ArXiv:hep-ph/0212231]. 147

[5] M. Knecht, S. Peris, M. Perrottet and E. de Rafael, *"New nonrenormalization theorems for anomalous three point functions,"* JHEP **0403**, 035 (2004) [ArXiv:hep-ph/0311100]. 147, 161

[6] D. T. Son and N. Yamamoto, *"Holography and Anomaly Matching for Resonances,"* [ArXiv:1010.0718][hep-ph]. 148, 149, 151, 161, 163

[7] D. T. Son and M. A. Stephanov, *"QCD and dimensional deconstruction,"* Phys. Rev. D **69** (2004) 065020 [ArXiv:hep-ph]0304182. 148, 149

[8] M. Knecht, S. Peris and E. de Rafael, *"On Anomaly Matching and Holography,"* [ArXiv:1101.0706][hep-ph]. 149, 161, 163

[9] T. Sakai, S. Sugimoto, *"Low energy hadron physics in holographic QCD,"* Prog. Theor. Phys. **113** (2005) 843-882. [ArXiv:hep-th/0412141]. 148, 149, 150, 152

[10] U. Gursoy and E. Kiritsis, *"Exploring improved holographic theories for QCD: Part I,"* JHEP **0802** (2008) 032 [ArXiv:0707.1324][hep-th];
U. Gursoy, E. Kiritsis and F. Nitti, *"Exploring improved holographic theories for*

QCD: Part II," JHEP **0802** (2008) 019 [ArXiv:0707.1349][hep-th];
E. Kiritsis, *"Dissecting the string theory dual of QCD,"* Fortsch. Phys. **57** (2009) 396 [ArXiv:0901.1772][hep-th];
U. Gursoy, E. Kiritsis, L. Mazzanti, G. Michalogiorgakis and F. Nitti, *"Improved Holographic QCD,"* Lect. Notes Phys. **828** (2011) 79 [ArXiv:1006.5461][hep-th]. 150, 152, 153, 155, 165

[11] A. Sen, *"Tachyon dynamics in open string theory,"* Int. J. Mod. Phys. A **20** (2005) 5513 [ArXiv:hep-th/0410103]. 150, 152

[12] R. Casero, E. Kiritsis and A. Paredes, *"Chiral symmetry breaking as open string tachyon condensation,"* [ArXiv:hep-th/0702155]. 150, 152, 153, 154, 156, 157, 159

[13] I. Iatrakis, E. Kiritsis and A. Paredes *"An AdS/QCD model from Sen's tachyon action,"* [ArXiv:1003.2377][hep-ph]. 150, 151, 152, 154, 155, 162, 163, 164

[14] I. Iatrakis, E. Kiritsis and A. Paredes *"An AdS/QCD model from tachyon condensation: II,"* JHEP **1011**, 123 (2010) [ArXiv:1010.1364][hep-ph]. 150, 151, 152, 153, 154, 156, 161, 162, 163

[15] O. Aharony and D. Kutasov, *"Holographic Duals of Long Open Strings,"* Phys. Rev. D **78** (2008) 026005 [ArXiv:0803.3547][hep-th]. 152

[16] J. Erlich, E. Katz, D. T. Son and M. A. Stephanov, *"QCD and a holographic model of hadrons,"* Phys. Rev. Lett. **95** (2005) 261602 [ArXiv:hep-ph/0501128];
L. Da Rold and A. Pomarol, *"Chiral symmetry breaking from five dimensional spaces,"* Nucl. Phys. B **721** (2005) 79 [ArXiv:hep-ph/0501218]. 149, 150, 154, 163

[17] A. Karch, E. Katz, D. T. Son and M. A. Stephanov, *"Linear confinement and AdS/QCD,"* Phys. Rev. D **74** (2006) 015005 [ArXiv:hep-ph/0602229]. 150, 155

[18] L. Cappiello, O. Cata, G. D'Ambrosio, *"Antisymmetric tensors in holographic approaches to QCD,"* Phys. Rev. **D82** (2010) 095008. [ArXiv:1004.2497][hep-ph];
S. K. Domokos, J. A. Harvey and A. B. Royston, *"Completing the framework of AdS/QCD: h_1/b_1 Mesons and excited omega/rho's,"* JHEP **1105** (2011) 107 [ArXiv:1101.3315][hep-th];
R. Alvares, C. Hoyos and A. Karch, *"An improved model of vector Mesons in holographic QCD,"* [ArXiv:1108.1191][hep-ph]. 150

[19] T. Imoto, T. Sakai, S. Sugimoto, *"Mesons as Open Strings in a Holographic Dual of QCD,"* Prog. Theor. Phys. **124** (2010) 263-284. [ArXiv:1005.0655][hep-th]. 150

[20] S. Kuperstein and J. Sonnenschein, *"Non-critical supergravity (d > 1) and holography,"* JHEP **0407** (2004) 049 [ArXiv:hep-th/0403254];
153

[21] S. Kuperstein and J. Sonnenschein, *"Non-critical, near extremal AdS_6 background as a holographic laboratory of four dimensional YM theory,"* JHEP **0411** (2004) 026 [ArXiv:hep-th/0411009]. 153, 155

[22] E. Witten, *"Anti-de Sitter space and holography,"* Adv. Theor. Math. Phys. **2** (1998) 253 [ArXiv:hep-th/9802150]. 153

[23] D. Z. Freedman, S. D. Mathur, A. Matusis and L. Rastelli, *"Correlation functions in the CFT(d) / AdS(d+1) correspondence,"* Nucl. Phys. B **546** (1999) 96 [ArXiv:hep-th/9804058]. 153

[24] A. Sen, *"Dirac-Born-Infeld action on the tachyon kink and vortex,"* Phys. Rev. D **68**, 066008 (2003) [ArXiv:hep-th/0303057]. 153

[25] A. A. Tseytlin, *"On nonAbelian generalization of Born-Infeld action in string theory,"* Nucl. Phys. B **501** (1997) 41 [ArXiv:hep-th/9701125].

[26] M. Kruczenski, D. Mateos, R. C. Myers and D. J. Winters, *"Towards a holographic dual of large-N(c) QCD,"* JHEP **0405**, 041 (2004) [ArXiv:hep-th/0311270]. 154

[27] T. Takayanagi, S. Terashima and T. Uesugi, *"Brane-antibrane action from boundary string field theory,"* JHEP **0103**, 019 (2001) [ArXiv:hep-th/0012210]. 151, 156

[28] C. Kennedy and A. Wilkins, *"Ramond-Ramond couplings on brane-antibrane systems,"* Phys. Lett. B **464**, 206 (1999) [ArXiv:hep-th/9905195]. 156

[29] P. Kraus and F. Larsen, *"Boundary string field theory of the DD-bar system,"* Phys. Rev. D **63**, 106004 (2001) [ArXiv:hep-th/0012198]. 156

[30] J. Bijnens, L. Girlanda and P. Talavera, *"The Anomalous chiral Lagrangian of order p**6,"* Eur. Phys. J. C **23** (2002) 539 [ArXiv:hep-ph/0110400]. 161

[31] M. A. Shifman, A. I. Vainshtein and V. I. Zakharov, *"QCD and Resonance Physics: Applications,"* Nucl. Phys. B **147** (1979) 448. 164

[32] J. Sonnenschein, *"What does the string / gauge correspondence teach us about Wilson loops?,"* [ArXiv:hep-th/0003032]. 155

[33] I. R. Klebanov and J. M. Maldacena, *"Superconformal gauge theories and non-critical superstrings,"* Int. J. Mod. Phys. A **19** (2004) 5003 [ArXiv:hep-th/0409133].

[34] F. Bigazzi, R. Casero, A. L. Cotrone, E. Kiritsis and A. Paredes, *"Non-critical holography and four-dimensional CFT's with fundamentals,"* JHEP **0510**, 012 (2005) [ArXiv:hep-th/0505140].

[35] T. Gherghetta, J. I. Kapusta and T. M. Kelley, *"Chiral symmetry breaking in the soft-wall AdS/QCD model,"* Phys. Rev. D **79**, 076003 (2009) [ArXiv:0902.1998][hep-ph]; Y. Q. Sui, Y. L. Wu, Z. F. Xie and Y. B. Yang, *"Prediction for the mass Spectra of Resonance Mesons in the Soft-Wall AdS/QCD with a Modified 5D Metric,"* Phys. Rev. D **81**, 014024 (2010) [ArXiv:0909.3887][hep-ph]. 155

[36] J. P. Shock and F. Wu, *"Three flavour QCD from the holographic principle,"* JHEP **0608**, 023 (2006) [ArXiv:hep-ph/0603142]. 155

[37] A. L. Cotrone, A. Dymarsky and S. Kuperstein, *"On vector meson masses in a holographic SQCD"* [ArXiv:1010.1017][hep-ph]. 155

[38] U. Gursoy, E. Kiritsis, L. Mazzanti and F. Nitti, *"Deconfinement and Gluon Plasma Dynamics in Improved Holographic QCD,"* Phys. Rev. Lett. **101**, 181601 (2008) [ArXiv:0804.0899][hep-th];
U. Gursoy, E. Kiritsis, L. Mazzanti and F. Nitti, *"Holography and Thermodynamics of 5D Dilaton-gravity,"* JHEP **0905** (2009) 033 [ArXiv:0812.0792][hep-th]. 155

[39] D. Kutasov, M. Marino and G. W. Moore, *"Some exact results on tachyon condensation in string field theory,"* JHEP **0010** (2000) 045. [ArXiv:hep-th/0009148] 156

[40] M. Alishahiha, H. Ita and Y. Oz, *"On superconnections and the tachyon effective action,"* Phys. Lett. B **503** (2001) 181 [ArXiv:hep-th/0012222]. 151, 156

[41] M. jarvinen and E. Kiritsis, *"Holographic Models for QCD in the Veneziano Limit,"* [ArXiv:1112.1261][hep-ph]. 153

[42] P. Colangelo, F. De Fazio, F. Giannuzzi, S. Nicotri and J. J. Sanz-Cillero, *"Anomalous AV^*V vertex function in the soft-wall holographic model of QCD,"* [ArXiv:1108.5945][hep-ph]. 165

6

V-QCD: Spectra, the dilaton and the S-parameter

Authors : Daniel Areán[a], Ioannis Iatrakis[c], Matti Järvinen[c] and Elias Kiritsis[b,c]

[a] International Centre for Theoretical Physics (ICTP) and INFN - Sezione di Trieste
Strada Costiera 11; I 34014 Trieste, Italy

[b] APC, Université Paris 7, Diderot,
CNRS/IN2P3, CEA/IRFU, Obs. de Paris, Sorbonne Paris Cité,
Bâtiment Condorcet, F-75205, Paris Cedex 13, France (UMR du CNRS 7164)

[c] Crete Center for Theoretical Physics, Department of Physics, University of Crete,
71003 Heraklion, Greece

6.1 Abstract

Zero temperature spectra of mesons and glueballs are analyzed in a class of holographic bottom-up models for QCD (named V-QCD), as a function of $x = \frac{N_f}{N_c}$ with the full back-reaction included. It is found that spectra are discrete and gapped (modulo the pions) in the QCD regime, for x below the critical value x_c where the conformal transition takes place. The masses uniformly converge to zero in the walking region $x \to x_c$ due

to Miransky scaling. The ratio of masses all asymptote to non-zero constants as $x \to x_c$ and therefore there is no “dilaton" in the spectrum. The S-parameter is computed and found to be of $\mathcal{O}(1)$ in the walking regime.

6.2 Introduction

The dynamics of “walking" (or nearly conformal) quantum field theories, have been the subject of intensive study, since they have been argued to be an important ingredient, [1; 2; 3] in providing viable non-perturbative mechanisms for electroweak symmetry breaking like technicolor, [4]. This regime is expected to appear in standard QCD with N_c colors and N_f flavors, just below the boundary of the conformal window, $N_f \simeq 4N_c$, as well as in other quantum field theories, [5].

The transition between the conformal window and QCD-like IR behavior, has been called a conformal transition [6]. The “walking" regime has been conjectured to display Miransky scaling, [7]. It was recently suggested that in holographic theories this conformal transition is associated with a violation of the BF bound in the dual bulk theory, [8]. Moreover, in QCD, this correlates with fermion bilinear operators reaching a scaling dimension equal to 2, another prerequisite of viable extended technicolor.

Apart from Miransky scaling several other phenomena have been associated with the “walking regime" of QFT:

(a) The appearance of a light scalar state, the “dilaton", due to the almost unbroken scale invariance, [2].

(b) The strong suppression of the S-parameter, a crucial ingredient for the experimental viability of technicolor theories, [9].

Both issues are controversial, especially as “walking regimes" appear at strong coupling, and perturbative techniques do not apply.

In recently studied holographic models with walking behavior, the lightest state is often a scalar, [10], [11]. Whether this state can be identified as the dilaton is, however, a difficult question and appears to depend on the model. The S-parameter has been studied in popular holographic bottom-up [12] as well as brane-antibrane models [13] with a variety of answers found. Recently, it was argued that in a class of holographic models the S-parameter is substantial and definitely bounded below, [14].

What we plan to do in this letter is to report on these and related issues in a class of holographic theories that have been proposed recently, under the name of V-QCD, [15] which has physics that is very close to QCD in the Veneziano limit.

6.3 V-QCD

The class of models in question combine two sectors whose dynamics are inspired by string holographic models. The first is improved holographic QCD (IHQCD), which is a holographic model for large-N Yang Mills in 4 dimensions, [16]. The second is a model for flavor inspired by tachyon condensation in string theory, [17]. The relevant fields in the gravity description that are kept in these models (in order to describe the vacuum structure) are as follows: apart for the five-dimensional metric, there is a scalar, (the dilaton, ϕ) that is dual to the YM 't Hooft coupling constant, and a complex $N_f \times N_f$ matrix field, (the tachyon, T_{ij}) transforming in the $(N_f, \bar{N}_f)$ of the $U(N_f) \times U(N_f)$ flavor group. We will be working in the Veneziano limit, $N_c, N_f \to \infty$ with $\frac{N_f}{N_c} = x$ fixed, [18].

The complete action for V-QCD models can be written as

$$S = S_g + S_f + S_a \tag{6.3.1}$$

where S_g, S_f, and S_a are the actions for the glue, flavor and CP-odd sectors, respectively[1]. The glue action was introduced in [16; 21],

$$S_g = M^3 N_c^2 \int d^5x \, \sqrt{-g} \left(R - \frac{4}{3} \frac{(\partial\lambda)^2}{\lambda^2} + V_g(\lambda) \right) \, , \tag{6.3.2}$$

with $\lambda = e^{\phi}$. The dilaton potential V_g asymptotes to a constant near $\lambda = 0$, and diverges as $V_g \sim \lambda^{\frac{4}{3}} \sqrt{\log \lambda}$ as $\lambda \to \infty$, generating confinement, a mass gap, discrete spectrum and asymptotically linear glueball trajectories.

The flavor action is[2]

$$S_f = -\frac{1}{2} M^3 N_c \int d^4x \, dr \, \mathrm{Tr}\Big[V_f(\lambda, T^\dagger T) \sqrt{-\det \mathbf{A}_L} + V_f(\lambda, T T^\dagger) \sqrt{-\det \mathbf{A}_R} \Big] \, . \tag{6.3.3}$$

The quantities inside the square roots are defined as

$$\begin{aligned} \mathbf{A}_{(R)MN} &= g_{MN} + w(\lambda) F^{(R)}_{MN} + \frac{\kappa(\lambda)}{2} \Big((D_M T)(D_N T)^\dagger + (D_N T)(D_M T)^\dagger \Big) \\ \mathbf{A}_{(L)MN} &= g_{MN} + w(\lambda) F^{(L)}_{MN} + \frac{\kappa(\lambda)}{2} \Big((D_M T)^\dagger (D_N T) + (D_N T)^\dagger (D_M T) \Big) \end{aligned} \tag{6.3.4}$$

[1] We will not discuss S_a here. We will address its physics (that contains the $U(1)_A$ anomaly) in a future publication, [19].

[2] This is inspired by the Sen's action for tachyon condensation, [22]. The non-abelian action is not well understood, but its knowledge is not needed for this paper.

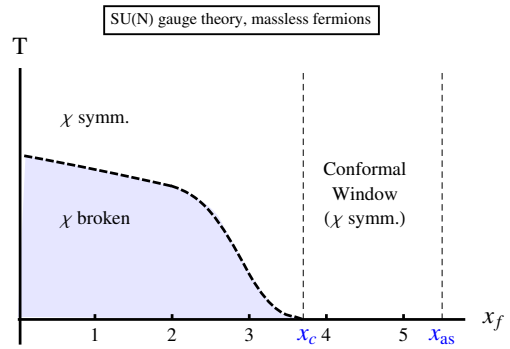

Figure 6.1: Qualitative behavior of the transition temperature between the low and high temperature phases of V-QCD matter, [23].

with $(i) = L, R$, and the fields $A_{(i)}$ as well as T are $N_f \times N_f$ matrices in the flavor space. The covariant derivative of the tachyon field is defined as

$$D_M T = \partial_M T + iTA_M^L - iA_M^R T \ . \tag{6.3.5}$$

The class of tachyon potentials that we will explore are

$$V_f(\lambda, T) = V_{f0}(\lambda) e^{-a(\lambda)\, TT^\dagger} \ . \tag{6.3.6}$$

For the vacuum solutions (with flavor independent quark mass) we set $T = \tau(r)\mathbf{1}_{N_f}$ where $\tau(r)$ is real, and the flavor gauge fields are trivial. $V_g(\lambda)$ has been fixed already from glue dynamics [21]. The other undetermined functions in the flavor action ($V_{f0}(\lambda)$, $\kappa(\lambda)$, $a(\lambda)$, $w(\lambda)$) must satisfy the following generic requirements:

(a) There should be two extrema in the potential for τ: an unstable maximum at $\tau = 0$ with chiral symmetry intact and a minimum at $\tau = \infty$ with chiral symmetry broken.

(b) The dilaton potential at $\tau = 0$, namely $V_{\rm eff}(\lambda) = V_g(\lambda) - xV_{f0}(\lambda)$, must have a non-trivial IR extremum at $\lambda = \lambda_*(x)$ that moves from $\lambda_* = 0$ at $x = \frac{11}{2}$ to large values as x is lowered.

In [15; 23], the flavor potential was parametrized as $V_f(\lambda, \tau) = V_{f0}(\lambda) \exp(-a(\lambda)\tau^2)$ in order to satisfy the first requirement, and several choices for the remaining functions were explored. The models were classified according to the IR behavior of the tachyon (I or II) and the constant W_0, that controls the flavor dependence of the UV AdS scale. We refer to [23] for a detailed exposition.

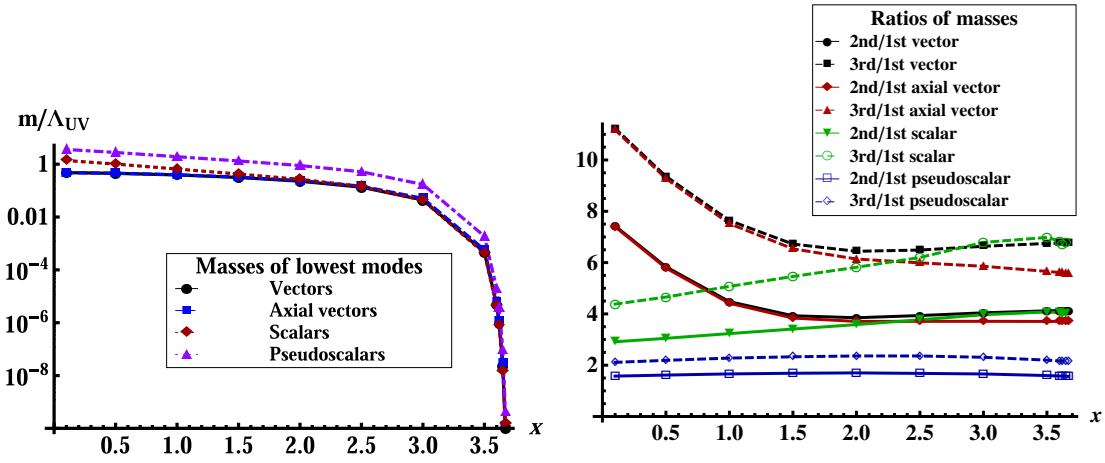

Figure 6.2: Non-singlet meson spectra in the potential II class with Stefan-Boltzmann (SB) normalization for W_0 (see [23]), with $x_c \simeq 3.7001$. Left: the lowest non-zero masses of all four towers of mesons, as a function of x, in units of $\Lambda_{\rm UV}$, below the conformal window. Right, the ratios of masses of up to the fourth massive states in the same theory as a function of x.

At zero temperature the phase diagram as a function of $0 < x < \frac{11}{2}$, is essentially universal. In the region $0 < x < x_c$, the (massless) theory has chiral symmetry breaking, and flows to a massless $SU(N_f)$ pion theory in the IR. For $x_c < x < \frac{11}{2}$ (the conformal window) the theory flows to a non-trivial IR fixed point and there is no chiral symmetry breaking. It was found that $x_c \simeq 4$, its precise value depends on the details of the potential. In the regime just below the conformal window, $x \simeq x_c$ the theory exhibits Miransky scaling, [7] where in particular for the chiral condensate $\sigma \sim \Lambda_{\rm UV}^3 \exp(-\frac{\kappa}{\sqrt{x_c - x}})$ with κ calculable from the flavor action, [15]. This regime is also known as the "walking" regime as the coupling flows to almost λ_*, stays there for many decades in the RG time, and then at the end the non-trivial tachyon drives the theory away from the non-trivial fixed point and towards $\lambda = \infty$.

At finite temperature a rich structure of hairy black holes was found, with one and two scalar hairs, [23]. The general structure of their phase diagram is depicted in figure 6.1. The chiral restoration transition is first order at low values of x but typically becomes second order as we approach x_c. In this region extra chirally broken phases can appear and several extra first-order transitions (up to two), depending on the detailed potentials. The transition temperatures also exhibit Miransky scaling, [23].

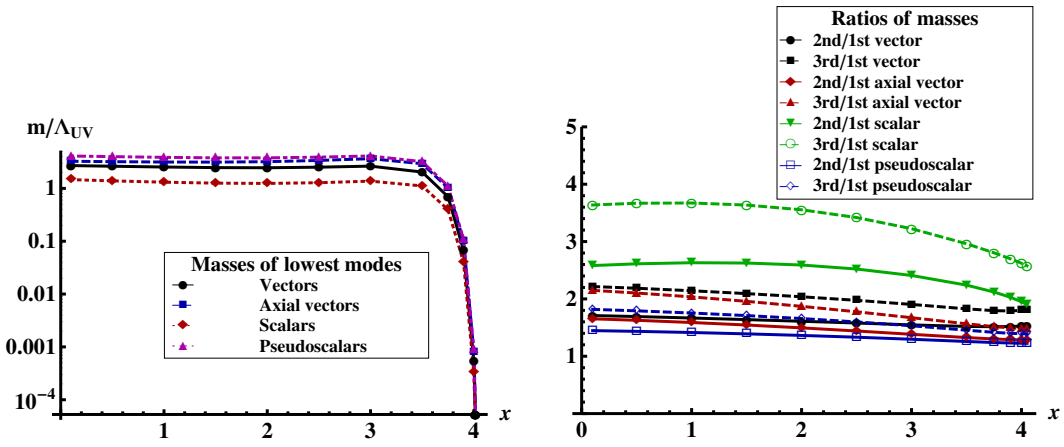

Figure 6.3: Non-singlet meson spectra in the potential I class ($W_0 = \frac{3}{11}$), with $x_c \simeq 4.0830$. Left: the lowest non-zero masses of all four towers of mesons, as a function of x, in units of $\Lambda_{\rm UV}$, below the conformal window. Right, the ratios of masses of up to the fourth massive states in the same theory as a function of x.

6.4 Quadratic fluctuations and spectra

The purpose of this letter is to study further interesting aspects of the physics of V-QCD models and address several interesting questions that are now accessible to calculation. In this paper we consider the theory with massless quarks.

The strategy is to consider small (quadratic) fluctuations of all the fields in V-QCD ($g_{\mu\nu}, \phi, T, A_\mu^{L,R}$) around the vacuum (zero temperature) solutions of [15], involving a Poincaré invariant metric, no vectors and radially depended scalars,

$$ds^2 = e^{2A(r)}(dx_{1,3}^2 + dr^2) \quad , \quad \phi(r) \quad , \quad T = \tau(r)\ \mathbf{1}_{N_f}\ . \tag{6.4.1}$$

There are several fluctuations that we will classify into two distinct classes: singlet fluctuations under the flavor group, and non-singlet fluctuations.

- The non-singlet fluctuations include the L and R vector meson fluctuations, packaged into an axial and vector basis, V_μ, A_μ, the pseudoscalar mesons (including the massless pions), and the scalar mesons. Their second order equations are relatively simple, and we present those of the vectors below. We work in axial gauge $V_r = 0$ and write the factorized Ansatz $V_\mu(x^\mu, r) = \psi^V(r)\,\mathcal{V}_\mu(x^\mu)$. The radial wave functions satisfy

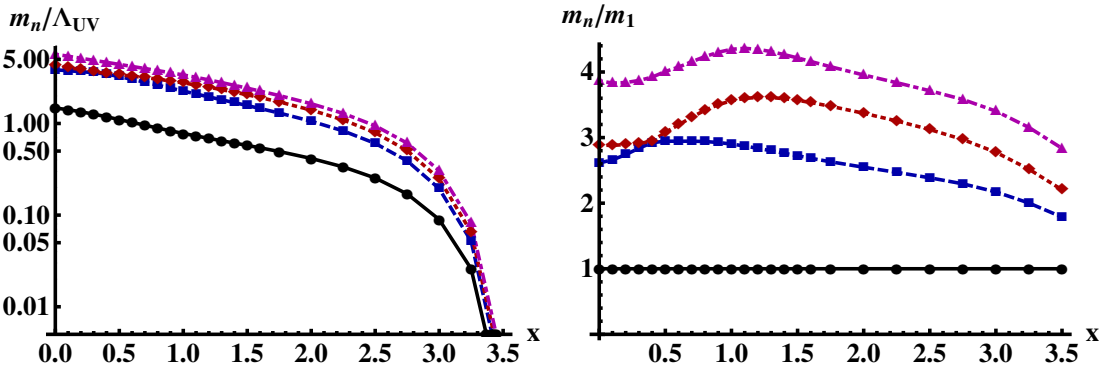

Figure 6.4: Singlet scalar meson spectra in the potential II class with SB normalization for W_0. They contain the 0^{++} glueballs and the singlet 0^{++} mesons that mix here at leading order. Left: the four lowest masses as a function of x in units of $\Lambda_{\rm UV}$. Right: the ratios of masses of up to the fourth massive states as a function of x.

$$\frac{\partial_r\left(V_f(\lambda,\tau)w(\lambda)^2e^A G^{-1}\,\partial_r\psi^V\right)}{V_f(\lambda,\tau)w(\lambda)^2e^A G}+m_V^2\psi^V=0\quad,\quad G\equiv\sqrt{1+e^{-2A}\kappa(\lambda)(\partial_r\tau)^2} \tag{6.4.2}$$

For the axial vectors we define transverse and longitudinal parts as $A_\mu(x^\mu,r)=A_\mu^\perp(x^\mu,r)+A_\mu^\parallel(x^\mu,r)$ with $A_\mu^\perp(x^\mu,r)=\psi^A(r)\,\mathcal{A}_\mu(x^\mu)$ and $\partial^\mu\mathcal{A}_\mu=0$. The radial wave function satisfies

$$\frac{\partial_r\left(V_f(\lambda,\tau)w(\lambda)^2e^A G^{-1}\,\partial_r\psi^A\right)}{V_f(\lambda,\tau)w(\lambda)^2e^A G}-\frac{4\tau^2e^{2A}\kappa(\lambda)}{w(\lambda)^2}\psi^A+m_A^2\psi^A=0\ . \tag{6.4.3}$$

The non-singlet scalar and pseudoscalar fluctuation equations are more complicated and we will present them in [19]. A few general properties are as follows:

1. In the conformal window all spectra are continuous.
2. Below the conformal window, $x<x_c$, the spectra are discrete and gapped. The only exception are the $SU(N_f)$ pseudoscalar pions that are massless, due to chiral symmetry breaking.
3. All masses in the Miransky scaling region (aka "walking region") are obeying Miransky scaling $m_n\sim\Lambda_{\rm UV}\exp(-\frac{\kappa}{\sqrt{x_c-x}})$. This is explicitly seen in the case of the ρ mass in figure 6.5, left.
4. All non-singlet mass ratios asymptote to non-zero constants as $x\to x_c$.

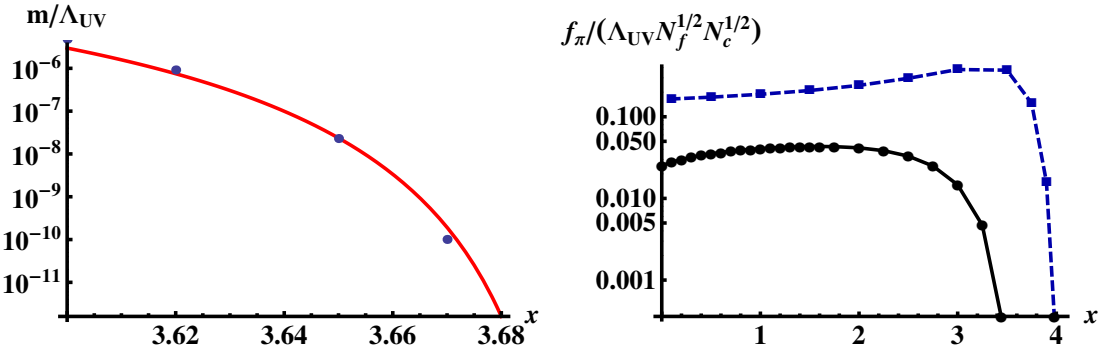

Figure 6.5: Potential II with SB normalization for W_0. Left: A fit of the ρ mass to the Miransky scaling factor, showing that it displays Miransky scaling in the walking region. Right, f_π as a function of x in units of $\Lambda_{\rm UV}$. The blue dashed curve corresponds to potential I and the black to potential II. In both cases, it vanishes near x_c following again Miransky scaling.

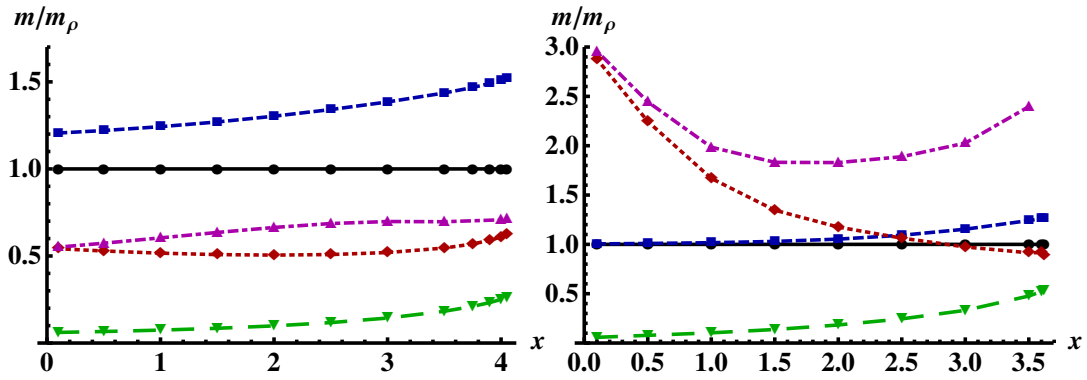

Figure 6.6: The masses of the lightest states of various towers, and $f_\pi/\sqrt{N_f N_c}$ as a function of x in units of the ρ mass. Left: potentials I with $W_0 = 3/11$. Right: potentials II with SB normalization for W_0. Solid black, dashed blue, dotted red, and dotdashed magenta curves show the masses of the lightest vector, axial, flavor nonsinglet scalar, and flavor singlet scalar states, respectively, while the long-dashed green curve is $f_\pi/\sqrt{N_f N_c}$.

In figures 6.2 and 6.3 we present the results for the non-singlet meson spectra (note that the plots on the left of those figures are in logarithmic scale). The lowest masses of the mesons vary little with x until we reach the walking region. There, Miransky scaling takes over and the lowest masses dip down exponentially fast. The $\Lambda_{\rm UV}$ scale is extracted as usual from the logarithmic running of λ in the UV.

- The singlet fluctuations, that include the 2^{++} glueballs, the 0^{++} glueballs and scalar mesons that mix to leading order in $1/N$ in the Veneziano limit, and the 0^{-+} glueballs and the η' pseudoscalar tower. Although the spin-two fluctuation equations are always simple, summarized by the appropriate Laplacian, the scalar and pseudoscalar equations are involved and we refrain from presenting them here. They will appear in a future publication, [19].

  A few general properties of the singlet spectra are as follows: Both items 1 and 3 above remain as such (see figure 6.4 for 0^{++} scalars). In addition we find that

  - Below the conformal window, $x < x_c$, the singlet spectra are discrete and gapped. The $U(1)_A$ anomaly appears at leading order and the mixture of the 0^{-+} glueball and the η' has a mass of $\mathcal{O}(1)$.
  - In the scalar sector, for small x, where the mixing between glueballs and mesons is small, the lightest state is a meson, the next lightest state is a glueball, the next a meson and so on. However, with increasing x, non-trivial mixing sets in and level-crossing seems to be generic. This can be seen in figure 6.3, right.
  - All singlet mass ratios asymptote to constants as $x \to x_c$ (see figure 6.4, right). The same holds for mass ratios between the flavor singlet and nonsinglet sectors, as confirmed numerically in figure 6.6. There seems to be no unusually light state (termed the "dilaton") that reflects the nearly unbroken scale invariance in the walking region. The reason is a posteriori simple: the nearly unbroken scale invariance is reflected in the *whole* spectrum of bound states scaling exponentially to zero due to Miransky scaling.

The asymptotics of the spectra at high masses is in general a power-law with logarithmic corrections, with the powers depending on the potentials. The trajectories are approximately linear ($m_n^2 \sim cn$) for type I potentials and quadratic ($m_n^2 \sim cn^2$) for type II potentials. There is the possibility, first seen in [17] that the proportionality coefficient c in the linear case is different between axial and vector mesons[1]. These possibilities do not affect substantially the issues of the dilaton and the S-parameter.

Finally, let us comment on the possibility of using as background the non-trivial saddle points, found in [15], where the tachyon solution has at least one zero (analogous to the Efimov minima). We have verified explicitly that such saddle points are unstable

[1] A careful analysis of the effects of different potentials on the asymptotics of the spectra will be presented in [19].

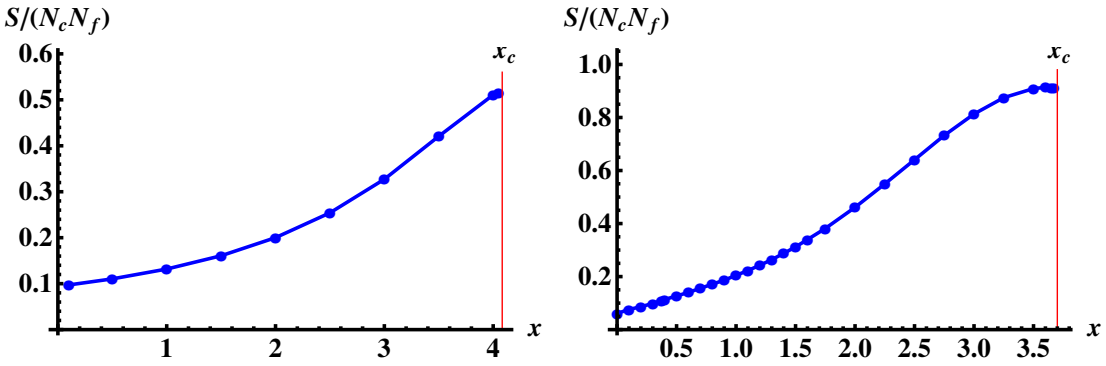

Figure 6.7: Left: The S-parameter as a function of x for potential class I with $W_0 = \frac{3}{11}$. Right: The S-parameter as a function of x for potential class II with SB normalization for W_0. In both cases S asymptotes to a finite value as $x \to x_c$.

(also pointed out in [11]), as the scalar meson equation has a single mode with a negative mass squared, both in the singlet and non-singlet channels. This mass is small for small x, but becomes large as $x \to x_c$. Therefore the Efimov minima are strongly unstable in the walking regime.

6.5 Two-point functions and the S-parameter

We have computed the two-point functions of several operators including the axial and vector currents as well as the scalar mass operator. We will focus here on the two-point function of the vector and axial currents which can be written in momentum space as

$$\langle V^a_\mu(q) V^b_\nu(p)\rangle = \Pi^{ab}_{\mu\nu,V,A}(q,p) = -(2\pi)^4\delta^4(p+q)\,\delta^{ab}\left(q^2\eta_{\mu\nu} - q_\mu q_\nu\right)\Pi_V(q)\ . \quad (6.5.1)$$

and similarly for the axial vector. We have $V_\mu(x) = \int \frac{d^4q}{(2\pi)^4} e^{iqx} V^a_\mu(q) t^a\,\psi_V(r)$, where t^a, $a = 1,\ldots,N_f^2-1$ are the flavor group generators.

Using the expansions

$$\Pi_A = \frac{f_\pi^2}{q^2} + \sum_n \frac{f_n^2}{q^2+m_n^2-i\epsilon} \quad , \quad \Pi_V = \sum_n \frac{F_n^2}{q^2+M_n^2-i\epsilon} \quad (6.5.2)$$

we determine f_π as

$$f_\pi^2 = -\frac{N_c N_f}{12\pi^2}\left.\frac{\partial_r \psi^A}{r}\right|_{r=0,\,q=0} \quad (6.5.3)$$

where the normalization was fixed by matching the UV limit of the two point functions to QCD and we chose $\psi^A(r=0)=1$.

A typical example is plotted in figure 6.5, right. The pion scale changes smoothly for most x, but is affected directly by Miransky scaling which makes it vanish exponentially in the walking regime.

The S-parameter is

$$S = 4\pi \frac{d}{dq^2}\left[q^2(\Pi_V - \Pi_A)\right]_{q=0} = -\frac{N_c N_f}{3\pi}\frac{d}{dq^2}\left(\frac{\partial_r \psi^V(r)}{r} - \frac{\partial_r \psi^A(r)}{r}\right)\Bigg|_{r=0,\, q=0} \tag{6.5.4}$$

$$= 4\pi \sum_n \left(\frac{F_n^2}{M_n^2} - \frac{f_n^2}{m_n^2}\right) \ .$$

As both masses and decay constants in (6.5.2,6.5.4) are affected similarly by Miransky scaling, the S-parameter is insensitive to it. Therefore its value cannot be predicted by Miransky scaling alone. Our results show that generically the S-parameter (in units of $N_f N_c$) remains finite in the QCD regime, $0 < x < x_c$ and asymptotes to a finite constant at x_c (see figure 6.7). The S-parameter is identically zero inside the conformal window (massless quarks) because of unbroken chiral symmetry. This suggests a subtle discontinuity of correlators across the conformal transition.

This behavior of S is in qualitative agreement with recent estimates based on analysis of the BZ limit in field theory [24]. We have also found choices of potentials where the S-parameter becomes very large as we approach x_c. Our most important result is that generically the S parameter is an increasing function of x, reaching it highest value at x_c contrary to previous expectations, [24].

6.6 Outlook

We have analyzed zero temperature spectra of glueballs and mesons in a class of holographic theories (V-QCD) that are in the universality class of QCD in the Veneziano limit. We have verified some generic properties of such spectra in the theory with massless quarks.

- In the conformal window all spectra are continuous.
- Below the conformal window, $x < x_c$, the spectra are discrete and gapped (except for the pions).

- All masses in the Miransky scaling region (aka “walking region") are obeying Miransky scaling $m_n \sim \Lambda_{\rm UV} \exp(-\frac{\kappa}{\sqrt{x_c - x}})$. The same applies to other mass parameters like f_π.

- All singlet and non-singlet mass ratios asymptote to non-zero constants as $x \to x_c$. Therefore there is no “dilaton" state. The approximate conformal symmetry is correlated with Miransky scaling instead.

- For finite values of x there is strong mixing between singlet mesons and glueballs, and occasional level crossings as we vary x.

- The S-parameter in units of $N_f N_c$ is generically $\mathcal{O}(1)$. It is an increasing function of x and asymptotes to a finite constant as $x \to x_c$. This suggests subtle discontinuities at the conformal transition.

The results on the S-parameter suggest that making S arbitrarily small in a walking theory may be more difficult than expected before. Moreover our results indicate that is probably not the case in QCD in the Veneziano limit. In [25] that appeared while this work was being finalized, similar conclusions are reached in a different context (probe tachyon-flavor dynamics in AdS). We find that in the walking region of V-QCD, backreaction of flavor to matter (that is fully implemented here) is important, among other things, for the spectra, and therefore the two results are not directly comparable.

6.7 Acknowledgments

We are grateful to T. Alho, K. Kajantie and K. Tuominen for useful discussions and comments. This work was in part supported by grants PERG07-GA-2010-268246, PIEF-GA-2011-300984, the EU program “Thales” ESF/NSRF 2007-2013, and by the European Science Foundation “Holograv" (Holographic methods for strongly coupled systems) network. It has also been co-financed by the European Union (European Social Fund, ESF) and Greek national funds through the Operational Program “Education and Lifelong Learning” of the National Strategic Reference Framework (NSRF) under “Funding of proposals that have received a positive evaluation in the 3rd and 4th Call of ERC Grant Schemes”. D.A. would like to thank the Crete Center for Theoretical Physics for hospitality and the FRont Of pro-Galician Scientists for unconditional support. I. Iatrakis’ work was supported by the project “HERAKLEITOS II - University of Crete" of the Operational Programme for Education and Lifelong Learning 2007 -

2013 (E.P.E.D.V.M.) of the NSRF (2007 - 2013), which is co-funded by the European Union (European Social Fund) and National Resources.

Bibliography

[1] B. Holdom, *"Techniodor,"* Phys. Lett. B **150** (1985) 301. 171

[2] K. Yamawaki, M. Bando and K. -i. Matumoto, *"Scale Invariant Technicolor Model and a Technidilaton,"* Phys. Rev. Lett. **56** (1986) 1335. 171

[3] T. W. Appelquist, D. Karabali and L. C. R. Wijewardhana, *"Chiral Hierarchies and the Flavor Changing Neutral Current Problem in Technicolor,"* Phys. Rev. Lett. **57** (1986) 957. 171

[4] S. Dimopoulos and L. Susskind, *"Mass Without Scalars,"* Nucl. Phys. B **155** (1979) 237. 171

[5] E. T. Neil, *"Exploring Models for New Physics on the Lattice,"* PoS LATTICE **2011** (2011) 009 [ArXiv:1205.4706][hep-lat]. 171

[6] V. A. Miransky and K. Yamawaki, *"Conformal phase transition in gauge theories,"* Phys. Rev. D **55** (1997) 5051 [Erratum-ibid. D **56** (1997) 3768] [ArXiv:hep-th/9611142]. 171

[7] V. A. Miransky, *"Dynamics of Spontaneous Chiral Symmetry Breaking and Continuum Limit in Quantum Electrodynamics,"* Nuovo Cim. **A90**, 149-170 (1985). 171, 174

[8] D. B. Kaplan, J. -W. Lee, D. T. Son, M. A. Stephanov, *"Conformality Lost,"* Phys. Rev. **D80**, 125005 (2009) [ArXiv:0905.4752][hep-th]. 171

[9] T. Appelquist and F. Sannino, *"The Physical spectrum of conformal SU(N) gauge theories,"* Phys. Rev. D **59** (1999) 067702 [ArXiv:hep-ph/9806409]. 171

[10] D. Elander, C. Nunez and M. Piai, *"A Light scalar from walking solutions in gauge-string duality,"* Phys. Lett. B **686**, 64 (2010) [ArXiv:0908.2808][hep-th];
K. Haba, S. Matsuzaki and K. Yamawaki, *"Holographic Techni-dilaton,"* Phys. Rev. D **82**, 055007 (2010) [ArXiv:1006.2526][hep-ph];

J. Alanen, T. Alho, K. Kajantie and K. Tuominen, *"Mass spectrum and thermodynamics of quasi-conformal gauge theories from gauge/gravity duality,"* Phys. Rev. D **84**, 086007 (2011) [ArXiv:1107.3362][hep-th];
L. Anguelova, P. Suranyi and L. C. R. Wijewardhana, *"Scalar Mesons in Holographic Walking Technicolor,"* Nucl. Phys. B **862**, 671 (2012) [ArXiv:1203.1968][hep-th]. 171

[11] D. Kutasov, J. Lin and A. Parnachev, *"Conformal Phase Transitions at Weak and Strong Coupling,"* Nucl. Phys. B **858**, 155 (2012) [ArXiv:1107.2324][hep-th]; 171, 179

[12] D. K. Hong and H. -U. Yee, *"Holographic estimate of oblique corrections for technicolor,"* Phys. Rev. D **74**, 015011 (2006) [ArXiv:hep-ph/0602177];
K. Agashe, C. Csaki, C. Grojean and M. Reece, *"The S-parameter in holographic technicolor models,"* JHEP **0712**, 003 (2007) [ArXiv:0704.1821][hep-ph];
K. Haba, S. Matsuzaki and K. Yamawaki, *"S Parameter in the Holographic Walking/Conformal Technicolor,"* Prog. Theor. Phys. **120**, 691 (2008) [ArXiv:0804.3668][hep-ph]. 171

[13] O. Mintakevich and J. sonvnenschein, *"Holographic technicolor models and their S-parameter,"* JHEP **0907** (2009) 032 [ArXiv:0905.3284][hep-th]. 171

[14] D. G. Levkov, V. A. Rubakov, S. V. Troitsky and Y. A. Zenkevich, *"Constraining Holographic Technicolor,"* Phys. Lett. B **716** (2012) 350 [ArXiv:1201.6368][hep-ph]. 171

[15] M. Järvinen and E. Kiritsis, *"Holographic Models for QCD in the Veneziano Limit,"* [ArXiv:1112.1261][hep-ph]. 171, 173, 174, 175, 178

[16] U. Gursoy and E. Kiritsis, *"Exploring improved holographic theories for QCD: Part I,"* JHEP **0802** (2008) 032 [ArXiv:0707.1324][hep-th];
U. Gursoy, E. Kiritsis, F. Nitti, *"Exploring improved holographic theories for QCD: Part II,"* JHEP **0802**, 019 (2008) [ArXiv:0707.1349][hep-th];
U. Gursoy, E. Kiritsis, L. Mazzanti, G. Michalogiorgakis and F. Nitti, *"Improved Holographic QCD,"* Lect. Notes Phys. **828** (2011) 79 [ArXiv:1006.5461][hep-th]. 172

[17] R. Casero, E. Kiritsis and A. Paredes, "Chiral symmetry breaking as open string tachyon condensation," Nucl. Phys. B **787** (2007) 98 [ArXiv:hep-th/0702155][hep-th];

I. Iatrakis, E. Kiritsis and A. Paredes, *"An AdS/QCD model from Sen's tachyon action,"* Phys. Rev. D **81** (2010) 115004 [ArXiv:1003.2377][hep-ph];
"An AdS/QCD model from tachyon condensation: II," JHEP **1011** (2010) 123 [ArXiv:1010.1364][hep-ph]. 172, 178

[18] G. Veneziano, *"Some Aspects of a Unified Approach to Gauge, Dual and Gribov Theories,"* Nucl. Phys. B **117** (1976) 519. 172

[19] D. Arean, I. Iatrakis, M. Järvinen, E. Kiritsis, to appear. 172, 176, 178

[20] U. Gursoy, E. Kiritsis, L. Mazzanti, F. Nitti, *"Deconfinement and Gluon Plasma Dynamics in Improved Holographic QCD,"* Phys. Rev. Lett. **101** (2008) 181601 [ArXiv:0804.0899][hep-th];
"Holography and Thermodynamics of 5D Dilaton-gravity," JHEP **0905**, 033 (2009) [ArXiv:0812.0792][hep-th].

[21] U. Gursoy, E. Kiritsis, L. Mazzanti, F. Nitti, *"Improved Holographic Yang-Mills at Finite Temperature: Comparisonv with Data,"* Nucl. Phys. **B820** (2009) 148-177 [ArXiv:0903.2859][hep-th]. 172, 173

[22] A. Sen, *"Tachyon dynamics in open string theory,"* Int. J. Mod. Phys. A **20** (2005) 5513 [ArXiv:hep-th/0410103]. 172

[23] T. Alho, M. Järvinen, K. Kajantie, E. Kiritsis and K. Tuominen, *"On finite-temperature holographic QCD in the Veneziano limit,"* [ArXiv:1210.4516][hep-ph]. 173, 174

[24] F. Sannino, *"Mass Deformed Exact S-parameter in Conformal Theories,"* Phys. Rev. D **82**, 081701 (2010) [ArXiv:1006.0207][hep-lat];
F. Sannino, *"Magnetic S-parameter,"* Phys. Rev. Lett. **105**, 232002 (2010) [ArXiv:1007.0254][hep-ph];
S. Di Chiara, C. Pica and F. Sannino, *"Flavor Dependence of the S-parameter,"* Phys. Lett. B **700**, 229 (2011) [ArXiv:1008.1267][hep-ph]. 180

[25] M. Goykhman and A. Parnachev, *"S-parameter, Technimesons, and Phase Transitions in Holographic Tachyon DBI Models,"* [ArXiv:1211.0482][hep-th]. 181

7 The Chern-Simons Diffusion Rate in Improved Holographic QCD

Authors : U. Gürsoy[a,b], I. Iatrakis[c], E. Kiritsis[c,d], F. Nitti[d], A. O'Bannon[e]

[a]Institute for Theoretical Physics, Utrecht University
Leuvenlaan 4, 3584 CE Utrecht, The Netherlands
[b]Instituut voor Theoretische Fysica, KU Leuven
Celestijnenlaan 200D, B-3001 Leuven, Belgium
[c]Crete Center for Theoretical Physics, Department of Physics
University of Crete, PO Box 2208, 71003 Heraklion, Greece
[d]APC, Université Paris 7, CNRS/IN2P3, CEA/IRFU, Obs. de Paris, Sorbonne Paris Cité, Bâtiment Condorcet, F-75205, Paris Cedex 13, France (UMR du CNRS 7164)
[e]Department of Applied Mathematics and Theoretical Physics University of Cambridge, Cambridge CB3 0WA, United Kingdom

7.1 Abstract

In $(3+1)$-dimensional $SU(N_c)$ Yang-Mills (YM) theory, the Chern-Simons diffusion rate, Γ_{CS}, is determined by the zero-momentum, zero-frequency limit of the retarded

two-point function of the CP-odd operator $\mathrm{tr}\,[F \wedge F]$, with F the YM field strength. The Chern-Simons diffusion rate is a crucial ingredient for many CP-odd phenomena, including the chiral magnetic effect in the quark-gluon plasma. We compute Γ_{CS} in the high-temperature, deconfined phase of Improved Holographic QCD, a refined holographic model for large-N_c YM theory. Our result for $\Gamma_{CS}/(sT)$, where s is entropy density and T is temperature, varies slowly at high T and increases monotonically as T approaches the transition temperature from above. We also study the retarded two-point function of $\mathrm{tr}\,[F \wedge F]$ with non-zero frequency and momentum. Our results suggest that the CP-odd phenomena that may potentially occur in heavy ion collisions could be controlled by an excitation with energy on the order of the lightest axial glueball mass.

7.2 Introduction

(3+1)-dimensional $SU(N_c)$ Yang-Mills (YM) theory has an infinite number of degenerate classical vacua distinguished by a topological invariant, the Chern-Simons number, N_{CS}. Normalizing the YM kinetic term as $-\frac{1}{4g^2}\mathrm{tr}[F_{\mu\nu}F^{\mu\nu}]$, N_{CS} is

$$N_{\mathrm{CS}} \equiv \frac{1}{8\pi^2}\int d^3x\,\epsilon_{ijk}\,\mathrm{tr}\left[A_i\partial_j A_k - \frac{2ig}{3}A_iA_jA_k\right], \tag{7.2.1}$$

where $i,j,k = 1,2,3$ and the trace is over gauge indices. A change in the Chern-Simons number is thus

$$\Delta N_{\mathrm{CS}} = \int d^4x\, q(x^\mu), \tag{7.2.2a}$$

$$q(x^\mu) \equiv \frac{1}{16\pi^2}\mathrm{tr}\,[F\wedge F] = \frac{1}{64\pi^2}\,\epsilon^{\mu\nu\rho\sigma}\mathrm{tr}F_{\mu\nu}F_{\rho\sigma}, \tag{7.2.2b}$$

where $x^\mu = (t,\vec{x})$. In a state invariant under translations in space and time, the rate of change of N_{CS} per unit volume V per unit time t is called the Chern-Simons diffusion rate, denoted Γ_{CS},

$$\Gamma_{\mathrm{CS}} \equiv \frac{\langle(\Delta N_{\mathrm{CS}})^2\rangle}{Vt} = \int d^4x\ \langle q(x^\mu)q(0)\rangle_{\mathrm{W}}\,, \tag{7.2.3}$$

where the subscript W denotes the Wightman function. In an equilibrium state with non-zero temperature T, let $G_R(\omega,\vec{k})$ denote the retarded Green's function of $q(x^\mu)$ in Fourier space, with frequency ω and spatial momentum $\vec{k}$. In such states, eq. (7.2.3) can be rewritten as

$$\Gamma_{CS} = -\lim_{\omega\to 0}\frac{2T}{\omega}\,\mathrm{Im}\,G_R(\omega,\vec{k}=0). \tag{7.2.4}$$

Gauge field configurations for which $\int d^4x\, q(x^\mu)$ is non-zero produce a non-zero $\Delta N_{\rm CS}$. At zero temperature, such gauge field configurations, called instantons, represent quantum tunneling events between vacua. At both zero and non-zero T, the contribution of instantons to $\Gamma_{\rm CS}$ is exponentially suppressed [1; 2]. When T is non-zero, however, classical thermal fluctuations can also produce a non-zero $\Delta N_{\rm CS}$, for example by exciting unstable gauge field configurations called sphalerons [3; 4] which generate non-zero $\Delta N_{\rm CS}$ upon decay. Such classical thermal processes are not exponentially suppressed [5; 6; 7]: in YM perturbation theory $\Gamma_{\rm CS} \propto \lambda_t^5 \log(\lambda_t)\, T^4$, where $\lambda_t \equiv g^2 N_c$ is the 't Hooft coupling [8; 9; 10; 11].

In YM coupled to fundamental-representation fermions, $\int d^4x\, q(x^\mu)$ also contributes to chiral anomalies in global symmetries. In the electroweak theory, gauge field configurations with non-zero $\int d^4x\, q(x^\mu)$ play a role in electroweak baryogenesis [12; 13], while in Quantum Chromodynamics (QCD), for sufficiently high T they may play a role in generating bubbles of net chirality (more left-handed than right-handed quarks, for example), in which parity, P, and charge conjugation times parity, CP, are broken [14].[1]

Such CP-odd domains in hot QCD may have observable consequences in heavy ion collisions at the Relativistic Heavy Ion Collider (RHIC) and Large Hadron Collider (LHC). These collisions produce a hot soup of QCD matter with T on the order of two to four times the QCD crossover temperature. The resulting state behaves as a nearly-ideal fluid of strongly-interacting quarks and gluons, the quark-gluon plasma (QGP) [15; 16; 17]. A non-central collision may produce a QGP with non-zero angular momentum and hence a magnetic field, both pointing perpendicular to the reaction plane (spanned by the beam axis and impact parameter). In the presence of a magnetic field, a net chirality will produce an electric current parallel to the magnetic field, due to the axial anomaly. This is the Chiral Magnetic Effect (CME) [18; 19]. A detection of the CME in heavy ion collisions would thus be a detection of CP-odd processes in QCD.

One observable consequence of the CME in a heavy ion collision is charge separation: positive charges will move to one side of the reaction plane, negative charges to the other. We know from experiment that the strong interactions preserve P and CP, however, so any charge separation from CP-odd sources will, over many events, average to zero. An observable that could serve as a "smoking gun" for the CME is thus hard to find. For heavy ion collsions at RHIC and LHC the focus so far has been on three-particle correlations [20; 21; 22], which indeed indicate that charge separation occurs in

[1] Sometimes $\Gamma_{\rm CS}$ is also called the "sphaleron transition rate" or, in the context of electroweak baryogenesis, the "baryon number violation rate."

heavy ion collisions. These correlations are sensitive to event-by-event charge separation from both CP-odd and CP-even processes, however, making a positive identification of a signal from the CME difficult [23]. In short, to date the experimental evidence for the detection of the CME in heavy ion collisions at RHIC and LHC is inconclusive.

The experimental situation raises a number of urgent questions for theorists. Can we compute the size of the signal from the CME, relative to backgrounds? How will that signal depend on temperature, magnetic field, centrality, etc.? Clearly an auxiliary question is: how big is the rate of chirality production, which is $\propto \Gamma_{\rm CS}$, in a heavy ion collision?

Unfortunately, $\Gamma_{\rm CS}$ is difficult to calculate for the QGP, for the same reasons that the shear viscosity, η, is difficult to calculate. The quarks and gluons are strongly-interacting, so perturbation theory is *a priori* unreliable. Calculating transport coefficients, such as $\Gamma_{\rm CS}$ and η, from lattice QCD requires a problematic analytic continuation from Euclidean signature.[1] Currently no reliable technique exists to compute $\Gamma_{\rm CS}$ or η for QCD at the temperatures reached in the QGP.

An alternative approach is holography [26; 27; 28], which equates certain strongly-coupled gauge theories in the large-N_c limit with weakly-coupled theories of gravity in spacetimes of one higher spatial dimension. A deconfined thermal state of the gauge theory is dual to a black hole spacetime [29], and transport coefficients are relatively straightforward to calculate [30; 31; 32]. Remarkably, the ratio of η to entropy density, s, for *any* theory dual to higher-dimensional Einstein gravity is $\eta/s = 1/(4\pi)$ [33], which is close to the estimate for η/s for the QGP extracted from data [34]. Such universality serves as encouragement for computing other transport coefficients, like $\Gamma_{\rm CS}$, from holography.

Previous calculations of $\Gamma_{\rm CS}$ in holography employed "top-down" models, *i.e.* models descending from a known string theory or supergravity construction. The best-understood example is $\mathcal{N} = 4$ supersymmetric YM (SYM) with large N_c and large λ_t, dual to supergravity in an Anti-de Sitter (AdS) space, for which $\Gamma_{\rm CS} \propto \lambda_t^2 T^4$ [30]. Other holographic calculations included the effects on $\Gamma_{\rm CS}$ due to a magnetic field [35] or confinement [36]. To our knowledge, in all previous cases the holographic results for $\Gamma_{\rm CS}$ were ultimately fixed by some underlying (perhaps "hidden" [36]) conformal symmetry.

In this paper we compute $\Gamma_{\rm CS}$ in Improved Holographic QCD (IHQCD) [37; 38; 39;

[1] In fact, $\Gamma_{\rm CS}$ may be *more* difficult to calculate from lattice QCD than other transport coefficients. The operator $q(x^\mu)$ obeys various constraints. For example, $\Delta N_{CS} = \int d^4x\, q(x^\mu)$ must be an integer, the second Chern character. Defining a lattice version of the operator $q(x^\mu)$ that obeys all of the constraints can be difficult, as discussed for example in refs. [11; 24; 25].

40; 41; 42; 43; 44], a holographic model of large-N_c YM theory. The model is "bottom-up," *i.e.* does not descend from a known string theory or supergravity construction, but is tailored to model string theory systems very closely, unlike other bottom-up models. The bulk theory is Einstein-dilaton gravity, where the dilaton Φ is dual to $\mathrm{tr}\, F_{\mu\nu}F^{\mu\nu}$. A non-trivial dilaton solution will describe non-trivial running of the YM coupling, hence the choice of dilaton potential is crucial. The simplest choice involves only two free parameters, which can be adjusted such that the model reproduces both the $T = 0$ glueball spectrum and the thermodynamics of large-N_c YM, including a first-order deconfinement transition at a critical temperature T_c. In particular, the model has no (hidden) conformal symmetry. We briefly review IHQCD in section 7.3.

In IHQCD the operator $q(x^\mu)$ is dual holographically to an axion field in the bulk [37; 38; 40; 42; 44]. Defining for convenience a holographic 't Hooft coupling $\lambda \equiv e^\Phi$, the normalization of the axion's kinetic term includes a dilaton-dependent factor, $Z(\lambda)$. In principle, $Z(\lambda)$ could be fixed by matching to lattice results for the Euclidean correlator of $q(x^\mu)$, as we explain in section 7.3. We work instead with several simple choices for $Z(\lambda)$, in part to study the generic behavior of $\Gamma_{\rm CS}$ in holographic models. Specifically, we consider a $Z(\lambda)$ with two free parameters, which we fix by demanding that the model match large-N_c YM lattice results for the topological susceptibility and for axial glueball mass ratios to within one sigma.

In section 7.4 we compute $\Gamma_{\rm CS}$ in the high-temperature, deconfined phase of IHQCD. Letting s denote the entropy density and λ_h the value of λ at the black hole horizon, our result for $\Gamma_{\rm CS}$ is of the form

$$\Gamma_{CS} = \frac{1}{N_c^2}\frac{sT}{2\pi}\, Z(\lambda_h). \tag{7.2.5}$$

Figs. 7.4, 7.5, and 7.6 show our numerical results for $\Gamma_{\rm CS}/(sT/N_c^2) = Z(\lambda_h)/(2\pi)$. For our choices of $Z(\lambda)$, the value of $Z(\lambda_h)$ is bounded from below as a function of T by its value in the $T \to \infty$ limit, and increases monotonically as T approaches T_c from above, with most of the increase occurring between $2T_c$ and T_c. We will argue that such behavior is generic in a large class of confining theories with classical gravity duals. In a scan through various choices of $Z(\lambda)$, each of which reproduces the first two axial glueball mass ratios to within one sigma, we find that the increase can be as large as 60%. For our optimal choice of $Z(\lambda)$, which provides the best fit to the lattice results for the first two axial glueball mass ratios, the increase is only 0.01%.

To obtain $\Gamma_{\rm CS}$, we compute the low-frequency limit of $G_R(\omega, \vec{k} = 0)$ holographically. In section 7.5 we initiate the study of $G_R(\omega, \vec{k})$ at non-zero ω and $|\vec{k}|$, in the $T \geq T_c$ regime. We focus in particular on $\mathrm{Im}\, G_R(\omega, \vec{k})$, which is proportional to the

spectral function of $q(x^\mu)$. After suitably subtracting the high-frequency asymptotics, by computing the difference in the value of the correlator at two temperatures, our results suggest the presence of a reasonably long-lived excitation with energy of order of the lightest axial glueball mass at $T = 0$. That is sufficiently light to prompt the speculation that perhaps such an excitation could dominate many CP-odd phenomena in the QGP created in heavy ion collisions.

In section 7.6 we summarize our results and discuss directions for future research.

7.3 Improved Holographic QCD

The holographic model that we consider as the dual to pure large-N_c YM is (4+1)-dimensional Einstein-dilaton gravity with a well-chosen dilaton potential [37; 38; 39; 40; 41; 42; 43; 44]. In terms of the holographic 't Hooft coupling $\lambda \equiv e^\Phi$, the bulk action is

$$S = M_p^3 N_c^2 \int d^5x \sqrt{-g} \left[R - \frac{4}{3}\frac{(\partial\lambda)^2}{\lambda^2} + V(\lambda) \right] + S_{\text{bdry}}, \tag{7.3.1}$$

where M_p is the Planck Mass, related to the (4+1)-dimensional Newton's constant G_5 as $M_p^3 = 1/(16\pi G_5 N_c^2)$, g and R are the determinant and Ricci scalar of the bulk metric, $V(\lambda)$ is the dilaton potential, and S_{bdry} represents all boundary terms, including the Gibbons-Hawking term as well as counterterms.

If $V(\lambda) = 12/\ell^2$ with a constant length scale ℓ, then the equations of motion arising from eq. (7.3.1) admit a solution with constant λ and an AdS metric with radius of curvature ℓ,

$$ds^2_{AdS} = \frac{\ell^2}{r^2}\left(dr^2 - dt^2 + d\vec{x}^2\right), \qquad 0 < r < \infty. \tag{7.3.2}$$

Here r is the holographic radial coordinate, dual to the field theory energy scale: the region near the AdS boundary at $r \to 0$ is dual to the ultra-violet (UV) of the field theory, while the region near the Poincaré horizon at $r \to \infty$ is dual to the infra-red (IR). Such a solution describes a conformal field theory.

For non-trivial $V(\lambda)$, the equations of motion admit vacuum solutions in which λ depends only on r and the metric takes the form

$$ds^2 = b_0(r)^2(dr^2 - dt^2 + d\vec{x}^2), \qquad 0 < r < \infty, \tag{7.3.3}$$

with warp factor $b_0(r)$. In IHQCD we demand that as $r \to 0$ the metric approach that of AdS, $b_0(r) \to \ell/r$ (up to corrections logarithmic in r) and that λ vanish logarithmically, $\lambda \to -1/\log r$, to mimic the running of the large-N_c YM coupling.

Large-N_c YM approaches a free theory in the UV, so we expect the holographic dual in the $r \to 0$ region to be a string theory, not just a classical gravity theory like IHQCD. On the other hand, in large-N_c YM, λ_t diverges in the IR, so a classical gravity theory may be a reliable description in the $r \to \infty$ region. IHQCD is intended to be such a *low-energy effective* description of large-N_c YM, reliable in the $r \to \infty$ region. In practice, the role of the $r \to 0$ region in IHQCD is simply to provide boundary conditions for the fields in the $r \to \infty$ region. We impose those boundary conditions at a cutoff, *i.e.* at some small but finite $r = \epsilon$. We then compute low-energy quantities that are insensitive to the cutoff, some of which we match to large-N_c YM, while the rest are predictions of the model. A more detailed discussion of these issues appears for example in ref. [41].

Using classical gravity in the $r \to 0$ region has an important consequence, however: IHQCD will actually be dual to a theory that flows to a *non-trivial* UV fixed point. Generically, the UV physics of large-N_c YM and IHQCD will thus be different. For example, in IHQCD, $\eta/s = 1/(4\pi)$ [33], which is much smaller than the high-T perturbative result for η/s in large-N_c YM [45]. Nevertheless, in order to match IHQCD to known results for IR quantities in large-N_c YM, we must match some quantities in the UV. For example, to reproduce lattice results for the free energy of large-N_c YM for $T \gtrsim T_c$ with the correct normalization, we must demand that at high T the free energy of IHQCD obey a Stefan-Boltzmann law. That requirement fixes the value of ℓ in the asymptotic AdS region in units of the Planck mass: $(M_p \ell)^{-3} = 45\pi^2$ [39; 40].

By matching to another UV quantity, the perturbative large-N_c YM β-function, we can also constrain $V(\lambda)$. In the $r \to 0$ region, where λ is small, $V(\lambda)$ has a regular series expansion

$$V(\lambda) = \frac{12}{\ell^2}\left(1 + v_0\lambda + v_1\lambda^2 + \mathcal{O}\left(\lambda^3\right)\right). \tag{7.3.4}$$

Committing to an identification of the field theory renormalization scale $E \equiv E_0\, b_0(r)$, where E_0 can be fixed by matching to the lowest glueball mass or to the result for T_c from lattice large-N_c YM, we can fix the coefficients v_0 and v_1 in terms of the coefficients of the perturbative large-N_c YM β-function [37; 38; 44]:

$$\beta(\lambda_t) = -\beta_0\lambda_t^2 - \beta_1\lambda_t^3 + \mathcal{O}(\lambda_t^4), \qquad \beta_0 = \frac{22}{3(4\pi)^2}, \qquad \beta_1 = \frac{51}{121}\beta_0^2, \tag{7.3.5a}$$

$$v_0 = \frac{8}{9}\beta_0, \qquad v_1 = \frac{4}{9}\beta_1 + \frac{23}{81}\beta_0^2. \tag{7.3.5b}$$

In the vacuum solutions, generically λ diverges as $r \to \infty$. The large-λ expansion of $V(\lambda)$ must take the form $V(\lambda) \propto \lambda^{\frac{4}{3}}\sqrt{\log\lambda}$ in order for the glueball spectrum to be

gapped and discrete with asymptotically linear trajectories [37; 38; 41; 44]. With this asymptotic form for $V(\lambda)$, as $r \to \infty$ the warp factor and $\lambda(r)$ take the form

$$b_0(r) \propto e^{-(r/L)^2}, \qquad \lambda(r) \propto \frac{r}{L}\, e^{\frac{3}{2}(r/L)^2}, \qquad (r \to \infty) \tag{7.3.6}$$

where L is a length scale determined by the value of λ at $r = \epsilon$. The form of $b_0(r)$ in eq. (7.3.6) is sufficient to guarantee that the dual field theory is confining [37; 38]. The metric actually has a mild singularity[1] at $r = \infty$ that can be cloaked by a regular horizon and hence is a "good" singularity [46]. Moreover, the singularity is repulsive [38; 40], which guarantees that the low-energy spectrum and other observables are insensitive to the details of the resolution of the singularity.

The black hole solutions of the model defined by the action in eq. (7.3.1) have non-trivial $\lambda(r)$ and a metric of the form [39; 40]

$$ds^2 = b(r)^2 \left(\frac{dr^2}{f(r)} - f(r)dt^2 + d\vec{x}^2 \right), \qquad 0 < r < r_h. \tag{7.3.7}$$

The surface $r = r_h$ is the horizon, where $f(r_h) = 0$, and the corresponding Hawking temperature is $T = 4\pi f'(r_h)$. Black hole solutions only exist for temperatures above a value $T_{\rm min}$, and in fact two branches of solutions exist, the large and small black holes (comparing r_h to ℓ). Fig. 7.1 depicts the typical form of T as a function of r_h, including the two branches of black hole solutions. For both large and small black holes, as $r \to r_h$, the warp factor $b(r)$ asymptotes to a constant whose value determines the entropy density, $s = b(r_h)^3/(4G_5)$, and as $r \to 0$, $b(r) \to r/\ell$, up to $\mathcal{O}(r^4)$ (times logarithmic) corrections, indicating that in the field theory the thermal energy density and pressure are both of order N_c^2.

In large black hole solutions, $\lambda(r)$ decreases monotonically as T increases, so that $\lambda \to 0$ as $T \to \infty$. In small black hole solutions, $\lambda(r)$ increases as T increases. In particular, as discussed in refs. [40; 42], the value of $\lambda(r)$ at the horizon, $\lambda_h \equiv \lambda(r_h)$, is a monotonically increasing function of r_h, so a plot of T versus λ_h is qualitatively similar to fig. 7.1: in the $T \to \infty$ limit, $\lambda_h \to 0$ on the large black hole branch and $\lambda_h \to \infty$ on the small black hole branch (see for example fig. 2 (a) of ref. [40]).

If we Wick-rotate to a compact Euclidean time direction of length $1/T$, then for $T \geq T_{min}$ three bulk solutions exist: the Wick-rotated version of eq. (7.3.3), which describes a thermal gas of gravitons and is dual to a confined state, and the Wick-rotated large and small black holes, which are dual to deconfined states. To determine which

[1] On the other hand, in the string frame, where the metric scale factor is $\lambda^{2/3}(r)b_0(r)$, the curvature approaches zero as $r \to \infty$.

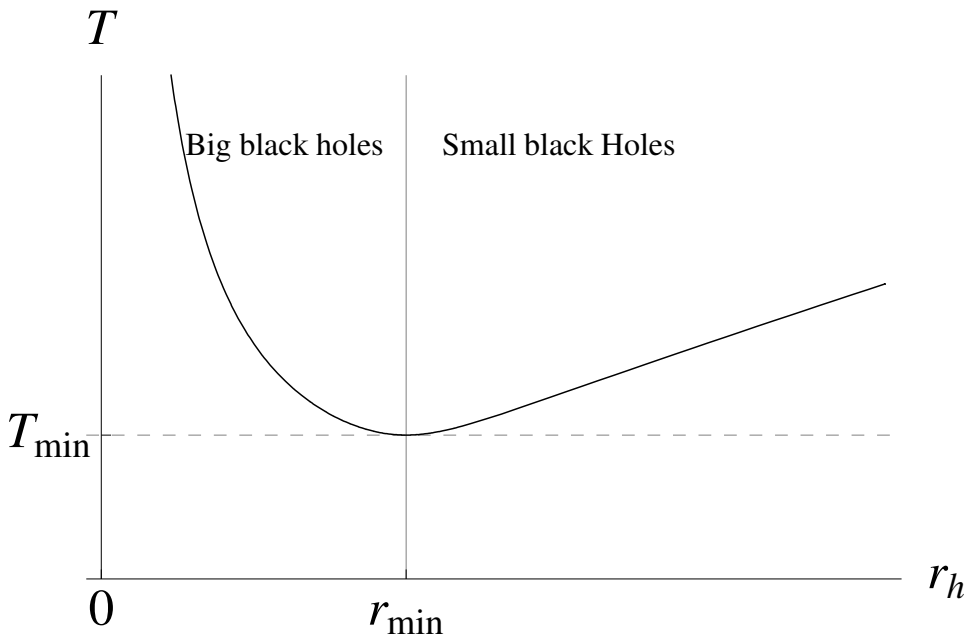

Figure 7.1: Schematic plot for the typical form of the black hole Hawking temperature T as a function of the horizon position r_h, for a generic choice of $V(\lambda)$ (with the correct small- and large-λ asymptotics). The temperature exhibits a minimum, T_{min}, at $r_{\rm min}$, which separates the large black hole ($r_h < r_{\rm min}$) from the small black hole ($r_h > r_{\rm min}$) branches.

solution is thermodynamically preferred at any given T, we must determine which has the smallest on-shell Euclidean action, dual to the field theory's free energy (times $1/T$). As shown in refs. [39; 40; 42], the small black hole solutions are never thermodynamically preferred, but at some $T_c > T_{min}$ the large black hole solutions become thermodynamically preferred. Indeed, the system exhibits a first-order Hawking-Page type transition at T_c, dual to a confinement-deconfinement transition.

In general, for a given potential $V(\lambda)$ we cannot solve the equations of motion arising from eq. (7.3.1) exactly, so we resort to numerics. Here we will only sketch our numerical procedure, which is described in detail for example in ref. [42]. At the cutoff $r = \epsilon$ we impose a Dirichlet condition on each field, and in particular we demand that the metric take the AdS form. We then fix the remaining integration constants, including λ_h, by a shooting algorithm. Given a choice of $V(\lambda)$ and the Dirichlet conditions at $r = \epsilon$, we obtain a one-parameter family of solutions labeled by T, or equivalently by λ_h. Following refs. [42; 43], in our numerics we use a simple form for $V(\lambda)$ with the correct

small- and large-λ asymptotics,

$$V(\lambda) = \frac{12}{\ell^2}\left[1 + V_0\lambda + V_1\lambda^{4/3}\sqrt{\log\left(1 + V_2\lambda^{4/3} + V_3\lambda^2\right)}\right]. \tag{7.3.8}$$

Expanding eq. (7.3.8) about $\lambda = 0$ and matching to eq. (7.3.4), we find $v_0 = V_0$ and $v_1 = V_1\sqrt{V_2}$. The coefficients V_0 and V_2 can be determined in terms of V_1 by imposing the conditions in eq. (7.3.5b). The potential thus has two free parameters, V_1 and V_3. We fit these two parameters by matching to lattice results for two thermodynamic quantities in large-N_c YM: the latent heat of the deconfinement transition, which is proportional to the entropy density at the transition, $s(T_c)/(N_c^2T_c^3) \simeq 0.31$ [47], and the pressure at $T = 2T_c$ [47; 48; 49]. Upon fixing V_1 and V_3 in this fashion, IHQCD describes very well both the $T = 0$ glueball spectra (0^{++} and 2^{++}) as well as the finite T thermodynamics of large-N_c YM [42; 50].

The instanton number density operator, $q(x^\mu)$ in eq. (7.2.2b), is dual to a bulk pseudoscalar, the axion α (as in many top-down models). In the field theory, the source for $q(x^\mu)$ is an angular variable, the θ-angle. As a result, the action of the bulk axion must be invariant under shifts of α, and hence must depend only on derivatives[1] $\partial\alpha$. General arguments in string theory and in YM theory, including the argument that θ dependence should appear in the YM vacuum energy only at order one in the large-N_c limit rather than at order N_c^2 [51], imply that the axion action is suppressed by $\mathcal{O}(1/N_c^2)$ compared to the action S in eq. (7.3.1) [37; 38; 41; 44]. We thus add to the model an axion with an action S_α of the form [37; 38; 41; 44]

$$S_\alpha = -\frac{1}{2}M_p^3\int d^5x\sqrt{-g}\; Z(\lambda)(\partial\alpha)^2, \tag{7.3.9}$$

where, following the rules of effective field theory, we have included a dimensionless, λ-dependent normalization function, $Z(\lambda)$, consistent with the symmetries.

Being a massless pseudo-scalar, in an expansion of $\alpha(r)$ about $r = 0$, the leading, non-normalizable term is a constant, which is proportional to the YM θ-angle defined in the UV,

$$\alpha(r = 0) = \kappa\,\theta, \tag{7.3.10}$$

where in top-down models the proportionality constant κ will be fixed, but not in bottom-up models. In other words, in our model the normalization of the operator dual to α is ambiguous: α is dual to $q(x^\mu)/\kappa$. Nevertheless, by fixing the normalization of the topological susceptibility we will be able to compute two-point functions of $q(x^\mu)$ unambiguously, as we explain below.

[1] Instanton effects may produce a non-trivial axion potential, such as a term $\cos\alpha$. These instanton effects are exponentially suppressed in the large-N_c limit, however.

To specify S_α completely we must specify $Z(\lambda)$. In principle, $Z(\lambda)$ can be fixed as follows. First, perform a lattice calculation of the Euclidean two-point function of $q(x^\mu)$ with non-zero T for some set of frequencies. Second, compute the same Euclidean two-point function holographically for all frequencies for some choice of $Z(\lambda)$. A least squares fit of the holographic results to the lattice results should then determine $Z(\lambda)$. To study generic behavior of holographic models, we will instead proceed by using simple forms for $Z(\lambda)$ that we constrain by matching to lattice results for the topological susceptibility and axial glueball mass spectrum. Notice that matching to any lattice data will always have room for improvement: lattice definitions of $q(x^\mu)$ generically suffer from power-law divergences that dominate in the continuum limit, making lattice calculations of correlators of $q(x^\mu)$ noisy [24]. Accurate calculations may be possible in the near future[1].

We can constrain $Z(\lambda)$ as follows. Since $Z(\lambda)$ is the coefficient of a kinetic term, we demand that $Z(\lambda) \geq 0$. We can also constrain $Z(\lambda)$'s small- and large-λ asymptotics [37; 38; 41; 44]:

$$Z(\lambda) \propto \begin{cases} Z_0 + \mathcal{O}(\lambda), & \lambda \to 0, \\ \lambda^4 + \mathcal{O}(1/\lambda), & \lambda \to \infty, \end{cases} \tag{7.3.11}$$

where Z_0 is a dimensionless constant. The small-λ form follows from the rules of effective field theory: a constant is the most general allowed term. The large λ behavior is fixed by glueball universality [38]. Various towers of glueballs have linear asymptotic trajectories: for large excitation number n, their squared masses go as $(m_n^i)^2 = c^i n + \cdots$, with constants c^i, where the integer i labels different towers. Glueball universality is the statement that all the slopes c^i are similar, *i.e.* do not depend on i. That is automatic for the 0^{++} and 2^{++} glueballs. Requiring the same for the 0^{-+} glueballs forces $Z(\lambda)$ to go as λ^4 at large λ [38].

We will use the simplest form of $Z(\lambda)$, also used for example in ref. [42],

$$7Z(\lambda) = Z_0(1 + c_4\lambda^4), \tag{7.3.12}$$

where c_4 is a dimensionless constant. To fix Z_0 we match to the large-N_c YM lattice result for the Euclidean topological susceptibility, χ, defined in terms of the $T = 0$ vacuum energy density $\mathcal{E}(\theta)$ as

$$\chi \equiv \frac{d^2\mathcal{E}(\theta)}{d\theta^2} = \int d^4x \, \langle q(x^\mu)q(0)\rangle_{\rm E} \,, \tag{7.3.13}$$

[1]We thank F. Bruckmann, H. Panagopoulos, and A. Schäfer for discussions on this issue.

where the subscript E denotes the Euclidean correlator. The holographic result for χ is[2] [38],

$$\chi = \frac{\kappa^2 M_p^3}{\int_0^\infty \frac{dr}{b_0^3(r) Z(\lambda(r))}}. \tag{7.3.14}$$

Clearly χ will be proportional to $\kappa^2 Z_0$. Thus, for any given value of the parameter c_4, matching the holographic result for χ to the lattice result, $\chi \approx (191\,\mathrm{MeV})^4$ [24; 52], fixes the product $\kappa^2 Z_0$. On the other hand, since the locations of poles in the two-point function of $q(x^\mu)$ are independent of the overall normalization $\kappa^2 Z_0$, we can fix c_4 independently by matching the mass of the lowest 0^{-+} glueball to the lattice result of ref. [53],

$$m_{0^{-+}}/m_{0^{++}} = 1.50(4). \tag{7.3.15}$$

The resulting values are[1] [42]

$$\kappa^2 Z_0 = 33.25, \qquad c_4 = 0.26. \tag{7.3.16}$$

These values can then be used to predict the masses in the full tower of 0^{-+} glueballs. As shown in refs. [37; 38; 41; 44], the holographic result for the first excited 0^{-+} glueball mass, $m_{0^{*-+}}$, agrees very well with the lattice result [53],

$$m_{0^{*-+}}/m_{0^{++}} = 2.11(6). \tag{7.3.17}$$

Crucially, notice that by fixing the normalization of χ we have fixed the normalization of *any* two-point function of $q(x^\mu)$, and thus have eliminated the normalization ambiguity mentioned below eq. (7.3.10). In other words, the holographic calculation of the two-point functions of $q(x^\mu)$ will only depend on the combination $\kappa^2 Z_0$ (as we will see explcitly in section 7.4), which we have fixed to the value in eq. (7.3.16).

Solutions for α as a function of T were studied in refs. [40; 42]. When $T = 0$, a non-trivial UV θ-angle forces $\alpha(r)$ to be non-trivial. The resulting normalizable solution then indicates that the non-zero UV θ-angle flows to zero in the IR, as shown in fig. 7.2, and additionally triggers a non-zero $\langle q(x)\rangle/\kappa$. The $T = 0$ solution for $\alpha(r)$ is unchanged when $T < T_c$: Wick-rotating the metric in eq. (7.3.3) to a compact Euclidean time does not affect the static solution $\alpha(r)$. Such behavior is expected in a confined phase at leading order in N_c, due to large-N_c volume independence. When $T > T_c$, however, the only non-singular solution for the axion is a constant, $\alpha(r) = \kappa\,\theta$, indicating that $\langle q(x)\rangle = 0$, in agreement with evidence from lattice data for large-N_c YM [24].

[2] The holographic calculation of χ in ref. [38] assumed $\kappa = 1$. Here we allow for arbitrary κ.

[1] The result for $\kappa^2 Z_0$ in ref. [42] was too large by a factor of four, producing an erroneous result, $\kappa^2 Z_0 = 133$. In eq. (7.3.16) we present the correct value, $\kappa^2 Z_0 = 133/4 = 33.25$.

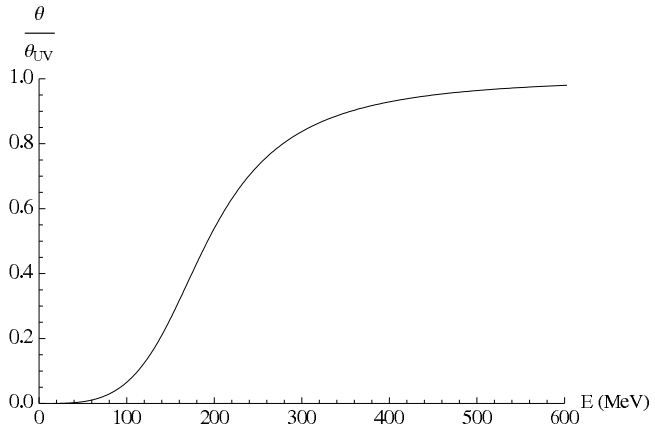

Figure 7.2: The normalizable solution $\alpha(r)$ for the axion at $T = 0$, expressed as a running θ-angle normalized to the UV value, as a function of the energy scale, $E(r) = E_0 b(r)$. We fix E_0 by matching our holographic result for T_c to the large-N_c YM lattice result.

What is the behavior of the topological susceptibility as a function of temperature, $\chi(T)$? When $T < T_c$, $\chi(T)$ is independent of T, *i.e.* takes the same value as at $T = 0$, eq. (7.3.14), again due to large-N_c volume independence. When $T > T_c$, the holographic result for the topological susceptibility is

$$\chi(T) = \frac{\kappa^2 M_p^3}{\int_0^{r_h} \frac{dr}{b^3(r) f(r) Z(\lambda(r))}}. \qquad (T > T_c) \tag{7.3.18}$$

The denominator on the right-hand-side of eq. (7.3.18) diverges at the black hole horizon, so in fact $\chi(T) = 0$ when $T > T_c$, up to $\mathcal{O}(e^{-N_c})$ corrections [40; 42].

We will also consider a form for $Z(\lambda)$ more general than that of eq. (7.3.12). On the large black hole branch, if T is large then λ is small, in which case we expect the largest polynomial correction to the $Z(\lambda)$ in eq. (7.3.12) to be a term linear in λ, hence we consider

$$Z(\lambda) = Z_0 \left(1 + c_1 \lambda + c_4 \lambda^4\right), \tag{7.3.19}$$

where c_1 is a dimensionless constant, which we choose to be positive. If we continue to fit only to the lattice result for the lowest 0^{-+} glueball mass, we find a substantial degeneracy (which is not surprising, given that we have introduced an additional parameter, c_1). Specifically, for any positive value of c_1, a value of c_4 exists such that, upon matching to the lowest axial glueball mass in eq. (7.3.15), the value of the first excited axial glueball mass is in rough agreement with the value in eq. (7.3.17), exhibiting at most a 3% discrepancy, as shown in fig. 7.3. To constrain c_1 we will demand

that our holographic results for the axial glueball masses fall within one sigma of the lattice values in eqs. (7.3.15) and (7.3.17). That results in the constraints

$$0 \lesssim c_1 \lesssim 5, \qquad 0.06 \lesssim c_4 \lesssim 50. \tag{7.3.20}$$

In fact, the optimal values, which provide the best fit, are the ones in eqs. (7.3.12) and (7.3.16): $(c_1, c_4) = (0, 0.26)$.

Figure 7.3: Our holographic results for the masses of the 0^{-+} glueball states with excitation number n, normalized to the lowest 0^{++} glueball mass, obtained by varying the coefficients c_1 and c_4 in the $Z(\lambda)$ in eq. (7.3.19). From the top (red) dots (visible only for $n = 2$ and $n = 4$) to the bottom (blue) dots, $(c_1, c_4) = (0, 0.26), (0.5, 0.87), (1, 2.2), (5, 24), (10, 75), (20, 230), (40, 600)$. The lowest axial glueball mass, $n = 1$, is always fixed to be the value in eq. (7.3.15). The two horizontal blue lines with surrounding blue bands indicate the results and errors, respectively, of the large-N_c YM lattice calculations for the masses of the lowest and first excited states, $n = 1$ and $n = 2$ (see eqs. (7.3.15) and (7.3.17)) [53]. Only the mass of the $n = 2$ state is appreciably sensitive to changes of c_1 and c_4, differing from the lattice result by 3% at most.

As we have seen, the function $Z(\lambda)$ must be non-negative and is constrained in the $\lambda \to 0$ and $\lambda \to \infty$ limits. For intermediate values of λ, the most natural assumption

is that $Z(\lambda)$ is monotonic. At least, we are not aware of any compelling evidence for the existence of maxima or minima in $Z(\lambda)$. Our choices for $Z(\lambda)$ were thus monotonic functions of λ, namely polynomials in λ with strictly positive coefficients. To test the effect of maxima and minima in $Z(\lambda)$, we considered two changes to the $Z(\lambda)$ in eq. (7.3.19). First, we allowed slightly negative c_1, while maintaining $Z(\lambda) \geq 0$. Second, we introduced a maximum by a adding a Gaussian peak to $Z(\lambda)$. In each case we computed the axial glueball mass spectrum. After matching to the lattice result for the lowest axial glueball mass, we found that the fit to the first excited axial glueball mass was worse, deviating from the lattice result by about 10%. We consider that a preliminary indication that monotonic $Z(\lambda)$ may indeed be the best choice. We leave more thorough tests for future research.

Our assumption that $Z(\lambda)$ is monotonic in λ determines the qualitative behavior of $Z(\lambda)$ as a function of T. On the large black hole branch, as $T \to \infty$, $\lambda \to 0$, and as T decreases towards T_c, λ increases monotonically. As a result, for our choices of $Z(\lambda)$—simple polynomials in λ with positive coefficients—when $T \to \infty$, $Z(\lambda) \to Z_0$, and when $T \to T_c$, $Z(\lambda)$ will increase monotonically. As functions of T, our $Z(\lambda)$ are thus bounded from below by their value in the $T \to \infty$ limit: $Z(\lambda) \geq Z_0$. The behavior of $Z(\lambda)$ as a function of T will translate directly into the behavior of $\Gamma_{\rm CS}$ as a function of T, as we will show in the next section. In particular, the dimensionless combination $\Gamma_{\rm CS}/(sT)$ will be bounded from below by its value in the $T \to \infty$ limit, and will increase as $T \to T_c$. In the next section we will also present a more general argument that $\Gamma_{\rm CS}/(sT)$ must increase as T approaches T_c from above.

7.4 The Chern-Simons Diffusion Rate

7

We will compute $\Gamma_{\rm CS}$ using eq. (7.2.4), rewritten as

$$\Gamma_{CS} = -\kappa^2 \lim_{\omega \to 0} \frac{2T}{\omega} \operatorname{Im} \hat{G}_R(\omega, \vec{k} = 0), \tag{7.4.1}$$

where $\hat{G}_R(\omega, \vec{k})$ is the retarded two-point function of $q(x^\mu)/\kappa$, the operator dual to our axion α.

In holography, the on-shell bulk action is the generating functional for field theory correlation functions [27; 28]. To compute the two-point function $\hat{G}_R(\omega, \vec{k})$ in the high-temperature, deconfined phase of IHQCD, we must solve the linearized equation of motion of the axion in the black hole spacetime with metric in eq. (7.3.7), with $T \geq T_c$.

We thus introduce a fluctuation of the axion, $\delta\alpha(r, x^\mu)$, where $x^\mu = (t, \vec{x})$. When $T \geq T_c$, the background solution for the axion is trivial, hence the linearized equation of motion for $\delta\alpha(r, x^\mu)$ is simply

$$\frac{1}{Z(\lambda(r))\sqrt{-g}}\,\partial_r\left[Z(\lambda(r))\sqrt{-g}\,g^{rr}\partial_r\delta\alpha(r,x^\mu)\right] + g^{\mu\nu}\partial_\mu\partial_\nu\,\delta\alpha(r,x^\mu) = 0, \tag{7.4.2}$$

where the metric is that of eq. (7.3.7). Notice in particular that $\delta\alpha$ will not couple to the fluctuations of any other fields because the background solution preserves CP and the axion is the only CP-odd field in the bulk. We must solve eq. (7.4.2) with Dirichlet boundary condition at the asymptotically AdS boundary and with in-going wave boundary condition at the horizon [30]. The solution takes the form

$$\delta\alpha(r, x^\mu) = \int \frac{d^4k}{(2\pi)^4}\, e^{ikx}\,\delta\alpha(r, k^\mu)\, a(k^\mu), \tag{7.4.3}$$

where $k^\mu = (\omega, \vec{k})$ and where $a(k^\mu)$ is fixed by the Dirichlet boundary condition,

$$\lim_{r\to 0}\delta\alpha(r, x^\mu) = \int \frac{d^4k}{(2\pi)^4}\, e^{ikx}\, a(k^\mu), \tag{7.4.4}$$

while $\delta\alpha(r, k^\mu)$ obeys the equation

$$\frac{1}{Z(\lambda(r))\sqrt{-g}}\,\partial_r\left[Z(\lambda(r))\sqrt{-g}\,g^{rr}\partial_r\delta\alpha(r,k^\mu)\right] - g^{\mu\nu}k_\mu k_\nu\,\delta\alpha(r,k^\mu) = 0, \tag{7.4.5}$$

with unit normalization at the asymptotically AdS boundary, $\lim_{r\to 0}\delta\alpha(r, k^\mu) = 1$, and in-going wave boundary condition at the horizon. The on-shell axion action is then

$$S_\alpha^{\text{on-shell}} = \int \frac{d^4k}{(2\pi)^4}\, a(-k^\mu)\,\mathcal{F}(r, k^\mu)\, a(k^\mu)\Big|_0^{r_h}, \tag{7.4.6}$$

where

$$\mathcal{F}(r, k^\mu) \equiv -\frac{M_p^3}{2}\,\delta\alpha(r, -k^\mu)\, Z(\lambda(r))\,\sqrt{-g}\,g^{rr}\,\partial_r\delta\alpha(r, k^\mu). \tag{7.4.7}$$

The retarded Green's function is then [30]

$$\hat{G}_R(\omega, \vec{k}) = -2\,\lim_{r\to 0}\mathcal{F}(r, k^\mu). \tag{7.4.8}$$

To compute Γ_{CS}, we need to solve eq. (7.4.5) with $\vec{k} = 0$ and with small ω. We will do so in two ways, first using near-horizon matching and second using the membrane paradigm, following ref. [32]. In each case we can determine Γ_{CS} analytically, essentially because $\delta\alpha$ is a massless fluctuation.

In the near-horizon matching technique, we first solve eq. (7.4.5) with $\omega = 0$ and then expand the solution near the horizon. We then reverse the order of operations, solving the equation in the near-horizon region and then expanding the solution in ω. Finally, we match the two solutions to obtain $\mathcal{F}(r, k^\mu)$.

When $\vec{k} = 0$ and $\omega = 0$ the solution of eq. (7.4.5) is

$$\delta\alpha = C_1 + C_2 \int_0^r \frac{dr'}{Z(\lambda(r'))b(r')^3 f(r')}, \tag{7.4.9}$$

with constant coefficients C_1 and C_2. The second term on the right-hand side of eq. (7.4.9) diverges as $r \to r_h$. As a result, when $\omega = 0$ a normalizable solution must have $C_2 = 0$. When ω is small but non-zero, a normalizable solution may have $C_2 \propto \omega$. Plugging eq. (7.4.9) into eq. (7.4.7), we find

$$\lim_{r\to 0} \mathcal{F}(r, k^\mu) = -\frac{M_p^3}{2} C_1 C_2. \qquad (\omega \ll T, \vec{k} = 0) \tag{7.4.10}$$

We will choose $C_1 = 1$ so that our $\delta\alpha$ has unit normalization at the asymptotically AdS boundary. Our task is thus to determine C_2. Expanding the solution in eq. (7.4.9) around the horizon, we find

$$\delta\alpha = C_1 + \frac{C_2}{Z(\lambda_h)\, b(r_h)^3\, f'(r_h)} \log(r_h - r) + \mathcal{O}(r_h - r), \tag{7.4.11}$$

where $f'(r_h) = 4\pi T$. Now we reverse the order of operations. Expanding eq. (7.4.5) in $(r_h - r)$, we find the solution in the near-horizon region,

$$\delta\alpha = C_+ (r_h - r)^{\frac{i\omega}{4\pi T}} + C_- (r_h - r)^{-\frac{i\omega}{4\pi T}}, \tag{7.4.12}$$

with coefficients $C_\pm$ that depend on ω but not on r. We set $C_+ = 0$ so that the near-horizon solution is an in-going wave [30]. Now we expand the solution in eq. (7.4.12) for small ω:

$$\delta\alpha = C_- - i\frac{\omega}{4\pi T} C_- \log(r_h - r) + \mathcal{O}(\omega^2/T^2). \tag{7.4.13}$$

By matching the constant and logarithmic terms in eqs. (7.4.11) and (7.4.13), we find

$$C_1 = C_-, \qquad C_2 = -i\omega\, Z(\lambda_h)\, b(r_h)^3\, C_-. \tag{7.4.14}$$

Setting $C_1 = 1$, we obtain $\lim_{r\to 0} \mathcal{F}(r, k^\mu)$ via eq. (7.4.10) and then $\hat{G}_R(\omega, \vec{k})$ via eq. (7.4.8),

$$\hat{G}_R(\omega, \vec{k} = 0) = -i\,\omega\, M_p^3\, Z(\lambda_h)\, b(r_h)^3. \qquad (\omega \ll T) \tag{7.4.15}$$

We thus obtain our main result for $\Gamma_{\rm CS}$,

$$7\Gamma_{CS} = -\kappa^2 \lim_{\omega\to 0} \frac{2T}{\omega} \operatorname{Im} \hat{G}_R(\omega, \vec{k} = 0) = \frac{1}{N_c^2} \frac{sT}{2\pi} \kappa^2 Z(\lambda_h), \tag{7.4.16}$$

where we have used $M_p^3 = 1/(16\pi G_5 N_c^2)$ and where $s = \frac{b^3(r_h)}{4G_5}$ is the entropy density. Notice that the normalization of this result is fixed by the product $\kappa^2 Z_0$, which we fixed in section 7.3 by matching to the topological susceptibility at $T = 0$.

The second equivalent, but more efficient, method that we will use to obtain $\hat{G}_R(\omega, \vec{k})$ is the membrane paradigm [32]. Kubo's formula for the retarded Green's function is

$$\Pi(\omega, \vec{k}) = \hat{G}_R(\omega, \vec{k})\delta\alpha(\omega, \vec{k}), \tag{7.4.17}$$

where $\Pi(\omega, \vec{k})$ is the one-point function of $q(x^\mu)/\kappa$ in Fourier space. Following ref. [32], we extend eq. (7.4.17) into the bulk by defining an r-dependent response function,

$$\zeta(r, \omega, \vec{k}) \equiv \frac{\Pi(r, \omega, \vec{k})}{\omega\, M_p^3\, \delta\alpha(r, \omega, \vec{k})}, \tag{7.4.18}$$

where $\Pi(r, \omega, \vec{k})$ is the canonical momentum of $\delta\alpha(r, \omega, \vec{k})$ with respect to the r-foliation of the bulk space-time,

$$7\Pi(r, \omega, \vec{k}) \equiv \frac{\delta S_\alpha}{\delta\partial_r\delta\alpha} = -M_p^3\, Z(\lambda(r))\sqrt{-g}\, g^{rr}\, \partial_r\delta\alpha(r, \omega, \vec{k}). \tag{7.4.19}$$

The retarded Green's function is then proportional to the boundary value of ζ:

$$7\hat{G}_R(\omega, \vec{k}) = -M_p^3\, \omega \lim_{r\to 0} \zeta(r, \omega, \vec{k}). \tag{7.4.20}$$

An equation of motion for ζ is straightforward to derive using eq. (7.4.19) and $\delta\alpha$'s equation of motion, eq. (7.4.5),

$$\begin{aligned} \partial_r\zeta &= \frac{\omega}{Z(\lambda(r))\sqrt{-g}\, g^{rr}} \left[\zeta^2 + Z(\lambda(r))^2 g\, g^{rr} g^{tt} \left(1 + \frac{g^{xx}}{g^{tt}} \frac{\vec{k}^2}{\omega^2}\right)\right] \\ &= \frac{\omega}{Z(\lambda(r))b(r)^3 f(r)} \left[\zeta^2 + Z(\lambda(r))^2 b(r)^6 \left(1 - f(r)\frac{\vec{k}^2}{\omega^2}\right)\right]. \end{aligned} \tag{7.4.21}$$

To obtain the retarded Green's function $\hat{G}_R(\omega, \vec{k})$, we must impose regularity at the horizon, meaning $\partial_r\zeta$ is finite there [32], hence the term in brackets in eq. (7.4.21) must vanish[1] at $r = r_h$:

$$\zeta(r_h) = +iZ(\lambda_h)b(r_h)^3. \tag{7.4.22}$$

We can now easily derive $\Gamma_{\rm CS}$. In eq. (7.4.21) we take $\vec{k} = 0$ and observe that if $\omega \to 0$ then ζ becomes independent of r. The value of ζ for all r is then the same as the value

[1] When $\vec{k} \neq 0$ but $\omega = 0$, the boundary condition is modified from that in eq. (7.4.22), as discussed in ref. [32]. In what follows, whenever we consider $\vec{k} \neq 0$ we will work with $\omega \neq 0$, hence we will use the boundary condition in eq. (7.4.22).

at the horizon, eq. (7.4.22), and via eq. (7.4.20) we trivially obtain $\hat{G}_R(\omega, \vec{k} = 0)$, which is identical to eq. (7.4.15). We thus find again

$$7\Gamma_{CS} = -\kappa^2 \lim_{\omega\to 0} \frac{2T}{\omega} \operatorname{Im} \hat{G}_R(\omega, \vec{k} = 0) = \frac{1}{N_c^2} \frac{sT}{2\pi} \kappa^2 Z(\lambda_h). \tag{7.4.23}$$

Our result suggests a natural dimensionless quantity to study,

$$\frac{\Gamma_{CS}}{sT/N_c^2} = \frac{\kappa^2 Z(\lambda_h)}{2\pi}, \tag{7.4.24}$$

which has implicit dependence on T through $Z(\lambda_h)$, and is constant in T if and only if $Z(\lambda)$ is a constant in λ, that is, if the axion does not couple to the dilaton. Indeed, as we mentioned at the end of section 7.3, the behavior of $Z(\lambda)$ as a function of T determines the behavior of $\Gamma_{CS}/(sT/N_c^2)$ as a function of T. In particular, on the large black hole branch, $\Gamma_{CS}/(sT/N_c^2)$ is bounded from below by its value in the $T \to \infty$ limit,

$$\lim_{T\to\infty} \frac{\Gamma_{CS}}{sT/N_c^2} = \frac{\kappa^2 Z_0}{2\pi}. \tag{7.4.25}$$

If we use the preferred value $\kappa^2 Z_0 = 33.25$ [42] then $\kappa^2 Z_0/(2\pi) \simeq 5.29$. Moreover, $\Gamma_{CS}/(sT/N_c^2)$ will increase monotonically as T approahces T_c from above.

For the simplest choice of $Z(\lambda)$, given in eq. (7.3.12), $\Gamma_{CS}/(sT/N_c^2)$ has extremely mild dependence on T: as T approaches T_c from above, $\Gamma_{CS}/(sT/N_c^2)$ is nearly constant, experiencing an increase of only about 0.01%, mostly between $2T_c$ and T_c, as shown in fig. 7.4. In bulk terms, the reason for this mild T dependence is that between $T \to \infty$ and $T = T_c$, λ_h increases from zero up to only $\lambda_h \approx 0.14$, which for the $Z(\lambda)$ in eq. (7.3.12) translates into a very small change in $\Gamma_{CS}/(sT/N_c^2)$.

On the other hand, for the $Z(\lambda)$ in eq. (7.3.19), for different values of the coefficients c_1 and c_4 we find more variation in $\Gamma_{CS}/(sT/N_c^2)$ as T approaches T_c from above, as shown in fig. 7.5. For example, if $c_1 = 40$ and $c_4 = 600$, then $\Gamma_{CS}/(sT/N_c^2)$ increases near T_c by more than a factor of six. For all values of c_1 and c_4 that we considered, most of the increase occurs between $2T_c$ and T_c. Fig. 7.6 shows $\Gamma_{CS}/(sT/N_c^2)$, normalized to the $T \to \infty$ value $\kappa^2 Z_0/(2\pi)$, as a function of T/T_c for values of c_1 and c_4 that reproduce the lattice results for axial glueball mass ratios to within one sigma, eq. (7.3.20). At the upper limits of the allowed (c_1, c_4) values, namely $(c_1, c_4) = (5, 50)$, we find that as T approaches T_c from above, $\Gamma_{CS}/(sT/N_c^2)$ increases by about 60%, with most of the increase occuring between $2T_c$ and T_c.

In heavy ion collisions at RHIC and LHC, T reaches two to four times the QCD crossover temperature. We would thus like to know the value of $\Gamma_{\rm CS}$ in QCD near

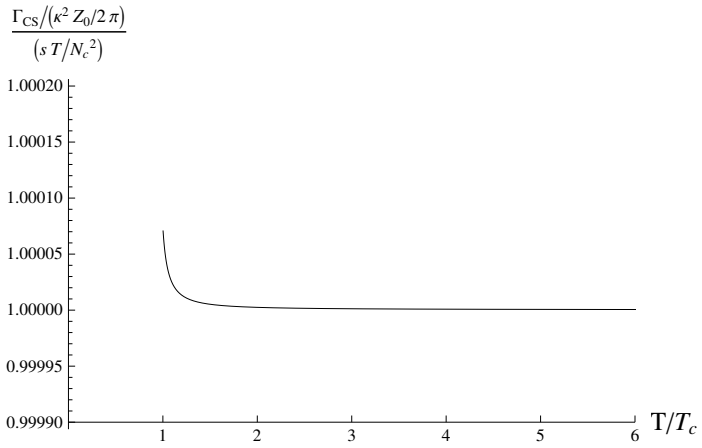

Figure 7.4: Our numerical result for $\Gamma_{CS}/(sT/N_c^2)$, normalized to the $T \to \infty$ value $\kappa^2 Z_0/(2\pi)$, as a function of T/T_c for the $Z(\lambda)$ given in eq. (7.3.12), with $c_4 = 0.26$ [42]. As T decreases, $\Gamma_{CS}/(sT/N_c^2)$ remains nearly constant, experiencing only an approximately 0.01% increase, mostly between $2T_c$ and T_c.

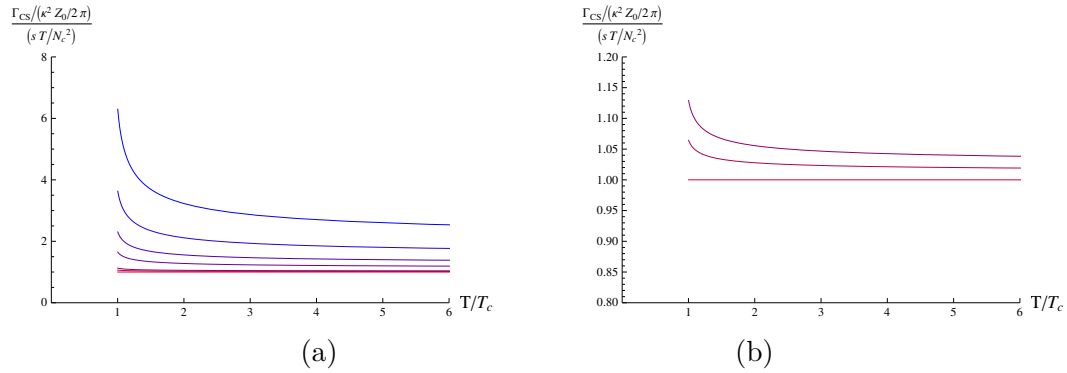

Figure 7.5: (a) Our numerical results for $\Gamma_{CS}/(sT/N_c^2)$, normalized to the $T \to \infty$ value $\kappa^2 Z_0/2\pi$, as functions of T/T_c, for the $Z(\lambda)$ in eq. (7.3.19), for different choices of the dimensionless parameters (c_1, c_4). From the bottom (red) curve to the top (blue) curve, $(c_1, c_4) = (0, 0.26), (0.5, 0.87), (1, 2.2), (5, 24), (10, 75), (20, 230), (40, 600)$. (b) Close-up of the curves for (from bottom to top) $(c_1, c_4) = (0, 0.26), (0.5, 0.87), (1, 2.2)$. In all of these cases, as T approaches T_c from above $\Gamma_{CS}/(sT/N_c^2)$ increases by anywhere from 0.01% up to a factor greater than six. The increase occurs mostly between $2T_c$ and T_c.

the crossover temperature, which is a key ingredient determining the magnitude of any current produced via the CME [18].[1] No controlled calculation of $\Gamma_{\rm CS}$ from QCD at

[1] We thank D. Kharzeev for a discussion on this point.

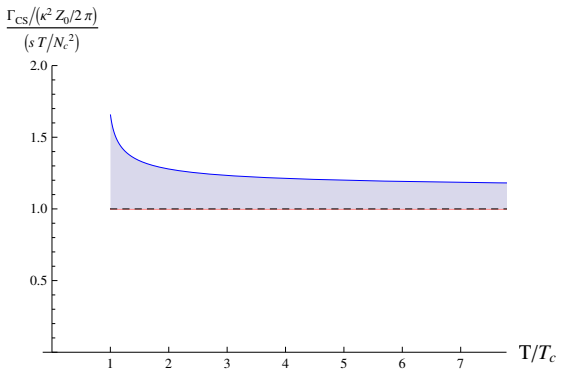

Figure 7.6: Our numerical results for $\Gamma_{CS}/(sT/N_c^2)$, normalized to the $T \to \infty$ value $\kappa^2 Z_0/2\pi$, as functions of T/T_c, for the $Z(\lambda)$ in eq. (7.3.19) with (c_1, c_4) constrained such that the holographic model reproduces the lattice results for axial glueball mass ratios to within one sigma: $0 \lesssim c_1 \lesssim 5$ and $0.06 \lesssim c_4 \lesssim 50$. A generic choice of (c_1, c_4) within these limits will produce a curve inside the shaded region. The lower bound of the shaded region, given by the solid pink curve, has the lowest values, $(c_1, c_4) = (0, 0.06)$, while the upper bound, given by the solid blue curve, has the largest values, $(c_1, c_4) = (5, 50)$. At the upper bound we see that as T approaches T_c from above, $\Gamma_{CS}/(sT/N_c^2) \times (2\pi)/(\kappa^2 Z_0)$ increases by about 60%. The dashed line is the result for the optimal values $(c_1, c_4) = (0, 0.26)$, as shown also in fig. 7.4.

these temperatures exists, hence we turn to holography. Suppose we use $\mathcal{N} = 4$ SYM as a holographic proxy for QCD near the crossover temperature. The result for $\Gamma_{\rm CS}$ in large-N_c, strongly-coupled $\mathcal{N} = 4$ SYM is [30],

$$\Gamma_{\rm CS}^{\mathcal{N}=4} = \frac{\lambda_t^2}{2^8\pi^3}\, T^4. \tag{7.4.26}$$

Being a conformal field theory, $\mathcal{N} = 4$ SYM has no phase transitions at non-zero T, so to obtain a sensible result we should consider the dimensionless quantity $\Gamma_{\rm CS}/T^4$. As a crude estimate we take $\alpha_s \equiv g^2/(4\pi) = 0.5$ and we use $N_c = 3$, so that $\lambda_t = 6\pi$, in which case we find

$$\Gamma_{\rm CS}^{\mathcal{N}=4}/T^4 \approx 0.045. \qquad (\lambda_t = 6\pi) \tag{7.4.27}$$

For a better estimate, let us consider $\Gamma_{\rm CS}(T_c)/T_c^4$ in IHQCD. As discussed above, if $Z(\lambda)$ is monotonic in λ, then $\Gamma_{\rm CS}/(sT/N_c^2)$ is bounded from below by its value in the $T \to \infty$ limit, eq. (7.4.25). We can obtain a lower bound on $\Gamma_{\rm CS}(T_c)/T_c^4$ by using the large-N_c YM lattice result for the entropy density at T_c [47], $s(T_c) = 0.31 N_c^2 T_c^3$. Letting λ_c denote the value of λ_h at T_c, we find

$$\Gamma_{CS}(T_c)/T_c^4 = 0.31 \times \frac{\kappa^2 Z(\lambda_c)}{2\pi} > 0.31 \times \frac{\kappa^2 Z_0}{2\pi} = 1.64, \tag{7.4.28}$$

which is about 36 times larger than the $\mathcal{N} = 4$ SYM estimate, eq. (7.4.27). In fact, eq. (7.4.28) is closer to the perturbative QCD result, if we naïvely extrapolate to $\alpha_s = 0.5$: $\Gamma_{CS}(T)/T^4 \approx 30\alpha_s^5 \approx 0.94$ (up to logarithms) [8; 9; 10; 11]. If we consider the $Z(\lambda)$ in eq. (7.3.19), and constrain c_1 and c_4 to the values in eq. (7.3.20), then we can also place an upper bound on $\Gamma_{CS}(T_c)/T_c^4$, given by the solid blue curve in fig. 7.6. For these choices of $Z(\lambda)$, we thus find

$$1.64 \leq \Gamma_{CS}(T_c)/T_c^4 \leq 2.8. \tag{7.4.29}$$

Finally, we have also calculated Γ_{CS} using the small black hole solutions [39; 40; 42]. Our results for those cases appear in the appendix. Although the small black hole branch is always thermodynamically disfavored, we can actually use the results for $\Gamma_{\rm CS}/(sT/N_c^2)$ on the small black hole branch to argue quite generally that on the large black hole branch $\Gamma_{\rm CS}/(sT/N_c^2)$ should increase as T approaches T_c from above. A similar argument also applies for the bulk viscosity, as discussed in ref. [43]. The key result, shown in fig. 11 in the appendix, is that for $T > T_{min}$ $\Gamma_{\rm CS}/(sT/N_c^2)$ is larger on the small black hole branch than on the large black hole branch, but the two branches meet at T_{min}. On the large black hole branch, then, $\Gamma_{\rm CS}/(sT/N_c^2)$ must increase as $T \to T_{min}$ from above, in order to meet $\Gamma_{\rm CS}/(sT/N_c^2)$ from the small black hole branch. In fact, we can show in full generality that on the large black hole branch $\Gamma_{\rm CS}/(sT/N_c^2)$ must increase as $T \to T_{min}$: we simply take $(d/dT)(\Gamma_{CS}/(sT/N_c^2)) = (d\lambda_h/dT)(d/d\lambda_h)(\kappa^2 Z(\lambda_h)/2\pi)$ and observe that by definition $(d\lambda_h/dT)$ diverges when $T \to T_{min}$, while $(d/d\lambda_h)(\kappa^2 Z(\lambda_h)/2\pi)$ remains finite. Notice also that $\Gamma_{\rm CS}/(sT/N_c^2)$ itself remains finite when $T \to T_{min}$. Given that T_{min} is generally very close to T_c, we are then guaranteed that $\Gamma_{\rm CS}/(sT/N_c^2)$ will be increasing as $T \to T_c$ from above, if we assume that $Z(\lambda)$ is monotonic as a function of T between T_{min} and T_c. In principle, $Z(\lambda)$ could exhibit maxima or minima for $T \in (T_{min}, T_c)$, although such behavior seems un-natural. On the large black hole branch an increase of $\Gamma_{\rm CS}/(sT/N_c^2)$ as $T \to T_c$ from above seems to be the generic behavior. We thus learn that the increase in $\Gamma_{\rm CS}/(sT/N_c^2)$ in the vicinity of T_c on the large black hole branch is tied to the existence of T_{min}, and hence to the existence of small black hole solutions. As argued in ref. [40], the existence of small black hole solutions follows from the fact that the zero-temperature theory is confining. These arguments suggest that perhaps any confining, strongly-interacting, large-N_c gauge theory with a (4+1)-dimensional holographic dual[1] may exhibit an increase in $\Gamma_{CS}/(sT/N_c^2)$ in the vicinity of T_c.

[1] Our arguments may not apply for (3+1)-dimensional confining theories obtained from higher-dimensional theories with compact spatial directions, such as the low-energy worldvolume theory on D4-branes with one spatial direction compactified and anti-periodic boundary conditions for fermions [29].

7.5 The Spectral Function

7 We now turn our attention to $G_R(\omega, \vec{k})$ with non-zero ω and $\vec{k}$. Generically $G_R(\omega, \vec{k})$ is a complex-valued function of the real variables ω and $\vec{k}$. A pole in $G_R(\omega, \vec{k})$ indicates a large response to an infinitesimal source for $q(x^\mu)$, and is thus associated with a resonant excitation of the system. Being complex-valued, $G_R(\omega, \vec{k})$ is not directly observable. To study the excitations of our system, we thus turn to the spectral function, $-2\,\mathrm{Im}\, G_R(\omega, \vec{k})$, which is real and hence observable in principle.[2] Typically, a pole in $G_R(\omega, \vec{k})$ produces a peak in the spectral function. In this section we initiate the study of these peaks in our system.

To be precise, we will compute $\mathrm{Im}\, G_R(\omega, \vec{k})$. To do so, we will compute $G_R(\omega, \vec{k})$ using the membrane paradigm [32], as explained in section 7.4. In particular, we must solve eq. (7.4.21), which we reproduce here for convenience

$$\partial_r \zeta = \frac{\omega}{Z(\lambda(r))b(r)^3 f(r)} \left[\zeta^2 + Z(\lambda(r))^2 b(r)^6 \left(1 - f(r) \frac{\vec{k}^2}{\omega^2} \right) \right], \tag{7.5.1}$$

with the boundary condition in eq. (7.4.22),

$$\zeta(r_h) = +iZ(\lambda_h) b(r_h)^3, \tag{7.5.2}$$

and then obtain $G_R(\omega, \vec{k})$ via eq. (7.4.20),

$$7G_R(\omega, \vec{k}) = -\kappa^2 M_p^3\, \omega \lim_{r \to 0} \zeta(r, \omega, \vec{k}). \tag{7.5.3}$$

We have not been able to solve eq. (7.5.1) exactly for all values of ω and $\vec{k}$, hence we turn to numerical solutions. In this section we exclusively use the $Z(\lambda)$ in eq. (7.3.12), with $c_4 = 0.26$.

We consider first the case $\vec{k} = 0$. Fig. 7.7 shows our numerical result for $\mathrm{Im}\, G_R(\omega, \vec{k} = 0)/(T_c M_p^3)$ at T_c as a function of ω/T_c. As we saw in section 7.4, for ω sufficiently small, $\mathrm{Im}\, G_R(\omega, \vec{k} = 0) \propto \omega$. On the other hand, at asymptotically large ω we expect $\mathrm{Im}\, G_R(\omega, \vec{k} = 0) \propto \omega^4$ because in the UV the theory is conformally invariant and $q(x^\mu)$ is dimension four. Our results are consistent with that expectation: fig. 7.7 shows that the function $(1.6 \times 10^{-7}) \times (\omega/T_c)^{4.051}$ provides an excellent fit to our data.

The ω^4 scaling of $\mathrm{Im}\, G_R(\omega, \vec{k} = 0)$, and hence of $G_R(\omega, \vec{k} = 0)$, at asymptotically large ω is a divergence in the coincidence limit of the two-point function that prevents

[2] Given $\mathrm{Im}\, G_R(\omega, \vec{k})$ we can obtain $\mathrm{Re}\, G_R(\omega, \vec{k})$ via a Kramers-Kroning relation, provided the large-ω and large-$|\vec{k}|$ asymptotics have been suitably regulated.

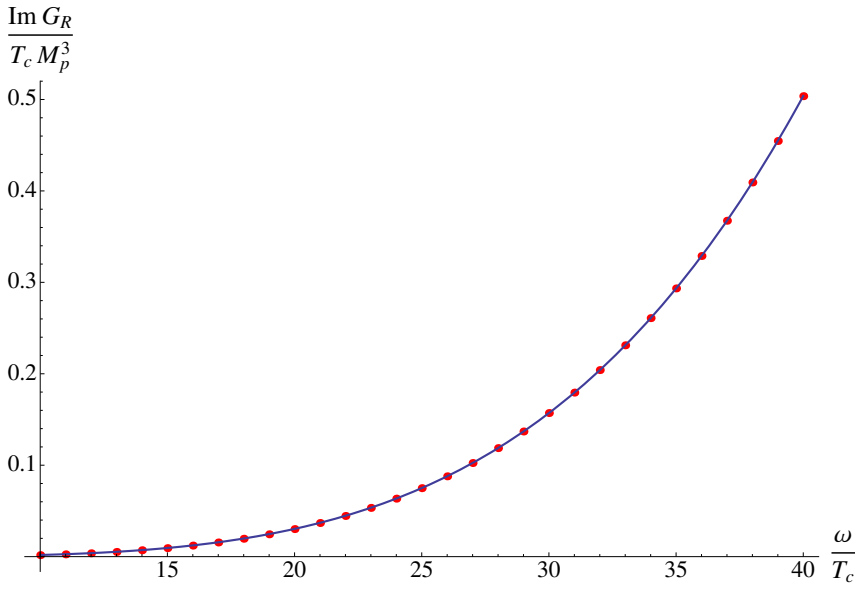

Figure 7.7: Our numerical results for $\mathrm{Im}\, G_R(\omega, \vec{k}=0)/(T_c M_p^3)$ as a function of ω/T_c, at T_c, for the $Z(\lambda)$ in eq. (7.3.12) with $\kappa^2 Z_0 = 33.25$ and $c_4 = 0.26$. The red dots are our numerical results while the solid blue curve is the function $(1.6\times 10^{-7})\times(\omega/T_c)^{4.051}$. Our results are clearly consistent with the expectation that $\mathrm{Im}\, G_R(\omega, \vec{k}=0) \propto \omega^4$ at large ω.

the correlator from obeying the sum rules and dispersion relations typically used to give physical meaning to the poles of $G_R(\omega, \vec{k})$ in the complex ω plane, which require $G_R(\omega, \vec{k})$ to *vanish* at large frequency. Such a divergence may overwhelm peaks in $\mathrm{Im}\, G_R(\omega, \vec{k})$, rendering them practically invisible.

One way to improve the large-ω behavior of $\mathrm{Im}\, G_R(\omega, \vec{k})$ is to consider subtracted correlators. For example, one possible option is to determine the form of $\mathrm{Im}\, G_R(\omega, \vec{k})$ at large ω exactly by solving eq. (7.5.1) in a WKB approximation, and then subtracting that large-ω form from all subsequent calculations of $\mathrm{Im}\, G_R(\omega, \vec{k})$. That approach encounters ambiguities in sub-leading divergences in ω, as discussed for example in ref. [54]. We will instead eliminate the large-ω divergence by computing $G_R(\omega, \vec{k})$ at two different temperatures, T_1 and T_2, and then taking the difference,

$$7\Delta G_R(\omega, \vec{k}; T_1, T_2) \equiv G_R(\omega, \vec{k})\Big|_{T_2} - G_R(\omega, \vec{k})\Big|_{T_1} . \tag{7.5.4}$$

We could also imagine subtracting the $T = 0$ result for $G_R(\omega, \vec{k})$, that is, by taking $T_1 = 0$, but that is difficult to do numerically. When $T = 0$, $G_R(\omega, \vec{k})$ is a sequence of delta-functions whose locations and amplitudes correspond to the masses and wave-function normalizations of axial glueballs. We would need to subtract the enveloping

function of this sequence of delta-functions, which is difficult to implement numerically. We will thus always consider $T_1, T_2 \geq T_c$. Fig 7.8 shows our numerical results for $\mathrm{Im}\, G_R(\omega, \vec{k} = 0)$ at two different temperatures, T_c and $2T_c$, while fig. 7.9 shows our numerical results for $\Delta\mathrm{Im}\, G_R(\omega, \vec{k} = 0; T_c, 2T_c)$. In each figure we observe that the difference in $\mathrm{Im}\, G_R(\omega, \vec{k} = 0)$ between T_c and $2T_c$ approaches zero as $\omega/T_c \to \infty$, at least within our numerical precision. Our numerical subtraction thus appears to be reliable, so we may interpret peaks in $\mathrm{Im}\, G_R(\omega, \vec{k})$ as physical excitations.

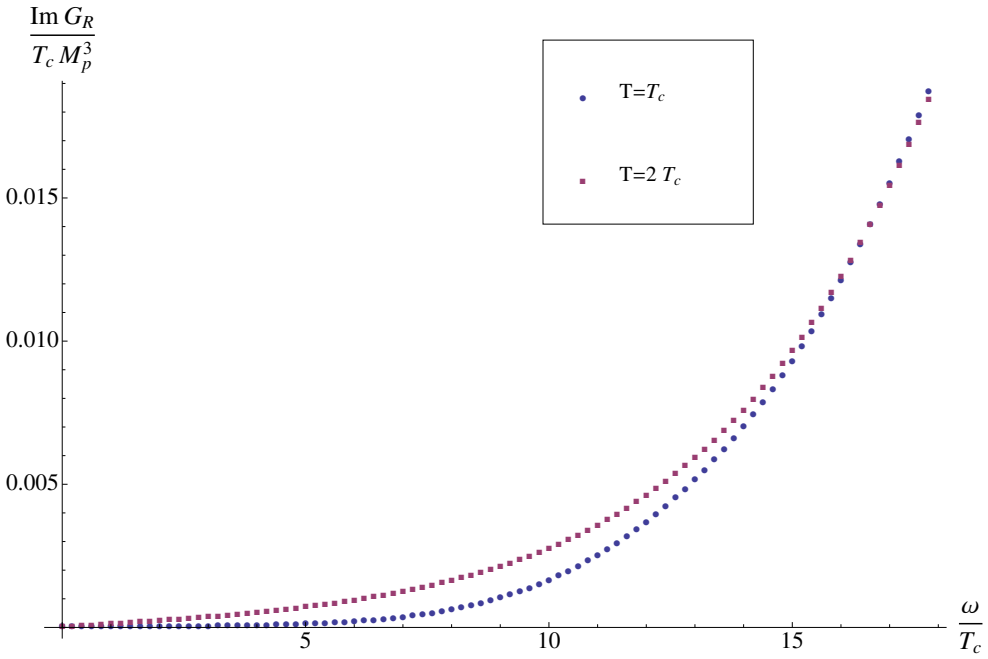

Figure 7.8: Our numerical results for $\mathrm{Im}\, G_R(\omega, \vec{k} = 0)/(T_c M_p^3)$ as a function of ω/T_c, at T_c (lower blue dots) and at $2T_c$ (upper red dots), for the $Z(\lambda)$ in eq. (7.3.12) with $\kappa^2 Z_0 = 33.25$ and $c_4 = 0.26$. A both T_c and $2T_c$, for ω/T_c sufficiently large $\mathrm{Im}\, G_R(\omega, \vec{k} = 0) \propto \omega^4$.

From figs. 7.8 and 7.9, we see that as T increases from T_c to $2T_c$, $\mathrm{Im}G_R(\omega, \vec{k} = 0)$ changes by at most 10%. Fig. 7.9 also clearly reveals a minimum in $\Delta\mathrm{Im}\, G_R(\omega, \vec{k} = 0; T_c, 2T_c)$ near $\omega/T_c \approx 10$ and a maximum near $\omega/T_c \approx 22$, indicating a shift in spectral weight towards higher ω as T increases. Indeed, fig. 7.9 strongly suggests that a peak in the spectral function is moving to higher ω as T increases. The location of the peak, at ω on the order of twenty times T_c, is roughly the same as the scale of the lightest 0^{-+} glueball mass at $T = 0$, around 2600 MeV [53]. In other words, fig. 7.9 provides evidence that the plasma supports an excitation with roughly the same energy as the lightest 0^{-+} glueball at $T = 0$. The width of the peak in fig. 7.9 is about $10T_c \approx 1300$ MeV, so

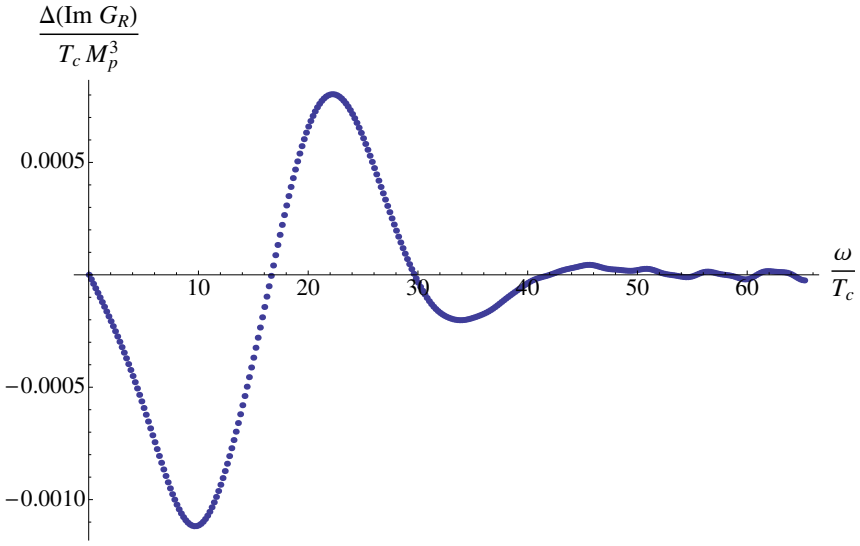

Figure 7.9: Our numerical results for the difference $\Delta \mathrm{Im}\, G_R(\omega, \vec{k} = 0; T_c, 2T_c)/(T_c M_p^3)$ as a function of ω/T_c, for the $Z(\lambda)$ in eq. (7.3.12) with $\kappa^2 Z_0 = 33.25$ and $c_4 = 0.26$. The difference goes to zero (within our numerical precision) as $\omega/T_c \to \infty$, as expected. The prominent minimum at $\omega/T_c \approx 10$ and maximum at $\omega/T_c \approx 22$ indicate a shift in spectral weight with increasing T, presumably from the motion of a peak in the spectral function.

the excitation is reasonably long-lived.

Figure 7.10 shows our result for the subtracted correlator with non-zero ω and $|\vec{k}|$, using the same two temperatures as above. We observe that as $|\vec{k}|$ increases up to $|\vec{k}|/T_c \approx 10$, the largest peak shifts from $\omega/T_c \approx 22$ up to $\omega/T_c \approx 30$. Although this change in the position of the peak is roughly order one, the change in the shape of the peak is very mild. In particular, the width of the peak changes very little, indicating that the lifetime of the excitation stays nearly constant as $|\vec{k}|$ increases.

The typical time scale for dynamical processes in the QGP created in heavy ion collisions is about $1\,\mathrm{fm/c} \approx (200\,\mathrm{MeV})^{-1}$. Our results suggest the existence of a relatively long-lived excitation with energy on the order of 2600 MeV, corresponding to a time scale of about 0.1 fm/c. We cannot resist speculating that perhaps such an excitation, if present in the QGP, could dominate correlators of $q(x^\mu)$ and hence many dynamical CP-odd phenomena. Regrettably, we will leave a detailed analysis of this excitation, and its effect on CP-odd physics, for the future.

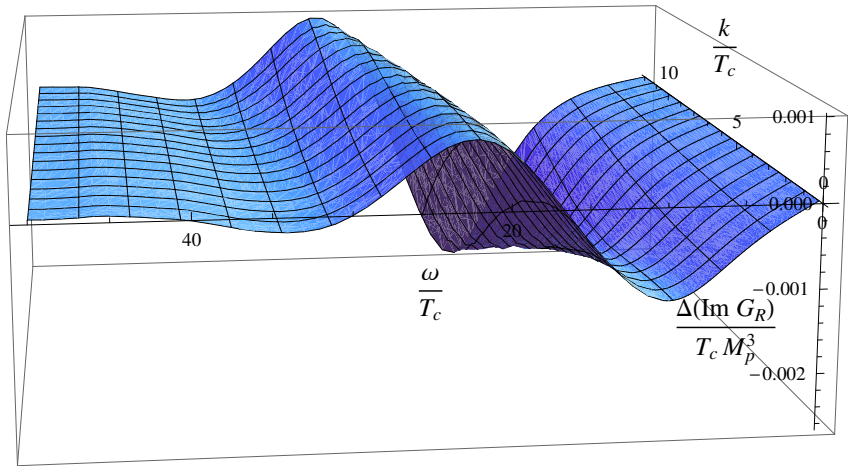

Figure 7.10: Our numerical results for $\Delta \mathrm{Im}\, G_R(\omega, \vec{k} = 0; T_c, 2T_c)/(T_c M_p^3)$ as a function of ω/T_c and $|\vec{k}|/T_c$, for the $Z(\lambda)$ in eq. (7.3.12) with $\kappa^2 Z_0 = 33.25$ and $c_4 = 0.26$. As $|\vec{k}|$ increases up to $|\vec{k}|/T_c \approx 10$, the largest peak shifts from $\omega/T_c \approx 22$ up to $\omega/T_c \approx 30$. The width of the peak changes very little.

7.6 Discussion and Outlook

IHQCD is a state-of-the-art bottom-up holographic model for the low-energy physics of (3+1)-dimensional large-N_c YM theory. In this paper we computed the retarded Green's function of the instanton density operator $q(x^\mu)$ in the high-temperature, deconfined phase of IHQCD. Our primary motivation was to compute the Chern-Simons diffusion rate, $\Gamma_{\rm CS}$, with the result in eq. (7.2.5). In particular, our result for $\Gamma_{\rm CS}$ is proportional to $Z(\lambda_h)$, where $Z(\lambda)$ is the normalization factor of the bulk axion action, and λ_h is the value of the holographic 't Hooft coupling at the black hole horizon. A combination of available data for the topological susceptibility and axial glueball spectrum of large-N_c YM, and glueball universality, are sufficient to determine the small and large λ limits of $Z(\lambda)$ [37; 38; 41; 44]. We considered several forms for $Z(\lambda)$. Assuming that $Z(\lambda)$ is a monotonic function of λ, we found quite generally that $\Gamma_{\rm CS}/(sT/N_c^2)$ is bounded from below by its value in the $T \to \infty$ limit and increases monotonically as $T \to T_c$ from above. Indeed, we presented an argument that the same will be true in many (3+1)-dimensional, confining, strongly-coupled, large-N_c theories with holographic duals. For the $Z(\lambda)$ producing our optimal fit to the lattice results for the axial glueball spectrum, we found that the increase was only 0.01%. Fixing $Z(\lambda)$ completely by a least-squares fit to lattice results for the Euclidean two-point function of $q(x^\mu)$, as

explained in section 7.3, is an important task for the future. We also presented evidence for a relatively long-lived excitation in the system with energy roughly on the order of the mass at $T = 0$ of the lightest 0^{-+} glueball, which prompted us to speculate that perhaps such an excitation could dominate CP-odd phenomena in the QGP created in heavy ion collisions.

IHQCD is dual to pure large-N_c YM, so an important goal for the future is to include the effects of quarks in the holographic calculation of $\Gamma_{\rm CS}$. Some key questions are how the quark mass and chiral symmetry breaking affect $\Gamma_{\rm CS}$. The axial and vector flavor $U(1)$ currents are dual to two $U(1)$ Maxwell fields in the bulk, and the quark mass operator is dual to a complex scalar field, a tachyon, that is bi-fundamental under these two gauge fields. In the bulk, the axion couples to the axial $U(1)$ gauge field and the to phase of the tachyon, as explained in refs. [55; 56]. A solution for the tachyon describing either a non-zero quark mass or chiral symmetry breaking can thus influence the axion and affect $\Gamma_{\rm CS}$.

Introducing flavors fields would also enable us to compute holographically the current produced via the CME. A preliminary requirement is a bulk solution describing a magnetic field and a net chirality.

We plan to study these and other related issues in the future.

7.7 Acknowledgements

We would like to thank F. Bruckmann, D. Kharzeev, H. Panagopoulos, A. Schäfer, D.T. Son and L. Yaffe for helpful conversations and correspondence. This work was supported in part by grants PERG07-GA-2010-268246, PIF-GA-2011-300984, the EU program “Thales” and "HERAKLEITOS II” ESF/NSRF 2007-2013 and was also co-financed by the European Union (European Social Fund, ESF) and Greek national funds through the Operational Program “Education and Lifelong Learning” of the National Strategic Reference Framework (NSRF) under “Funding of proposals that have received a positive evaluation in the 3rd and 4th Call of ERC Grant Schemes”. The research leading to these results has also received funding from the European Research Council under the European Community’s Seventh Framework Programme (FP7/2007-2013) / ERC grant agreement no. 247252.

Appendix: The Small Black Hole Branch

As discussed in section 7.3, when $T > T_{min}$ IHQCD admits two branches of black hole solutions, large black holes and small black holes [40]. In this appendix we compute $\Gamma_{\rm CS}$ using the small black hole solutions.

We can determine the dependence of $\Gamma_{\rm CS}$ on T in the large-T limit of the small black hole solutions as follows. For generality, we will consider a dilaton potential $V(\lambda)$ whose large-λ asymptotic form is $V(\lambda) \propto \lambda^{4/3} (\log \lambda)^P$, with P a non-negative real number. In the body of the paper we used $P = 1/2$. From fig. 7.1, we observe that for the small black hole solutions, when T is large, r_h is also large. When r_h is large, λ_h is also large, in which case we can approximate $Z(\lambda_h) \approx Z_0 c_4 \lambda_h^4$ and hence $\Gamma_{\rm CS}/(sT/N_c^2) \approx \kappa^2 Z_0\, c_4\, \lambda_h^4/(2\pi)$. As shown in refs. [37; 38; 41; 44], in the $r \to \infty$ limit, $\lambda(r) \propto \exp(r^{1/(1-P)})\, r^{\frac{3}{4}\frac{P}{1-P}}$. Evaluating at r_h gives us λ_h in terms of r_h. From ref. [40] we know r_h in terms of T on the small black hole branch in the $r_h \to \infty$ limit, $r_h \propto T^{(1-P)/P}$. We thus find

$$\frac{\Gamma_{\rm CS}}{sT/N_c^2} \propto \frac{\kappa^2 Z_0 c_4}{2\pi} (T/T_c)^3\, e^{C(T/T_c)^{\frac{1}{P}}}, \tag{.1}$$

where C is a dimensionless positive constant that depends on the choice of $V(\lambda)$.

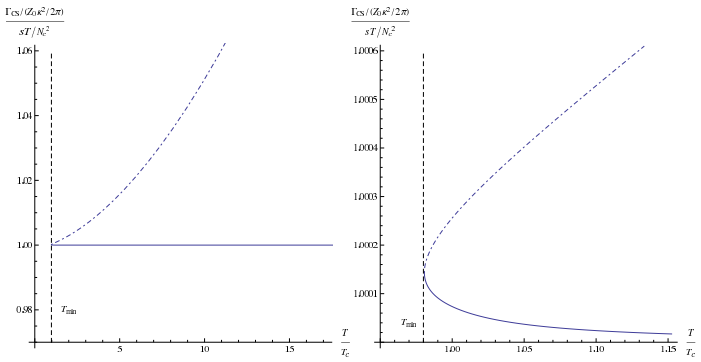

Figure 11: (a.) Our numerical result for $\Gamma_{CS}/(sT/N_c^2)$, divided by $Z_0\kappa^2/(2\pi)$, as a function of T/T_c, for the $Z(\lambda)$ in eq. (7.3.12) with $c_4 = 0.26$. The upper dot-dashed blue curve is our result obtained from small black hole solutions, while the lower solid blue curve is the result obtained from large black hole solutions. Both curves begin at T_{min}, indicated by the vertical dashed black line, which is slightly below T_c. The result on the small black hole branch increases as T increases, and in the $T \to \infty$ limit approaches the form in eq. (.1). (b.) Close-up of (a.) near T_{min}.

To compute $\Gamma_{\rm CS}$ in the entire range $T_{min} < T < \infty$, we resorted to numerics. For the $Z(\lambda)$ in eq. (7.3.12) with $c_4 = 0.26$, our results appear in fig. 11, where we see clearly

that the result grows as T increases, and in the $T \to \infty$ limit approaches the form in eq. (.1). Fig. 11 also shows that the result for $\Gamma_{CS}/(sT/N_c^2)$ is always larger on the small black hole branch than on the large black hole branch, except at T_{min} where the two are equal. This result is important for our argument at the end of section 7.4 that $\Gamma_{CS}/(sT/N_c^2)$ computed on the large black hole branch will increase as T approaches T_c from above.

Bibliography

[1] E. Shuryak, *Suppression Of Instantons As The Origin Of Confinement*, *Phys.Lett.* **B79** (1978) 135. 188

[2] D. Gross, R. Pisarski, and L. Yaffe, *QCD and Instantons at Finite Temperature*, *Rev.Mod.Phys.* **53** (1981) 43. 188

[3] N. Manton, *Topology in the Weinberg-Salam Theory*, *Phys.Rev.* **D28** (1983) 2019. 188

[4] F. Klinkhamer and N. Manton, *A Saddle Point Solution in the Weinberg-Salam Theory*, *Phys.Rev.* **D30** (1984) 2212. 188

[5] V. Kuzmin, V. Rubakov, and M. Shaposhnikov, *On the Anomalous Electroweak Baryon Number Nonconservation in the Early Universe*, *Phys.Lett.* **B155** (1985) 36. 188

[6] P. Arnold and L. McLerran, *Sphalerons, Small Fluctuations and Baryon Number Violation in Electroweak Theory*, *Phys.Rev.* **D36** (1987) 581. 188

[7] P. Arnold and L. McLerran, *The Sphaleron Strikes Back*, *Phys.Rev.* **D37** (1988) 1020. 188

[8] P. Arnold, D. Son, and L. Yaffe, *The Hot Baryon Violation Rate is $O(\alpha_w^5\ T^4)$*, *Phys.Rev.* **D55** (1997) 6264–6273, [hep-ph/9609481]. 188, 204

[9] D. Bodeker, *On the Effective Dynamics of Soft Non-Abelian Gauge Fields at Finite Temperature*, *Phys.Lett.* **B426** (1998) 351–360, [hep-ph/9801430]. 188, 204

[10] D. Bodeker, G. D. Moore, and K. Rummukainen, *Chern-Simons Number Diffusion and Hard Thermal Loops on the Lattice*, *Phys.Rev.* **D61** (2000) 056003, [hep-ph/9907545]. 188, 204

[11] G. Moore and M. Tassler, *The Sphaleron Rate in SU(N) Gauge Theory*, *JHEP* **1102** (2011) 105, [arXiv:1011.1167]. 188, 189, 204

[12] A. Cohen, D. Kaplan, and A. Nelson, *Progress in Electroweak Baryogenesis*, *Ann.Rev.Nucl.Part.Sci.* **43** (1993) 27–70, [hep-ph/9302210]. 188

[13] V. Rubakov and M. Shaposhnikov, *Electroweak Baryon Number Non-conservation in the Early Universe and in High-energy collisions*, *Usp.Fiz.Nauk* **166** (1996) 493–537, [hep-ph/9603208]. 188

[14] D. Kharzeev, R. Pisarski, and M. Tytgat, *Aspects of Parity, CP, and Time Reversal Violation in Hot QCD*, *Int.J.Mod.Phys.A* (2000) [hep-ph/0012012]. 188

[15] M. Gyulassy and L. McLerran, *New Forms of QCD Matter Discovered at RHIC*, *Nucl.Phys.* **A750** (2005) 30–63, [nucl-th/0405013]. 188

[16] E. Shuryak, *Physics of Strongly-Coupled Quark-Gluon Plasma*, *Prog.Part.Nucl.Phys.* **62** (2009) 48–101, [arXiv:0807.3033]. 188

[17] B. Müller, J. Schukraft, and B. Wyslouch, *First Results from Pb+Pb Collisions at the LHC*, arXiv:1202.3233. 188

[18] D. Kharzeev, L. McLerran, and H. Warringa, *The Effects of Topological Charge Change in Heavy Ion Collisions: 'Event by Event P and CP Violation'*, *Nucl.Phys.* **A803** (2008) 227–253, [arXiv:0711.0950]. 188, 204

[19] K. Fukushima, D. Kharzeev, and H. Warringa, *The Chiral Magnetic Effect*, *Phys.Rev.* **D78** (2008) 074033, [arXiv:0808.3382]. 188

[20] S. Voloshin, *Parity Violation in Hot QCD: How to Detect It*, *Phys.Rev.* **C70** (2004) 057901, [hep-ph/0406311]. 188

[21] **STAR Collaboration** Collaboration, B. Abelev *et. al.*, *Observation of Charge-dependent Azimuthal Correlations and Possible Local Strong Parity Violation in Heavy Ion Collisions*, *Phys.Rev.* **C81** (2010) 054908, [arXiv:0909.1717]. 188

[22] **ALICE Collaboration** Collaboration, B. Abelev *et. al.*, *Charge Separation Relative to the Reaction Plane in Pb-Pb Collisions at* $\sqrt{s_{NN}} = 2.76$ *TeV*, arXiv:1207.0900. 188

[23] A. Bzdak, V. Koch, and J. Liao, *Charge-Dependent Correlations in Relativistic Heavy Ion Collisions and the Chiral Magnetic Effect*, arXiv:1207.7327. 189

[24] E. Vicari and H. Panagopoulos, *Theta Dependence of SU(N) Gauge Theories in the Presence of a Topological Term*, *Phys.Rept.* **470** (2009) 93–150, [arXiv:0803.1593]. 189, 196, 197

[25] N. Iqbal and H. Meyer, *Spatial Correlators in Strongly Coupled Plasmas*, *JHEP* **0911** (2009) 029, [arXiv:0909.0582]. 189

[26] J. Maldacena, *The Large N Limit of Superconformal Field Theories and Supergravity*, *Adv.Theor.Math.Phys.* **2** (1998) 231–252, [hep-th/9711200]. 189

[27] S. Gubser, I. Klebanov, and A. Polyakov, *Gauge theory Correlators from Non-critical String Theory*, *Phys.Lett.* **B428** (1998) 105–114, [hep-th/9802109]. 189, 199

[28] E. Witten, *Anti-de Sitter Space and Holography*, *Adv.Theor.Math.Phys.* **2** (1998) 253–291, [hep-th/9802150]. 189, 199

[29] E. Witten, *Anti-de Sitter Space, Thermal Phase Transition, and Confinement in Gauge Theories*, *Adv.Theor.Math.Phys.* **2** (1998) 505–532, [hep-th/9803131]. 189, 205

[30] D. Son and A. Starinets, *Minkowski Space Correlators in AdS / CFT Correspondence: Recipe and Applications*, *JHEP* **0209** (2002) 042, [hep-th/0205051]. 189, 200, 201, 204

[31] G. Policastro, D. Son, and A. Starinets, *From AdS / CFT Correspondence to Hydrodynamics*, *JHEP* **0209** (2002) 043, [hep-th/0205052]. 189

[32] N. Iqbal and H. Liu, *Universality of the Hydrodynamic Limit in AdS/CFT and the Membrane Paradigm*, *Phys.Rev.* **D79** (2009) 025023, [arXiv:0809.3808]. 189, 200, 202, 206

[33] P. Kovtun, D. Son, and A. Starinets, *Viscosity in Strongly-Interacting Quantum Field Theories from Black Hole Physics*, *Phys.Rev.Lett.* **94** (2005) 111601, [hep-th/0405231]. 189, 192

[34] M. Luzum and P. Romatschke, *Conformal Relativistic Viscous Hydrodynamics: Applications to RHIC results at s(NN)**(1/2) = 200-GeV*, *Phys.Rev.* **C78** (2008) 034915, [arXiv:0804.4015]. 189

[35] G. Basar and D. Kharzeev, *The Chern-Simons Diffusion Rate in Strongly-Coupled N=4 SYM Plasma in an External Magnetic Field*, *Phys.Rev.* **D85** (2012) 086012, [arXiv:1202.2161]. 189

[36] B. Craps, C. Hoyos, P. Surowka, and P. Taels, *Chern-Simons Diffusion Rate in a Holographic Yang-Mills Theory*, arXiv:1209.2532. 189

[37] U. Gursoy and E. Kiritsis, *Exploring Improved Holographic Theories for QCD: Part I*, *JHEP* **0802** (2008) 032, [arXiv:0707.1324]. 189, 190, 191, 192, 193, 195, 196, 197, 208, 216

[38] U. Gursoy, E. Kiritsis, and F. Nitti, *Exploring Improved Holographic Theories for QCD: Part II*, *JHEP* **0802** (2008) 019, [arXiv:0707.1349]. 189, 190, 191, 192, 193, 195, 196, 197, 208, 216

[39] U. Gursoy, E. Kiritsis, L. Mazzanti, and F. Nitti, *Deconfinement and Gluon Plasma Dynamics in Improved Holographic QCD*, *Phys.Rev.Lett.* **101** (2008) 181601, [arXiv:0804.0899]. 189, 191, 192, 193, 204

[40] U. Gursoy, E. Kiritsis, L. Mazzanti, and F. Nitti, *Holography and Thermodynamics of 5D Dilaton-gravity*, *JHEP* **0905** (2009) 033, [arXiv:0812.0792]. 189, 190, 191, 192, 193, 197, 198, 204, 205, 216

[41] E. Kiritsis, *Dissecting the String Theory Dual of QCD*, *Fortsch.Phys.* **57** (2009) 396–417, [arXiv:0901.1772]. 189, 191, 192, 195, 196, 197, 208, 216

[42] U. Gursoy, E. Kiritsis, L. Mazzanti, and F. Nitti, *Improved Holographic Yang-Mills at Finite Temperature: Comparison with Data*, *Nucl.Phys.* **B820** (2009) 148–177, [arXiv:0903.2859]. 189, 190, 191, 193, 194, 195, 196, 197, 198, 203, 204, 211

[43] U. Gursoy, E. Kiritsis, G. Michalogiorgakis, and F. Nitti, *Thermal Transport and Drag Force in Improved Holographic QCD*, *JHEP* **0912** (2009) 056, [arXiv:0906.1890]. 189, 191, 194, 204

[44] U. Gursoy, E. Kiritsis, L. Mazzanti, G. Michalogiorgakis, and F. Nitti, *Improved Holographic QCD*, *Lect.Notes Phys.* **828** (2011) 79–146, [arXiv:1006.5461]. 189, 190, 191, 192, 195, 196, 197, 208, 216

[45] P. Arnold, G. Moore, and L. Yaffe, *Transport Coefficients in High Temperature Gauge Theories. 1. Leading Log Results*, *JHEP* **0011** (2000) 001, [hep-ph/0010177]. 192

[46] S. S. Gubser, *Curvature Singularities: The Good, the Bad, and the Naked*, *Adv.Theor.Math.Phys.* **4** (2000) 679–745, [hep-th/0002160]. 193

[47] B. Lucini, M. Teper, and U. Wenger, *Properties of the Deconfining Phase Transition in SU(N) Gauge Theories*, *JHEP* **0502** (2005) 033, [hep-lat/0502003]. 195, 204

[48] G. Boyd, J. Engels, F. Karsch, E. Laermann, C. Legeland, *et. al.*, *Thermodynamics of SU(3) Lattice Gauge Theory*, *Nucl.Phys.* **B469** (1996) 419–444, [hep-lat/9602007]. 195

[49] B. Bringoltz and M. Teper, *The Pressure of the SU(N) Lattice Gauge Theory at Large-N*, *Phys.Lett.* **B628** (2005) 113–124, [hep-lat/0506034]. 195

[50] M. Panero, *Thermodynamics of the QCD Plasma and the Large-N limit*, *Phys.Rev.Lett.* **103** (2009) 232001, [arXiv:0907.3719]. 195

[51] E. Witten, *Theta Dependence in the Large-N Limit of Four-dimensional Gauge Theories*, *Phys.Rev.Lett.* **81** (1998) 2862–2865, [hep-th/9807109]. 195

[52] L. Del Debbio, L. Giusti, and C. Pica, *Topological Susceptibility in the SU(3) Gauge Theory*, *Phys.Rev.Lett.* **94** (2005) 032003, [hep-th/0407052]. 196

[53] C. Morningstar and M. Peardon, *The Glueball Spectrum from an Anisotropic Lattice Study*, *Phys.Rev.* **D60** (1999) 034509, [hep-lat/9901004]. 197, 207, 210

[54] K. Kajantie, M. Krssak, M. Vepsalainen, and A. Vuorinen, *Frequency and Wave Number Dependence of the Shear Correlator in Strongly Coupled Hot Yang-Mills Theory*, *Phys.Rev.* **D84** (2011) 086004, [arXiv:1104.5352]. 206

[55] R. Casero, E. Kiritsis, and A. Paredes, *Chiral Symmetry Breaking as Open String Tachyon Condensation*, *Nucl.Phys.* **B787** (2007) 98–134, [hep-th/0702155]. 208

[56] M. Jarvinen and E. Kiritsis, *Holographic Models for QCD in the Veneziano Limit*, *JHEP* **1203** (2012) 002, [arXiv:1112.1261]. 208

8 Conclusions and Outlook

In this thesis a class of holographic models, namely IHQCD, Tachyon AdS/QCD and V-QCD were studied in order to understand low-energy phenomena of QCD. In chapters 3 and 4, Tachyon AdS/QCD in a simple gravitational background was studied in order to address several aspects of the low energy meson sector of QCD. Even if this is a bottom-up phenomenological holographic model it is string inspired. Therefore, we readily recognize the bulk fields as the lightest fields of a brane-antibrane system. AdS/QCD models can be thought as small field expansion of the above model, since upon expansion of Sen's DBI action we find the usual AdS/QCD quadratic action. The UV (near boundary) behavior of the model is very close to other AdS/QCD models, but the IR significantly changes.

In other holographic models, physics is determined by boundary conditions in the IR while now we have a consistency condition that the tachyon potential becomes zero in the IR and consequently the tachyon infinite. Moreover, brane-antibrane system has a natural Wess-Zumino part in its action which gives the correct anomaly, parity and charge conjugation symmetries. The model incorporates confinement in the sense that the quark-antiquark potential, computed with the usual AdS/CFT prescription (see section 2.7), confines. The gravitational background comes from an action that allows, black hole solutions as well. Thus, one can describe thermal phase transitions within these backgrounds as described in section 2.8.

The flavor vacuum of the model has spontaneously broken chiral symmetry at zero

temperature. While, it is restored at the confinement-deconfinement transition. An advantage of the present model is that the IR consistency condition for the tachyon allows us to determine the vacuum expectation value of the quark bilinear in terms of the quark mass. So, we have one less parameter with respect to hard wall AdS/QCD. Having quark mass as a parameter in our model we find that meson masses depend on it linearly in the limit of small quark mass. The pion and the quark mass are shown to obey the Gell Mann-Oakes Renner relation and in case of zero quark mass there are N_f^2 Goldstone bosons in the spectrum. It is also found that the masses of highly excited states follow linear Regge trajectories. Finally, the comparison of the model to the experimental data is quite successfull since we find an error, $\epsilon_{rms} = 14.5\%$.

The Tachyon AdS/QCD model also has some disadvantages. One main issue is that in order for the bulk tachyon to be dual to the dimension three quark bilinear, its mass should be $m_T^2 R_{AdS}^2 = -3$, where the mass of the tachyon is $m_T^2 = -\frac{1}{2\alpha'}$. This shows that $R_{Ads}^2 = 6\alpha'$, meaning that background spacetime is highly curved and higher derivative corrections to the gravitational action could be important. This is a general problem of non-critical holographic models. However, even if we do not have top-down controlled model, we notice that incorporating top-down ingredients to a simple effective holographic model we achieve unifying all the good predictions of different AdS/QCD models in one simple construction automatically.

In the context of Tachyon AdS/QCD model, we have shown that the relation, which was proposed by Son and Yamamoto connecting the vector-axial vector flavor current correlator in weak electric field to the difference of the vector and axial vector two-point functions is valid only for low Euclidean momenta. This seems to be a feature of a general class of holographic models which have similar UV asymptotics (hard/soft wall, tachyon AdS/QCD). In addition, the dependence of the correlator on q^2 for large q^2 is $1/q^8$ while in QCD it is $1/q^6$.

As explained in chapter 5, the $1/q^6$ contribution in the OPE of the vector-axial correlator comes from the operator $\bar{\psi}_R \sigma^{\mu\nu} \psi_L$. The bulk dual of this operator is a two-index antisymmetric tensor which is absent in the most common AdS/QCD models. This field transforms as $(N_f, \bar{N}_f)$ under the flavor group and is a higher massive string state in the tower of the tachyon. Sen's action, describing our bulk fields, is supposed to arise as an effective action after integrating out higher stringy states as the one mentioned above. Hence, we were expecting that we could find the correct large q^2 expansion of the axial-vector correlator. It turned out that the correlator is similar to other simple holographic models and different from QCD.

The chapter 6 contains the main results of the fluctuation analysis of V-QCD model

at zero temperature. We have considered all the fluctuations classified in two categories: singlets and non-singlets under the flavor group. Singlets include the 2^{++} glueballs, the 0^{++} glueballs and scalar mesons which were found to mix to leading order in $1/N$ in the Veneziano limit, and the 0^{-+} glueballs and the η' pseudoscalar tower. The non-singlet fluctuations contain vector and axial-vetor meson fluctuations, the pseudoscalar mesons (including the massless pions), and the scalar mesons. The main result of this analysis is that masses and in general the observables, which have non-zero mass dimension, follow Miransky scaling as $x \to x_c$, where x_c is the place where a conformal phase transition takes place. Moreover, there is no light dilaton state in spectrum which has been proposed as a signal of the conformal symmetry breaking at x_c. This breaking is correlated to the Miransky scaling close to x_c.

The S-parameter of the model is found to asymptote to a finite value at x_c. This analysis is generalized in a publication that will soon follow. There is a thorough analysis of the model where different classes of potentials that appear in Sen's action are constrained in terms of their prediction about the spectrum. For instance, their IR behavior affects the behavior of the spectra at large excitation number. Hence, demanding that the spectrum follows linear Regge trajectories constraints are set to the model.

Finally, the chapter 7 describes the calculation of Chern-Simons diffusion rate, Γ_{CS}, in IHQCD. Γ_{CS} is shown to be proportional to the dilaton dependent function, $Z(\lambda)$, which multiplies the axion kinetic term. We have found that the value of Γ_{CS} as a function of temperature is bounded from below by it's value at infinite T. This seems to be a generic result for confining theories with classical gravity duals. Γ_{CS} is computed for various choices of $Z(\lambda)$, which are such that $Z(\lambda)$ matches the lattice results for topological susceptibility and for axial glueball mass ratios. Γ_{CS} is always increasing as the temperature approaches the confinement/deconfinement transition temperature. By requiring that the choices of $Z(\lambda)$ reproduce the lattice results for the axial glueball mass ratios to within one sigma, we set an upper bound on Γ_{CS}. Therefore, we found $1.64 \leq \Gamma_{CS}(T_c)/T_c^4 \leq 2.8$. We also calculate the axion spectral function which is proportional to the imaginary part of the retarded Green function $G_R(\omega, \vec{k})$, for $T \geq T_c$. The renormalized spectral function suggests the presence of a reasonably long-lived excitation with energy of order of the lightest axial glueball mass at $T = 0$. Such an excitation could dominate many CP-odd phenomena in the quark gluon plasma.

8.1 Outlook

It is observed that the tachyon AdS/QCD model does not work very well for large quark mass. For example, we studied the spectral function of the vector excitations in the deconfined phase in order to argue if there is a peak corresponding to J/Ψ meson, but no peak was found. As it has been argued a step-like Schrödinger potential for the bulk excitation gives the desired quasi-particle behavior, see 4.6. In the present model the potentials in the deconfined phase do not appear to have step-like behavior, therefore they do not create sharp peaks in the spectral function. Having only one scale in our model, which does not really affect the deconfined phase physics, does not seem possible to introduce the desired dip in the potentials. The Schrödinger potentials do not depend on Λ_{QCD}. Indeed, z_Λ only sets the temperature at which the confinement/deconfinement transition takes place. An interesting future direction is to try to address this issue in the context of V-QCD. In this case, there are two scales ($\Lambda_{UV/IR}$) in the problem defined by the UV and the IR expansions of the fields. For $x < x_c$ the two scales are of the same order. They become distinct as $x \to x_c$. Λ_{UV} is the scale where the coupling starts decreasing and Λ_{IR} sets the location where it starts increasing. In the intermediate region the coupling walks. The Schrödinger potentials of the fluctuations depend on the gravitational and dilaton background and the Λ_{IR} scale may set the location of a possible dip of Schrödinger potentials. Exploring the fluctuation spectrum on the finite temperature backgrounds of V-QCD is important in order to find possible long-lived fluctuations in thermal backgrounds.

We also observe in the spectrum fits to the experimental data that the Tachyon AdS/QCD model tends to consistently overestimate the masses of the excited axial vectors and pseudoscalars. This is connected to the fact that the model yields larger Regge slope for axial mesons than for the vectors. In V-QCD the normalization factors of the kinetic terms in Sen's DBI action depend on the dilaton as well. So, their functional form can be contrained by requiring that they produce the same slopes for vectors with axial-vectors and scalars with pseudoscalars. This is an imprortant improvement that will soon be published. Hence, the phenomenological fit of the specra and decay constants of those models is expected to be of better accuracy. Therefore, this is another interesting future task.

Moreover, the result for the vector-axial vector flavor current correlator in weak electric field indicates that the Son-Yamamoto relation is valid in the IR for a general class of models where chiral symmetry breaking is properly described. However, we are

lacking something like a Ward identity which would explain where this relation comes from. This is would be an important improvement since from the point of view of chiral perturbation theory this relation connects couplings of the CP odd and even sector of the chiral Lagrangian. In case of large momenta, it is shown that the holographic calculation of the vector-axial vector correlator does not agree with the OPE answer of QCD. Even if holographic models are not guaranteed to give correct predictions in the UV, we expect that the UV behavior of the above correlator can be corrected. A modified tachyon potential ($W(TT^\dagger)$) in the Wess-Zumino (WZ) term may change the result. For instance, in the Tachyon AdS/QCD, a WZ potential with UV expansion of the form $W(TT^\dagger) = W(0) + \mathcal{O}(TT^\dagger)^{\frac{2}{3}})$ gives the proper behavior of the correlator. This is a fit though, which is not supported by any other argumentation. However, in V-QCD the normalization factors of the kinetic terms, the tachyon potential and the Wess-Zumino potential become non-trivial functions of the dilaton. Therefore, the result for the correlator will change in V-QCD since the on-shell action and the equations of the vector and axial vector fluctuations will change. Hence, It is important to check how the dilaton dependence of those functions affects the result for the correlator.

Moreover, we start examining the model in the case of finite baryon density. We aim to construct the finite temperature (T) and baryon chemical potential (μ) phase diagram of V-QCD. The real QCD phase diagram exhibits many interesting features. At zero baryon chemical potential QCD passes from the chirally broken to the chirally symmetric phase through a crossover. In case of finite chemical potential, the crossover turns into a first order transition. This happens at a critical point on the $(T-\mu)$ plane, which has not been reached experimentally until now. Therefore, not much is known about the properties of matter in the viccinity of that point. Future experiments are believed to create quark-gluon plasma close to that point. In the limit of large chemical potential several exotic phases have been proposed to exist, like color superconducting phase. Lattice methods cannot be applied appropriately for finite chemical potential due to the sign in the path integral. Therefore, studying holographically the QCD phase diagram in terms of the temperature and baryon chemical potential is of great importance. States with finite chemical potential in QCD correspond to bulk solutions with non-trivial vector field. Hence, working in the context of V-QCD, we aim to study gravitational backgrounds with non-zero dilaton, tachyon and vetor field.

The generalization of the IHQCD calculation of Γ_{CS} by including the flavor degrees of freedom is very important as well. Non-zero quark mass and chiral symmetry breaking are expected to affect $\Gamma_C S$. The information about both the quark mass and quark condensate is in the bulk tachyon field. Therefore, through the coupling of the tachyon

phase to the axion field the Chern-Simons diffusion rate will be changed by the tachyon vacuum. Moreover, in order to describe the chiral magnetic effect holographically one should consider a background axial-vector field in the bulk corresponding to the chiral chemical potential of the field theory. A non-zero bulk vector gauge field is dual to the neccesary background magnetic field which causes the effect. In this construction, a non-zero electric current parallel to the magnetic field should appear in the dual field theory.

List of Figures

List of Tables


European Union
European Social Fund

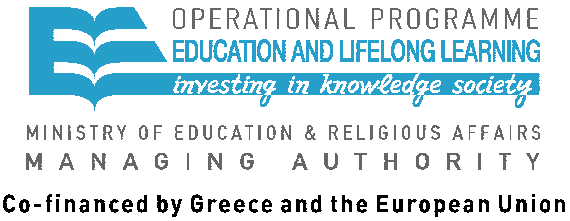
OPERATIONAL PROGRAMME
EDUCATION AND LIFELONG LEARNING
investing in knowledge society
MINISTRY OF EDUCATION & RELIGIOUS AFFAIRS
MANAGING AUTHORITY
Co-financed by Greece and the European Union


NSRF
2007-2013
programme for development
EUROPEAN SOCIAL FUND